A molecular and behavioural analysis of descending facilitation in a model of joint inflammation

Fiona Brigid Carr

UCL

Thesis submitted for the degree of Doctor of Philosophy

I, Fiona Brigid Carr, confirm that the work presented in this thesis is my own. Where information has been derived from other sources, I confirm that this has been indicated in the thesis.

Abstract

Descending facilitation of nociceptive processing via the rostral ventromedial medulla (RVM) has been shown to contribute to behavioural hypersensitivity in a number of models of pain. Pain arising from the joints is a significant clinical problem, and studies to date have focused largely on the underlying peripheral causes. The aim of this study was to investigate the contribution of central mechanisms of descending facilitation to pain in a model of joint inflammation.

To determine if the RVM is activated following ankle injection of Complete Freund's adjuvant (CFA), a model of joint inflammation, pERK immunohistochemistry and labelling of active GABAergic synapses were carried out. At 6h post CFA, pERK labelling was increased, predominantly within 5-HT expressing neurons. Later, at 3d post CFA a decrease in GABAergic transmission was identified. This suggests time dependent changes in neuronal function occur within the RVM following joint inflammation. Selective lesion of descending 5-HT fibres and mu opioid receptor expressing (MOR+) cells of the RVM combined with behavioural studies indicated that both descending pathways contribute to mechanical hypersensitivity of the ipsilateral hindpaw. As the dorsal horn mechanisms underlying descending facilitation are not well understood, microarray analysis was carried out to identify changes in dorsal horn gene expression associated with descending facilitation. This led to the identification of a number of immune system related genes, including the chemokine *Cxcl10* and its receptor *Cxcr3* suggesting descending facilitation is mediated in part by neuronal - immune system interactions.

These findings demonstrate for the first time that behavioural hypersensitivity in joint pain is dependent in part on descending facilitation via the RVM. In addition to peripheral pathology and spinal cord sensitisation, brainstem contributions should also be taken into account in the study and treatment of joint pain.

List of abbreviations

5,7-DHT	5,7-dihydroxytryptamine
5-HT	5-hydroxytryptamine (serotonin)
ACC	anterior cingulate cortex
AMPA	2-amino-3-(3-hydroxy-5-methyl-isoxazol-4-yl)propionic acid
ANOVA	analysis of variance
ASIC	acid sensing ion channel
ATP	adenosine triphosphate
BDNF	brain derived neurotrophic factor
BP	biological process
CaMKII	calcium-calmodulin dependent protein kinase II
cAMP	cyclic adenosine monophosphate
CC	cellular compartment
CCK	cholecystokinin
CCL2	chemokine (C-C motif) ligand 2
Ccnb2	cyclin b2
cDNA	complementary deoxyribonucleic acid
Ce	central nucleus of the amygdala
CFA	Complete Freund's adjuvant
CGRP	calcitonin gene related peptide
Chrnb3	nicotinic receptor β3 subunit
CL	central lateral nucleus (thalamus)
CNS	central nervous system
CO_2	carbon dioxide
COX-2	cyclooxygenase 2
CREB	camp response element binding protein
Ct	cycle threshold
CVLM	caudal ventrolateral medulla
CX3CL1	fractalkine
CXCL10	chemokine (C-X-C motif) ligand 10
CXCL9	chemokine (C-X-C motif) ligand 9
CXCR3	chemokine (C-X-C motif) receptor 3
DAB	3,3’-diaminobenzidine
DAPI	4',6-diamidino-2-phenylindole
DRG	dorsal root ganglion

DS	dermorphin-saporin
ERK	extracellular signal related kinase
EtOH	ethanol
GABA	gamma-amino butyric acid
GAD65/67	glutamate decarboxylase (65kDa isoform)
GAD65/67	glutamate decarboxylase (65kDa and 67kDa isoforms)
GDNF	glial cell line derived neurotrophic factor
GFAP	glial fibrillary acidic protein
GiA	nucleus reticularis gigantocellularis
GO	gene ontology
GPCR	G protein-coupled receptor
HRP	horseradish peroxidase
Htr1d	5-HT1D receptor
IBA1	ionised calcium binding adaptor molecule 1
IC	insular cortex
IFN-γ	interferon gamma
Il-16	interleukin 16
IL-1β	interleukin 1 beta
Il-6	interleukin 6
iNOS	inducible nitric oxide synthase
LSD	least significant difference
MAPK	mitogen activated protein kinase
MAPKK (MEK)	mitogen activated protein kinase kinase
MAPKKK	mitogen activated protein kinase kinase kinase
MeCP2	methyl CpG binding protein 2
MeOH	methanol
MF	molecular function
MIA	monosodium iodoacetate
MNK	MAPK (Mitogen-Activated Protein Kinase)-interacting kinase
MOPS	3-(N-morpholino)propanesulfonic acid
MOR	mu opioid receptor
mRNA	messenger ribonucleic acid
mTOR	mammalian target of rapamycin
NaV	voltage gated sodium channel
NeuN	neuronal nuclear antigen
NGF	nerve growth factor

NK1	neurokinin 1
NMDA	N-methyl-D-aspartic acid
nNOS	neuronal nitric oxide synthase
NO	nitric oxide
Nos2	nitric oxide synthase 2
NRM	nucleus raphe magnus
NS	nociceptive specific
NSAID	non-steroidal anti-inflammatory
NTS	nucleus tractus solitarus
O_2	oxygen
OA	osteoarthritis
PAG	periaqueductal gray
PB	lateral parabrachial area
PB	phosphate buffer
PFA	paraformaldehyde
PGE2	prostaglandin E2
PKA	protein kinase A
PKC	protein kinase C
Py	pyramidal tract
qPCR	quantitative real time polymerase chain reaction
RA	rheumatoid arthritis
RIPA	radioimmunoprecipitation assay buffer
RNA	ribonucleic acid
ROb	nucleus raphe obscurus
RPa	nucleus raphe pallidus
Rpl	ribosome protein like
rRNA	ribosomal RNA
RT-qPCR	quantitative reverse transcriptase real time polymerase chain reaction
RVM	rostral ventromedial medulla
SDS-PAGE	sodium dodecyl sulphate polyacrylamide gel electrophoresis
serpin	serine protease inhibitor
SS	somatosensory cortex
TNF-α	tumor necrosis factor alpha
TPH	tryptophan hydroxylase
TrkB	tyrosine related kinase B receptor
TRP	transient receptor potential

TSA	tyramide signal amplification
TTBS	Triton Tris buffered saline
VGAT	vesicular GABA transporter
VGAT-C	C terminus of vesicular GABA transporter
VGAT-N	N terminus of vesicular GABA transporter
VGKC	voltage gated potassium channel
VMH	ventromedial hypothalamus
VPL	ventroposterior lateral nucleus (thalamus)
VPM	ventroposterior medial nucleus (thalamus)
WDR	wide dynamic range

Contents

List of figures

List of tables

Acknowledgements

I would first like to thank my supervisor, Professor Stephen Hunt, for his enthusiasm and encouragement throughout my PhD. His support and wisdom has been invaluable and I could not ask for a better mentor.

Thanks also to Professor Tony Dickenson, for his support as my secondary supervisor and throughout my time with the LPC. I am very grateful to the LPC and the Wellcome Trust for funding my research.

Many thanks go to Dr Sandrine Géranton for her time and endless patience in teaching me lab techniques. Thanks also to Dr Ilona Obara for her Western blot expertise. I also thank my BSc students, Theo Bartholomew and Affreen Matin who were wonderful to teach, and have contributed to the immunohistochemistry in chapter 3 and 6.

A big thanks to my friends and fellow PhD students, Keri Tochiki, Julia Dudley and Ruth Weir. Without you this would have been a lot more difficult, and a lot less fun, so thank you for the many laughs in the lab, the bar and the wider world! Thanks also to Jacqueta Meredith-Middleton for looking after us over the years, and to all my colleagues in the Hunt and Fitzgerald labs, thank you for making the Medawar corridor such a lovely place to work.

Thanks to my Aunt Angela, for being my home from home in London. Thanks also to my brothers and sisters for their support and encouragement.

Finally, thank you to my parents, for everything you have done for us and supporting me at every step. I hope I've made you proud and can continue to do so in the years to come.

1. Introduction

Pain has an important protective role as it alerts the individual to harmful or potentially harmful external stimuli, and provokes prompt behavioural responses to minimise injury. The essential role of pain perception for survival is most apparent in individuals suffering from a congenital inability to feel pain. The absence of this important protective mechanism leads to failure to respond to harmful stimuli which can result in severe injuries throughout life. Although the sensation of pain is unpleasant, these cases illustrate the importance of an intact pain system for the wellbeing of the individual (Cox et al., 2006; Goldberg et al., 2007; Verpoorten et al., 2006).

In contrast to these rare cases of insensitivity to pain, a more widespread clinical problem is chronic pain. This is pain which persists after the injury has healed or for periods beyond it being useful as a warning signal. Chronic pain, lasting for longer than 3 months, is highly prevalent with reports of up to 20% incidence in the general population (Breivik et al., 2006; Reid et al., 2011). Chronic pain is a symptom of many underlying pathologies, including arthritis, nerve injury, and cancer. Despite its prevalence, many patients suffering from chronic pain receive inadequate relief from existing therapies. This has a negative impact on quality of life for the affected individual, and is a considerable economic burden for society due to the costs of healthcare management and the inability of some chronic pain patients to work (Reid et al., 2011). For this reason basic research on the neurobiology of pain and identification of potential pharmacological targets remains an important goal.

1.1 Classification of pain

Pain is defined as an unpleasant sensory and emotional experience associated with actual or potential tissue damage, or described in terms of such damage (International Association for the Study of Pain, 2011). This

precise definition illustrates some important points about the nature of pain. Importantly, pain is an experience with both sensory and affective components and cannot be considered only in terms of sensory input. In addition pain can occur even in the absence of tissue damaging stimuli. It has been proposed that there are three main types of pain which differ in terms of cause, duration and function (Scholz and Woolf, 2002).

1. Nociceptive pain occurs in the presence of an acute noxious stimulus. This form of pain serves an important protective role in that it alerts the individual to tissue damaging stimuli (Basbaum et al., 2009). Nociceptive pain is typically of short duration and stops once the noxious stimulus is removed.

2. Pathological pain does not serve a useful biological function. Conditions in this category often lead to pain in the absence of noxious input, and can be chronic. One widely studied example of a pathological pain condition is neuropathic pain, caused by direct lesion of the nervous system (Costigan et al., 2009b). A range of other conditions also come under this category, which produce the sensation of pain without obvious noxious input, such as irritable bowel syndrome and fibromyalgia (Woolf, 2010).

3. Inflammatory pain is caused by inflammation associated with tissue damage and has some characteristics in common with both nociceptive and pathological pain. Inflammatory pain arises as a direct result of tissue injury and therefore like nociceptive pain has a protective role, alerting the individual to a physical injury and preventing further damage. However it is also problematic for patients, as it can be chronic, like many of the pathological pain states.

Chronic pain conditions are characterised by hyperalgesia, allodynia, and spontaneous pain. Hyperalgesia is defined as increased pain from a stimulus that normally provokes pain, and allodynia is defined as pain due to a

stimulus that does not normally provoke pain (International Association for the Study of Pain, 2011). These symptoms arise due to sensitisation of the nociceptive system. This is defined as a reduction in the threshold and an increase in the magnitude of a response to noxious stimulation, and is driven by both peripheral and central mechanisms (Gold and Gebhart, 2010). Table 1.1 summarises the characteristics of the three forms of pain.

	Nociceptive	**Inflammatory**	**Pathological**
Cause	Acute noxious stimuli: heat, cold, mechanical	Inflammation caused by tissue injury	Neuropathic: nervous system injury Others idiopathic, e.g. irritable bowel syndrome
Function	Protective function: reflex withdrawal	Protective function: reduce further injury, promotes repair	Dysfunctional, serves no protective role
Duration	Acute	Variable: can be acute or chronic	Chronic
Sensations	Intense heat, cold or mechanical pain	Hyperalgesia Allodynia Spontaneous pain	Hyperalgesia Allodynia Spontaneous pain
Treatment	Not always necessary	Reduce peripheral inflammation, e.g. non-steroidal anti-inflammatories Disease modification e.g. joint replacement or immunosuppression in arthritis	Poor treatment options available

Table 1.1 Characteristics of nociceptive, inflammatory and pathological pain.

Adapted from Scholz and Woolf, 2002.

1.2 Overview of the nociceptive system

Nociceptive stimuli are detected by nociceptors innervating peripheral tissues, and are relayed to the dorsal horn of the spinal cord which forms the first synapse of the pathway (Hunt and Mantyh, 2001). From here the signal is conveyed to the brain which leads to the perception of pain.

Understanding the normal function of these peripheral, spinal and supraspinal mechanisms is crucial to understanding maladaptations that occur in chronic pain states.

1.2.1 Nociceptors

The concept of a sensory fibre specific to the detection of tissue damaging stimuli was first proposed by Sherrington in 1903 (Sherrington, 1903), however the existence of nociceptive specific sensory fibres was only demonstrated in the mid-1960s. A subset of thinly myelinated Aδ-fibres were identified which responded exclusively to noxious mechanical stimulation (Burgess and Perl, 1967). Unmyelinated C-fibres were also discovered which were either polymodal nociceptors, responding to a variety of noxious stimuli such as heat, cold, chemical and mechanical stimulation, or high threshold mechanoreceptors (Bessou and Perl, 1969). Aδ-fibres conduct more rapidly than C-fibres, and for this reason the Aδ-fibres are thought to be responsible for rapid, sharp pain and C-fibres for the slow, dull pain that occurs upon noxious stimulation. Aβ-fibres are also myelinated and are the largest diameter sensory fibres in the DRG, however these do not act as nociceptors, and instead conduct rapidly in response to low intensity mechanical stimulation (Julius and Basbaum, 2001; Woolf and Ma, 2007). The cell bodies of nociceptors are located in the dorsal root ganglion (DRG) or trigeminal ganglion in the case of head and neck areas.

As with all sensory afferents, nociceptors innervate various peripheral tissues including the skin, joints and viscera. The transduction of noxious stimuli into an action potential is achieved by the activation of transducer molecules on the nociceptor endings by high intensity, tissue damaging stimuli. This distinguishes nociceptors from other sensory fibres, which express low threshold transducers. Among the nociceptor transducers that have been identified are the transient receptor potential (TRP) family of ion channels. This includes TRPV1 which is responsible for the transduction of

noxious heat, and contributes to inflammatory pain and thermal hyperalgesia (Caterina et al., 1999). TRPA1 is activated by noxious cold and can also respond to chemical irritants such as formalin and mustard oil, and may play a role in mediating mechanical nociception (Vay et al., 2012). Another important family of noxious stimuli transducers are the acid sensing ion channels (ASICs). These are activated by protons in the extracellular environment, which are increased during tissue acidosis and so contribute to inflammatory pain (Deval et al., 2010). Recently, a mechanosensitive ion channel Piezo has been identified which may contribute to the transduction of noxious mechanical stimuli (Kim et al., 2012).

Activation of these transducer channels leads to depolarisation of the membrane, producing a generator potential which is converted into an action potential if the stimulus is of large enough magnitude or spread (Raouf et al., 2010). Action potentials are propagated along the axon by voltage gated sodium channels (Nav). The subtypes Nav 1.7, 1.8, 1.9 are present in nociceptors and local anaesthetics act by inhibiting these channels (Eijkelkamp et al., 2012). Nav 1.7 plays an important role in inflammatory pain (Nassar et al., 2004). Nav 1.8 contributes to transmission of noxious heat and mechanical stimuli, and also contributes to cold pain sensitivity (Zimmermann et al., 2007).

Glutamate is the major excitatory neurotransmitter released by nociceptors at their terminals in the dorsal horn. However other transmitters are also present in nociceptors, allowing them to be classified neurochemically. Nociceptors can be divided into a subpopulation that contain peptides such as substance P and calcitonin gene related peptide (CGRP) and those that do not (Hunt and Rossi, 1985; Nagy and Hunt, 1982). Non-peptidergic C-fibres are associated with the epidermis of the skin whereas peptidergic C-fibres are associated with deeper parts of the skin as well as other tissues such as the joints and viscera (Todd, 2010). These non-peptidergic C-fibres can be

identified histochemically by their ability to bind isolectin B4 (IB4) (Plenderleith and Snow, 1993). Figure 1.1 summarises the mechanisms of noxious stimuli detection by nociceptors.

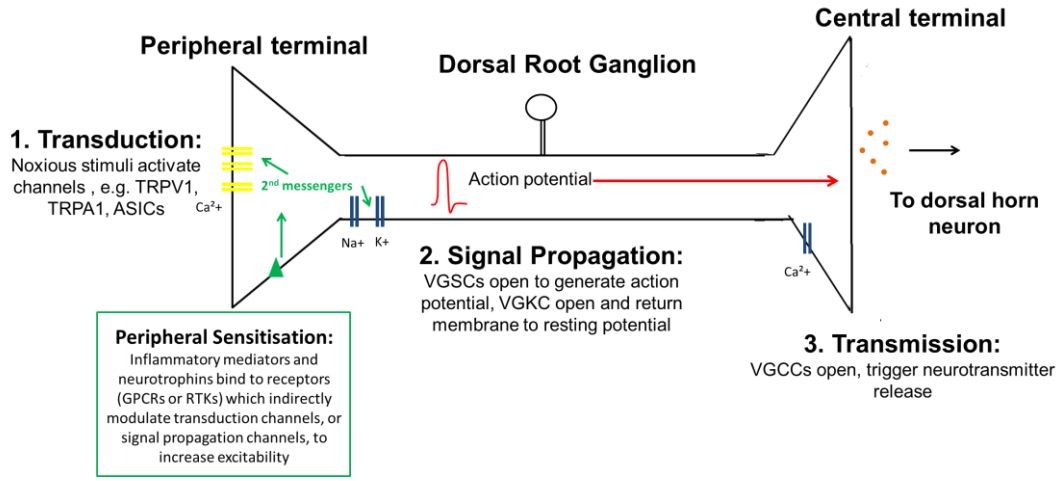

Figure 1.1 Detection of noxious stimuli by the nociceptor.

1). Specialised ion channels (noxious signal transducers) on the peripheral terminal of the nociceptor are activated by noxious stimuli, leading to the generation of a local potential. **2).** Action potentials are generated and propagated along the axon by voltage gated Na^+ channels and the membrane returns to resting potential via opening of voltage gated K^+ channels. **3).** Arrival of the action potential at the central terminal triggers influx of Ca^{2+} which leads to neurotransmitter release in the dorsal horn. The green box and arrows highlight the basic mechanisms of peripheral sensitisation (discussed below in section 1.4.1). Both the transducer channels and voltage gated Na^+ channels can be modulated by various peripheral mediators such as cytokines and neurotrophins via their target receptors (G protein-coupled receptors and receptor tyrosine kinases) on the peripheral terminals. Adapted from Raouf et al., 2010.

1.2.2 Dorsal horn of the spinal cord and projections to the brain

Primary afferent fibres terminate in the dorsal horn of the spinal cord, forming the first synapse of the pain pathway. Within the dorsal horn is a complex circuitry of excitatory and inhibitory interneurons which modulate the nociceptive signal before it is relayed to the brain. The gray matter of the spinal cord has a precise laminar organisation which was first described by Rexed (Rexed, 1952). Nociceptive fibres terminate in the outer laminae of

the dorsal horn, within lamina I and II. Peptidergic C-fibres terminate in both lamina I and IIo, while non-peptidergic C-fibres terminate mainly in lamina IIi. Non-nociceptive Aβ-fibres terminate in deeper layers, from lamina IIi– V (Todd, 2010, 2002). Figure 1.2 outlines the distribution of primary afferent terminals in the laminae of the dorsal horn.

Electrophysiological recordings can be used to classify dorsal horn neurons on the basis of their responses to peripheral stimulation. Proprioceptive dorsal horn neurons respond only to Aα-fibre input. Nociceptive specific (NS) neurons respond only to noxious stimulation and are found largely within lamina I and II. Wide dynamic range neurons (WDRs) can respond to all types of afferent input, both nociceptive and non-nociceptive. These are located in the deeper laminae of the dorsal horn (lamina V) (D'Mello and Dickenson, 2008). The majority of the neurons within the dorsal horn are locally projecting interneurons which play an important role in modulating the output of the dorsal horn in response to nociceptive input. Both inhibitory and excitatory interneurons are present, with GABA and glycine as the main inhibitory transmitters and glutamate as the main excitatory transmitter (Todd, 2010).

Projection neurons in the dorsal horn relay nociceptive information to the brain. These are located largely in lamina I (Spike et al., 2003). There are two main targets of the lamina I projection neurons. The lateral parabrachial area (PB) receives input from lamina I, and from here projects to brain areas responsible for the affective components of the pain experience such as the central nucleus of the amygdala and the hypothalamus (Gauriau and Bernard, 2002). The lateral thalamus (ventroposterior lateral nucleus, VPL, and ventroposterior medial nucleus, VPM) also receives input from lamina I and from there projects to areas such as the insular (IC) and somatosensory (SS) cortices, involved in the sensory-discriminative aspects of pain (Gauriau and Bernard, 2004). Other target structures of lamina I projection neurons

include the caudal ventrolateral medulla (CVLM), nucleus tractus solitarus (NTS) and periaqueductal gray (PAG) (Todd, 2010). Many lamina I projection neurons have collateral projections to more than one brain area (Al-Khater and Todd, 2009).

Some projection neurons are also found within the deeper laminae of III – V. The projections from the deeper laminae terminate in the medial thalamus (central lateral nucleus, CL), which projects to areas such as the anterior cingulate cortex (ACC) (Van der Werf et al., 2002). This pathway is implicated in the attentional and motivational aspects of the pain experience. Some deep projection neurons also terminate in the reticular nuclei, which may mediate motor responses associated with pain (Gauriau and Bernard, 2002). A summary of the main ascending projection pathways is shown below in figure 1.3. This figure indicates ascending pathways that have been characterised for the rat, and it is important to note that there may be some species differences in the relative importance of these pathways. For example, there are fewer direct projections from lamina I to the thalamus in the lumbar spinal cord segment in the rat (Al-Khater and Todd, 2009) than in the primate (Zhang and Craig, 1997), and the rat has greater numbers of projections to the PAG and Pb (Todd, 2010).

Many projection neurons express the neurokinin 1 (NK1) receptor, which binds substance P. These neurons are nociceptive specific (Salter and Henry, 1991). Depletion of these neurons selectively by the neurotoxin substance P-saporin prevents the development of behavioural hypersensitivity in models of inflammatory and neuropathic pain in the rat (Mantyh et al., 1997; Nichols et al., 1999). Furthermore it has been shown that these projection neurons are critical to the activation of descending controls in chronic pain states (Géranton et al., 2010; Suzuki et al., 2002).

Dorsal horn projection neurons allow the nociceptive signal to reach the brain, where pain is perceived. There are many brain areas activated during

acute noxious stimulation. Data from human brain imaging experiments during noxious stimulation has shown that some of the most common areas activated during painful stimulation are the primary and secondary somatosensory, insular, anterior cingulate, and prefrontal cortices and the thalamus (Apkarian et al., 2005). In addition to these core regions other areas are also activated, depending on the circumstances, including the amygdala, hippocampus, basal ganglia (Tracey and Mantyh, 2007). Importantly, there is no one brain area that is uniquely activated by painful stimulation, and indeed many of these brain areas have also been shown to be involved in the detection of non-noxious, novel sensory stimuli. Therefore these regions may not form a pain specific network, but rather function in the detection of any novel sensory information (Iannetti and Mouraux, 2010).

Figure 1.2 Termination of primary afferents in the dorsal horn.

Nociceptors innervate the periphery, and terminate in a structured manner in the dorsal horn of the spinal cord. Aδ-fibres terminate largely in lamina I and to a lesser extent in lamina II outer (IIo). Peptidergic C-fibres terminate in both lamina I and lamina IIo and non-peptidergic C-fibres terminate in lamina II inner (IIi). Non-nociceptive Aβ-fibres terminate in the deeper laminae (Iii to V), and Aδ hair-follicle fibres terminate on the border of lamina II-III. Image from Todd, 2010.

1.2.3 Descending modulation of pain

The relationship between nociceptive input and pain perception is not always linear. Under conditions of danger or stress, pain perception may be blunted, or completely abolished even under conditions of extensive noxious input (Fields, 2004). One example is that of injured soldiers in battle, many of whom do not report feelings of pain until some time after the injury (Melzack et al., 1982). Emotional state also has a large effect on pain perception, for example it is known that anxiety can increase pain perception (Ossipov et al., 2010). These examples demonstrate that

nociceptive signalling is subject to top-down modulation by the brain, and this provides a mechanism by which the brain can increase or decrease pain processing in the dorsal horn depending on the context.

Early evidence from animals to suggest the existence of a descending modulatory system came from studies of spinal cord transection. This procedure was found to increase nociceptive reflexes, suggesting the presence of a tonic descending inhibitory system (Sherrington, 1906). Later it was found that electrical stimulation of the periaqueductal gray (PAG) produced analgesia in the unanaesthetised animal (Reynolds, 1969) and transection of the spinal cord prevents the inhibitory effects of PAG stimulation (Basbaum et al., 1977). This endogenous descending inhibitory system is activated in situations of fear or stress when intensely noxious input does not produce pain (Siegfried et al., 1990; Terman et al., 1984). The PAG is an important site of action of many analgesic drugs such as opiates (Herz et al., 1970; Yaksh et al., 1976).

Information from the PAG is relayed indirectly to the dorsal horn via the rostral ventromedial medulla (RVM) to the dorsal horn (Ossipov et al., 2010). The RVM consist of two structures, the midline nucleus raphe magnus (NRM) and the more dorsal and lateral nucleus reticularis gigantocelluaris (GiA) (Fields and Heinricher, 1985). The RVM can exert both inhibitory and excitatory effects on spinal nociception. This bidirectional role of the RVM in pain processing can be explained in part by the heterogeneity of cells within the region. *In vivo* electrophysiological experiments have allowed for the classification of three cell types in the RVM depending on their firing properties immediately prior to the tail flick reflex in response to heat (Fields et al., 1983). ON cells show a brief burst in firing prior to the reflex, OFF cells show a decrease in firing and NEUTRAL cells show no alteration in their firing pattern. It has therefore been suggested that the ON cells are facilitatory and OFF cells are inhibitory in the modulation of the nociceptive reflex

(Heinricher et al., 2009). The role, if any, of NEUTRAL cells in the nociceptive reflex is unclear. However interestingly it has been suggested that these cells may change phenotype under certain conditions such as during an inflammatory pain state, becoming either ON-cells or OFF-cells (Miki et al., 2002). This suggests that cells defined as NEUTRAL during an acute nociceptive reflex in the naïve animal may contribute to descending modulation in chronic pain states.

The different RVM cell types also have different responses to morphine. OFF cells increase firing and ON cells decrease firing in response to morphine microinjection (Barbaro et al., 1986). Microinjection of morphine to the PAG, a region which has projections to the RVM and is an important site in morphine mediated analgesia, also led to an increase in OFF cell firing and a decrease in ON cell firing at the time of a nociceptive reflex. NEUTRAL cells did not change firing properties (Cheng et al., 1986).

Initially studies suggested that electrical stimulation of the RVM region always resulted in inhibition of spinal neuronal responses (Fields and Heinricher, 1989). Later it was demonstrated that electrical stimulation of the RVM could also lead to increased excitability of neurons in the dorsal horn (Light et al., 1986). This work highlighted the bidirectional nature of RVM modulation of nociception, with both inhibition and facilitation possible arising from the same site. It was found that low intensity stimulation of the RVM either electrically, of by administration of a low dose of glutamate has excitatory effects on spinal neurons, while higher intensity stimulation leads to inhibitory effects. This further illustrated that the RVM is capable of both inhibition and facilitation (Zhuo and Gebhart, 1992a, 1992b). This facilitation is also evident at the behavioural level as these procedures can enhance the tail flick reflex in the lightly anaesthetised animal (Zhuo and Gebhart, 1997). Therefore in the acute nociceptive reflex,

it is clear that both descending inhibition and facilitation are possible through the same brainstem region.

Importantly physiologically defined ON, OFF and NEUTRAL cell types cannot be separated anatomically within the RVM itself (Fields and Heinricher, 1985; Fields et al., 1983) and neurochemically it is not known which transmitters are involved in ON and OFF cell signalling. The RVM contains many 5-HT neurons and initially it was thought that only NEUTRAL cells contain 5-HT (Potrebic et al., 1994) however it has since been shown that a subset of all three physiologically defined cell types contain 5-HT (Marinelli et al., 2002). To date the role of RVM 5-HT in descending modulation remains controversial, but it now appears that 5-HT can play a pronociceptive or antinociceptive role in the dorsal horn, depending on the receptor subtype activated (Bardin, 2011).

GABA is another prominent transmitter in the RVM and these cells are also heterogeneous in their physiology (Kalyuzhny and Wessendorf, 1998). Although many RVM neurons project directly to the dorsal horn, some may also form local connections within the RVM region itself. In the case of OFF cells, these could form inhibitory projections onto projecting ON cells. For locally projecting ON cells, these could act to inhibit OFF cell output (Fields et al., 1991). In addition there are a number of spinally projecting GABAergic neurons within the RVM, and recently these have been shown to coexpress glycine, presumably forming an important inhibitory pathway to the dorsal horn (Hossaini et al., 2012).

Figure 1.3 Ascending and descending pathways.

Projection neurons are located in lamina I and laminae III-V of the dorsal horn. Lamina I projection neurons (shown in black) convey information to the lateral thalamic nuclei (including the ventroposterior medial nucleus (VPM) and ventroposterior lateral nucleus (VPL)), and from there to the insular (IC) and somatosensory cortices (SS). Lamina I

projection neurons also project to the lateral parabrachial nucleus (PB), and from there neurons project to limbic structures such as the central nucleus of the amygdala (Ce) and hypothalamus (VMH). Other structures targeted by the lamina I projection neurons are the caudal ventrolateral medulla (CVLM), nucleus tractus solitarus (NTS) and periaqueductal gray (PAG). Projection neurons from the deeper laminae III-V (shown in red) convey information primarily to the medial thalamus (CL, central lateral nucleus), and from there information is conveyed to cortical areas such as the anterior cingulate cortex (ACC). Descending modulation of pain is relayed from cortical areas such as the ACC, as well as limbic structures such as the Ce and VMH (shown in blue). This descending information is relayed to the PAG. The PAG does not project directly to the dorsal horn. Instead information is conveyed indirectly via the rostral ventromedial medulla (RVM). The numbers on the left hand side of the image indicate the approximate distance of the coronal section from Bregma (mm). Adapted from Todd 2010, and Paxinos and Watson, 1998. These pathways are based on data from the rat literature, and some species differences may exist in the ascending pathways of the rodent and the primate.

1.3 Animal models of pain

1.3.1 Measuring pain hypersensitivity in animals

To understand how animal models relate to human pain conditions, a behavioural outcome measure of the pain experience is needed. By definition pain is a subjective and individual experience. In studying pain in a human subject it is possible to ask questions about the pain to determine its severity however in animal models this is not possible. Therefore most studies using animal models do not measure pain directly, and instead use hypersensitivity to noxious stimuli as a surrogate measure of pain.

Pain hypersensitivity can be measured in animals by studying the spinal reflex withdrawal from a noxious stimulus (Mogil, 2009). A number of measures have been developed to address hypersensitivity to noxious thermal (Hargreaves et al., 1988), cold, chemical and mechanical (Chaplan et al., 1994) stimuli and to deep pressure (Randall and Selitto, 1957). Thermal sensitivity is measured using the Hargreaves apparatus, which involves placing the animal in a box with a plastic floor, and applying radiant heat to

the individual paws. The time taken to withdraw the paw is the latency and is the measure used to assess thermal sensitivity, the more time taken the less the sensitive the animal. Mechanical thresholds are widely studied using von Frey hairs. These are a set of graded plastic filaments with a blunt end, applied to skin until the filament bends. At this point a calibrated force is exerted. In most cases the hairs are applied from lowest to highest force, and the lowest force at which paw withdrawal is observed is deemed the paw withdrawal threshold.

Although difficult to measure, spontaneous pain is also important clinically and attempts are being made to address this in animal models. For example paradigms have been established to study tonic pain in animal models by using conditioned place preference with analgesic drugs (King et al., 2009; Sufka, 1994). Other attempts to measure spontaneous pain include monitoring innate behaviour such as vocalisation, scratching, biting and burrowing (Mogil, 2009), which may be altered when the animal is in pain. In addition attempts have been made to study comorbidities such as anxiety in animal models of pain, using paradigms that measure these complex behaviours such as the elevated plus maze and open field tests (Wallace et al., 2008). To date however measures of hypersensitivity using reflex withdrawal from a noxious stimulus remain the most widely used in pain research.

1.3.2 Inflammatory pain models

Tissue injury leads to an inflammatory response which aims to clear pathogens and aid repair of the damaged area. Inflammation also results in pain, which in some cases can persist beyond the time of healing. Common causes of inflammatory pain are surgical procedures, diseases of the joint and autoimmune disorders (Ren and Dubner, 2010). Various substances are used to model inflammation and pain in animals. Most commonly these are injected subcutaneously to induce localised inflammation and thermal and

mechanical hypersensitivity. Formalin injection can be considered a short term model of inflammatory pain (Dubuisson and Dennis, 1977). Longer lasting inflammatory compounds include carrageenan and Complete Freund's adjuvant (CFA), which are more useful in modelling long term aspects of inflammatory pain.

Clinically, joint inflammation is a leading cause of pain (Breivik et al., 2006) and a variety of methods are used to cause joint injury and inflammation in animals. Osteoarthritis is the most common cause of joint pain, and arises due to structural changes to the affected joint including loss of cartilage, synovial inflammation and destruction of the bone.
In animals this can be modelled by injection of monosodium iodoacetate (MIA) to the joint (Fernihough et al., 2004). This is a NADPH inhibitor, which inhibits chondrocyte metabolism and leads to rapid destruction of the joints, which mimics that seen in osteoarthritis patients. High doses of MIA may also induce some primary afferent injury, which could contribute to neuropathic-like symptoms in the animal (Thakur et al., 2012). An alternative surgical method of inducing OA in the animal is to destabilise the medial meniscus, a cartilaginous component of the knee joint, by transecting the medial meniscotibial ligament (Inglis et al., 2008).

Rheumatoid arthritis (RA) is an autoimmune disorder which causes inflammation of the joints, and is another common cause of pain (Lee et al., 2011a). RA can be modelled in animals by inducing systemic inflammation, for example by injecting CFA or a collagen and CFA emulsion into the tail (Clark et al., 2012; Neugebauer et al., 2007). This adjuvant-induced arthritis results in pathology at a number of joints, with an initial acute phase of inflammation up to 5d post injection, and a chronic phase which can last for weeks or months. At later stages joint destruction is observed which is similar to that seen in RA patients (Neugebauer et al., 2007). Adjuvant induced polyarthritis is used to model the chronic and systemic nature of RA

in humans and is helpful in the study of potential disease modifying or analgesic therapies (Neugebauer et al., 2007).

Importantly however systemic inflammation results in other adverse effects, such as skin lesions and weight loss, in addition to the joint pathology. This may affect the overall wellbeing of the animal, and confound the assessment of pain (Neugebauer et al., 2007). To address this problem, models of inflammatory monoarthritis have also been developed, including injection of CFA to the ankle joint (Butler et al., 1992). Although not a model of human RA per se, this method produces a reliable, localised inflammation of the ankle joint and results in stable behavioural hypersensitivity lasting up to 2 weeks post inflammation. It can be considered an experimental model of inflammatory joint pain, and has been useful in characterising sensitisation that occurs during prolonged nociceptive input from the joint. For example our group has previously characterised dorsal horn gene expression changes that occur in this model (Géranton et al., 2007).

Cutaneous inflammatory pain is often assessed by measuring thermal and mechanical hypersensitivity of the targeted hindpaw. In models of joint inflammation, it is more difficult to measure hypersensitivity of the affected area directly, however some measures such as withdrawal or vocalisation following compression of the joint have been developed (Neugebauer et al., 2007). Indirect measures of joint hypersensitivity are also widely used including weight bearing and gait analysis, which are disrupted following inflammation or injury to the joint (Neugebauer et al., 2007). In addition, many studies use thermal or mechanical hypersensitivity of the hindpaw of the affected limb as outcome measures in models of joint pain (Fernihough et al., 2004; Sagar et al., 2011; Thakur et al., 2012). As these measure cutaneous hypersensitivity away from the affected joint, it is considered to be a reflection of secondary hyperalgesia or allodynia (Neugebauer et al., 2007).

1.3.3 Primary and secondary hyperalgesia

There are two forms of stimulus evoked hypersensitivity described in humans. Allodynia is defined as pain due to a stimulus that does not normally provoke pain. Hyperalgesia is defined as increased pain from a stimulus that normally provokes pain. A distinction can be made between primary and secondary hyperalgesia. Primary hyperalgesia refers to increased pain sensitivity that occurs at the site of injury while secondary hyperalgesia occurs at sites adjacent to but not at the site of injury (Hardy et al., 1950; Treede et al., 1992). Importantly it has been demonstrated in human studies that primary hyperalgesia is associated with both thermal and mechanical modalities, while secondary hyperalgesia is only associated with mechanical hypersensitivity (Ilkjaer et al., 1996; Treede et al., 1992). Primary and secondary hyperalgesia are also believed to have different neurobiological mechanisms. Primary hyperalgesia is thought to be driven largely by peripheral sensitisation, whereas secondary hyperalgesia is driven by central sensitisation (Treede et al., 1992).

Although hyperalgesia is a term that can only be correctly used in human studies this distinction is important to consider when using animal models of pain hypersensitivity. In the context of joint inflammation, this suggests that sensitivity of the joint (primary hyperalgesia) is driven largely by peripheral mechanisms, while sensitivity of the ipsilateral hindpaw (secondary hyperalgesia) is driven largely by central mechanisms. In models of plantar inflammation however it is not clear if hindpaw sensitivity reflects primary or secondary hyperalgesia, and may be a combination of both.

1.4 Sensitisation in pain states

1.4.1 Peripheral sensitisation

Under normal circumstances, nociceptors respond only to high intensity stimulation. However in conditions of injury or inflammation nociceptor

sensitivity is increased such that normally innocuous stimuli produce pain and noxious stimuli produce a greater pain response. These changes are produced in part by sensitisation of the peripheral nociceptor, which refers to a decrease in threshold and increase in magnitude of response to noxious stimulation (Gold and Gebhart, 2010).

Tissue damage causes a local inflammatory response which leads to release of a variety of mediators from immune cells which can increase the sensitivity of the nociceptor terminals. These include GPCR activators (for example 5-HT, prostaglandins, and bradykinin), ion channel activators (ATP and H+), growth factors (NGF and GDNF) and cytokines (TNFα and interleukins) (Woolf and Ma, 2007). Peripheral sensitisation occurs by binding of these substances to their target receptors on the peripheral terminals and subsequent activation of intracellular signalling cascades that drive functional plasticity of the nociceptor (see figure 1.1). This allows the nociceptor to become sensitive to normally non-noxious stimuli as well as increasing the magnitude of responses to noxious stimuli.

There are a number of ways in which the excitability of the peripheral nociceptor terminal can be increased. One is via modulation of the sensory transducer molecules directly. Modifications which increase the numbers or availability of transducer molecules at the nociceptor terminal will increase the ability of the nociceptor to convert noxious stimuli to a pain signal. One established example of this is the increased expression of the TRPV1 channel at the nociceptor membrane during inflammation. TRPV1 is a transducer of noxious heat (Caterina et al., 1999). Growth factors such as NGF acting at receptors on the nociceptor terminals lead to the activation of intracellular signalling pathways which result in TRPV1 phosphorylation. This leads to increased trafficking of the channel and insertion to the membrane, therefore increasing nociceptor excitability (Zhang et al., 2005). Other inflammatory mediators, including bradykinin, PGE_2 and ATP, can also

contribute to increased TRVP1 phosphorylation. This provides a direct mechanism by which inflammatory mediators can increase transduction of a pain signal (Schaible et al., 2011).

Another mechanism by which nociceptor sensitivity can be increased in pain states is via the mediators of signal propagation. In the sensory axon these are primarily the voltage gated Na+ channels Nav1.7, Nav1.8 and Nav1.9. These channels are sensitised by exposure to inflammatory mediators including the cytokines TNF-α and IL-1β (Linley et al., 2010).

Direct modulation of ion channels explains the relatively rapid onset of sensitisation which occurs during acute injury and local inflammation. More long term changes in nociceptor function involve transcriptional changes, within the cell bodies of the DRG (Woolf and Costigan, 1999). Among the genes that are increased during inflammation include transducers such as TRPV1, and the peptides CGRP and substance P. In the non peptidergic, IB4 expressing population, other transcriptional changes occur such as upregulation of the protein Reg-2, a survival factor for motoneurons (Nishimune et al., 2000), following plantar inflammation (Averill et al., 2008).

Peripheral sensitisation is an important mechanism underlying nociception during acute tissue injury and inflammation, and indeed many common analgesics act through decreasing the availability of sensitising mediators at the peripheral terminal, for example the non-steroidal anti-inflammatory agents (NSAIDs) which inhibit the production of prostaglandins. However some aspects of chronic pain symptoms such as secondary hyperalgesia at non-injured sites cannot be accounted for by peripheral drive alone.

1.4.2 Central sensitisation

In addition to peripheral sensitisation it is known that plasticity within the dorsal horn can contribute to pain hypersensitivity. This was first demonstrated in animals by using repeated high intensity noxious input,

which was found to cause increased excitability of dorsal horn neurons which persisted even after the conditioning stimulus has ceased. This is termed central sensitisation (Woolf, 1983) and is a mechanism by which an initial noxious input can enhance later responses to further noxious stimulation. Central sensitisation also results in the ability of nociceptive dorsal horn neurons to be activated by low threshold stimuli that would not normally be able to do so, such as that from Aβ-fibres. Central sensitisation requires repeated activation of C-fibres and cannot be activated by Aδ nociceptors or Aβ-fibres. Following nerve injury or peripheral inflammation increased nociceptor input to the dorsal horn can also induce central sensitisation and it is now well established that central sensitisation is a common feature of models of chronic pain (Latremoliere and Woolf, 2009). Central sensitisation accounts for secondary hyperalgesia, which is pain beyond the site of injury (Woolf and Salter, 2000).

1.4.2.1 Mechanisms of central sensitisation

Since its discovery there have been many developments in understanding the molecular and cellular basis underlying central sensitisation. Increased neurotransmitter release by primary afferent fibres is a trigger for central sensitisation, and activation of the NMDA receptor is crucial to its induction (Woolf and Thompson, 1991). Under conditions of persistent noxious input the release of transmitters such as glutamate, substance P and CGRP occurs, and leads to depolarisation of the post-synaptic membrane and the removal of the Mg^{2+} ion block in the pore of the NMDA receptor (Mayer et al., 1984). This enhances the membrane depolarisation by glutamate, and allows rapid entry of Ca^{2+} to the post-synaptic neuron. Increased intracellular Ca^{2+} mediated by the NMDA receptor, as well as other mechanisms such as activation of Ca^{2+} permeable AMPA channels, voltage gated Ca^{2+} channels, and release from intracellular stores (Latremoliere and Woolf, 2009) is important in central sensitisation.

Elevated intracellular Ca^{2+} leads to the activation of Ca^{2+} dependent kinases, including protein kinase C (PKC) and calcium-calmodulin dependent protein kinase II (CaMKII) (Kuner, 2010). These kinases can influence neuronal excitability in a number of ways. One is by direct phosphorylation of ion channels, such as the NMDA and AMPA. This increases trafficking of the channels to the membrane and therefore increases postsynaptic excitability (Latremoliere and Woolf, 2009). Another aspect of Ca^{2+} mediated plasticity is the activation of the extracellular signal related kinase (ERK) cascade by upstream activation of PKA (Kawasaki et al., 2004). This leads to transcriptional changes downstream of ERK. Other enzymes activated by increased intracellular Ca^{2+} include cyclooxygenase 2 (COX-2) and neuronal nitric oxide synthase (nNOS). These produce prostaglandin E2 (PGE2) and nitric oxide, respectively, both of which contribute to increased excitability in the dorsal horn (Samad et al., 2001; Wu et al., 2001).

1.4.2.2 Contribution of non-neuronal cells to central sensitisation

Non-neuronal cells contribute to plasticity in a number of CNS structures (Ben Achour and Pascual, 2010), including the dorsal horn in chronic pain states. Microglia are the resident immune cells of the CNS and in the normal resting state are involved in surveillance of the environment. During CNS infection or trauma they become active (Aguzzi et al., 2013). This is reflected in morphological changes of the microglia and in the chemical mediators released. Among these mediators are neuroactive molecules such as glutamate, ATP, nitric oxide (NO), cytokines and chemokines, all of which may interact with dorsal horn neurons (Palygin et al., 2010). Microglial activation occurs following peripheral nerve injury. The injured afferents release the chemokines fractalkine (CX3CL1) and CCL2, which attract microglia to the dorsal horn. This contributes to increased dorsal horn excitability (Calvo et al., 2012). One of the established mechanisms by which microglia increase spinal excitability in neuropathic pain states is through

the release of BDNF, which activates TrkB receptors on neurons of the dorsal horn and disrupts chloride homeostasis, which reduces the inhibitory effects of GABA and glycine on these neurons (Coull et al., 2005). The release of cytokines such as IL-1β, IL-16 and TNF-α from microglia may also contribute directly to increased excitability in the dorsal horn (Kawasaki et al., 2008). Inhibition of microglial activation within the spinal cord by administration of agents such as minocycline has been shown to reverse behavioural hypersensitivity in models of neuropathic pain (Raghavendra et al., 2003). Although the contribution of microglia has been more widely examined in neuropathic pain states, studies have demonstrated that microglial activation also contributes to behavioural hypersensitivity in models of joint (Clark et al., 2012; Sagar et al., 2011; Shan et al., 2007), visceral (Cho et al., 2012) and inflammatory (Raghavendra et al., 2004) pain.

Astrocytes are another important cell type within the CNS, providing homeostatic support for neurons. Astrocytes are more abundant than microglia, and have structural connections with synapses and blood vessels. Astrocytes contribute to synaptic plasticity by releasing neuroactive substances and by taking in released neurotransmitters from the synapse (Barres, 2008). Astrocyte activation within the dorsal horn has been reported in a number of pain models, including neuropathic and inflammatory pain states (Gao et al., 2010). As with microglial activation, activated astrocytes produce pro-inflammatory cytokines, such as IL-1β, which may increase neuronal excitability. Interestingly astrocyte activation occurs later than microglial activation in models of neuropathic pain, suggesting that astrocytes may play a role in the maintenance of behavioural hypersensitivity (Gao and Ji, 2010).

1.4.3 Plasticity of descending controls

In addition to modulation by peripheral input, dorsal horn excitability is subject to descending modulation from the brain. As discussed above

(section 1.2.3) the RVM is the main relay site involved in conveying information from the brain to the spinal cord, and can have both inhibitory and facilitatory effects on spinal processing of acute nociception (Ossipov et al., 2010). In models of persistent pain however evidence suggests that a shift towards increased descending facilitation occurs, contributing to increased behavioural responses (Pertovaara, 2000; Vanegas and Schaible, 2004).

1.4.3.1 Sensitisation of RVM neurons in models of pain

Although not as extensively studied as central sensitisation within the spinal cord, a number of studies have demonstrated that RVM neurons alter their firing properties during chronic pain. In models of neuropathic pain, both ON and OFF cells in the RVM become responsive to normally innocuous stimuli, and develop longer responses to noxious stimuli prior to the tail flick reflex (Carlson et al., 2007; Gonçalves et al., 2007). Similar changes in RVM neuron physiology have been reported in a model of cutaneous inflammation (Kincaid et al., 2006) and in visceral pain (Sanoja et al., 2010). These studies suggest that as with neurons in the dorsal horn, RVM neurons can be sensitised in persistent pain models, and this may contribute to behavioural sensitivity.

1.4.3.2 Behavioural studies following RVM lesion

The role of the RVM in behavioural hypersensitivity in chronic pain models has also been studied using a number of approaches. For example, in a model of opioid-withdrawal induced hypersensitivity the behavioural response was found to be attenuated by RVM microinjection of lidocaine suggesting that in this model, suggesting descending facilitation contributes to behavioural hypersensitivity (Kaplan and Fields, 1991). Injection of lidocaine to the RVM also attenuated mechanical hypersensitivity in rats with neuropathic pain (Pertovaara et al., 1996).

Spinalisation of an animal removes descending modulation, and this technique has been used to investigate the role of descending modulation in a number of pain models. This manipulation attenuates secondary hyperalgesia associated with mustard oil application to the skin (Mansikka and Pertovaara, 1997). In the carrageenan model of inflammation, and the spinal nerve ligation model of neuropathy, spinalisation has also been shown to attenuate mechanical hypersensitivity (Kauppila et al., 1998).

Other studies addressing the role of descending facilitation in behavioural hypersensitivity have used an electrolytic lesion to non-selectively destroy neurons of the RVM region. In one such study cutaneous application of mustard oil, which normally results in a robust secondary hyperalgesia of the surrounding region, had a lesser effect in animals with prior lesion of the region (Urban et al., 1996). Silencing of the RVM has also been shown to prevent mechanical hyperalgesia associated with muscle injection of hypotonic saline, a model strongly associated with central sensitisation (Tillu et al., 2008).

While much information on the role of the RVM has been elucidated from such studies, the complicated heterogeneous nature of the region requires a more selective approach to address individual components of the system. One method of achieving this is to selectively target cells based on receptor expression. The ON cell population are believed to be the only RVM neurons which respond directly to morphine, and therefore express the mu opioid receptor (Heinricher et al., 1994; Marinelli et al., 2002). This characteristic has been exploited by using a toxin which targets cells expressing the mu opioid receptor (MOR+ cells). Saporin is a cytotoxin which needs to be internalised in order to have its effects. Conjugating saporin to an agonist for a particular receptor allows it to be taken in to those cells expressing the receptor and results in cell death within that population. Dermorphin-saporin, which selectively ablates MOR+ neurons, has been used within the

RVM to characterise the role of these cells in chronic pain states. It has been shown repeatedly that these cells are required for the maintenance of mechanical hypersensitivity in models of neuropathic pain, but not in the induction phase (Bee and Dickenson, 2008; Burgess et al., 2002; Porreca et al., 2001; Zhang et al., 2009). This indicates a crucial role for descending facilitation in the maintenance of neuropathic pain. These cells have also been shown to contribute to visceral pain behaviour (Sikandar et al., 2012; Vera-Portocarrero et al., 2006)

An alternative strategy to study the role of a particular subset of RVM neurons in a chronic pain state is to address the role of a particular neurotransmitter. 5-HT has been the most widely studied in this regard. The RVM is the major source of 5-HT within the dorsal horn (Kwiat and Basbaum, 1992), and 5-HT can have either inhibitory or facilitatory effects on spinal processing of pain, depending on the receptor type activated (Bardin, 2011). The ionotropic 5-HT_3 receptor is the most widely implicated in mediating the pro-nociceptive actions of 5-HT in the dorsal horn (Millan, 2002). Lesion of the descending 5-HT pathway by the selective toxin 5,7-dihydroxtryptamine has been used to demonstrate a facilitatory role for this system in pain behaviour following both neuropathic injury (Rahman et al., 2006) and cutaneous inflammation (Géranton et al., 2008). Recently, silencing of the tryptophan hydroxylase (TPH) enzyme (responsible for 5-HT synthesis) within the RVM has confirmed the facilitatory role of descending 5-HT in these pain states (Wei et al., 2010).

1.4.3.3 Molecular changes in the RVM

In addition to behavioural evidence for alterations in RVM activity, molecular changes have also been shown to occur in persistent pain states. For example, upregulation of NMDA receptor gene expression (Miki et al., 2002), and AMPA receptor expression (Guan et al., 2003) and phosphorylation (Guan et al., 2004) has been shown to occur following

peripheral inflammation. Recently it has been demonstrated that a pentraxin protein, involved in recruiting AMPA receptors to the synapse, is upregulated in the RVM during neuropathic pain and contributes to hyperalgesia (Zapata et al., 2012). These molecular changes in the RVM during peripheral inflammation may contribute to enhanced excitability in the region, and in some ways mimic aspects of dorsal horn changes that occur in chronic pain states (Latremoliere and Woolf, 2009).

1.4.3.4 The role of immune cells in the RVM

As with central sensitisation in the dorsal horn, it has recently emerged that glial cells within the RVM may contribute to behavioural hypersensitivity in neuropathic pain. Activation of microglia occurs within days, and a more prolonged activation of astrocytes occurs in the later phases. Using selective inhibitors of microglia and astrocytes within the RVM regions, it has been demonstrated that microglia contribute to hypersensitivity in the early induction phase, and astrocytes contribute to the maintenance of the pain state (Wei et al., 2008). Microglia are also activated in the RVM after plantar inflammation, and local inhibition of microglia in the region attenuates behavioural hypersensitivity (Roberts et al., 2009).

1.4.3.5 The role of the RVM in primary and secondary hyperalgesia

It has been argued that the RVM plays different roles in primary and secondary hyperalgesia. This is most apparent in models of cutaneous and joint inflammation (Vanegas and Schaible, 2004; Vanegas, 2004). For example initial evidence suggested that in cutaneous inflammation increased descending inhibition from the RVM occurs, which suppresses central sensitisation. This was shown by measuring thermal hypersensitivity following plantar injection of CFA in animals with prior lesion of the dorsolateral funiculus, the main pathway from the RVM to the dorsal horn (Ren and Dubner, 1996). A later study addressed both primary and secondary hyperalgesia following cutaneous inflammation. Secondary

hyperalgesia was assessed by measuring thermal sensitivity of the hindpaw following knee injection of carrageenan or application of mustard oil to the skin, while primary hyperalgesia was assessed by injection of carrageenan to the hindpaw. This study illustrated that lesion of the RVM by ibotenic acid resulted in attenuation of secondary thermal hyperalgesia, but not primary thermal hyperalgesia (Urban et al., 1999). These studies suggest descending modulation of secondary hyperalgesia is facilitatory, while descending inhibition may predominate in primary hyperalgesia. Notably however these studies used thermal hyperalgesia as an outcome measure, and as discussed in section 1.3.3, secondary hyperalgesia is not generally thought to be associated with thermal sensitivity (Treede et al., 1992).

1.5 Joint Pain

1.5.1 Clinical features of joint pain

Among the most common causes of pain in the general population is that arising from the joints (Breivik et al., 2006). The term arthritis refers to inflammatory diseases of the joint, and there are many forms and causes (Kidd et al., 2007). Pain of the affected joint and surrounding areas is a common feature to all arthritic diseases. Osteoarthritis (OA) is a leading cause of chronic pain and disability particularly among the elderly (Bennell et al., 2012). This is caused by structural changes to the affected joint including loss of cartilage, synovial inflammation and destruction of the bone. Interestingly the extent of joint destruction is not always correlated with the degree of pain in OA (Bedson and Croft, 2008). In addition joint replacement, which is a common procedure in patients with advanced OA, is not always successful in the relief of pain. Severe persistent pain after joint replacement is reported to be a problem in 15% of patients (Wylde et al., 2011). Together these observations suggest that although joint destruction and inflammation are the initial cause of pain in OA, chronic pain may be due in part to changes within the nociceptive system.

Rheumatoid arthritis (RA) is another common cause of pain affecting about 1% of the general population (Lee and Weinblatt, 2001). It differs from OA in that patients have systemic inflammation due to autoimmune processes, rather than physical destruction of the joint (Lee et al., 2011a). Although less common than OA, RA generally has an earlier age of onset and therefore can have a greater impact on quality of life for the patient. As with OA, pain associated with RA is not always directly correlated to the extent of joint pathology, as many patients have persistent pain despite treatment with disease-modifying, anti-inflammatory agents (Wolfe and Michaud, 2007). In addition it is known that patients have increased pain sensitivity at sites away from the inflamed joints (Edwards et al., 2009). Application of capsaicin to the skin results in mechanical hyperalgesia in normal individuals, and in patients with RA this effect is more pronounced. This reflects increased central sensitisation within the dorsal horn of these patients (Kidd et al., 2007; Morris et al., 1997) and implies central sensitisation may be an important component of chronic pain in joint diseases (Lee et al., 2011a).

1.5.2 Differences in joint and cutaneous pain processing

It has long been noted that pain from the deep tissue and viscera tends to be more dull and aching, rather than sharp, and poorly localised in comparison to cutaneous pain (Lewis, 1938; Schaible et al., 2009). This suggests that there are differences in the processing of nociceptive information from the skin and the joints. As in cutaneous tissue joints are innervated by Aβ-, Aδ- and C-fibres, however there are some differences in their roles within the joint. In cutaneous tissue activation of Aβ-fibres relays the sensation of innocuous pressure, but this does not occur in the joint under normal circumstances. Indeed the only sensations known to arise from the healthy joint occur in response to noxious input for example following a twisted ankle (Schaible et al., 2009). Increased pressure in the

joint capsule during inflammation is one mechanism by which nociceptors are activated during arthritis.

Another difference between cutaneous and joint innervation is the unique localisation of C-fibre low threshold mechanoreceptors in the cutaneous tissue, and not in other tissues such as the joint. In the human these have been shown to play a role in pleasant touch (Löken et al., 2009). These cutaneous fibres can be identified in the rodent by their expression of the vesicular glutamate transporter VGLUT3, and they contribute to the development of mechanical hypersensitivity to previously innocuous stimuli, following inflammation and nerve injury (Seal et al., 2009).

The content of the C-fibres also differs between cutaneous tissue and the joint. In the skin, both peptidergic and non-peptidergic fibres are present. In the joints there is no evidence of a non-peptidergic C-fibre population, identified by IB4 labelling (Ivanavicius et al., 2004; Jimenez-Andrade et al., 2010; Nakajima et al., 2008). Recently it has been demonstrated that cutaneous C-fibres expressing the G-protein coupled receptor Mgrpd, which correspond to the IB4+ (non-peptidergic) population, are required for the development of cutaneous mechanical hyperalgesia in the mouse (Cavanaugh et al., 2009). However, the bone and joints are sensitive to noxious mechanical stimulation, despite the absence of these non-peptidergic C-fibres. This indicates that mechanical hypersensitivity in the joint may be mediated solely by the peptidergic population, unlike cutaneous inflammation (Jimenez-Andrade et al., 2010). Interestingly this implies that treatments targeting the peptidergic population of afferents may be more effective in joint pain than cutaneous pain, and highlights the importance of studying the joint as a separate entity to the skin (Jimenez-Andrade et al., 2010).

IB4+ C-fibres terminate largely within lamina II of the dorsal horn (Hunt and Mantyh, 2001; Zylka et al., 2005). In contrast, it is known that joint fibres

terminate preferentially in lamina I (Doyle and Hunt, 1999; Mense and Prabhakar, 1986; Neugebauer et al., 1994). Therefore joint and cutaneous nociceptors have different patterns of termination in the dorsal horn, which suggests that cutaneous nociceptors are better able to induce changes in excitability of lamina II dorsal horn neurons, than those from the joint. Lamina II consists of interneurons, which modulate nociceptive input (Todd, 2010). The absence of significant input from the joint to lamina II may lead to reduced recruitment of these interneurons in joint pain states.

1.5.3 Peripheral sensitisation during joint inflammation

As discussed in section 1.3.2, a variety of animal models of joint pain have been developed which address aspects of OA and RA. Models of inflammatory monoarthritis have also been very useful in establishing the basic mechanisms of peripheral and central sensitisation following joint inflammation (Neugebauer et al., 2007). During joint inflammation, sensitisation of the primary afferents occurs. Aβ-fibres show an increase in responses to mechanical stimulation of the knee, which may result from swelling and increased pressure within the joint (Schaible and Schmidt, 1988). Low threshold Aδ-fibres have increased responses to both noxious and innocuous mechanical stimulation, and high threshold Aδ- and C-fibre nociceptors develop a lower threshold of activation (Guilbaud et al., 1985). Joint inflammation also leads to activation of 'silent nociceptors', C-fibres which do not respond to noxious stimulation under normal circumstances (Schaible and Grubb, 1993). Increased spontaneous firing of nociceptors has also been shown to occur which may contribute to spontaneous pain at rest during joint inflammation (Schaible and Schmidt, 1988).

In arthritic disorders inflammation of the joint is the source of pain and therefore peripheral sensitisation plays an important role in these conditions. The dominant feature of joint pain is mechanical hyperalgesia, which contrasts with cutaneous inflammation in which thermal hyperalgesia

is more prominent. Although extensive work has been carried out regarding the mechanisms of peripheral sensitisation in cutaneous nociceptors, including the contribution of TRPV1 sensitisation to thermal hyperalgesia (Woolf and Ma, 2007), less is known regarding the molecular mechanisms of sensitisation of the joint afferents. Some of the modulators proposed include prostaglandins, bradykinin, and 5-HT suggesting that peripheral sensitisation in joint afferents may share at least some of the same mediators as cutaneous inflammation (Gold and Gebhart, 2010)

Immune cell infiltration to the joint is a key feature of RA, and these act as a source of inflammatory mediators. In addition to contributing to the pathogenesis of the disease state, these mediators can act directly on joint afferents to induce sensitisation. DRG neurons express the IL-6 receptor (Obreja et al., 2005; von Banchet et al., 2005) and intra-articular injection of Il-6 increases C-fibre responses to noxious mechanical stimuli (Brenn et al., 2007). Another cytokine implicated in joint afferent sensitisation is tumour necrosis factor alpha (TNF-α). TNF-α is important in regulating B and T cell infiltration in RA, however it also acts as a mediator of peripheral sensitisation. Primary afferents express the TNF-α receptor, and direct injection of TNF-α injection to the joint increases afferent excitability (Boettger et al., 2008; Sommer and Kress, 2004). Administration of a TNF-α neutralising antibody in animal models of RA had both disease-modifying and analgesic effects (Boettger et al., 2008; Inglis et al., 2007). The humanised anti-TNFα antibody Etanercept is now widely used in the treatment of RA to reduce the inflammatory component of the disease. These recent discoveries suggest that the benefits of these drugs may be due in part to direct inhibition of peripheral sensitisation at the nociceptor.

1.5.4 Central sensitisation during joint inflammation

As described above central sensitisation is an important factor in chronic pain following nerve injury and cutaneous inflammation (Latremoliere and

Woolf, 2009). Increased excitability also contributes to hyperalgesia in animal models of joint pain. Following joint inflammation, dorsal horn neurons shown an increased responsiveness to noxious and non-noxious stimuli (Grubb et al., 1993; Neugebauer et al., 1993; Schaible et al., 1987). Behaviourally, in the MIA model of knee OA, mechanical hypersensitivity of the ipsilateral hindpaw develops which is indicative of central sensitisation (Fernihough et al., 2004). Interestingly it has been suggested that primary afferents from deep tissue such as the joints and muscle are better able to induce central sensitisation than those from cutaneous tissue (Sluka, 2002; Woolf and Wall, 1986). This implies that pain in arthritis is heavily dependent on dorsal horn adaptations however less is known about the mechanisms underlying central sensitisation following in joint pain than in neuropathic and cutaneous conditions.

Many mechanisms are likely to be common to neuropathic and cutaneous injury. For example increased release of glutamate (Sluka and Westlund, 1992), activation of NMDA receptors (Neugebauer et al., 1993) and metabotropic glutamate receptors (Zhang et al., 2002) are required for central sensitisation following joint injury. Increased release of peptides by primary afferents (Naeini et al., 2005; Neugebauer et al., 1994), activation of voltage gated calcium channels (Neugebauer et al., 1996) and production of prostaglandins (Bär et al., 2004) have also been implicated. Protective mechanisms may also be in place, as it has been demonstrated that the induction of OA increases expression of endocannabinoids in the dorsal horn, which may serve to counteract increased spinal excitability in arthritis (Sagar et al., 2010).

Activation of dorsal horn immune cells is also important in central sensitisation in joint pain. Inhibition of microglial activation attenuates behavioural hypersensitivity in the MIA model of OA (Sagar et al., 2011). Similarly the collagen-CFA induced model of RA is associated with increased

microglial and astrocytic activation in the dorsal horn, and inhibition of fractalkine signalling attenuates mechanical hypersensitivity of the hindpaw (Clark et al., 2012).

1.5.5 Molecular changes in the dorsal horn during joint inflammation

As in other forms of long term plasticity (Bailey et al., 1996) changes in dorsal horn gene expression are important in central sensitisation (Kim et al., 1998). Gene expression changes in the dorsal horn have been characterised at various time points following ankle joint inflammation using microarray analysis (Géranton et al., 2007a). This study revealed that upregulation of a number of genes occurs in the acute stage of inflammatory pain (up to 24h post inflammation). In contrast at a later time point (7d), when mechanical hypersensitivity is still present, downregulation of a separate set of genes was observed. This suggests that different programs of gene expression mediate the development and maintenance of inflammatory joint pain (Géranton et al., 2007). The transcriptional repressor MeCP2 was found to play a role in mediating some of these early gene changes. Phosphorylation of MeCP2 relieves its repression of target genes and accordingly it was shown that phosphorylation of MeCP2 goes up in the early time points after inflammatory insults, enhancing activation of its target genes. Recently it has also been shown that upregulation of MeCP2 levels occurs in the maintenance phase following ankle joint inflammation which would be reflected by a decrease in expression of MeCP2 target genes (Tochiki et al., 2012). Interestingly the opposite occurs in neuropathic injury in which downregulation of MeCP2 occurs, which would cause upregulation of target genes. This study suggests that the dorsal horn gene expression programs involved in joint and neuropathic pain are different.

1.5.6 Descending modulation in joint pain

Increased descending inhibition has been demonstrated following joint inflammation. Spinalisation of the animal results in increased responses of

dorsal horn neurons to noxious stimulation of knee joint afferents, and this is more pronounced in animals with prior inflammation (Cervero et al., 1991; Schaible et al., 1991) suggesting that tonic inhibition from supraspinal regions is increased in the acute phase of joint inflammation (1-3h). However similar experiments in a model of ankle joint inflammation indicated that this increased inhibition of spinal excitability occurs only in the acute and not in the chronic phase of inflammation (Danziger et al., 2001).

Descending facilitation has been shown to be an important factor in a number of animal models of chronic pain (Ossipov et al., 2010). Descending facilitation via the RVM is required for the maintenance phase of neuropathic pain behaviour (Bee and Dickenson, 2008; Porreca et al., 2001; Rahman et al., 2009). Behavioural hypersensitivity following cutaneous inflammation is also enhanced by descending facilitation via the RVM (Géranton et al., 2008; Wei et al., 2010), as is that arising from muscle injury (Tillu et al., 2008). Less is known regarding descending facilitation via the RVM in animal models of joint pain. One electrophysiological study has demonstrated that descending 5-HT has contributes to enhanced spinal excitability in the MIA model of osteoarthritis (Rahman et al., 2009), but to date no behavioural studies have investigated the role of descending facilitation in animal models of joint pain.

1.6 Hypotheses

The RVM is an important site in the relay of descending information from the brain to the spinal cord. The aim of this thesis was to investigate the role of descending facilitation in a rat model of inflammatory joint pain. My experiments were designed to test the following hypotheses:

- RVM neurons are activated following ankle injection of CFA, which may be reflected in increased ERK phosphorylation and decreased GABAergic inhibition.
- Descending facilitation contributes to behavioural hypersensitivity associated with ankle joint inflammation, via both 5-HT and mu opioid receptor expressing neurons of the RVM.
- Gene expression changes within the dorsal horn following joint inflammation are regulated in part by descending facilitation.

2. Methods

This chapter describes methods used in more than one chapter of this thesis, with specific experimental details provided in the individual chapters. Techniques used only in one chapter are described in the methods section of that chapter.

2.1 Animals and surgical procedures

2.1.1 Animals

All studies presented in this thesis were carried out using male Sprague-Dawley rats which were bred and supplied by the Biological Services Unit at University College London. Rats were housed in cages in groups of 1 – 4 animals with a 12h light dark cycle (lights on at 8.00am). Access to food and water was *ad libitum*. Animals weighed between 180-250g at the start of the experiment, depending on the protocol. For the intrathecal injection experiments described in chapter 4, rats weighed 180-200g at the time of injection. For intra-RVM injections, described in chapter 3 and chapter 5, animals weighed 200-250g at the time of injection to ensure accuracy of the stereotaxic coordinates based on the rat brain atlas (George Paxinos, 1998). In all other experiments animals weighing 200-250g at the induction of the pain state were used.

2.1.2 Microinjection to the RVM

Isoflurane anaesthesia (5% for induction and 1.5-2% for maintenance combined with 100% O_2 (1l/min)) was used during the surgical procedures. Animals were secured using in a stereotaxic frame (Kopf instruments) and anaesthesia maintained via a facemask. The head was shaved and sterilised using 70% EtOH. A skin incision was made from the front to the back of the head and the skull was exposed. A dental drill was used to form a single hole at the site of microinjections. For the dermorphin-saporin lesion experiment

(chapter 5), two microinjections were carried out using a 5µl Hamilton syringe with 30 gauge needle at the following coordinates: anterior-posterior -10.5mm from Bregma, lateral: ± 0.6mm, and dorso-ventral -9mm from the surface of the brain. The toxin was dispensed slowly over the course of 5 minutes and the needle was held in place for 1 min after the injection to minimise the back flow of toxin. The needle was then removed gradually. VGAT-C antibody injections (chapter 3) were carried as above but only one lateral injection was made, on the left hand side of the animal. Following RVM microinjections the skin covering the skull was sutured using 5-0 Mersilk. Local anaesthetic cream (EMLA) was applied to the wound to reduce irritation. Following surgery animals were observed closely for weight loss, neurological impairments or general distress.

2.2 Inflammatory pain model and behavioural testing

2.2.1 Model of ankle joint inflammation

Joint inflammation was carried out using a modified version of the protocol first described by Butler et al. (Butler et al., 1992). Although not a direct model of human rheumatoid arthritis, as it does not involve systemic inflammation, this method produces a reliable, localised inflammation of the ankle joint. This results in stable behavioural hypersensitivity which mimics many aspects of joint pain and localised tenderness in RA patients (Neugebauer et al., 2007).

Inflammation of the left ankle joint was carried out by injection of 10µl of Complete Freund's adjuvant (CFA, Sigma) while the animals were under isoflurane anaesthesia (see above, section 2.1.2). The skin covering the area was sterilised, and the foot was flexed to allow access the joint capsule. A disposable needle on a 100µl Hamilton syringe was inserted to the inta-articular space. The needle was pushed until a loss of resistance was felt

and CFA was then injected. Sham animals were exposed to the same anaesthesia as the CFA treated group but received no injection.

Following CFA injection, the ankle became swollen and red. CFA treated rats were less mobile, with a visible reduction in weight bearing on the affected paw. These symptoms began within hours, and consistently peaked in severity at day 1 post injection. By day 7, some resolution of the swelling, redness and reduced weight bearing was observed. The adjacent cutaneous tissue of the hindpaw also became red and swollen, however this was less severe than in the immediate vicinity of the ankle joint. Signs of the cutaneous inflammation also resolved more rapidly, by day 1 post injection. The quantity of CFA used in the experiments described in this thesis is considerably lower than the 50µl used by others (for example, Uematsu et al., 2011; Yao et al., 2011) and as expected produced milder symptoms of inflammation which resolved more rapidly than described by these investigators. In all behavioural experiments, peak mechanical hypersensitivity of the ipsilateral hindpaw was reached by 6h post injection. By the 24h time point, a stable level of hypersensitivity was reached which was maintained for up 7 days post CFA injection.

2.2.2 Measuring mechanical paw withdrawal thresholds

On the day of testing, animals were transported to the testing room in their home cages, and placed in clear plastic containers on a wire mesh floor. The animals were allowed to settle for a minimum of 15min prior to testing. Habituation to the testing environment was achieved by taking a series of baseline measures, once daily for at least 3 days, prior to the initial experimental manipulation.

The mechanical paw withdrawal threshold was obtained for the ipsilateral and contralateral hindpaw of the animal. A series of calibrated von Frey hairs were applied to the centre of plantar surface of the hindpaw, between the footpads. The hairs were applied in ascending order, with 0.07g as the

minimum and 60g as the maximum cut off points. Each von Frey hair was applied until bending occurred. The hair was held in place for approximately 4s. For each hair the stimulus was applied five times at 5s intervals. The paw withdrawal threshold was defined as the lowest weight von Frey hair at which a brisk withdrawal was observed at least once out of the five repeated stimuli. When a withdrawal response was observed to a given hair, no further hairs were applied.

Both the ipsilateral and contralateral hindpaw thresholds were measured for each animal. The ipsilateral paw withdrawal thresholds for each animal were obtained first, followed by repetition of the procedure on the contralateral paw. Testing was carried out blind to treatment, except in pilot experiments (ondansetron experiment, figure 4.4 and dermorphin-saporin experiments 1 and 2, figures 5.2 and 5.4).

This method of analysis of manual von Frey thresholds has been described by our group and others previously for use in models of neuropathic pain (Bourquin et al., 2006; Géranton et al., 2009; Obara et al., 2011). Another widely used approach is the up-down method (Chaplan et al., 1994). This is used to calculate the 50% paw withdrawal threshold, a value which indicates the von Frey hair weight at which a brisk withdrawal response would be expected to occur 50% of the time (Mills et al., 2012). This method involves the sequential application of the von Frey hairs, in either ascending or descending order depending on whether a negative or positive response is obtained to the first hair applied. This up-down procedure is carried out at least 4 times following the first change in response, and so requires repeated withdrawals by the animal. In the ankle joint inflammatory model, obtaining repeated brisk withdrawals can be difficult on the ipsilateral hindpaw. In some instances the animal will produce a brisk withdrawal only once. This may be due to the pain within the joint itself, which would be exacerbated by the repeated withdrawal of the hindpaw. For this reason,

the up-down method of analysis was not deemed suitable for our study. Another alternative method is the use of electronic von-Frey apparatus, which has been used previously with this pain model (Géranton et al., 2007). However as with the up-down method this requires repeated withdrawals which can be difficult to obtain due to the ankle joint inflammation.

2.2.3 Statistical analysis of behavioural data

For all behavioural experiments data was analysed using SPSS (PASW) 18 (IBM). Logarithmic transformation (log2) was carried out on the paw withdrawal thresholds (g) before statistical analysis as Levene's test for equality of variance was significant (Bourquin et al., 2006; Géranton et al., 2009). Appendix A3 includes a table listing paw withdrawal threshold values in grams and corresponding log2 transformed values.

Analysis of variance (ANOVA) with repeated measures was used for all time course experiments. To proceed to further post hoc testing at least one main effect (CFA treatment or drug/toxin manipulation) or interaction was required to be statistically significant ($p < 0.05$). Post hoc analysis varied depending on the nature of the comparisons. Where appropriate a subsequent two-way ANOVA with repeated measures was carried out to determine if there was an overall effect of CFA or drug/toxin across a specific time window. Where this was not possible one-way ANOVA with LSD or Bonferroni post hoc test was carried out at individual time points.

2.3 Tissue collection

2.3.1 Perfusion

At the end of behavioural testing, animals for perfusion were deeply anaesthetised with pentobarbital (Euthatal, 0.5 – 1ml per animal, i.p.) and the ribs were sectioned to allow access the heart. A small incision was made in the left ventricle. A cannula, attached to a pump, was connected and

inserted into the ventricle and up through the aorta. This was held in place with a clamp, and saline containing 5000 IU/ml heparin was pumped through the animal at a rate of 30ml per min, for 4min. This was followed by 4% paraformaldehyde (PFA) in 0.1M phosphate buffer for 8min. Brains and spinal cords were dissected and post fixed in 4% PFA for 2 h. Tissue was then cryoprotected in 30% sucrose (in 0.1M PB) and stored at 4°C until sectioning.

2.3.2 Fresh tissue

To obtain fresh tissue for western blot and RNA analysis, animals were culled by CO_2 asphyxiation. Rats were placed in a chamber with a slow steady flow of CO_2 to allow the concentration to rise slowly. When the rat had stopped breathing, death was confirmed by cervical dislocation. The spinal cord segment corresponding to the lumbar L4-L6 region was rapidly dissected on ice, and the ipsilateral and contralateral quadrants of the dorsal horn separated using a blade. These were frozen rapidly on dry ice. Samples were stored at -80°C until further use for protein or RNA extraction.

2.4 Immunohistochemistry

Immunohistochemistry was carried out to enable visualisation of specific target antigens within fixed tissue. This process involves application of a primary antibody which has been generated to target the antigen of interest followed by detection by a secondary antibody. In this thesis three different detection methods were used: direct fluorescence labelling, tyramide signal amplification and fluorescence labelling, or avidin-biotin chromogenic labelling. An overview of the process involved in these three types of detection is given below, in figure 2.1. The details of primary antibodies used are given in the individual chapters. Details of laboratory solutions used in immunohistochemistry protocols are given in appendix A1.

2.4.1 Sectioning

40µm sections were obtained for the brainstem or spinal cord using a freezing microtome (Leica). These sections were stored in 5% sucrose (in 0.1M PB) at 4°C until staining was carried out. Tissue was sectioned in series across 4 or 6 wells on a plate depending on the experiment (see individual chapters). All immunohistochemistry was carried out on freely floating sections, in 1ml tubes placed on a rocker.

2.4.2 Direct fluorescence immunohistochemistry

To begin immunohistochemistry, the sections were transferred from 5% sucrose to 0.1M PB using a small paintbrush. The PB was removed and sections were blocked for one hour in 1ml 0.1MPB, 30µl serum (Goat, Chicken or Horse, depending on the host of the primary antibody, Vector) and 30ul 10% Triton X (Sigma). The blocking solution was removed with a pipette and the sections were incubated with the primary antibody diluted as required in Tris-Triton buffered saline (TTBS , 30ml 10% Triton, 50ml Tris Solution and 8g NaCl in 920ml 0.1M PB) overnight at room temperature. Following primary antibody incubation, and between additions of all other reagents, the sections were washed three times for ten minutes in 0.1MPB. The sections were incubated in the dark with the appropriate secondary Alexa Fluor antibody (Invitrogen) for 2h. Sections were mounted on gelatin coated slides in 0.1MPB, followed by drying at room temperature and coverslipping with fluoromount (Sigma), or used for detection of a second antigen.

2.4.3 Tyramide signal amplification fluorescence immunohistochemistry

Sections were blocked and incubated with the primary antibody as above. The appropriate biotinylated secondary antibody (Vector, 1:400) was added for 90min. The secondary antibody was removed sections washed. An avidin-biotinylated horseradish peroxidase solution was prepared using the

Vectastain Elite ABC kit using 4ul solution A (avidin)+ 4ul solution B (horseradish peroxidase) (Vector) in 1ml TTBS and allowed to conjugate for at least 30min. This solution was added to the sections for 30mins followed by washing. 13.3µl of biotinylated tyramide in 1ml diluent (Perkin Elmer) was prepared and added to the sections for exactly 7min. The reaction was stopped rapidly by saturating with 0.1MPB and two washes followed. Sections were then incubated in the dark with fluorescein (FITC) conjugated avidin D (1:600, Vector), or cyanine 3 conjugated Streptavidin (Cy3, 1:4000, Jackson Laboratories) in TTBS for 2h or used for detection of a second antigen.

2.4.4 Chromogenic immunohistochemistry

Sections were blocked as described above, with the addition of 2% H_2O_2 to the blocking solution. Incubation with primary antibody was as described above. Biotinylated secondary antibody was added for 2h at a concentration of 1:500. An avidin-biotinylated horseradish peroxidase solution was prepared using the Vectastain Elite ABC kit using 1ul solution A (avidin) + 1ul solution B (horseradish peroxidase) (Vector) in 1ml TTBS was prepared and allowed to conjugate for at least 30min. Sections were incubated in this solution, following washes, for 1h. Sections were washed, and then the chromogenic substrate was developed using a 3,3'-diaminobenzidine (DAB) substrate kit (Vector). DAB is a chromogenic electron donor, which produces a brown colour in the presence of H_2O_2 and the enzyme horseradish peroxidase (HRP). A solution containing DAB, H_2O_2 and the buffer (supplied in the kit) was prepared. pERK labelled sections were incubated in this solution for 7min, and the reaction was stopped rapidly by transferring sections into fresh wells containing distilled H_2O. Sections were then placed in 0.01M PB solution, and mounted on gelatin coated slides. These were left to dry at room temperature overnight, before dehydration in EtOH of decreasing increasing strength (10s in distilled H_2O, followed by 70% EtOH

for 1min, 95% EtOH for 1min, 100% EtOH for 1min), followed by placing in Histoclear (2 x 1min, National Diagnostics) and application of DPX mounting medium (VWR laboratories) and coverslipping.

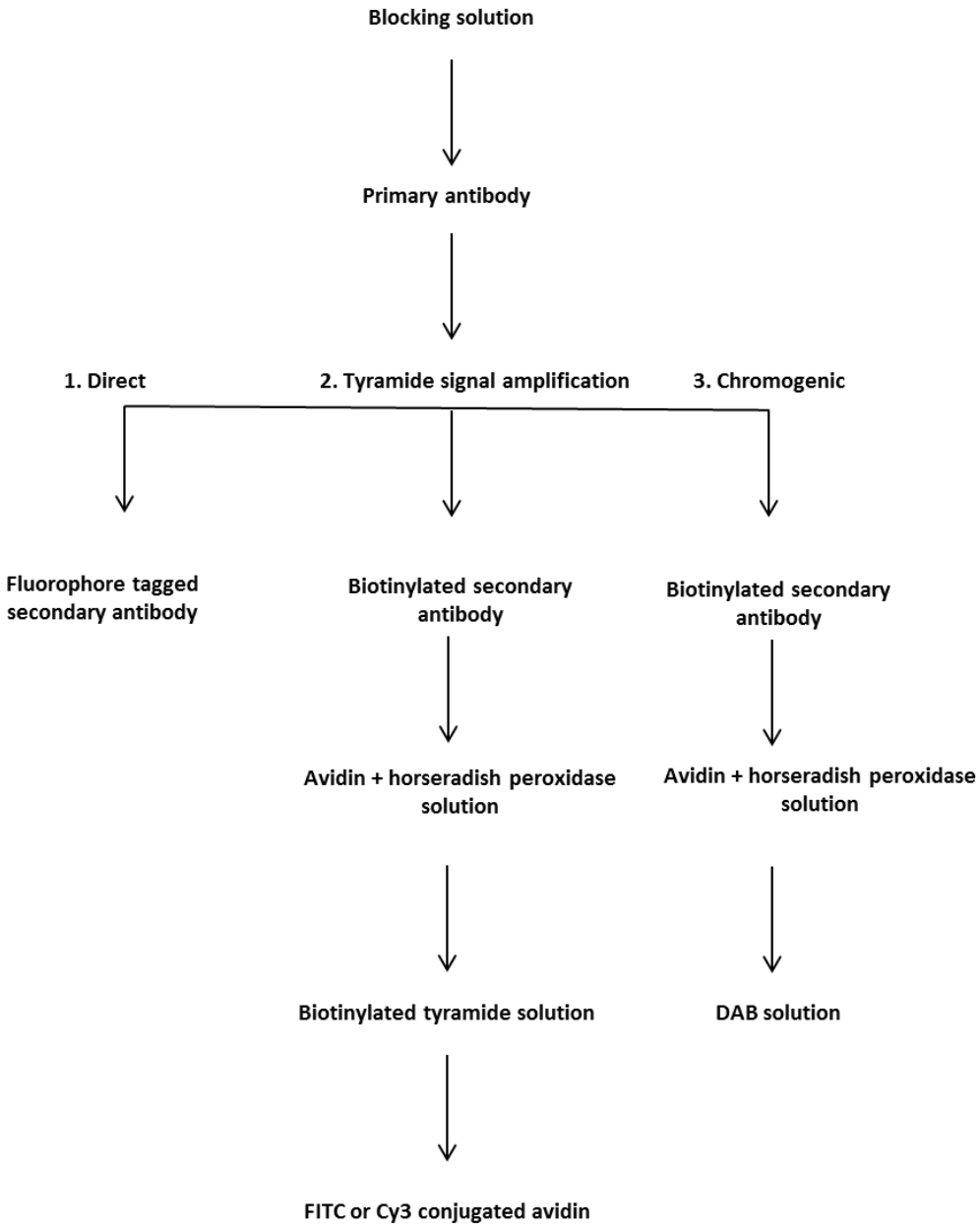

Figure 2.1 Immunohistochemistry detection methods.

2.4.5 Controls for antibody specificity

Control tubes of sections were prepared to ensure there was no non-specific binding of the antibodies. Control tubes were processed in parallel with the

experimental tubes, and underwent all steps of the staining protocol, except at the control step. At this point the tissue was placed in TTBS lacking the appropriate antibody. Four types of control were carried out, lacking either the first primary antibody, the first secondary antibody, the second primary antibody (for double labelling experiments) or the second secondary antibody (also for double labelling experiments).

2.4.6 Fluorescence and chromogenic imaging

Fluorescence labelled sections were viewed using a Leica DMR microscope (Leica Microsystems) and fluorescently tagged antigens were viewed using the appropriate excitation filter from a 50 W mercury lamp. Images were acquired using a Hamamatsu CCD digital camera (C5985, Hammamatsu Photonics) using Openlab 4.0.4 software (Improvision). Confocal imaging was carried out when required for double labelling studies using a laser scanning Leica TCS NT SP microscope (see below section 2.4.6).

Chromogenically labelled sections were viewed using bright-field conditions on a Nikon Eclispe E800 microscope (Nikon) and images acquired using a Nikon Coolpix 4500 digital camera (Nikon).

2.4.7 Confocal microscopy

A laser scanning confocal microscope (Leica TCS SPE) was used to acquire images of fluorescence immunohistochemistry with double labelling. Sequential laser channel acquisition was used to prevent bleed through. The z-plane thickness was 0.5-0.7µm. Following acquisition, the series of z-plane images was viewed using Leica LAS lite software to determine if colabelling of the two channels could be observed. Where confocal images are presented in this thesis, they indicate single z-planes from each channel, and a merged image of both channels.

2.4.8 Photoshop and image presentation

Images were prepared for presentation using Adobe Photoshop CS4 software (Adobe Systems). The only adjustments made were the individual curves for each colour channel, to improve the clarity of the image. Image sizes were adjusted as necessary while maintaining the original ratio of dimensions.

2.4.9 Cell counts and statistical analysis

Positively labelled neurons in the RVM were counted manually, using a Nikon Eclispe E800 microscope for DAB immunoreactivity, and Leica DMR microscope for fluorescence immunoreactivity. The RVM was defined by the boundaries of the NRM and GiA, from approximately -10.3mm to -11.3mm from Bregma, according to the rat brain atlas (George Paxinos, 1998). Counts were carried out while blind to treatment group. All sections per animal were counted, and the top 5 scoring RVM sections per animal were used for analysis. These were summed to generate a total number of positive cells per animal, and data is plotted as the mean ± SEM per group.

Statistical analysis was carried out in SPSS. Two-way analysis of variance was used when comparing two variables (e.g. CFA treatment, and time point). A significant main effect or interaction of the variables was a prerequisite for subsequent one-way ANOVA, or post hoc testing as appropriate. In cases in which there was only one variable but more than one group, one-way ANOVA with LSD or Bonferroni post hoc testing was used. In cases where only two groups were compared, independent samples t-tests were used.

3. Increased ERK activation and decreased GABAergic signalling in the RVM following joint inflammation

3.1 Introduction

Changes in neuronal activity in the rostral ventromedial medulla (RVM) has been demonstrated in a number of models of cutaneous inflammation and neuropathic injury (Géranton et al., 2010; Imbe et al., 2005; Terayama et al., 2000). These changes are believed to correlate with increased descending facilitation from the RVM and contribute to behavioural hypersensitivity in these pain states (Porreca et al., 2001; Wei et al., 2010). This chapter describes two experiments which aimed to determine if the RVM is activated following joint inflammation.

3.1.1 Phosphorylation of extracellular signal related kinase (ERK): a marker of neuronal activity

The mitogen activated protein kinase (MAPK) cascades are signalling pathways which convey information from cell surface receptors to intracellular compartments and lead to changes in gene transcription and protein translation. One example of a mammalian MAPK cascade is the extracellular signal related kinase (ERK) cascade, which plays a role in cell growth, differentiation and survival as well as in neuronal activation and plasticity (Impey et al., 1999; Sweatt, 2004). A well characterised role of the ERK signalling pathway is in growth factor signalling (Widmann et al., 1999). Binding of growth factors to their corresponding receptor tyrosine kinases leads to activation of the canonical ERK signalling cascade, resulting in the phosphorylation of ERK on threonine 202 and tyrosine 204 residues (see figure 3.1).

There are three levels of kinases involved in this cascade. The small GTP-ase Ras phosphorylates the MAPK kinase kinase (MAPKK) Raf, followed by activation of the MAPK kinase (MAPKK) MEK, which phosphorylates ERK. This sequential activation of multiple kinases allows for interaction with other signalling pathways, in addition to the activation of growth factor receptors (see figure 3.1). Within the CNS many different intracellular signalling mechanisms can converge upon ERK activation, including Ca^{2+} influx which activates protein kinase C (PKC), and increased cAMP levels which activates protein kinase A (PKA) (Ji et al., 2009). Phosphorylated ERK (pERK) then phosphorylates and activates downstream protein targets. Short term responses mediated by ERK include the phosphorylation of cell surface receptors and channels, leading to increased neuronal excitability. Long term cellular effects mediated by ERK include the activation of transcription factors such as CREB, or components of the translational machinery such as MNK (Impey et al., 1999)

Figure 3.1 The ERK pathway.

The classical mitogen activated protein kinase (MAPK) pathway involves activation of a cell surface receptor, followed by sequential activation of a MAPK kinase kinase kinase (MAPKKK), MAPK kinase kinase (MEKK), and MAPK kinase (MAPKK). This general pathway is outlined in red. One well studied example of a MAPK pathway is the activation of growth factor receptors, which leads to activation of the MAPPKKK Ras, the MEKK Raf, the MAPKK MEK, and ERK (outlined in blue). Other intracellular signalling pathways can also converge on this pathway, for example Ca^{2+} influx can trigger the protein kinase C (PKC) – ERK pathway, and cAMP can trigger the protein kinase A (PKA) – ERK pathway. Adapted from Ji et al. 1999.

In the CNS, ERK activation is as a hallmark of neuronal activation and plasticity. Activation of ERK occurs in the hippocampus in a variety of learning and memory tasks, and inhibition of ERK activation can prevent memory formation (Impey et al., 1999). ERK activation also occurs within the CNS during nociceptive processing. Following noxious stimulation ERK is

activated within dorsal horn neurons. This has been demonstrated in a number of models of peripheral inflammation, including plantar injection of the irritant capsaicin (Ji et al., 1999) and Complete Freund's adjuvant (CFA) (Ji et al., 2002). Movement of an inflamed joint can also induce ERK activation in the dorsal horn (Cruz et al., 2005). Activation of ERK in dorsal horn neurons correlates with pain in these models, as inhibition of ERK phosphorylation by intrathecal administration of a MEK inhibitor attenuates behavioural hypersensitivity (Cruz et al., 2005; Ji et al., 1999).

3.1.2 ERK activation in the RVM

pERK has also been used as a marker of neuronal activation in the RVM in a number of pain models. Intraplantar injection of CFA leads to increased ERK phosphorylation in the RVM which peaks at 7h post CFA injection, but remains elevated for 1d. Approximately 60% of the pERK neurons contained 5-HT, as indicated by colabelling with tryptophan hydroxylase (TPH), the enzyme responsible for 5-HT synthesis (Imbe et al., 2005). Administration of an ERK inhibitor to the RVM attenuated thermal hyperalgesia in this model (Imbe et al., 2008). In a model of neuropathic pain ERK activation also occurs, largely within 5-HT neurons, with 60% of pERK+ neurons expressing TPH (Géranton et al., 2010). These studies suggest that ERK activation in the 5-HT population of RVM neurons correlates with the development of behavioural hypersensitivity following cutaneous inflammation or nerve injury.

3.1.3 GABAergic signalling in the RVM

GABA is the other major neurotransmitter found in RVM neurons, and GABA containing neurons are distinct from those expressing 5-HT (Jones et al., 1991; Reichling and Basbaum, 1990). Recently it has been demonstrated that 45% of retrogradely labelled spinally projecting RVM neurons are GABAergic (Hossaini et al., 2012) indicating a direct inhibitory role for these neurons within the dorsal horn. However these projection neurons

represent a relatively small proportion of the GABA containing neurons within the RVM overall, and it is thought that the majority of GABAergic neurons in the region act as local inhibitory interneurons (Jones et al., 1991). In support of this many spinally projecting RVM neurons have GABAergic synaptic input (Jones et al., 1991) and most of these GABAergic terminals arise from intrinsic RVM neurons with little input from other brain regions (Cho and Basbaum, 1991). GABAergic inhibition of RVM projection neurons is therefore likely to play an important role in modulating output during nociception.

Injection of $GABA_A$ receptor antagonists to the RVM has an antinociceptive effect, while the injection of $GABA_A$ agonists is pronociceptive (Gilbert and Franklin, 2001; Heinricher and Kaplan, 1991). In addition, the analgesic effects of morphine are thought to occur at least in part by direct inhibition of GABAergic neurons in the RVM (Pan et al., 1997). This indicates that in the normal animal, the net effect of GABAergic signalling within the RVM is to enhance acute nociception.

3.1.4 Changes in GABAergic transmission associated with persistent pain

It has been proposed that during persistent pain states changes to neurotransmitter synthesis and release may occur in a maladaptive manner. Recently it has been shown that inhibitory GABAergic signalling in the amygdala is decreased early in the induction of the kaolin-carrageenan model of arthritis (Ren and Neugebauer, 2010). Within the RVM changes to GABAergic transmission have also been reported. A decrease in presynaptic GABA release was found within the RVM at 3 days following plantar injection of CFA, but not at earlier stages (Zhang et al., 2011). In addition microinjection of the $GABA_A$ agonist muscimol, which in the naive animal has a pronociceptive effect, led to attenuation of thermal hyperalgesia in the inflammatory pain state. These authors also described studies indicating that epigenetic suppression of the *Gad65* gene (which encodes the enzyme

responsible for GABA synthesis) by decreased histone acetylation at the promoter region, could underlie these changes (Zhang et al., 2011). This study provides important evidence that GABA synthesis and release may be altered within the RVM during inflammation, and could contribute to the enhancement of descending facilitation observed in these conditions. Therefore in addition to increased activation of 5-HT neurons, decreased GABAergic signalling may be an important mechanism underlying descending facilitation in persistent pain states.

3.1.5 Hypothesis

In this chapter I have tested two hypotheses concerned with the activation of the RVM following ankle inflammation:

- That ERK phosphorylation, a widely used marker of neuronal activation, is increased in RVM neurons following ankle injection of CFA.
- That Inhibitory GABAergic transmission within the RVM is decreased following ankle injection of CFA.

3.2 Methods

3.2.1 pERK expression in the RVM

3.2.1.1 Immunohistochemistry

Animals were divided into two groups, receiving either CFA injection (10µl) to the left ankle or undergoing a sham procedure (see section 2.1.1). These were then subdivided into groups and perfused at one of three time points, at 6h, 3d or 7d following CFA injection. 40µm sections were taken in series across four wells therefore sections in each well were at least 160µm apart. Two wells were used for each animal to carry out separate pERK immunohistochemistry protocols. 3,-3'diaminobenzidine (DAB) detection

was carried out to quantify pERK+ cell numbers in the RVM. Fluorescence immunohistochemistry with tyramide signal amplification was carried out for colabelling of pERK and tryptophan hydroxylase, a marker of 5-HT expressing neurons (see section 2.4 for full immunohistochemistry methods). Controls were included to ensure that the secondary antibodies were specific to their primary antibody targets. This was carried out by removing either the pERK primary antibody or the TPH primary antibody from the procedure, to ensure no non-specific labelling by the secondary antibodies. Table 3.1 lists the antibodies and detection methods used in this chapter.

3.2.1.2 Cell counting and image acquisition

Cells expressing pERK were counted manually using a Leica bright field microscope. Counts were carried out while blind to the treatment (CFA or sham) for that animal. For counting, the RVM was defined as the regions containing the NRM and GiA at approximately -10.3 to -11.3 mm from Bregma. Sections were deemed caudal of the RVM if the nucleus ambiguus was present (-11.6mm from Bregma). The number of pERK positive cell bodies per section was recorded. The five sections with the highest number of pERK+ neurons per animal were used for analysis. The total number of pERK+ cells across the five sections was calculated and the data is presented as the mean ± SEM per group. Representative images of DAB staining were acquired using a Nikon E4500 MDC digital camera.

Fluorescence immunohistochemistry was used to quantify the number of pERK+ neurons colabelled with tryptophan hydroxylase (TPH) at the 6h time point. Slides were viewed using a Leica DMR immunofluorescence microscope. The total number of pERK labelled neurons and double labelled neurons were recorded for each section. The five sections with the highest number of pERK+ neurons per animal were used for analysis. The numbers of pERK+/TPH+, pERK+/TPH- and total pERK+ neurons, and percentage of

pERK+/TPH+ cells as a proportion of total pERK+ cells was calculated for each animal (n = 3 - 4). Data is presented as the mean ± SEM per group. Representative images of fluorescence staining at 6h post CFA were captured using a Hamamatsu digital camera and using Openlab 4.0.4 software from Improvision.

3.2.2 Labelling of GABAergic synapses *in vivo*

3.2.2.1 Microinjection of a luminal domain specific VGAT antibody to the RVM

To label active GABAergic synapses *in vivo*, a rabbit polyclonal antibody raised against the luminal domain (C terminus) of the vesicular GABA transporter (VGAT) (from Synaptic Systems) was microinjected to the RVM. The VGAT transporter is expressed in all synaptic vesicles at GABAergic synapses however the luminal domain is only exposed to the cell surface during synaptic release and vesicle recycling. Therefore when applied extracellularly the VGAT-C specific antibody is incorporated only into active synapses (see figure 3.2). This antibody has been used by others to label active GABAergic synapses in the hippocampus (Martens et al., 2008). The same technique was used here to label GABAergic synapses in the RVM in naive, CFA or sham treated animals.

Microinjection was carried out as described in section 2.1.2, with a single unilateral injection of antibody (1.5µg in 1.5µl) made to the left side of the RVM (+0.6mm laterally). This concentration was chosen based on previous published work within the hippocampus, which described the use of 4µg/2µl injections to the hippocampi (Martens et al., 2008). An initial pilot experiment was carried out in naïve animals, and following confirmation of injection site and antibody specificity animals were microinjected at 3d following CFA or sham treatment.

Animals were perfused 24h after the microinjection. 40µm sections were taken in series across six wells therefore sections in each well were at least 240µm apart. Although the VGAT-C antibody is tagged with a fluorescent label (Oyster-550) the raw signal was found to be weak, and fluorescence immunohistochemistry using tyramide signal amplification with Cy3 as fluorophore was carried out to detect the VGAT-C antibody within the tissue (see section 2.4 for immunohistochemistry methods). Double labelling with glutamate decarboxylase (GAD65/67), the enzyme responsible for GABA synthesis at synapses, was also carried out to identify GABAergic terminals. Controls were carried out to ensure that the detection of GAD65/67 was not affecting the VGAT-C signal, by removing the GAD65/67 primary antibody.

Figure 3.2 Labelling of active GABAergic synapses.

This schematic outlines the structure of the VGAT transporter, with N-terminus located in the cytoplasm, a number of transmembrane segments and the C-terminus located inside the lumen of the synaptic vesicle. At the inactive GABAergic synapse, the C-terminus of the VGAT transporter is located inside the lumen of the synaptic vesicle and not accessible to the VGAT-C specific antibody. During active synaptic release and vesicle recycling the lumen of the vesicle is exposed extracellularly and accessible to the VGAT-C specific antibody. Adapted from Martens et al., 2008.

3.2.2.2 Imaging and analysis

Confirmation of injection site and the spread of the antibody in naive animals was carried out using a Leica DMR immunofluorescence microscope. For quantification of VGAT-C and GAD65/67 labelling, sequential images of the green and red channels were obtained using a Leica SPE confocal microscope, with a step size of approximately 0.5µm. Images were captured contralateral to the microinjection, immediately above the pyramidal tracts, and next to midline (see figure 3.5). All sections used for analysis were within the region of -10.8mm to -11mm from Bregma.

The image analysis program Fiji (an open source image processing package based on ImageJ, with plugins included) was used to quantify the extent of VGAT-C and GAD65/67 double labelled punctae in these sections. Manual thresholding was carried out to define VGAT-C and GAD65/67 labelled punctae for each animal, across the entire z stack of images. Thresholding was carried out while blind to treatment group of the section. Three sections were analysed per animal with the same threshold settings used for each section in that animal. Particle analysis was used to count the number of defined red punctae (VGAT-C) and green punctae (GAD65/67) throughout the z-stack of images. The image calculator function was then used to create an overlay of the two thresholded channels followed by the particle analysis function which allowed the quantification of VGAT-C and GAD65/67 colabelled punctae per stack. The number of colabelled punctae was expressed as a percentage of total GAD65/67 to control for the number of GABAergic synapses. Data is presented as mean ± SEM of all 9 sections imaged per treatment group.

Antigen	Host	Company	Concentration	Method	Fluorophore
pERK	Rabbit	Cell Signalling	1:250	TSA	FITC
pERK	Rabbit	Cell Signalling	1:500	DAB	Brown DAB
TPH	Mouse	Sigma	1:200	Direct	Alexa 594
GAD65/67	Rabbit	Millipore	1:1000	Direct	Alexa 488
VGAT-C	Rabbit	Synaptic systems	1.5µg in 1.5µl	TSA	Cy3

Table 3.1 Primary antibodies, concentrations and detection methods.

3.3 Results

3.3.1 ERK activation in the RVM: general observations

To determine the effect of ankle inflammation on ERK activation within the RVM rats were divided into groups and perfused at three time points following CFA or sham treatment. pERK DAB immunohistochemistry was

performed on 40µm RVM sections. The RVM was defined as consisting of the nucleus raphe magnus (NRM) and nucleus gigantocelluaris pars alpha (GiA) (figure 3.3a). In all groups, including shams, a high number of pERK positive (pERK+) neurons were observed. These were distributed mainly in the NRM and in the ventrolateral regions of the GiA (figure 3.3). Examples of pERK+ cells from the GiA and NRM are shown in figure 3.3b. Very few cells were identified in the more dorsal regions of the GiA. All sections falling within the rostral-caudal distribution of the RVM (approximately – 10.3 to -11.3mm from Bregma) were counted, however for analysis only the five sections with the highest number of pERK+ cells per animal were used. Positive cells were counted based on cell body labelling however extensive dendritic pERK immunoreactivity was also observed (figure 3.3b).

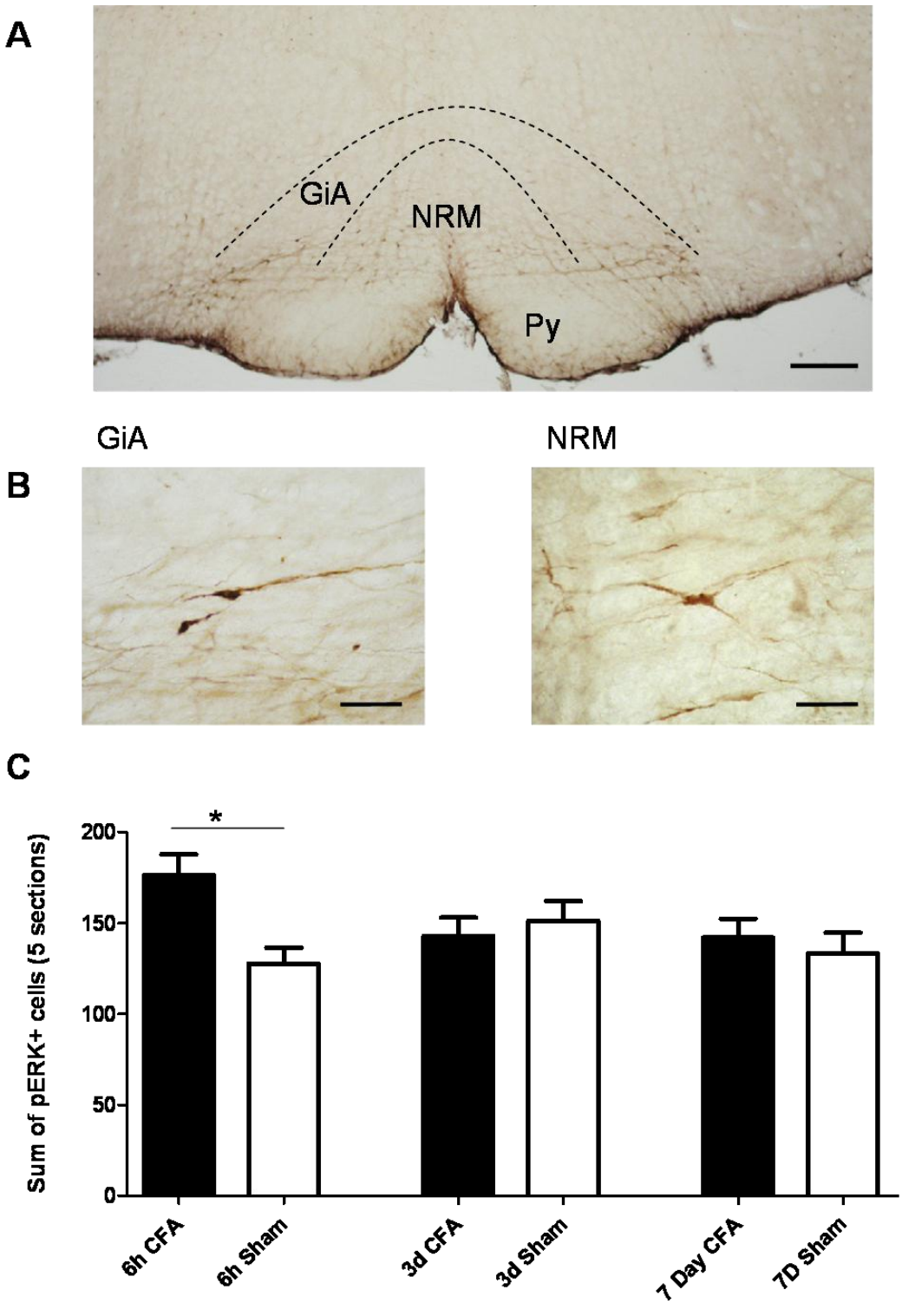

Figure 3.3 Increase in pERK+ neurons at 6h post CFA.

A). Representative section of the RVM corresponding to approximately -11mm from Bregma. The boundaries of the nucleus raphe magnus (NRM) and nucleus reticularis

gigantocelluaris pars alpha (GiA) are outlined by the dashed lines. The pyramidal tracts (Py) are also shown. Scale bar indicates 250µm. **B).** Examples of pERK+ cells from the lateral GiA and midline NRM. Intense labelling of both cell bodies and dendrites was observed. Scale bars indicate 100µm. **C).** Numbers of pERK+ neurons in the RVM region at 6h, 3d and 7d following ankle injection of CFA (black bars) or sham treatment (white bars). Counts for the top 5 pERK+ RVM sections were summed and are presented as mean ± SEM. n = 3 – 8, * $p < 0.05$, two-way ANOVA and Bonferroni post hoc test.

3.3.2 Increase in ERK phosphorylation in the RVM at 6h post CFA injection

The number of pERK+ neurons in CFA and sham treated animals at all three time points were compared (figure 3.3c). For each animal the five sections with the highest number of pERK+ neurons were summed to give a total number of pERK+ neurons per animal (n = 3 – 8 per group). Two-way analysis of variance (ANOVA) was carried out on the cell counts with treatment (CFA or sham) and time point (6h, 3d and 7d post CFA) as the between-subjects factors. There was no main effect of time or treatment ($p > 0.1$) however there was a significant time x treatment interaction ($p = 0.029$). A subsequent one-way ANOVA indicated there was an overall difference between all 6 groups ($p = 0.027$) and Bonferroni post-hoc analysis indicated the variation was due to a significant increase in pERK labelling in the CFA group compared to sham at 6h post injection ($p = 0.018$). The mean number of pERK+ neurons in the 6h CFA group was 176.4 ± 10.8 compared with 127.7 ± 8.3 in the 6h sham group, an increase of approximately 38%. No significant differences were found between CFA and sham groups at 3d or 7d ($p > 0.1$).

3.3.3 Proportion of pERK+ neurons double labelled with tryptophan hydroxylase

To characterise the population of pERK+ RVM neurons double fluorescence immunohistochemistry was carried out to determine the proportion of pERK+ neurons which colabelled with tryptophan hydroxylase (TPH), a

marker of 5-HT neurons, at 6h post CFA injection (figure 3.4a). Cell counts were carried out as for the DAB experiment, however in this case the number of pERK+ neurons double labelling with TPH (pERK+/TPH+) and not double labelling with TPH (pERK+/TPH-) were also recorded (n = 3 – 4). A high proportion of pERK+ neurons colabelled with TPH in (84.6% ± 5 in the CFA group, and 78% ± 2.8 in the sham group) however there was no significant increase in the percentage of pERK neurons expressing TPH in the CFA treated group and sham animals (p = 0.2743, independent samples t-test).

Nonetheless, by comparing the numbers of pERK+/TPH+ and pERK+/TPH- neurons, it was found that there was a significant increase in the number of pERK+/TPH+ double labelled neurons (p = 0.0309) and an overall increase in total pERK+ labelled neurons (p = 0.0082) at 6h post CFA injection (independent samples t-tests). No significant increase in the number of pERK+/TPH- neurons was found. This indicates that the increase pERK expression occurs within the TPH+ population of the RVM (figure 3.4b). Table 3.2 gives the numbers of pERK+/TPH+, pERK+/TPH- and total pERK+ neurons at 6h post CFA.

	CFA	**Sham**	**p value**
pERK+/TPH+	131 ± 15.3	83 ± 8.3	0.0309
pERK+/TPH-	23 ± 7	22.8 ± 2	0.9703
pERK+ total	154 ± 9.6	105.8 ± 6.7	0.0082
% pERK+/TPH+ over total pERK+	84.6 ± 5	78 ± 2.8	0.2743

Table 3.2 Numbers of pERK+/TPH+ neurons at 6h post CFA.

The number of pERK+/TPH+ double labelled neurons, pERK+/TPH- neurons and total pERK+ neurons are shown, along with the percentage of pERK+/TPH+ double labelled neurons over total pERK+ neurons. The p values for independent samples t-tests between CFA (n = 3) and sham (n = 4) groups are also shown.

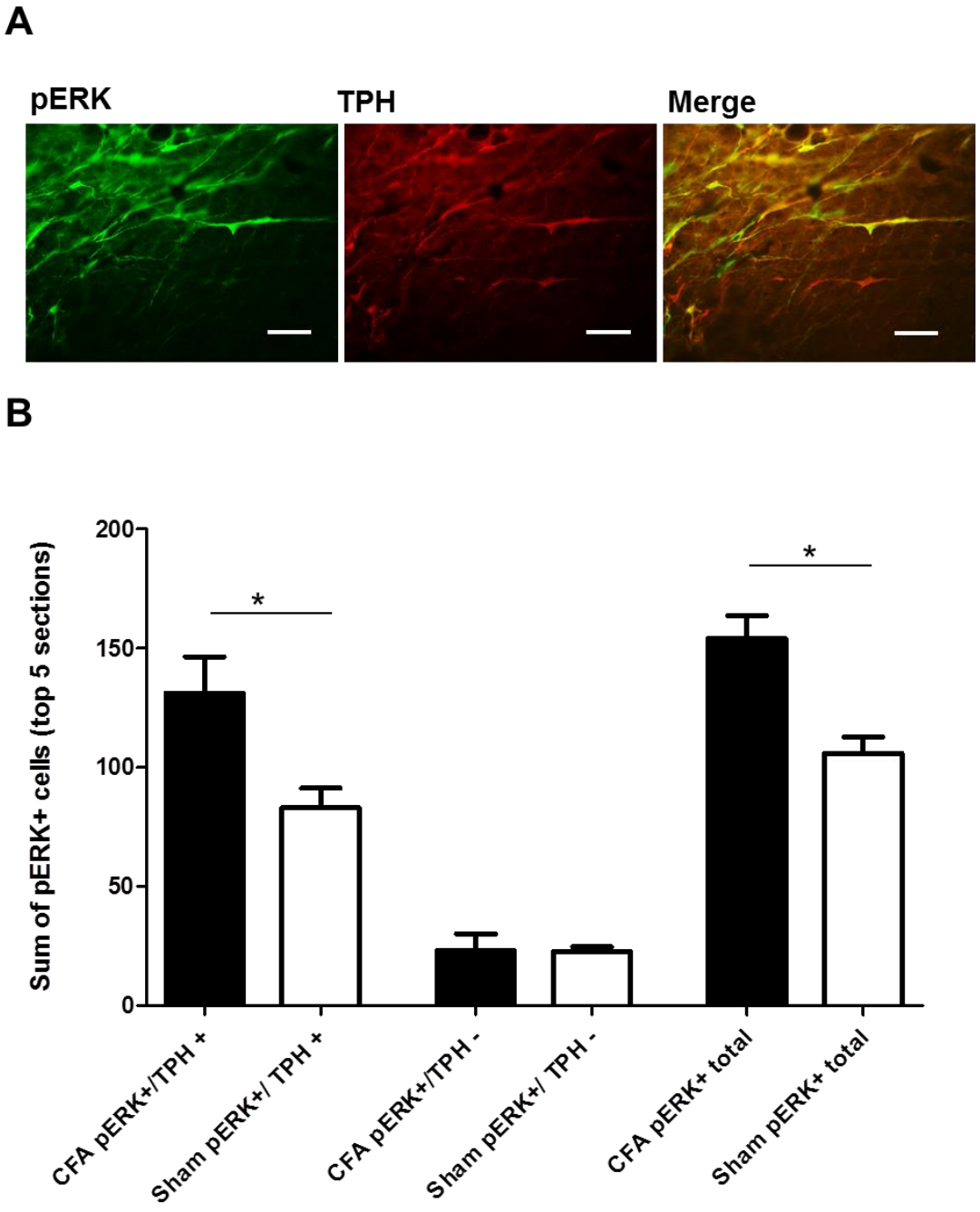

Figure 3.4 Increase in pERK+/TPH+ double labelled neurons at 6h post CFA.

A). Representative images of pERK+ (green) and TPH+ (red) cells within the NRM in the 6h CFA treated group. Scale bar indicates 100µm. **B).** Numbers of double labelled neurons in the RVM at 6h following ankle injection of CFA (black) or sham treatment (white). The numbers of pERK+/TPH+, pERK+/TPH- and total number of pERK+ cells for the top 5 pERK+

sections per animal are shown. n = 3 - 4, data is presented as mean ± SEM, * $p < 0.05$, independent samples t-test.

3.3.4 Labelling of active GABAergic synapses within the RVM

Pilot experiments were carried out to determine if injection of a VGAT-C specific antibody to the RVM in naive animals could be used as a measure of GABAergic activity within the region as described previously in the hippocampus (Martens et al., 2008). Animals were perfused 24h following a unilateral microinjection, and 40µm RVM sections were obtained. The VGAT-C antibody is tagged with Oyster-550, however weak fluorescence was observed following sectioning, and immunohistochemistry was carried out to enhance the signal. It was found that a single, unilateral microinjection of the VGAT-C antibody produced extensive labelling of the RVM region both ipsilateral and contralateral to injection site (figure 3.5). Punctate VGAT-C labelling was observed throughout the RVM with the most intense labelling close to the site of microinjection. The rostral-caudal distribution ran from approximately -9.5mm to -12mm from Bregma, with most intense labelling at approximately -11mm from Bregma.

Figure 3.5 Labelling of active GABAergic synapses *in vivo.*

Schematic illustrating the approximate site of VGAT-C antibody microinjection. The red asterix indicates the site of microinjection, at approximately -11mm from Bregma, +0.6mm laterally from the midline and -9.5mm from the surface of the brain. Immunohistochemistry using tyramide signal amplification allowed the visualisation of the VGAT-C antibody in RVM sections. The top panel illustrates a sample immunofluorescence image of VGAT-C staining in a naive animal, at approximately -11mm from Bregma. The white asterix indicates the site of injection. Below, higher power images of the ipsilateral and contralateral sides are shown. As clear labelling was observed contralaterally, these images were used for quantitative analysis (the area used for analysis is outlined in by the white box in the top panel). Scale bars indicate 50µm.

Notably, VGAT-C labelling appeared most prominent in the more ventral and lateral portions of the RVM, with considerable labelling spreading into the pyramidal tracts. This suggests there is dense GABAergic innervation of the area in which pERK labelling is observed following ankle injection of CFA (figure 3.3a). To determine if these active GABAergic synapses are formed onto 5-HT containing RVM neurons, double labelling of VGAT-C and TPH was carried out. It was found that although some close contact could be identified between VGAT-C labelled punctae and TPH, not all VGAT-C punctae are associated with TPH suggesting that GABAergic neurons synapse onto a mixed population of RVM neurons (figure 3.6).

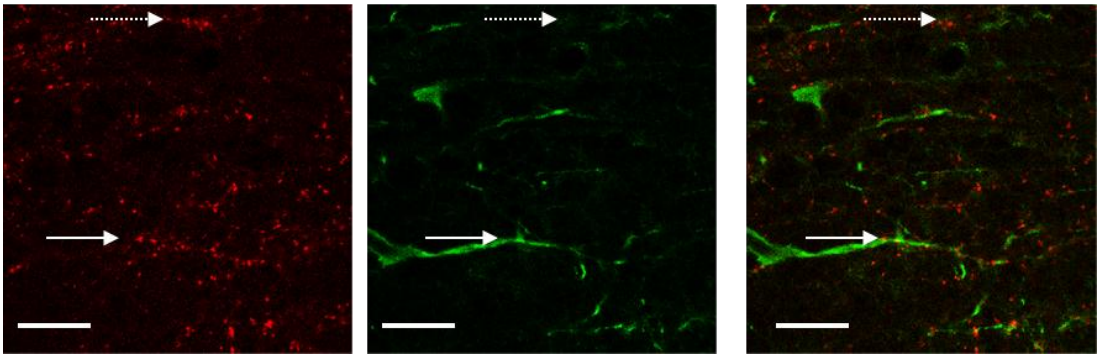

Figure 3.6 VGAT-C and TPH fluorescence immunohistochemistry.

Single plane confocal images illustrate that some VGAT-C punctae (red) appear to form close contact with TPH labelled neurons (green), with an example indicated by the solid white arrow. The dashed arrow indicates an example of VGAT-C labelling independent of TPH. Scale bar indicates 200µm.

3.3.5 Decrease in the proportion of active GABAergic synapses in the RVM at 3d following ankle injection of CFA

To determine if changes in GABAergic transmission occur within the RVM during persistent ankle inflammation, microinjection of the VGAT-C antibody was carried out in animals at 3d following injection of CFA or sham procedure (n = 3 per group). All quantitative analysis was carried out on the side contralateral to the injection site to minimise variation in labelling due to the minor damage caused by the microinjection needle tract (see figure

3.5). Animals were perfused at 24h following microinjection, and immunohistochemistry carried out to visualise the VGAT-C antibody. Double labelling for both isoforms of the glutamate decarboxylase enzyme (GAD65/67), a marker of GABAergic neurons, confirmed that the VGAT-C punctae corresponded to GABAergic synapses. A series of confocal images were taken for further analysis, with sample images from CFA treated and sham animals shown (figure 3.7a). Quantification of the total number of GAD65/67+ punctae and double labelled VGAT-C+ and GAD65/67+ punctae was carried out using the Fiji image analysis programme (see table 3.3). Two methods of statistical analysis were used.

The first analysis used each of the 9 sections per treatment group as individual data points. No significant difference in the number of GAD65/67+ punctae was observed between the groups ($p = 0.1563$, independent samples t-test, $n = 9$). Similarly no significant difference was found in the raw number of GAD65/67+ and VGAT-C+ overlapping punctae ($p = 0.957$, independent samples t-test, $n = 9$). However, when the data was expressed as the percentage of overlapping punctae over total GAD65/67+ punctae, a significant decrease was found in CFA treated animals compared to the sham treated group (figure 3.7b, independent samples t-test, $p = 0.0011$, $n = 9$).

The second analysis used the average of the 3 sections per animal as data points ($n = 3$). This analysis generates the same values for the group means, but results in a more stringent statistical test, due to the smaller n number. In this case the decrease in the percentage of overlapping punctae over total GAD65/67+ punctae in the CFA treated group fell just short of statistical significance (figure 3.7c, independent samples t-test, $p = 0.0559$, $n = 3$). Although this method is the preferred test for this type of data, as this was a small pilot experiment it was deemed appropriate to conclude that a

decrease in the proportion of double labelled punctae occurred in the CFA group.

	CFA	Sham	p value
Analysis 1: n = 9			
GAD65/67	21103 ± 8380.2	7439.6 ± 3758.3	0.1563
Double	3682.2 ± 1831.2	3849.9 ± 2336.5	0.9557
% Double/GAD65/67	14.63 ± 3.91	44.93 ± 6.6	0.0011
Analysis 2: n = 3			
GAD65/67	21103 ± 4841.46	7439.56 ± 2992.78	0.0743
Double	3682.22 ± 980.38	3849.9 ± 2263.47	0.9491
% Double/GAD65/67	14.63 ± 5.02	44.93 ± 10.18	0.0559

Table 3.3 Numbers of GAD65/67+ and VGAT-C+ punctae at 3d post CFA.

Values were determined by Fiji image analysis. The results of both statistical analyses are shown. Analysis 1 considered each section as a data point, with n = 9. Analysis 2 considered each animal as a data point, with n = 3 (based on the mean of 3 sections per animal). The p values for independent samples t-tests are shown for each comparison.

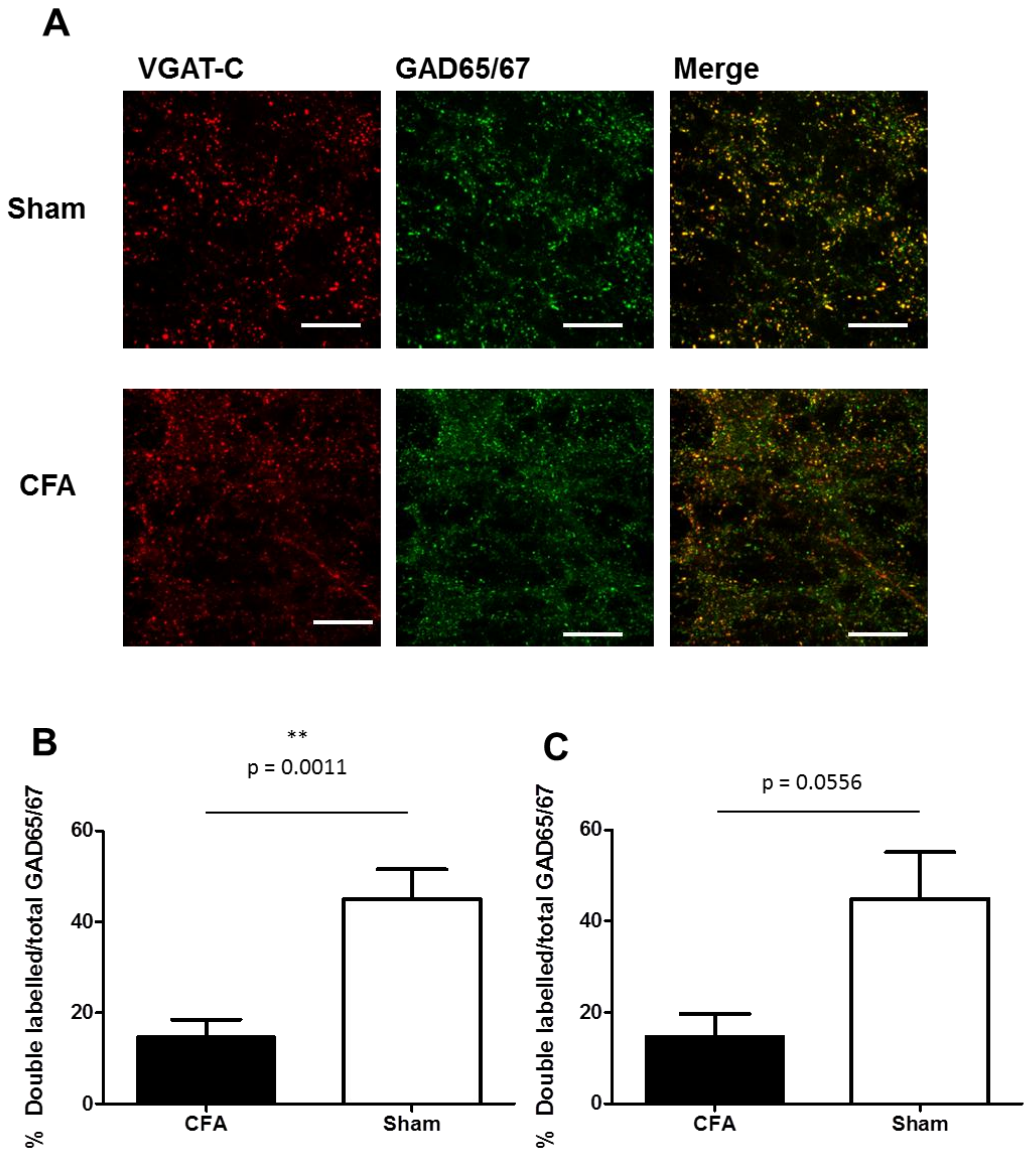

Figure 3.7 Decrease in the proportion of active GABAergic synapses at 3d post CFA.

A). Single plane confocal images from CFA and sham treated animals illustrate that the majority of VGAT-C labelled punctae (red) colabel with GAD65/67 (green). These double labelled punctae correspond to active GABAergic synapses. Not all the GAD65/67+ punctae are colabelled with VGAT-C, suggesting the antibody is specific for active synapses only. Scale bars indicate 50µm. **B).** Image analysis indicated that there is a decrease in the % of VGAT-C+ and GAD65/67+ double labelled punctae in the CFA treated group, over total GAD65/67 punctae. Data is expressed as the mean ± SEM of all 9 sections per group (n = 9, 3 sections per animal, 3 animals per group), p = 0.0011, independent samples t-test. **C).** The same image analysis data is presented as the group mean (n = 3 animals) where the value

per animal is calculated as the average of the 3 sections per animal. p = 0.0559, independent samples t-test.

3.4 Discussion

The RVM is a key structure involved in the relay of descending information to the dorsal horn of the spinal cord and is known to be activated in a number of models of persistent pain. Despite considerable evidence for a role of the RVM in descending facilitation of neuropathic pain as well as cutaneous inflammation (Burgess et al., 2002; Géranton et al., 2008; Wei et al., 2010), little is known regarding the role of the RVM in joint pain. This chapter describes experiments designed to determine if neuronal activation in the RVM is altered following ankle joint inflammation. Two separate immunohistochemistry approaches were used, investigating levels of pERK expression and GABAergic inhibition. Consideration of both findings together provides insight into the different time dependent changes that occur within the RVM in this model, with ERK activation within 5-HT neurons in the acute phase, and decreased GABAergic inhibition in the maintenance phase.

3.4.1 ERK activation in the RVM: a role in the induction of joint pain

ERK activation is widely used as a marker of stimulus induced activity in the CNS. In studies of nociception, ERK phosphorylation has been shown to occur in neurons of the dorsal horn in a number of pain models. RVM activation has also been demonstrated using pERK staining in the CFA model of cutaneous inflammation and spared nerve injury model of neuropathic pain (Géranton et al., 2010; Imbe et al., 2005). To investigate if similar RVM activation occurs in a model of joint pain, pERK immunohistochemistry was carried out at three time points following ankle injection of CFA. Interestingly it was found that in the sham treated animals there was a high level of ERK activation within the NRM and GiA regions of the RVM, suggesting that this region may be sensitive to the anaesthesia and

perfusion methods used. The RVM plays a role in acute nociception and phosphorylation of ERK is known to occur rapidly in stimulated neurons (Ji et al., 2002). This could explain the high level of ERK activation observed in the sham groups as the injection of pentobarbital and the perfusion process could cause rapid activation of ERK within the RVM.

Despite the high basal level of pERK+ neurons in sham animals, comparison of the number of pERK+ neurons in CFA and sham treated groups indicated there was an increase in pERK+ cells at 6h post inflammation. No significant increase was found at the later time points suggesting that ERK activation may play a role in the induction but not the maintenance of the pain state. The data presented here supports findings by others in the CFA model of cutaneous inflammation, in which peak ERK activation occurs at 7h post inflammation and pERK levels remain elevated until 1d (Imbe et al., 2005). Our findings suggest that the time course of ERK phosphorylation in the RVM is similar in models of joint and cutaneous inflammation.

Although the 6h time point correlates with peak mechanical hypersensitivity in our model, and can be considered representative of the acute phase of the pain state (Géranton et al., 2007), it is possible that ERK activation may occur at even earlier time points. For example in the Imbe et al. study an initial activation period was identified at 30min following plantar inflammation. This time point mirrors activation of ERK within spinal neurons following noxious stimulation (Ji et al., 1999). It is likely that a similar initial activation of ERK may occur in the RVM within minutes following ankle injection of CFA, and so an earlier time point may warrant investigation. If this proves to be the case, the two windows of ERK activation within the RVM may represent different aspects of nociceptive processing in the pain model. Activation of ERK within minutes may be arise due to the initial process of injection and inflammation, and could indicate activation of descending inhibitory neurons. Subsequent activation, within

hours, could represent recruitment of facilitatory pathways as mechanical hypersensitivity begins to stabilise and enters the maintenance phase.

Attenuation of cutaneous thermal hypersensitivity by microinjection of a MEK inhibitor to the RVM has been demonstrated (Imbe et al., 2008). Although ERK phosphorylation was decreased within hours of drug administration the effects of ERK inhibition on pain sensitivity did not occur until 1d post CFA injection. This suggests that the effects of ERK activation on behavioural hypersensitivity may not be observed until several hours later which would correlate with a role for ERK in long term transcriptional changes in the activated neurons. In the present study behavioural testing was not carried out, to eliminate the possibility that nociceptive testing itself could contribute to ERK activation in the RVM. Nonetheless behavioural testing may be of interest in future experiments, in particular to investigate if activation of ERK within the RVM has a facilitatory effect on mechanical paw withdrawal thresholds in this model. A useful future experiment would be to administer a MEK inhibitor directly to the RVM to establish if inhibition of ERK phosphorylation attenuates joint pain behaviour.

In the present study ERK activation is not observed at later time points, with no significant increase observed at either 3d or 7d post CFA injection. Again this correlates with previous findings in cutaneous inflammation (Imbe et al., 2005) but contrasts with work using the spared nerve injury model of neuropathic pain (Géranton et al., 2010). In this neuropathic pain model biphasic activation of ERK occurs, with increases in pERK+ neurons observed both during the induction phase of the pain state at (3d post nerve injury) and in the maintenance phase (8d post injury) (Géranton et al., 2010). This suggests that cutaneous and joint inflammation result in different patterns of ERK activation within the RVM when compared to neuropathic pain states. This may reflect differences in neuronal activity and descending modulation of pain in inflammatory and neuropathic models. It is possible

however that ERK activation could be maintained in the present model, at least up to 1d post inflammation as observed in cutaneous inflammation (Imbe et al., 2005). Further work is required to confirm that there is no further activation of ERK after the 6h time point, but at present the absence of activation at 3d and 7d suggests that in this model ERK activation does not occur in the later stages of inflammation. As mentioned above, pharmacological studies suggest there may be a delay between ERK activation and behavioural effects on descending modulation of pain, and it is possible that early ERK activation contributes to long term transcriptional changes and plasticity within the RVM.

It was found that approximately 80% of pERK expressing neurons in the RVM were TPH positive at 6h post inflammation. This proportion is higher than that reported in the cutaneous inflammation (Imbe et al., 2004) and may suggest greater activation of 5-HT neurons in the ankle joint model. 5-HT containing neurons represent approximately 20% of the RVM cell population (Gu and Wessendorf, 2007; Potrebic et al., 1994; Zhang et al., 2006) and many of these 5-HT neurons project to the dorsal horn (Bowker et al., 1982; Skagerberg and Björklund, 1985). Descending 5-HT fibres can have both pro- and anti-nociceptive effects within the dorsal horn, depending on the receptor subtype activated (Bardin, 2011; Millan, 2002). Increased activation of 5-HT neurons in the RVM following joint inflammation may therefore lead to increased descending inhibition, facilitation or a combination of the two. The next chapter describes experiments which aimed to investigate the role of descending 5-HT fibres in mediating behavioural hypersensitivity associated with joint inflammation.

Not all 5-HT neurons in the RVM project to the dorsal horn (Marinelli et al., 2002) and it would be of interest to determine the proportion of pERK+/TPH+ neurons that are projection neurons. Retrograde tracing from the dorsal horn would be useful in conjunction with pERK and TPH labelling.

Of those pERK+/TPH+ neurons that terminate within the RVM, it would be of interest to determine if these are either excitatory or inhibitory interneurons, by triple labelling with either VGLUT1 (the vesicular glutamate transporter) or GAD65/67.

Although these findings strongly suggest a role for 5-HT RVM neurons in the ankle joint model, the relatively low level of pERK expression in non-5-HT cell types is intriguing. The RVM is a heterogeneous population of cells, with physiologically defined ON, OFF and NEUTRAL cells being described throughout the region and these are not anatomically separated (Fields and Heinricher, 1985; Fields et al., 1983). It is interesting to note that little activation of ERK occurs in the more dorsal and lateral portions of the RVM, as at least some of these physiologically defined cells are present in the outer regions (Barbaro et al., 1986; Fields et al., 1983). This suggests that the signalling pathway contributing to ERK activation is not active in some of these electrophysiologically defined cells. Although ERK can be activated by Ca^{2+} influx via activated ionotropic receptors, another pathway which could contribute to ERK activation in TPH neurons is BDNF signalling (Pezet et al., 2002). Release of BDNF within the RVM from neurons arising in the PAG contributes to hyperalgesia (Guo et al., 2006) and this hyperalgesia appears to require release of 5-HT in the dorsal horn (Wei et al., 2010). Therefore BDNF activation of the TrkB receptor on 5-HT neurons of the RVM could lead to preferential activation of ERK in those neurons.

3.4.2 Decreased GABAergic transmission in the RVM following joint inflammation

In a separate experiment it was investigated if activity at GABAergic synapses within the RVM is altered in response to joint inflammation. In the normal animal GABAergic signalling in the RVM is pro-nociceptive, as microinjection of $GABA_A$ agonists to the region facilitates the tail flick reflex (Gilbert and Franklin, 2001; Heinricher et al., 1994). The proposed

mechanism underlying this effect is that increased GABAergic inhibition of inhibitory RVM neurons that project to the spinal cord results in a reduction in descending inhibition. Recently however it has been proposed that in persistent pain states decreased GABAergic inhibition within the RVM could lead to enhanced excitation of pain facilitating neurons projecting to the spinal cord. In the CFA model of plantar inflammation a decrease in inhibitory post synaptic currents occurs in the RVM. This effect is seen at 3 days but not at earlier time points following induction of the pain state (Zhang et al. 2011). In this study it was also shown that microinjection of a $GABA_A$ agonist to the RVM reduced thermal hypersensitivity. This strongly suggests that GABAergic transmission in altered in the maintenance phase of hypersensitivity (3d) following plantar inflammation.

To investigate if changes in GABAergic activity in the RVM occur in the ankle joint model a novel method of labelling active GABAergic synapses *in vivo* was used. Microinjection of the VGAT-C antibody to the RVM of naïve rats and subsequent detection by immunohistochemistry suggested that as described previously by others in the hippocampus (Martens et al., 2008) this technique could be a useful measure of GABAergic activity in the RVM. GAD65/67 double labelling indicated that the majority of these VGAT-C positive punctae were at GABAergic synapses. Furthermore the GAD65/67 labelling indicated that not all GAD65/67 positive punctae were positive for the VGAT-C terminus epitope, which is only exposed during synaptic release of neurotransmitter (figure 3.2). This suggests that as anticipated only a subset of active GABAergic synapses were labelled by VGAT-C (approximately 50% in the sham treated animals) and not all those containing GABA.

Using this labelling technique we wished to investigate if active GABAergic synapses are decreased in the RVM following ankle injection of CFA. Animals received VGAT-C microinjection at 3 days following CFA injection or sham

procedure. Analysis of the number of VGAT-C and GAD65/67 positive punctae in a sample of RVM sections from each group found that at 3 days following ankle inflammation there was a significant decrease in GABAergic signalling compared to sham controls. This supports the previous data on plantar inflammation in which GABAergic signalling is decreased at 3 days post CFA but not at earlier time points (Zhang et al., 2011). Although we have not carried out VGAT-C labelling at earlier time points, the results presented here indicate that decreased GABAergic transmission can be identified in the maintenance phase of the pain state. The origin of the GABAergic synapses characterised in this study is not addressed. Other brain regions which project to the RVM including the PAG may also be sources of GABAergic input however retrograde labelling from the PAG suggests that this GABAergic input is minimal (Jones et al. 1991). Therefore it is likely that many of the synapses quantified here arise from local inhibitory interneurons.

Further work is needed to characterise the functional role of GABAergic signalling within the RVM particularly in persistent pain states. Most previous studies have investigated GABAergic mechanisms in acute nociception using pharmacological manipulations (Drower and Hammond, 1988; Gilbert and Franklin, 2001; Heinricher and Kaplan, 1991; Heinricher et al., 1994). The role of the endogenous GABAergic signalling system within the RVM in pathological pain states following peripheral injury or inflammation is not well established. Increased descending facilitation from the RVM has been shown to play a role in behavioural hypersensitivity in neuropathic pain (Burgess et al., 2002; Porreca et al., 2001) and cutaneous inflammation (Géranton et al., 2008; LaGraize et al., 2010; Wei et al., 2010). The decrease in GABAergic signalling observed in this study and by others (Zhang et al., 2011) may therefore reflect a decrease in inhibitory control over facilitatory output neurons. Previously it has been reported that approximately 45% of all identified synapses in the rat RVM region are

GABAergic (Cho and Basbaum, 1991). The diffuse VGAT-C labelling observed throughout the RVM observed in naive rats is consistent with this. The high proportion of GABAergic synapses within the region and the presence of $GABA_A$ receptors on approximately 30% of RVM projection neurons (Hama et al., 1997) suggests that GABAergic inhibition is an important mechanism in the regulation of RVM to dorsal horn signalling.

It has been shown previously that at least some of the RVM 5-HT neurons have GABAergic input (Jones et al., 1991), and the finding that some TPH neurons have close labelling with VGAT-C supports this. Therefore the decreased GABAergic activity following ankle injection of CFA may result in a decrease in the inhibition of these neurons and increased 5-HT release in the spinal cord. However, only 20% of 5-HT neurons express the $GABA_A$ receptor (Hama et al., 1997) so it is likely that the decrease in GABAergic inhibition will also affect other cell types. Interestingly the Zhang et al. study (2011) suggested that decreased GABAergic inhibition may occur preferentially on cells expressing the mu opioid receptor (MOR), as MOR+ cell excitability is increased after inflammation. Further work is needed to determine if this is the case following ankle joint inflammation.

3.4.3 VGAT-C labelling technique: technical considerations

Labelling of active GABAergic synapses by application of a VGAT-C specific antibody is a relatively novel technique, and to date has been used *in vivo* only within the hippocampus in naïve animals, and not under experimental conditions (Martens et al., 2008). Although the results described in this chapter are promising, these should be considered pilot experiments and further work is needed to optimise the protocol. An important future experiment is to test a variety of VGAT-C concentrations *in vivo* to determine the optimal dose for TSA immunohistochemistry. As discussed above, the side contralateral to microinjection was used for analysis due to minor tissue damage caused at the injection site. A lower dose may reduce this effect and

allow for reliable analysis of the ipsilateral side. In addition, a single injection along the midline may be preferable as this would allow labelling and quantification of both sides of the RVM.

Specificity of the VGAT-C antibody for actively recycling GABAergic vesicles has been established by others previously (Hughes et al., 2010; Martens et al., 2008), however nonetheless a number of controls should be included in our future studies. Firstly, to ensure that the VGAT-C antibody is specific for active GABAergic synapses, a third antigen could be stained in addition to GAD65/67, such as VGAT-N or gephyrin, and only those punctae positive for all three would be counted as active GABAergic synapses. Secondly, to ensure that the VGAT-C antibody is not non-selectively labelling active synapses in all types of neurons, confirmation of a lack of double labelling with VGLUT1 (vesicular glutamate transporter) or SERT (5-HT transporter) could be carried out.

It has been reported that VGAT-C treatment of neurons *in vitro* does not impair vesicle filling, but may lead to a small reduction in vesicle release probability (Martens et al., 2008). The possibility that GABAergic transmission will be impaired following injection *in vivo* may warrant investigation, and suggests that combining behavioural studies with VGAT-C labelling may be problematic. Despite this limitation, and subject to confirmation of antibody specificity, the VGAT-C labelling technique may prove useful for quantifying GABAergic transmission within the RVM during ankle joint inflammation and other chronic pain states.

3.4.4 Conclusions

The aim of this chapter was to determine if changes in RVM activity occur following ankle joint inflammation, as described previously following induction of cutaneous inflammation or neuropathic injury. I have shown that following joint inflammation, ERK activation occurs mainly within 5-HT neurons. By labelling active GABAergic synapses *in vivo*, I have shown that

changes in inhibitory transmission also occur following joint inflammation. The following chapters describe experiments designed to determine the contribution of descending facilitation via the RVM to behavioural hypersensitivity in this model.

4. The role of descending 5-HT in inflammatory joint pain

4.1 Introduction

The majority of 5-HT fibres terminating in the dorsal horn originate in the RVM (Kwiat and Basbaum, 1992) and as demonstrated in chapter 3, activation of many of these neurons occurs in the hours following ankle joint inflammation. This chapter describes behavioural experiments carried out to investigate the role of spinal 5-HT in mediating behavioural hypersensitivity associated with this model.

4.1.1 The role of spinal 5-HT in nociceptive processing

5-hydroxytryptamine (5-HT) is a monoamine neurotransmitter found extensively in the periphery including the cardiovascular, gastrointestinal and pulmonary systems. Within the CNS 5-HT plays an important role in the modulation of many neurological processes including mood, sleep, autonomic function and sensory processing. Central 5-HT is produced largely in neurons of the midline raphe nuclei of the brainstem, which project to almost all brain areas and also the spinal cord (Berger et al., 2009).

The RVM is an important site in the descending modulation of nociceptive processing, and the majority of 5-HT fibres within the dorsal horn originate here (Kwiat and Basbaum, 1992). 5-HT containing fibres have been shown to form synapses onto projection neurons and local inhibitory interneurons (Millan, 2002; Ruda, 1988; Ruda et al., 1986). Therefore spinal 5-HT fibres arising from the RVM are ideally placed to modulate nociceptive processing in the dorsal horn.

In normal animals spinal 5-HT has been shown to play an inhibitory role in nociception. Direct application of 5-HT to the spinal cord in naive animals has an anti-nociceptive effect on behavioural responses to acute thermal (Crisp et al., 1991; Xu et al., 1994a; Yaksh and Wilson, 1979) and mechanical (Bardin et al., 1997) stimuli. In addition, the full analgesic effects of systemic morphine (Deakin and Dostrovsky, 1978) and clonidine (Duan and Sawynok, 1987) require an intact spinal 5-HT system suggesting 5-HT is a key component of endogenous inhibitory pathways.

These early studies established an important role for spinal 5-HT in mediating descending inhibition in the naive animal. Later work found that that in addition to mediating descending inhibition, the RVM could also play a role in facilitating nociception as high and low frequency stimulation of the region produced inhibition and facilitation respectively (Zhuo and Gebhart, 1990). It was found that the pro-nociceptive effect of low frequency stimulation in the RVM was blocked by 5-HT_1 receptor antagonism within the spinal cord (Zhuo and Gebhart, 1991) suggesting that spinal 5-HT may also facilitate spinal processing of pain.

4.1.2 5-HT receptor subtypes in the dorsal horn

At the spinal cord level the ability of 5-HT to enhance or inhibit nociceptive processing may be explained by activation of different receptor subtypes and multiple cellular locations within the dorsal horn (Millan, 2002). The 5-HT receptors are divided into 7 families, containing a total of 15 distinct receptors (Hannon and Hoyer, 2008). All are G protein-coupled, except for the 5-HT_3 receptor, which is a ligand gated ion channel. All the known 5-HT receptor subtypes are expressed within the spinal cord. The 5-HT_1 and 5-HT_2 groups and the individual 5-HT_3 and 5-HT_7 receptors are the most widely studied in terms of nociception (Millan, 2002). The functional response to 5-HT will depend on the physiological effect of receptor activation, i.e. if it has an inhibitory or excitatory role within the target neuron, and the cell type on

which it is located. The dorsal horn is a complex network of projection neurons, descending fibres, local inhibitory and excitatory interneurons, as well as containing the primary afferent terminals (Todd, 2010). 5-HT receptors are located on all of these cell types and therefore the net effect of 5-HT will depend on the balance between these components.

The 5-HT_1 subtype accounts for the majority of 5-HT receptors within the spinal cord. 5-HT_{1A} receptor activation has an inhibitory effect on neurons by negative coupling to adenylyl cyclase. 5-HT_{1A} activation has been shown to exert facilitatory effects on the nociceptive responses of spinal wide dynamic range neurons following carrageenan induced inflammation (Zhang et al., 2001) and are required for RVM stimulation induced facilitation of nociceptive reflexes (Ren, Randich, and Gebhart 1991; Zhuo and Gebhart 1991). Upregulation of this receptor occurs following peripheral carrageenan inflammation (Zhang et al. 2002) and hyperalgesia induced by plantar injection of bee venom (Wang et al., 2003). The facilitatory effects of 5-HT_{1A} receptor activation are thought to be mediated indirectly by inhibition of GABAergic interneurons (Wang et al., 2009). However inhibitory effects of 5-HT_{1A} on nociception have also been described, for example in the formalin test, and this may be mediated by direct inhibitory effects on projection neurons (Bardin et al., 2001; Oyama et al., 1996). Therefore the 5-HT_{1A} receptor subtype can have dual effects on nociception depending on the cell type activated.

The 5-HT_{2A} receptor has also been implicated in descending facilitation. It has an excitatory effect on neurons, by positive coupling to phospholipase C (Millan, 2002). The 5-HT_{2A} receptor is expressed at relatively low levels within the dorsal horn but is highly expressed in the DRG. Therefore the effects of 5-HT_{2A} activation in the spinal cord are likely to be mediated by the primary afferent terminals. Spinal administration of a 5-HT_{2A} antagonist has anti-nociceptive effects in models of neuropathic pain (Obata et al., 2004,

2001) and the formalin test (Nitanda et al., 2005). This receptor is therefore also a likely candidate in mediating descending facilitation via 5-HT.

The 5-HT_3 receptor has been the most widely studied in terms of mediating descending facilitation. This subtype is unique among the 5-HT receptors as it is a ligand gated ion channel. Activation of the 5-HT_3 receptor in neurons has an excitatory effect on target neurons, by positive coupling to phospholipase C. The 5-HT_3 receptor localises to primary afferent terminals (Maxwell et al., 2003) and one mechanism by which 5-HT_3 activation could enhance nociception is by increasing transmitter release from terminals. The 5-HT_3 receptor is also found on spinal interneurons and projection neurons (Conte et al., 2005; Huang et al., 2004; Kawasaki et al., 2004; Maxwell et al., 2003; Zeitz et al., 2002).

5-HT_3 knockout animals display normal acute pain behaviour but show an attenuated response to the second phase of the formalin test (Zeitz et al., 2002). This suggests that baseline pain responses are not modulated by 5-HT_3 but that in persistent pain states increased 5-HT drive to the spinal cord may activate these receptors. This is also observed pharmacologically whereby intrathecal administration of ondansetron, a selective 5-HT_3 antagonist, attenuates the second phase of the formalin response (Okamoto et al., 2004). Intrathecal administration of 5-HT_3 receptor antagonists has also been shown to attenuate behavioural hypersensitivity in a number of persistent pain models including spinal cord injury (Oatway et al., 2004), cancer induced bone pain (Donovan-Rodriguez et al., 2006), neuropathic pain (Dogrul et al., 2009) and cutaneous inflammation by CFA (LaGraize et al., 2010). Facilitation of dorsal horn neuronal excitability has also been shown to be mediated by the 5-HT_3 receptor in the formalin test (Suzuki et al., 2002) and in the monosodium iodoacetate (MIA) model of osteoarthritis (Rahman et al., 2009). Importantly these findings have been validated to some extent in patients with neuropathic pain, where a single intrathecal

dose of ondansetron led to a small decrease in overall pain scores, suggesting that targeting the spinal facilitation of pain via the 5-HT_3 receptor may a useful target in the treatment of chronic pain states (McCleane et al., 2003).

The 5-HT_7 receptor has only been studied in pain relatively recently, and most studies suggest it plays a role in the inhibitory effects of 5-HT. Activation of the 5-HT_7 receptor leads to excitatory effects within neurons and the receptor has been shown to localise both to primary afferent terminals and intrinsic dorsal horn neurons (Doly et al., 2005). In neuropathic pain, 5-HT_7 plays an inhibitory role (Dogrul et al., 2009) and this is thought to be mediated via activation of GABAergic interneurons in the dorsal horn (Yanarates et al., 2010). In addition, this receptor is required for morphine (Dogrul and Seyrek, 2006) and tramadol (Yanarates et al., 2010) mediated analgesia. These studies strongly support a role for the 5-HT_7 receptor in mediating descending inhibition by 5-HT.

4.1.3 The role of descending 5-HT in persistent pain states: evidence from lesion studies

The net effect of endogenous descending 5-HT in pain behaviour has been investigated using selective lesion of 5-HT containing fibres by the neurotoxin 5,7-dihydroxytryptamine. This technique has been used in a number of pain models, including the formalin model (Svensson et al., 2006), neuropathic injury (Rahman et al., 2006) and plantar inflammation by CFA (Géranton et al., 2008). These studies have illustrated that depletion of spinal 5-HT has no effect on baseline pain responses but that in models of persistent pain, lack of 5-HT fibres leads to an attenuation of behavioural hypersensitivity. This suggests that endogenous 5-HT exerts a net facilitatory effect on nociceptive processing in these pain models. More recently molecular depletion of descending 5-HT by silencing of tryptophan hydroxylase (TPH), the enzyme that synthesises 5-HT, has also been used to

demonstrate that descending 5-HT has a pro-nociceptive role in cutaneous inflammation (Wei et al., 2010). Collectively these studies suggest a role for descending 5-HT in increasing pain sensitivity across a variety of pain models.

4.1.4 Hypothesis

In this chapter I have tested the hypothesis that descending 5-HT facilitates behavioural hypersensitivity following joint inflammation and that this is mediated by the spinal 5-HT_3 receptor.

4.2 Methods

4.2.1 Intrathecal injection

Isoflurane anaesthesia (5% isoflurane for induction, 1.5 – 2% for maintenance, combined with 100% O2 (1l/min)) was used during surgery. Animals were secured in a stereotaxic frame and the head was shaved and sterilised. A skin incision was made from the base of the skull to the first vertebra, and the muscle separated in layers to reveal the atlanto-occipital membrane. A small incision was made and the membrane cleared to allow cannula access. Polyethene tubing (diameter 0.28mm), prefilled with solution and attached to a 50µl Hamilton syringe was then inserted carefully was into the subarachnoid space, terminating in L4-5 region. Care was taken to prevent damage to the spinal cord or roots. Toxin, drug or vehicle was injected in a volume of 10µl. The tubing was then withdrawn, and the muscle was sutured with 1 – 2 stiches of 3-0 Mersilk, and the skin sutured with 5-0 Mersilk. As with intra-RVM injections animals were monitored closely for weight loss, signs of neurological impairments or general distress.

4.2.1.1 5,7-Dihydroxytryptamine lesion

Animals were pre-treated with 25mg/kg i.p. desipramine hydrochloride (Sigma) dissolved in saline to protect against noradrenergic toxicity one hour

prior to surgery. Animals received 10µl of 5,7-dihydroxytryptamine (5,7-DHT) in saline (6µg/µl, Fluka) or saline only. The animals were allowed to recover over 6 days to allow for depletion of 5-HT fibres before CFA injection.

4.2.1.2 5-HT$_3$ antagonist

In a separate experiment animals were injected intrathecally with drug or vehicle at 1d following CFA injection to the ankle. Ondansetron hydrochloride (Tocris Bioscience), a selective 5-HT$_3$ antagonist was dissolved in saline and injected in a volume of 10µl at a dose of 1µg/1µl. This dose was chosen based on a previous study of thermal hyperalgesia following cutaneous inflammation (LaGraize et al., 2010).

4.2.2 Inflammatory pain model and behavioural testing

Animals received ankle injection of CFA or underwent a sham procedure. Paw withdrawal thresholds were measured and log2 transformation was carried out to normalise the data (see section 2.2).

To measure relative weight bearing on the ipsilateral and contralateral hindpaws following induction of joint inflammation an incapcitance tester (Linton Instrumentation) was used. Animals were placed in a plexiglass box with front paws leaning on a slope and each hindpaw on a separate weighing scale. The force of each hindpaw on its scale was then measured and averaged over a 5 second period, and 5 measurements were taken for each animal. Data is presented as the mean ipsilateral weight bearing over total weight bearing: (Ipsilateral weight (g)/ (Ipsilateral weight (g) + contralateral weight (g))) x 100.

Statistical analysis for both mechanical paw withdrawal thresholds and weight bearing data was carried out in SPSS. Analysis of variance (ANOVA) with repeated measures was carried out with time as the within subjects factor, and CFA and 5,7-DHT/ondansetron treatment as the between

subjects factors. A significant main effect of CFA was a prerequisite for subsequent ANOVAs or post hoc analysis.

4.2.3 5-HT immunohistochemistry

To determine the extent of 5,7-DHT lesion of spinal 5-HT fibres, direct fluorescence immunohistochemistry was carried out using a 5-HT specific antibody (rat host, concentration 1:75, Chemicon) in 40µm lumbar spinal cord sections from 5,7-DHT and saline injected animals. The 5-HT immunohistochemistry protocol used the avidin-biotin steps of the TSA protocol, but without the biotinylated tyramide step (section 2.4).

4.3 Results

4.3.1 Lesion of descending 5-HT fibres by 5,7-DHT attenuates mechanical hypersensitivity

Following intrathecal injection animals were monitored closely for neurological damage. In a small number of animals, cannula insertion resulted in dorsal root injury which caused clear motor deficits apparent upon recovery from the anaesthesia. These were culled immediately and removed from further analysis. Following a 6d recovery period animals were subjected to either ankle injection of CFA or sham procedure and paw withdrawal thresholds were monitored up to 7d post inflammation.

Three-way analysis of variance (ANOVA) with repeated measures was carried out on the ipsilateral paw withdrawal thresholds, with time as the within-subject factor and intrathecal injection (5,7-DHT or saline) and CFA injection (CFA or sham) as the between-subjects factors (n = 6 - 7). Main effects of time, CFA, and a time x CFA interaction were observed. The full results of this analysis are shown in table 4.1.

Subsequently a two-way ANOVA with repeated measures was carried out to determine if there was an overall effect of 5,7-DHT from 2h to 7d following

CFA treatment. The results of this analysis indicated there was no overall effect of 5,7-DHT treatment ($p = 0.271$) and no 5,7-DHT x CFA interaction ($p = 0.293$) but there was a main effect of time ($p < 0.001$). One-way ANOVAs at each time point following CFA injection were then carried out to determine the source of this variation. These indicated that there was a significant effect of 5,7-DHT treatment at days 1 and 2 post CFA injection ($p = 0.01$ and 0.037 respectively, LSD post hoc test, figure 4.1a).

Factor	df	F	Error	P
Time	13	20.8	286	< 0.001
CFA	1	64	22	< 0.001
5,7-DHT	1	0.36	22	0.555
5,7-DHT x CFA	1	16.5	22	0.198
Time x 5,7-DHT	13	0.771	286	0.691
Time x CFA	13	23.7	286	< 0.001
Time x CFA x 5,7-DHT	13	1.25	286	0.244

Table 4.1 Results of three-way ANOVA with repeated measures on ipsilateral paw withdrawal thresholds following 5,7-DHT.

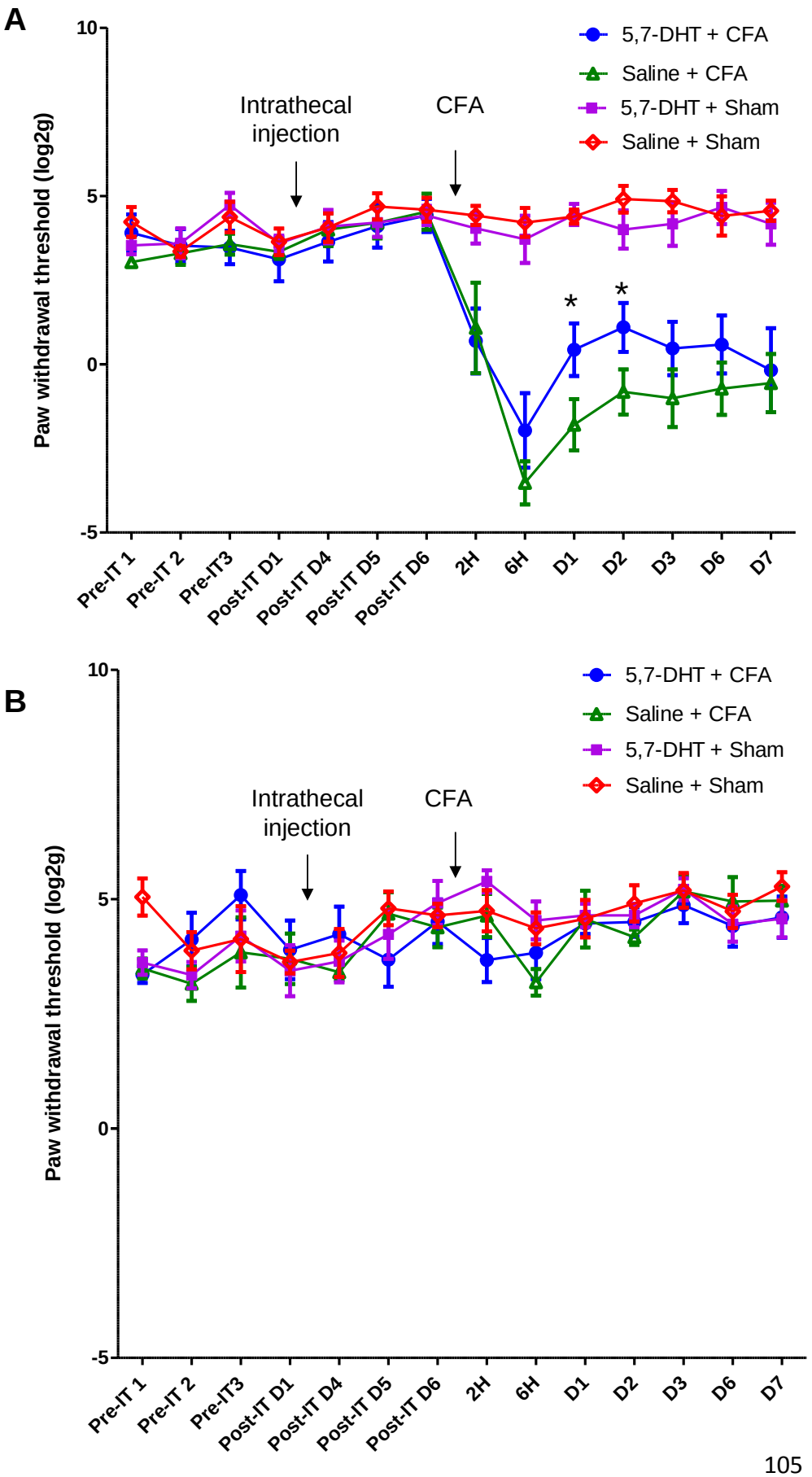
A
10
5
0
-5
Paw withdrawal threshold (log2g)
Intrathecal injection
CFA
5,7-DHT + CFA
Saline + CFA
5,7-DHT + Sham
Saline + Sham
*
*
Pre-IT 1
Pre-IT 2
Pre-IT3
Post-IT D1
Post-IT D4
Post-IT D5
Post-IT D6
2H
6H
D1
D2
D3
D6
D7
B
10
5
0
-5
Paw withdrawal threshold (log2g)
Intrathecal injection
CFA
5,7-DHT + CFA
Saline + CFA
5,7-DHT + Sham
Saline + Sham
Pre-IT 1
Pre-IT 2
Pre-IT3
Post-IT D1
Post-IT D4
Post-IT D5
Post-IT D6
2H
6H
D1
D2
D3
D6
D7

Figure 4.1 Attenuation of mechanical hypersensitivity by 5,7-DHT.

A). Attenuation of mechanical hypersensitivity in 5,7-dihydroxytryptamine treated rats following ankle joint inflammation. Ipsilateral paw withdrawal thresholds were significantly higher in 5,7-DHT treated animals compared with saline controls, at 1d and 2d following CFA injection. Pre-IT indicates the baseline prior to intrathecal injection, post-IT indicates baseline after IT injection. **B).** Paw withdrawal thresholds of the contralateral hindpaw were not altered by CFA injection or by 5,7-DHT pre-treatment. Data is presented as log2 (paw withdrawal threshold in g) and mean ± SEM. * $p < 0.05$, two-way ANOVA with repeated measures, and LSD post hoc analysis. n = 6 - 7.

A three-way ANOVA with repeated measures was also carried out on the paw withdrawal thresholds of the contralateral hindpaw (figure 4.1b). This analysis indicated that although there was a significant effect of time ($p < 0.001$) there was no time x 5,7-DHT interaction ($p = 0.59$), time x CFA interaction ($p = 0.651$) or time x 5,7-DHT x CFA interaction ($p = 0.604$). The between subjects effects indicated no effect of 5,7-DHT ($p = 0.922$), CFA (0.129) or CFA x 5,7-DHT interaction ($p = 0.393$). As there were no significant main effects of CFA treatment on paw withdrawal thresholds post hoc analysis was not carried out.

These findings indicate that 5,7-DHT treatment has no effect on baseline mechanical paw withdrawal thresholds, and attenuates mechanical hypersensitivity at 1d and 2d post inflammation only.

4.3.2 No effect of 5,7-DHT on weight bearing

Use of von Frey hairs allows the characterisation of cutaneous mechanical hypersensitivity of tissue adjacent to the inflamed joint, which may be considered a measure of secondary hyperalgesia. To study the sensitivity of the joint (primary hyperalgesia) weight bearing on the hindpaws was assessed. Readings were taken of weight placed on the ipsilateral and the contralateral hindpaws, and data is expressed as ipsilateral weight bearing/total hindpaw weight bearing (ipsilateral + contralateral). Three-way

ANOVA with repeated measures was carried out as for the paw withdrawal thresholds. The within-subjects tests indicated there was a main effect of time but no time x 5,7-DHT, time x CFA or time x 5,7-DHT x CFA interactions. The between-subjects tests indicated that there was no overall effect of drug or drug x treatment interaction but there was a main effect of treatment. The results of this analysis are shown in table 4.2.

As there was a main effect of time and CFA treatment, post-hoc analysis was carried out using one-way ANOVAs at each time point following CFA injection. This indicated that at all time points there was a significant effect of CFA treatment ($p < 0.03$) but no effect 5,7-DHT. These findings indicate that while CFA treatment reduces weight bearing on the ipsilateral hindpaw, there was no attenuation of this shift in weight bearing by 5,7-DHT treatment (figure 4.2).

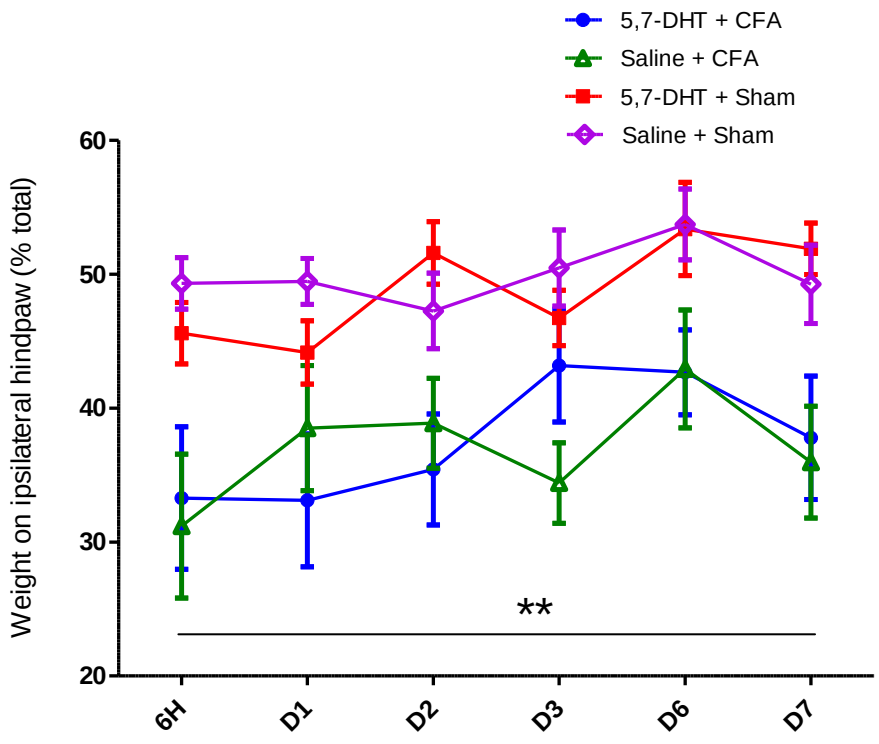

Figure 4.2 No effect on weight bearing following 5,7-DHT.

CFA treatment led to a decrease in weight bearing on the ipsilateral hindpaw in both 5,7-DHT and saline treated groups (** p = 0.001, three-way ANOVA with repeated measures)

however 5,7-DHT treatment had no effect on this decrease. Data is presented as mean ± SEM, n = 6 – 7.

Factor	df	F	Error	P
Time	5	4.72	110	0.001
CFA	1	14.892	303.737	0.001
5,7-DHT	1	0.06	303.737	0.809
5,7-DHT x CFA	1	0.034	303.737	0.855
Time x 5,7-DHT	5	1.225	110	0.302
Time x CFA	5	1.05	110	0.392
Time x CFA x 5,7-DHT	5	2.101	110	0.071

Table 4.2 Results of three-way ANOVA with repeated measures on weight bearing following 5,7-DHT.

4.3.3 Confirmation of 5-HT depletion by immunohistochemistry

Ablation of central 5-HT containing neurons by administration of 5,7-DHT is a widely used lesion technique in many areas of neuroscience and has been used by our research group previously to ablate descending 5-HT fibres within the dorsal horn of the spinal cord (Géranton et al., 2008). 5-HT immunohistochemistry was carried out in 40µm sections of the lumbar L4-L6 region spinal cord in a total of 8 rats (2 from each treatment group, in each of the two experimental batches). In all 5,7-DHT treated animals it was found that as expected, 5-HT positive punctae were almost completely absent within the dorsal horn, compared with saline injected controls in which extensive 5-HT labelling was observed. Representative images of 5,7-DHT treated and saline control animals are shown in figure 4.3.

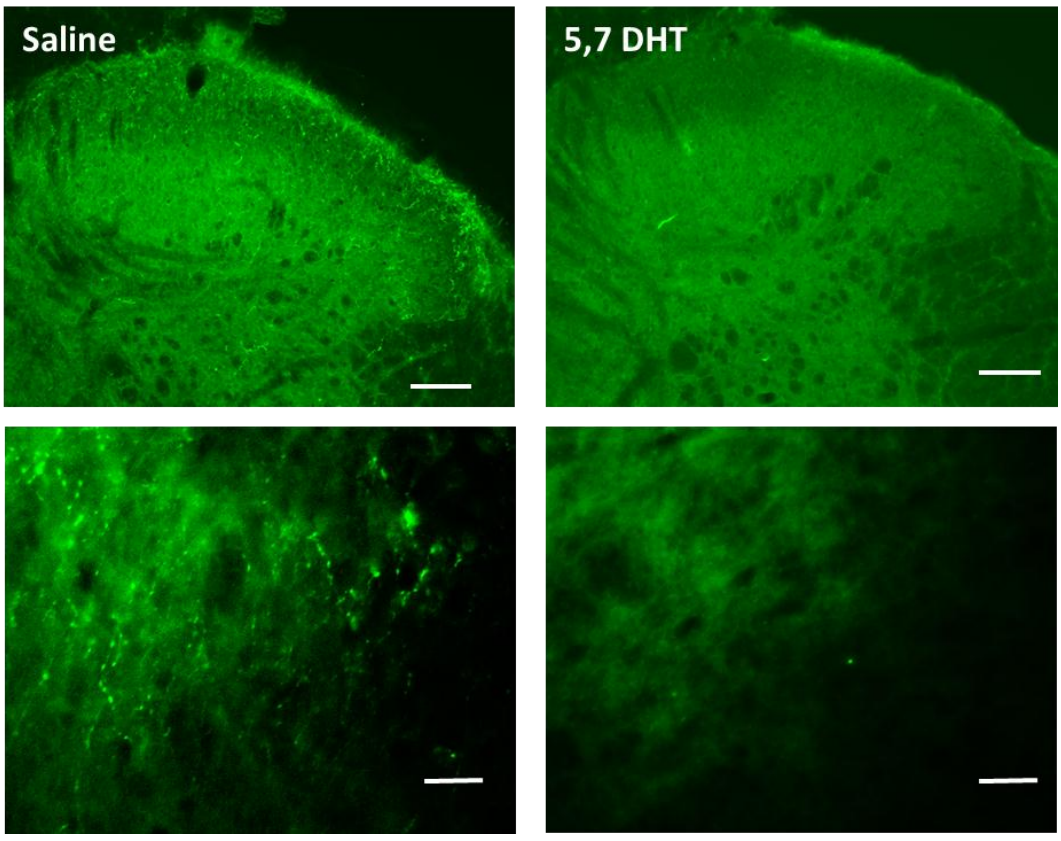

Figure 4.3 5-HT immunohistochemistry following at 13d following 5,7-DHT depletion (7d post CFA).

Representative images indicate that 5,7-DHT treatment leads to a complete loss of 5-HT punctate immunoreactivity within the dorsal horn. Top row x 5 magnification, scale bar indicates 400µm, bottom row x 10 magnification, scale bar indicates 200µm.

4.3.4 Effect of an intrathecal 5-HT$_3$ antagonist on established hypersensitivity

To determine the role of the 5-HT$_3$ receptor in mediating descending facilitation by 5-HT, the 5-HT$_3$ specific antagonist ondansetron was intrathecally administered to animals 24h following induction of inflammation. A two-way ANOVA with repeated measures was carried out with time as the within-subjects factor and drug treatment as the between-subjects factor. The results of this analysis are shown in table 4.4.

Factor	df	F	Error	P
Time	5	49.118	20	< 0.001
Drug	1	0.923	4	0.391
Time x Drug	5	3.805	20	0.014

Table 4.3 Results of two–way ANOVA with repeated measures on ipsilateral paw withdrawal thresholds following intrathecal ondansetron.

As there was a time x drug interaction, further analysis was carried out on time points after intrathecal injection of ondansetron. Two-way ANOVA with repeated measures from 2h – 3h indicated that at these time points there was an overall effect of ondansetron treatment ($p = 0.015$). This indicates that intrathecal antagonism of the 5-HT$_3$ receptor in animals with established inflammation can transiently attenuate behavioural hypersensitivity (figure 4.4).

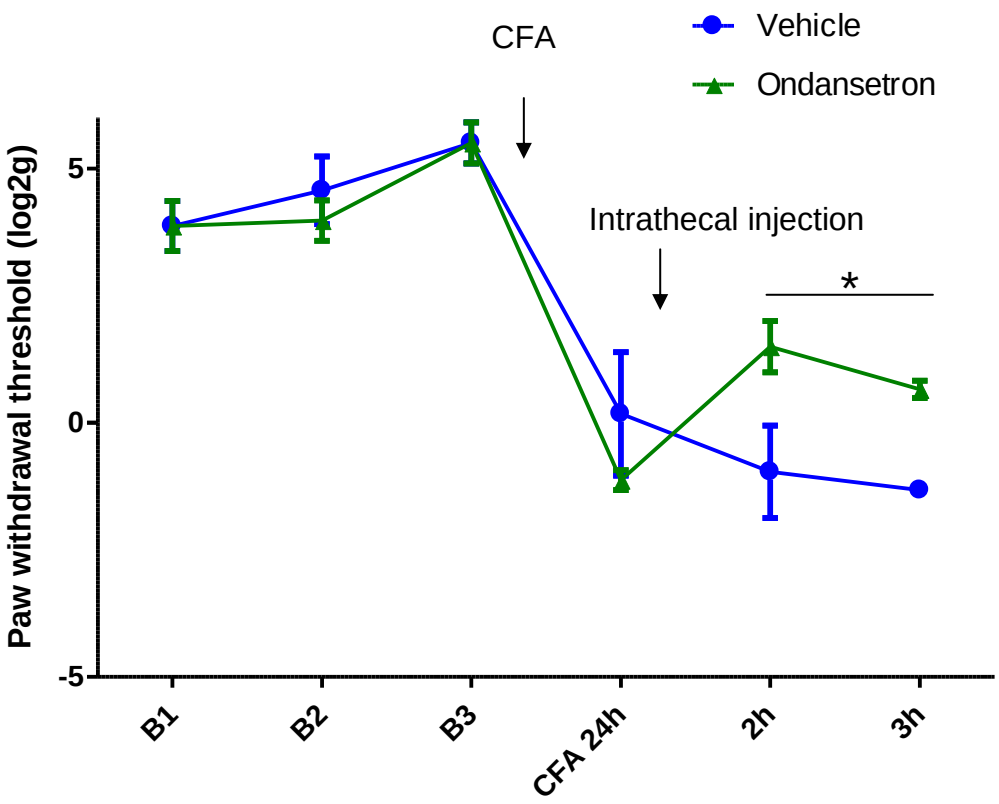

Figure 4.4 Attenuation of mechanical hypersensitivity by intrathecal ondansetron.
All animals received ankle injection of CFA which caused a decrease in paw withdrawal thresholds from baseline at 24h. They were then divided into two groups, one receiving intrathecal injection of ondansetron (10µg/10µl) and the other saline (10µl). Ondansetron treatment increased paw withdrawal thresholds at 2h and 3h post injection compared to saline injected controls, * $p < 0.05$, two-way ANOVA with repeated measures. Data is presented as log2 (paw withdrawal threshold in g) and mean ± SEM, n = 3. At the 3h time point no error bars are shown as the three values in each group were the same.

4.4 Discussion

Joint inflammation results in hyperalgesia and allodynia and this is driven partly by peripheral sensitisation by inflammatory mediators, however central sensitisation of the spinal cord has also been shown to contribute (Neugebauer and Schaible, 1990) and (Naeini et al., 2005). Interestingly enhanced descending inhibition of spinal excitability has also been shown to occur at least in the acute phase of joint inflammation (Cervero et al., 1991;

Schaible et al., 1991), however the potential contribution of descending facilitation to pain associated with joint inflammation is relatively unknown.

The role of 5-HT in models of pain is somewhat controversial, with some studies suggesting spinal 5-HT is anti-nociceptive and others describing a pronociceptive role. In this chapter the contribution of descending 5-HT fibres to behavioural hypersensitivity associated with CFA induced joint inflammation was investigated. It was found that 5-HT fibres play a small, time dependent role in the facilitation of joint pain behaviour. In a separate experiment it was shown that a single intrathecal injection of a 5-HT_3 receptor antagonist could transiently reverse mechanical hypersensitivity.

4.4.1 Time dependent role of 5-HT fibres in secondary mechanical hyperalgesia following joint inflammation

In studies of neuropathic pain it has been shown that descending 5-HT is required for the maintenance but not the induction of behavioural hypersensitivity (Rahman et al. 2006). In contrast our findings suggest that depletion of spinal 5-HT fibres attenuates mechanical hypersensitivity at days 1 and 2, but not days 3 – 7, after the induction of joint inflammation. One possible explanation is that the differences in the peripheral input generating hypersensitivity in these models leads to different patterns of activation of descending 5-HT neurons. In neuropathic pain, although mechanical hypersensitivity occurs within 24h, the peak behavioural response occurs days or weeks following the nerve injury (Decosterd and Woolf, 2000). In contrast following joint inflammation, peak mechanical hypersensitivity occurs within 6h, suggesting earlier activation of spinal and supraspinal neurons in this model. Therefore it seems likely that the different time course of 5-HT mediated facilitation observed in these models reflects the dynamics of peripheral input inducing the pain states.

Interestingly the role of descending 5-HT fibres in the ankle joint model also differs from that described previously following plantar inflammation in

which it has been demonstrated that in animals with 5,7-DHT pre-treatment, mechanical hypersensitivity is attenuated almost immediately following plantar injection of CFA (Géranton et al., 2008). The slightly later onset of 5-HT mediated facilitation in the present study may reflect subtle differences in the degree of peripheral inflammation and intensity of noxious input to the spinal cord. Peak mechanical hypersensitivity occurs at 6h following ankle injection of CFA, and the plantar model induces a more rapid decrease in paw withdrawal threshold. In addition the distribution of primary afferent terminals in the dorsal horn is different for cutaneous and joint nociceptors. Cutaneous fibres terminate in lamina I and II, while joint afferents terminate preferentially in lamina I (Doyle and Hunt, 1999; Neugebauer et al., 1994). These anatomical differences in the cutaneous and ankle models many explain the differences in behaviour observed following 5,7-DHT depletion.

Selective chemical depletion of 5-HT neurons by administration of 5,7-DHT is a widely used technique in the investigation of 5-HT function within the CNS (Baumgarten and Lachenmayer, 2004). Previous studies have demonstrated that axonal degeneration following 5,7-DHT treatment begins as early as 3d post injection (Frankfurt and Azmitia, 1984; Wiklund and Björklund, 1980). This suggests that the absence of an effect of 5,7-DHT treatment on paw withdrawal thresholds at 6h and 24h post CFA was not due to inadequate 5-HT depletion, as these time points correspond to 7d and 8d post 5,7-DHT treatment, at which time 5-HT axonal loss is optimal. In addition, although regeneration of 5-HT axons may occur after longer periods, this process does not begin until 14d post 5,7-DHT treatment and full restoration of 5-HT fibres takes many months (Wiklund and Björklund, 1980). Therefore the observation that paw withdrawal thresholds at 7d post CFA (corresponding to 13d post 5,7-DHT treatment) are unaffected by 5-HT fibre depletion is unlikely to be due to regeneration.

Immunohistochemistry using a 5-HT specific antibody allowed us to confirm this, indicating that 5-HT punctae are absent from the dorsal horn in rats at 13d following 5,7-DHT treatment. One limitation to this is the high background staining observed using the 5-HT antibody. It has been demonstrated that immunohistochemistry for the 5-HT transporter (SERT), which localises to 5-HT containing axons, has an equivalent distribution to staining for 5-HT itself, and produces a stronger signal with less background labelling (Nielsen et al., 2006). SERT labelling may therefore be useful as an additional marker of 5-HT fibres in the dorsal horn for future studies, in particular for a quantitative analysis of the depletion.

The time course of activation of the descending 5-HT system in ankle joint inflammation correlates with the pERK data presented in the previous chapter, in which activation of ERK in 5-HT producing RVM neurons was shown to occur at 6h but not at 3d or 7d following joint inflammation. Although the behavioural effect of 5,7-DHT lesion on paw withdrawal threshold is not significant at 6h following CFA treatment, activation of ERK at this time point may contribute to activation of the descending 5-HT pathway leading to subsequent behavioural facilitation at days 1 and 2. Indeed it has been demonstrated by others that injection of an ERK inhibitor to the RVM attenuates behavioural hypersensitivity at 24h post CFA. This attenuation does not occur at 7h, despite significant ERK activation at that time (Imbe et al., 2008). Our data supports this finding and suggests that although peripheral inflammation leads to molecular changes in the RVM within hours, the behavioural effects of those changes are not observed until later.

The time-dependence of facilitation by spinal 5-HT fibres identified here does support the findings of a recent study which investigated the contribution of 5-HT to inflammatory pain by molecular silencing of the tryptophan hydroxylase enzyme (TPH), required for 5-HT synthesis, within

the RVM (Wei et al., 2010). This method results in inhibition of 5-HT synthesis within all 5-HT neurons within the RVM, and not only those projecting to the spinal cord. The similarities between their findings and the data presented in this chapter are striking. In the Wei et al. study the greatest attenuation of mechanical hypersensitivity was detected at day 1 and day 3 following plantar inflammation, with only a small attenuation at earlier (6 hours) and later (5 days) time points. The magnitude of attenuation observed is larger than that identified here, but this may be due to the additional loss of 5-HT in locally terminating neurons of the RVM. Taken together these studies suggest a unique window of activation of the descending 5-HT system from 1 to 3 days after peripheral inflammation.

4.4.2 No effect of 5,7-DHT depletion on primary hyperalgesia

Paw withdrawal thresholds to mechanical stimuli using von Frey hairs reflect sensitivity to a punctate mechanical stimulus of the plantar surface adjacent to the inflamed ankle. As this measures pain hypersensitivity of a site removed from the initial inflammatory insult, this can generally be considered as a correlate of secondary hyperalgesia. Many studies of joint pain make use of additional outcome measures such as weight bearing asymmetry to reflect primary hyperalgesia of the joint itself (Sagar et al., 2011; Thakur et al., 2012). In this study it was found that as expected, CFA injection produces a significant shift in weight bearing from the ipsilateral paw. Notably 5,7-DHT treatment had no effect on weight bearing at any time point. This suggests that although cutaneous mechanical hypersensitivity is reduced by 5,7-DHT lesion, there is no effect on the primary hyperalgesia of the joint itself. It has long been suggested that descending facilitation is required for secondary but not primary hyperalgesia (Urban et al., 1996). Our finding that weight bearing is unaffected by 5,7-DHT depletion adds to this evidence suggesting

differences in the descending modulation of primary and secondary hyperalgesia.

4.4.3 The facilitatory effects of 5-HT are mediated via the 5-HT$_3$ receptor

The 5-HT$_3$ receptor has been implicated in the facilitatory actions of 5-HT within the spinal cord in a variety of pain models (Bardin, 2011). It is a ligand gated ion channel, unlike the other members of the 5-HT receptor family which are all G-protein coupled. Its permeability to cations means that activation of this receptor on the intrinsic neurons of the spinal cord would have an excitatory effect (Millan, 2002). Expression of the 5-HT$_3$ receptor has also been reported on the primary afferent terminals of the dorsal horn (Maxwell et al., 2003) and so 5-HT$_3$ receptor activation may also lead to enhanced neurotransmitter release. The Maxwell et al. study investigated expression of the 5-HT$_3$ receptor within the L4 region of the spinal cord, which receives input from the ankle joint. Notably the majority of the 5-HT$_3$ receptor positive afferent terminals double labelled with CGRP, and relatively few expressed IB4. As the joints are innervated largely with peptidergic afferents and few IB4 positive afferents (Ivanavicius et al., 2004), it is likely that many of the CGRP+ joint afferent terminals in the dorsal horn will express 5-HT$_3$ receptor. At the peripheral terminal, it has been directly established that ankle joint afferents express the 5-HT$_3$ receptor and respond directly to 5-HT (Birrell et al., 1990).

Intrathecal administration of 5-HT$_3$ specific antagonists has confirmed that this receptor plays a pro-nociceptive role in a number of pain models including the formalin test (Zeitz et al., 2002), spinal cord injury (Oatway et al., 2004), cancer induced bone pain (Donovan-Rodriguez et al., 2006), neuropathic pain (Dogrul et al., 2009) and plantar injection of CFA (LaGraize et al., 2010). The present finding that a single intrathecal injection of ondansetron transiently modifies secondary hyperalgesia following joint inflammation further supports the role of the 5-HT$_3$ receptor in descending

facilitation. Notably, the magnitude of attenuation was similar to that observed in the 5,7-DHT lesion experiment.

Interestingly it has been demonstrated that cannabinoids are also capable of binding to the 5-HT_3 receptor, and have an inhibitory effect (Oz et al., 2002; Yang et al., 2010). Within the dorsal horn, endogenous cannabinoids have been shown to have an antinociceptive effect and so may act as a protective mechanism to counteract central sensitisation in chronic joint pain (Sagar et al., 2010). This protective mechanism may be mediated via inhibition of the 5-HT_3 receptor.

The facilitatory role of other 5-HT receptors cannot be ruled out however, and in particular the contribution of 5-HT_{1A} and 5-HT_{2A} may warrant further investigation as these have been implicated in facilitation of pain behaviour in neuropathic and inflammatory models (Aira et al., 2012; Zhang et al., 2001). The 5-HT_{2A} receptor may be of particular interest in the modulation of spinal cord excitability, as it has been shown to form heterodimers with the mGluR2 receptor, suggesting activation of this 5-HT receptor subtype may enhance glutamatergic signalling (González-Maeso et al., 2008).

4.4.4 Modest effects of 5,7-DHT depletion: possible inhibitory effects of 5-HT

The modest and short lived magnitude of attenuation in hypersensitivity identified here may be due to the complexity of the role of 5-HT within the spinal cord. Considerable evidence exists to suggest that both inhibitory and facilitatory roles for 5-HT can occur within the spinal cord and that this is likely to be due to the activation of different receptor subtypes (Millan, 2002; Wei et al., 2010). Electrophysiological studies of joint inflammatory pain models have suggested that in the acute phase of inflammation there is

an increase in descending inhibition from the RVM (Cervero et al., 1991; Schaible et al., 1991). Therefore in addition to an increased facilitatory drive mediated by the 5-HT_3 receptor, there may be a parallel increase in inhibition at other receptor subtypes. The 5-HT_7 receptor has been shown to contribute to descending inhibition in neuropathic pain (Brenchat et al., 2010; Dogrul et al., 2009) and so may also be involved in the present model. Lesion of spinal 5-HT fibres would therefore include both of these aspects, and so these would 'cancel out' one another at the behavioural level in the animal. The window of attenuation observed at 1 and 2 days could reflect the period at which the pro-nociceptive influence of 5-HT predominates in this model. With this in mind it seems unlikely that loss of spinal 5-HT fibres would completely reverse behavioural hypersensitivity. The behavioural findings following 5,7-DHT depletion reflect the net effect of depletion of 5-HT fibres within the spinal cord, which incorporates both inhibitory and facilitatory influences.

The modest effects of 5,7-DHT depletion and 5-HT_3 receptor antagonism observed in this model may also be due to the reliance on paw withdrawal thresholds as our primary outcome measure. This method reflects evoked cutaneous hypersensitivity and does not reflect other features of joint pain such as spontaneous and movement-evoked pain (Mogil, 2009). Combining lesion of the descending 5-HT pathway with other measures to address these aspects may be of interest for future studies. For example measures such as burrowing behaviour (Andrews et al., 2011) and hind limb grip force (Chandran et al., 2009; Lee et al., 2011b) have been used effectively in models of neuropathic and osteoarthritic pain. These measures may also prove useful in understanding the contribution of descending facilitation to inflammatory joint pain.

4.4.5 Conclusion

The aim of this chapter was to determine if the descending 5-HT system contributes to pain behaviour following joint inflammation. A time-dependent role for descending 5-HT fibres in mechanical hypersensitivity in this pain model was identified, and this effect is mediated by the 5-HT_3 receptor.

5. The role of mu opioid receptor expressing RVM neurons in inflammatory joint pain

5.1 Introduction

The previous chapters have shown that the RVM is activated following joint inflammation, and that the descending 5-HT pathway arising in this region contributes in a time dependent manner to the associated mechanical hypersensitivity. However many of the electrophysiologically defined ON cells of the RVM do not contain 5-HT (Potrebic et al., 1994) suggesting that other facilitatory pathways are also in place. It has been shown previously that the mu opioid receptor (MOR+) expressing population plays a crucial role in the maintenance but not the initiation of neuropathic pain states (Bee and Dickenson, 2008; Burgess et al., 2002; Porreca et al., 2001). This chapter describes behavioural experiments carried out to investigate the role of MOR+ neurons in mediating behavioural hypersensitivity associated joint inflammation.

5.1.1 Role of mu opioid receptor expressing neurons in nociception

RVM neurons can be defined by their electrophysiological properties prior to a nociceptive reflex. OFF cells show a decrease in firing before the tail flick reflex, while ON cells show an increase in firing and NEUTRAL cells do not change their firing properties (Fields and Heinricher, 1985; Fields et al., 1983). These cell types can only be characterised in the lightly anaesthetised animal, by application of an acute noxious stimulus, and are not anatomically separated within the RVM. Nonetheless this classification system provides a physiological correlate for the bidirectional modulation of pain states by the RVM. ON cells are the only population which respond directly to morphine, resulting in decreased excitability (Heinricher et al.,

1994; Marinelli et al., 2002). This suggests that only ON cells express the mu opioid receptor (MOR).

MOR expressing (MOR+) cells have a pro-nociceptive role, as inhibition by MOR activation leads to reduced nociceptive responses (Heinricher and Kaplan, 1991; Heinricher et al., 1994; Marinelli et al., 2002). In contrast OFF cells are indirectly activated by MOR agonists, and this is thought to occur via inhibition of MOR+ GABAergic interneurons, which inhibit OFF cells (Heinricher et al., 1992). In addition to these MOR+ interneurons, some ON cells project directly to the spinal cord (Fields et al., 1995). This indicates that there are two ways by which MOR agonists may exert an antinociceptive role within the RVM. One proposed mechanism is that MOR+ neurons act indirectly by disinhibiting spinally projecting inhibitory neurons (Heinricher, Morgan, and Fields 1992; Heinricher et al. 1994; Fields and Heinricher 1985). The other is that some MOR+ neurons are excitatory and project directly to the spinal cord to enhance pain (Marinelli et al., 2002). Anatomical studies have demonstrated that a proportion of 5-HT (Marinelli et al. 2002), and GABA (Kalyuzhny and Wessendorf 1998) expressing RVM neurons also express the MOR. Therefore it is clear that MOR+ RVM neurons are a mixed population, which contain a number of transmitters, and may be either spinally projecting or non-projecting (Marinelli et al. 2002). The net effect of MOR agonism within the RVM is to reduce nociception, directly by decreasing the excitability of pro-nociceptive projection neurons and indirectly by disinhibition of anti-nociceptive projection neurons (figure 5.1).

Regardless of the precise nature of MOR mediated analgesia, it is likely that MOR+ cells are facilitatory in the context of persistent pain. A number of studies have demonstrated that in models of neuropathic (Carlson et al., 2007; Gonçalves et al., 2007) and visceral pain (Sanoja et al., 2010) ON cells show an increase in spontaneous firing.

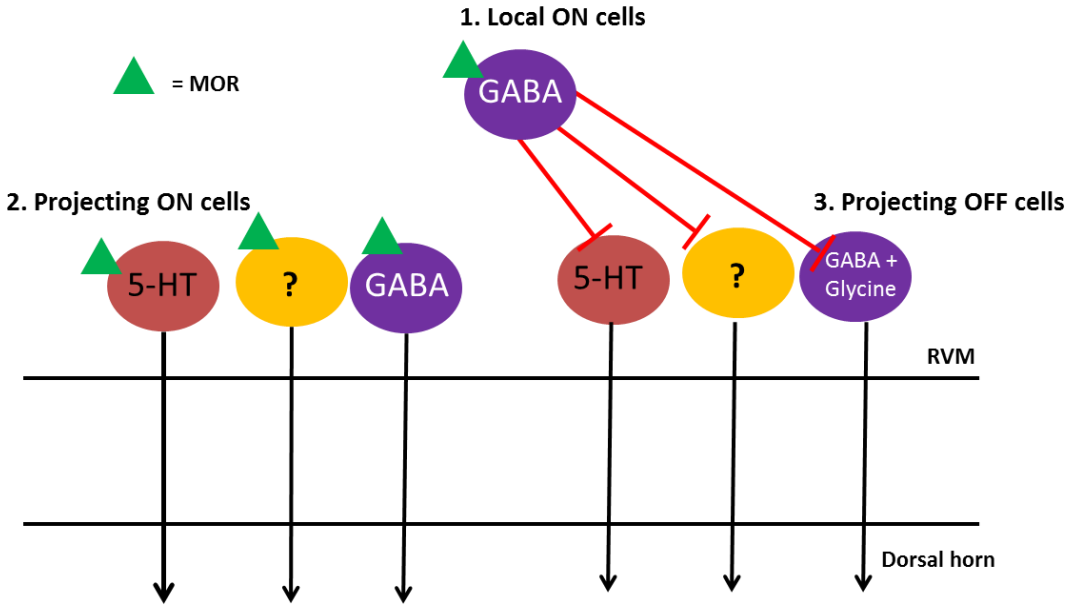

Figure 5.1 Cell types within the RVM.

ON cells are directly inhibited by morphine microinjection to the RVM (Heinricher et al., 1994) suggesting they express the mu opioid receptor (MOR+). OFF cells are not directly modulated by morphine as they do not express the MOR. **1).** Some ON cells are locally projecting GABAergic interneurons, which inhibit OFF cell firing (Kaplan and Fields, 1991). **2).** Other MOR+ cells express 5-HT, and many of these project to the dorsal horn (Marinelli et al., 2002). Some spinally projecting MOR+ cells also express GABA (Kalyuzhyny and Wessendorf, 1998). The '?' represents non-5-HT, non-GABAergic neurons. **3).** OFF cells are MOR-, and these may project directly to the spinal cord and may also contain 5-HT and GABA. GABA and glycine are co-expressed in dorsal horn projection neurons (Hossaini et al., 2012). These OFF cells may be inhibited by morphine indirectly via MOR expressing GABAergic interneurons. Non projecting 5-HT neurons, both MOR+ and MOR-, may also be found in the region, however for simplicity these are not illustrated here.

5.1.2 Saporin-conjugates as selective neurotoxins

The facilitatory role of MOR+ RVM neurons has been investigated previously using a selective targeted toxin delivered to the region. Saporin is a ribosomal inactivating protein which is derived from the plant *Saponaria officinalis*. Upon cell internalisation saporin inhibits protein synthesis and leads to cell death. Alone the saporin peptide cannot be endocytosed. However conjugation to a peptide which can be internalised, such as an

antibody or receptor agonist, allows for internalisation. By choosing peptides that can only be recognised by specific cell types this allows for selective internalisation (Wiley, 1992). Saporin conjugates have proved useful in a number of neurobiological studies by allowing the selective lesion of specific neuronal populations. This lesion technique was first described for NGF receptor expressing neurons of the cholinergic basal forebrain (Wiley et al., 1991). Since then a number of different saporin conjugates have been used to lesion specific cell populations of the nervous system. For example NK1 receptor expressing neurons can be targeted by use of substance P-saporin conjugate (Nichols et al., 1999). This technique allowed for a better understanding of the role of the NK1 receptor positive neurons of the dorsal horn in various models of pain.

5.1.3 Previous studies of pain using dermorphin-saporin

More recently the conjugate dermorphin-saporin has been used to elucidate the role of MOR+ RVM neurons in persistent pain states. In contrast to traditional lesion techniques which are non-selective, dermorphin-saporin microinjection allows for the selective lesion of a subpopulation of pro-nociceptive cells. Dermorphin-saporin has been used extensively to address the role of the RVM in neuropathic pain models, in which MOR+ neurons are required for the maintenance but not the induction of hypersensitivity (Burgess et al., 2002; Porreca et al., 2001). Similarly in a model of pancreatitis, a model of visceral pain, dermorphin-saporin lesion attenuates the maintenance phase of the pain state (Vera-Portocarrero et al., 2006). Furthermore studies using the conjugate CCK-saporin have shown that cholecystokinin receptor expressing RVM neurons are also required for maintenance of neuropathic pain (Zhang et al., 2009). Interestingly this population overlaps with the MOR+ population, adding further to the evidence that these neurons are facilitatory in nature and therefore may correspond to the electrophysiologically defined ON cell population.

Depletion of MOR+ RVM cells has also been used to demonstrate that these neurons contribute to increased neuronal excitability in the dorsal horn (Bee and Dickenson, 2008), as well as being required for enhanced evoked neurotransmitter release from primary afferent fibres (Gardell et al., 2003). These studies demonstrate an important contribution of the MOR+ cell descending pathway in a number of pain models.

5.1.4 Hypothesis

In this chapter I have tested the hypothesis that descending facilitation via MOR+ neurons of the RVM contributes to mechanical hypersensitivity associated with joint inflammation.

5.2 Methods

5.2.1 Dermorphin-saporin and microinjection to RVM

Bilateral microinjection to the RVM was carried out as described in section 2.1.2. Dermorphin-saporin was obtained from Advanced Targeting Systems. This was prepared in sterile saline to generate final injection volumes of 0.5µl for each side of the RVM. A dose of 3pmole dermorphin-saporin (1.5pmole per side) was used in our initial studies, based on previous work by others (Bee and Dickenson, 2008; Burgess et al., 2002; Porreca et al., 2001; Zhang et al., 2009).

The molecular weight of dermorphin-saporin is 32kDA and is purchased in solution, at a concentration of 1.4µg/µl. The number of moles per µl of purchased stock solution was calculated from the following:

Weight (g) = no. moles x MW (kDa) x 10^3

1.4µg = no. moles x 32kDA x 10^3

no. moles = 43.73pmole per 1µl of stock solution

The total injection volume used was 1µl (0.5µl each side) and dermorphin-saporin was made up to contain 3pmole (96ng) dermorphin-saporin in total. This corresponds to a final molarity of 3µM.

As adverse effects were observed at this dose (see below, section 5.3.1), it was decided to use two lower doses, of 1.5µM (containing 1.5pmole/48ng) and 0.75µM (containing 0.75pmole/24ng).

5.2.2 Inflammatory pain model and behavioural testing

Animals received ankle injection of CFA or underwent a sham procedure at 28-35 days post RVM injection. Paw withdrawal thresholds were measured and log2 transformation was carried out to normalise the data (see section 2.2). Statistical analysis was carried out in SPSS. Analysis of variance (ANOVA) with repeated measures was carried out with time as the within subjects factor, and CFA and dermorphin-saporin treatment as the between subjects factors. A significant main effect of CFA was a prerequisite for subsequent ANOVAs or post-hoc analysis.

5.2.3 MOR immunohistochemistry

To determine the accuracy of injection sites and extent of MOR+ cell depletion within the RVM dermorphin-saporin treated and control animals were perfused and immunohistochemistry carried out as described in section 2.4. For each animal a set of 40µm sections representing the RVM region, with all sections at least 240µm apart were used for MOR immunohistochemistry. Staining was carried out using a MOR specific antibody (1:10,000, rabbit, Neuromics) and tyramide signal amplification (see section 2.4.3). Counterstaining with NeuN (1:1000, mouse, Cell Signalling) was used to detect all neurons. Imaging was carried out using a fluorescence microscope (see section 2.4.5). MOR+ cells were counted manually, while blind to the treatment group of the animal. The RVM was defined as the regions containing the NRM and GiA at approximately -10.3

to -11.3 mm from Bregma. The anatomical boundaries used to define the region were the presence of the facial nuclei and pyramidal tracts. Sections were deemed caudal of the RVM if the nucleus ambiguus was present. The number of MOR+ cell bodies per section was counted and recorded. The five highest scoring sections per animal were used as representative of the RVM region. The total number of MOR+ cells across the five sections was calculated and the data is presented as the mean ± SEM per group. Representative images were acquired using a Hamamatsu digital camera and Openlab 4.0.4 software from Improvision. In some cases, confocal imaging was carried out using a laser scanning Leica TCS NT SP microscope.

5.2.4 Localisation of needle tracts

At the end of the final experiment which involved injection of 1.5pmole dermorphin-saporin (experiment 3, see below section 5.3.3) animals were culled by CO_2 asphyxiation to allow fresh tissue dissection for RNA extraction, brains were removed fresh and post fixed for 2 days in 4% PFA. Sectioning was carried out as for immunohistochemistry and sections were incubated briefly with DAPI (4',6-diamidino-2-phenylindole, 1:10,000 in 0.1M PB for 10mins). DAPI labelling was used to visualise the outline of the needle tracts for each animal. Using the rat brain atlas (George Paxinos, 1998) the approximate anterior-posterior, dorsal-ventral and lateral coordinates were noted for each animal.

5.3 Results

5.3.1 Experiment 1: Dermorphin-saporin (3pmole) microinjection to the RVM attenuates inflammatory pain

Animals underwent RVM microinjection of either dermorphin-saporin (1.5pmole each side) or saline and allowed to recover for 28-35 days. Baseline mechanical paw withdrawal thresholds were taken each day for three days prior to CFA injection. The saline injected animals were divided

into two groups, one receiving CFA injection to the ankle and the other a sham procedure (n = 8 in CFA groups, n = 4 in sham group). All dermorphin-saporin treated animals received CFA injection. A three-way analysis of variance (ANOVA) with repeated measures was carried out to determine if CFA and dermorphin-saporin treatment had significant effects on paw withdrawal threshold. Time was the within-subject factor and dermorphin-saporin treatment and CFA were the between-subjects factors. The tests of within-subjects effects indicated there was a significant effect of time ($p < 0.001$), a time x dermorphin-saporin interaction ($p < 0.001$) and a time x CFA interaction ($p < 0.001$). The between-subjects analysis indicated there was an overall effect of dermorphin-saporin ($p = 0.024$) and CFA ($p = 0.001$). See table 5.1 for a summary of this analysis.

Factor	df	F	Error	P
Time	10	11.4	170	< 0.001
CFA	1	17	14.8	0.001
Dermorphin-saporin	1	17	6.2	0.024
Time x CFA	10	6.9	170	<0.001
Time x Dermorphin-saporin	10	4.3	170	<0.001

Table 5.1 Results of three-way ANOVA with repeated measures on ipsilateral paw withdrawal thresholds following 3pmole dermorphin-saporin.

As there were main effects of both dermorphin-saporin and CFA, a subsequent two-way ANOVA with repeated measures was carried out on the two CFA injected groups, to determine if there was an overall effect of dermorphin-saporin from 2h to 7d post CFA injection (table 5.2). It was found that there was an overall effect of dermorphin-saporin on paw withdrawal thresholds ($p = 0.023$) from 2h to 7d following CFA injection (figure 5.2a).

Factor	df	F	Error	P
Time	7	9.3	98	0.0001
Dermorphin-saporin	1	6.479	14	0.023
Time x Dermorphin-saporin	7	2.6	98	0.018

Table 5.2 Results of two-way ANOVA with repeated measures on ipsilateral paw withdrawal

thresholds form 2h – 7d post CFA following 3pmole dermorphin-saporin.

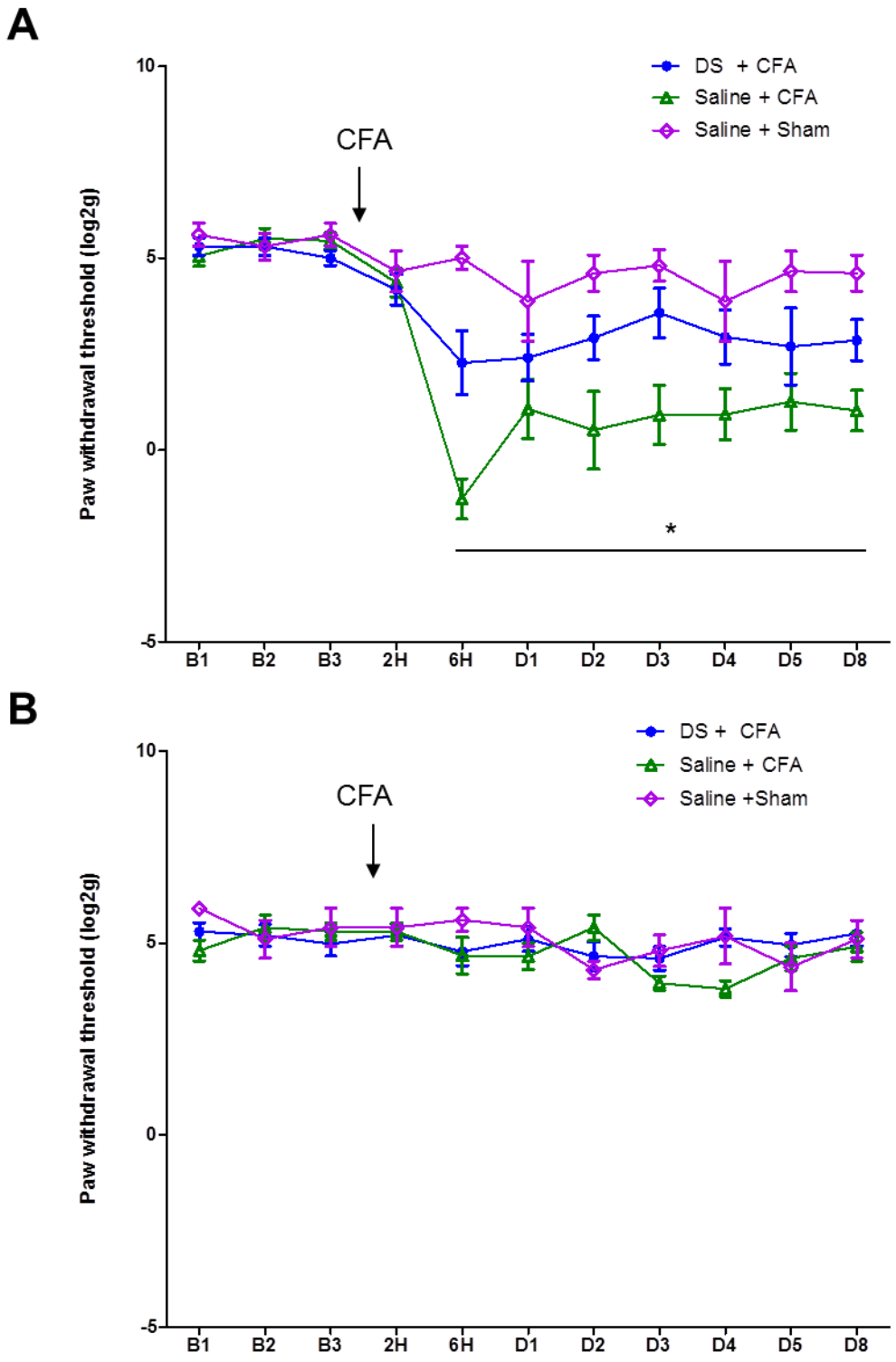

Figure 5.2 Attenuation of mechanical hypersensitivity by 3pmole dermorphin-saporin.

A). Attenuation of mechanical hypersensitivity in dermorphin-saporin (DS, 3pmole in total,

1.5pmole each side) microinjected rats following ankle joint inflammation by CFA injection. Ipsilateral paw withdrawal thresholds were significantly higher in the dermorphin-saporin group compared with saline injected controls. * p = 0.023, overall effect of dermorphin-saporin pre-treatment from 2h to 7d following ankle injection of CFA, two-way ANOVA with repeated measures. **B).** Paw withdrawal thresholds of the contralateral hindpaw were not altered by CFA injection or by dermorphin-saporin pre-treatment, p > 0.05, three-way ANOVA with repeated measures. Data is presented as log2 (paw withdrawal threshold in g) and mean ± SEM, n = 8 in CFA groups, n = 4 in saline + sham group.

On the contralateral paw, the within-subjects effects indicated that there a main effect of time (p = 0.011), but not of CFA or dermorphin-saporin (p > 0.05). As there was no main effects of CFA or dermorphin-saporin no further analysis was carried out. This indicates contralateral paw withdrawal thresholds were unaffected by either dermorphin-saporin pre-treatment or CFA injection (figure 5.2b).

To confirm the efficacy of dermorphin-saporin in ablating MOR+ RVM neurons, MOR immunohistochemistry was carried out at the end of the experiment in a subset of animals (n = 4 – 5, CFA treated groups only). Sample immunohistochemistry from animals treated with this dose of dermorphin-saporin compared with saline controls is shown (figure 5.3c). Cell counts indicated there was a significant decrease in MOR+ neurons with 197 ± 17.61 in saline compared with 131.4 ± 9.56 in the dermorphin-saporin treated group at this dose (3pmole in total, 1.5pmole each side) (independent samples t-test, p = 0.0145, figure 5.3d). The approximate area used for cell counts is outlined (figure 5.3a) and corresponds to approximately 1.56mm² per section. Notably the distribution of MOR+ cells identified by immunohistochemistry here is similar to that of a recent report, which studied MOR+ cell distribution in the RVM by microinjection of dermorphin conjugated to the fluorophore Alexa 594 (Phillips et al., 2012).

Figure 5.3 Decrease in MOR+ cell numbers by 3pmole dermorphin-saporin.

A). The area used for cell counting is outlined by the red triangle, with each section corresponding to approximately 1.56mm². Image adapted from the rat brain atlas (George Paxinos, 1998) **B).** The image in B is from Phillips et al., 2012, and illustrates the distribution of MOR expressing neurons within the RVM, based on labelling by microinjection of dermorphin conjugated to Alexa 594. **C).** Representative images illustrate MOR+ expression in a saline injected animal, illustrating that MOR immunohistochemistry identified a population of neurons similar to that in Phillips et al., 2012. Depletion of MOR+ cells can be observed in the bilaterally injected dermorphin-saporin (DS, 3pmole/96ng) animal. Scale bar indicates 200µm. **D).** Cell counts indicate a significant decrease in MOR+ cell number within the RVM of dermorphin-saporin animals. Cell counts were calculated as the sum of the top five sections per animal, and data is shown here as mean ± SEM per group. n = 5 in dermorphin-saporin group, n = 4 saline, * p = 0.0145 independent samples t-test.

A decrease in MOR mRNA expressing neurons within the RVM and attenuation of neuropathic pain behaviour had been shown previously using this dose of dermorphin-saporin (Bee and Dickenson, 2008; Burgess et al., 2002; Porreca et al., 2001). However in our study adverse effects were observed in a number of dermorphin-saporin treated animals. These effects included weight loss, motor impairment, and ataxia. These effects became noticeable at approximately 2 weeks following microinjection to the RVM. Of the 16 animals injected with dermorphin-saporin, 8 were culled due to these adverse effects. We attributed these effects to non-specific loss of neurons in the RVM and surrounding regions, as there was some evidence of necrosis at the sites of injection. For this reason we aimed to determine if lower doses of dermorphin-saporin could lead to attenuation of behavioural hypersensitivity without these adverse effects.

5.3.2 Experiment 2: Dose dependent effects of dermorphin-saporin

A pilot experiment was carried out to determine if lower doses of dermorphin-saporin would attenuate pain behaviour and decrease MOR+ neuron numbers in the RVM without adverse effects. Animals were injected with saline, 1.5pmole (0.75pmole each side) or 0.75pmole (0.375pmole each side) dermorphin-saporin and allowed to recover for 28 days. No adverse

effects were observed in either of the dermorphin-saporin groups (n = 3 – 4). Baseline mechanical paw withdrawal thresholds were measured each day for three days prior to CFA injection, and up to 7 days later. A two-way ANOVA with repeated measures was carried out to compare the ipsilateral paw withdrawal thresholds across these doses compared to saline microinjected animals, with time as the within-subjects factor and dose (1.5pmole, 0.75pmole or saline) as the between-subjects factor. The within-subjects effects indicated a significant effect of time ($p < 0.001$) and a significant time x dose interaction ($p = 0.015$). The between-subjects effects indicated an overall effect of dose ($p = 0.007$). The results of this analysis are shown in table 5.3. As there was a significant effect of dose and a dose x time interaction, one-way ANOVAs at each time point were subsequently carried out to identify the source of variation. LSD post hoc analysis indicated there was a significant difference in paw withdrawal thresholds at all time points post CFA between the 1.5pmole dose and saline groups ($p = 0.004$) and between the 0.75pmole dose and saline groups ($p = 0.005$). There was no difference between 1.5pmole and 0.75pmole groups ($p = 0.649$). This suggested that lower doses of dermorphin-saporin could be used to attenuate behavioural hypersensitivity (figure 5.4a).

	df	**F**	**Error**	**p**
Time	12	80.5	84	0.000
Dose	2	10.89	7	0.007
Time x dose	24	80.5	1.9	0.015

Table 5.3 Results of two-way ANOVA with repeated measures on ipsilateral paw withdrawal thresholds following 1.5pmole or 0.75pmole dermorphin-saporin.

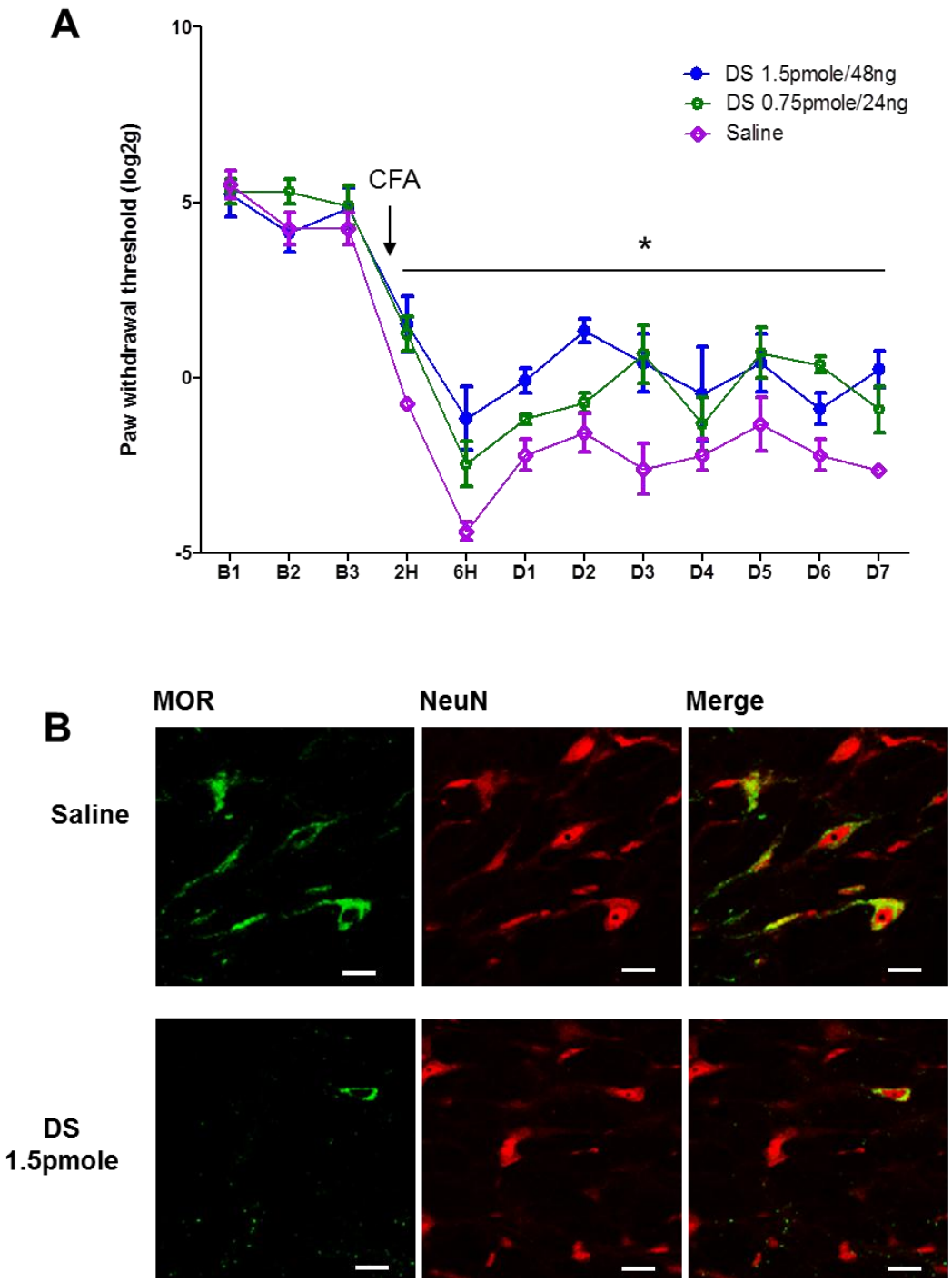

Figure 5.4 Attenuation of mechanical hypersensitivity and depletion of MOR+ cells by 1.5pmole and 0.75pmole dermorphin-saporin.

A). Attenuation of mechanical hypersensitivity of the ipsilateral hindpaw in dermorphin-saporin (1.5pmole in total, 0.75pmole each side) pre-treated rats following ankle joint inflammation. Both the 1.5pmole and 0.75pmole doses of dermorphin-saporin significantly attenuated paw withdrawal threshold from 2h – 7d post CFA injection. * indicates p = 0.004

for the 1.5pmole v saline comparison, and p = 0.005 for the 0.75pmole v saline comparison, two-way ANOVA with repeated measures and LSD post hoc test. Data is presented as log2 (paw withdrawal threshold in g) and mean ± SEM, n = 3 – 4. **B).** Representative confocal images of MOR immunohistochemistry in the 1.5pmole dermorphin-saporin group and saline control. Double labelling with NeuN indicated that although many MOR+ neurons are depleted at this dose, some surviving MOR- neurons remain in the region. Scale bars indicate 25μm.

Single plane confocal images taken from animals with and without dermorphin-saporin (1.5pmole dose) indicated that although this dose results in depletion of MOR+ neurons as expected, there are some NeuN positive cells remaining (figure 5.4b). This suggests that at this dose dermorphin-saporin is selectively toxic to MOR+ neurons. MOR+ cell counts were carried out at both doses as before. A decrease in MOR+ cell numbers in the 1.5pmole group (155 ± 4) was found when compared with saline control (208.7 ± 14.2) (one-way ANOVA with LSD post hoc test, p = 0.009, 1.5pmole v saline, see figure 5.5a). The decrease in cell numbers in the 0.75pmole treated group was not significant (188.75 ± 4.5, p = 0.124).

Plotting the number of MOR+ cells against paw withdrawal thresholds per animal in each of the three groups (figure 5.5b, illustrated for the 6h, d1, d2 and d7 time points) indicated that there was a significant correlation between cell number and paw withdrawal threshold at the 6h (R^2 = 0.4643 and p = 0.003), 1d (R^2 = 0.7548 and p = 0.0011), 2d (R^2 = 0.7337 and p = 0.016) and 7d (R^2 =0.416 and p=0.042) time points using the Pearson correlation. At other time points no significant correlation was found between MOR+ cell number and paw withdrawal threshold (table 5.4).

Time point	p	R^2
2H	0.151	0.2354
6H	0.003	0.4643
D1	0.0011	0.7548
D2	0.0016	0.7337
D3	0.2136	0.1786
D4	0.3224	0.1221
D5	0.4564	0.07110
D6	0.02948	0.6353
D7	0.0452	0.416

Table 5.4 Results of Pearson correlation analysis of number of MOR+ cells and ipsilateral paw withdrawal thresholds for individual animals following dermorphin-saporin.

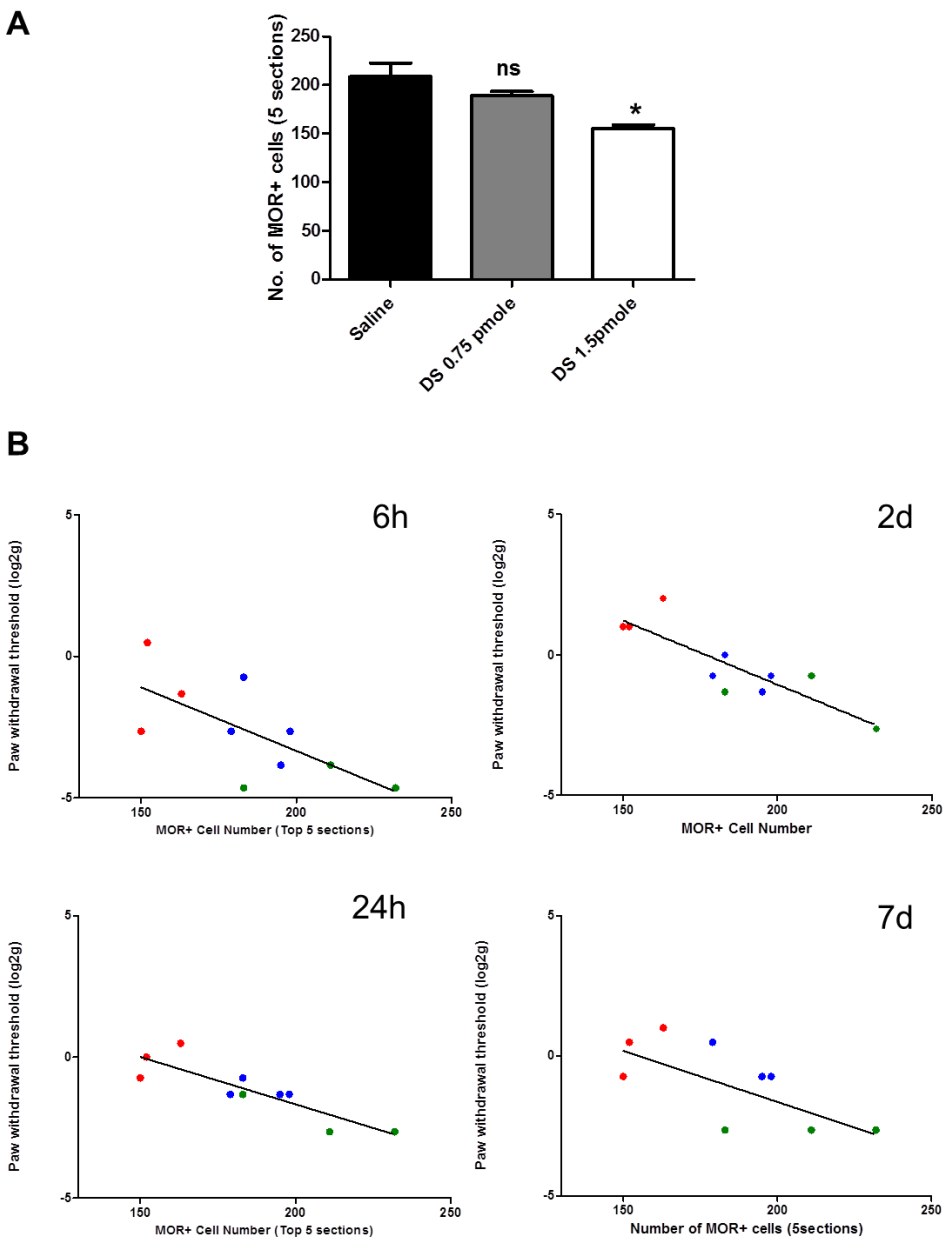

Figure 5.5 Dose dependent decrease in MOR+ cell number by dermorphin-saporin.

A). Cell counts indicate a significant decrease in MOR+ cell number in animals treated with 1.5pmole dermorphin-saporin (DS) but not 0.75pmole dermorphin-saporin. Cell counts were calculated as the sum of the top five sections per animal, and data shown here as mean ± SEM per group. n = 3 – 4, one-way ANOA with LSD post hoc test, * p = 0.009. **B).** Plot of paw withdrawal thresholds presented as log2 (paw withdrawal threshold in g), and number of MOR+ cells per animal at 6h, 1d, 2d and 7d following ankle injection of CFA. Green dots represent saline treated animals, blue dots represent 0.75pmole treated animals and red dots represent 1.5pmole treated animals. $p < 0.05$, Pearson correlation.

5.3.3 Experiment 3: Attenuation of behavioural hypersensitivity from 1 – 7d post CFA injection by microinjection of 1.5pmole dermorphin-saporin

In all further experiments the 1.5pmole dose (0.75pmole each size) was used. A complete, fully blind experiment was carried out with 4 groups of animals: dermorphin-saporin + CFA, saline + CFA, dermorphin-saporin + sham and saline + sham (figure 5.6). Three-way ANOVA with repeated measures was used to analyse the ipsilateral paw withdrawal thresholds. The within-subjects effects indicated a significant effect of time, time x CFA interaction and time x dermorphin-saporin x CFA interaction, but no time x dermorphin-saporin interaction ($p = 0.625$). The between-subjects tests indicated a significant effect of CFA ($p < 0.001$) but not of dermorphin-saporin ($p = 0.15$) or dermorphin-saporin x CFA interaction ($p = 0.534$). The tests of within-subjects effects indicated there was a significant effect of time ($p < 0.001$), a time x CFA interaction ($p < 0.001$) but no time x dermorphin-saporin interaction. The between-subjects analysis indicated there was no overall effect of dermorphin-saporin but there was an overall effect of CFA ($p < 0.001$). Table 5.5 is a summary of this analysis.

Factor	df	F	Error	P
Time	15	46	375	0.001
CFA	1	164	25	0.000
Dermorphin-saporin	1	2.21	25	0.15
CFA x Dermorphin-saporin	1	0.397	25	0.534
Time x CFA	15	44.2	375	0.001
Time x Dermorphin-saporin	15	0.847	375	0.625
Time x CFA x Dermorphin-saporin	15	2.416	375	0.002

Table 5.5 Results of three-way ANOVA with repeated measures on ipsilateral paw withdrawal thresholds following 1.5pmole dermorphin-saporin.

A subsequent two-way ANOVA with repeated measures was carried out on the two CFA treated groups, from 1d to 7d post CFA, and it was found that there was an overall main effect of dermorphin-saporin treatment on paw withdrawal thresholds from 1 to 7d post CFA injection ($p = 0.018$). Table 5.6 lists the results of this analysis. This indicates that dermorphin-saporin pre-treatment leads to attenuation of mechanical hypersensitivity from 1 to 7 days post CFA injection (figure 5.6a).

Factor	df	F	Error	p
Time	1	3.7	14	0.075
Dermorphin-saporin	1	7.161	14	0.018
Time x dermorphin-saporin	1	7.326	14	0.017

Table 5.6 Results of two-way ANOVA with repeated measures on ipsilateral paw withdrawal thresholds from 1 – 7 d post CFA following 1.5pmole dermorphin-saporin.

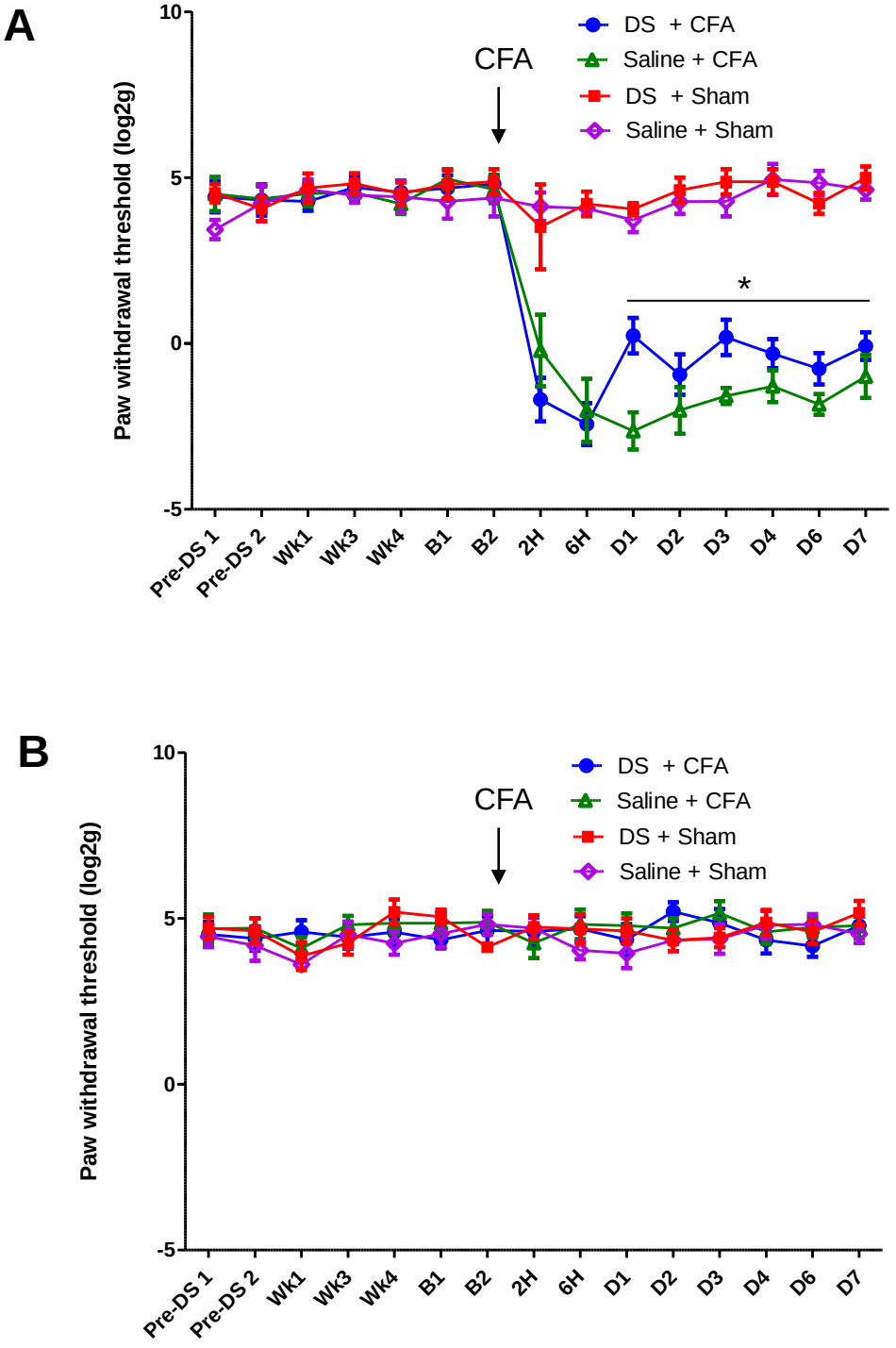

Figure 5.6 Attenuation of mechanical hypersensitivity by 1.5pmole dermorphin-saporin. **A).** Attenuation of mechanical hypersensitivity of the ipsilateral hindpaw in dermorphin-saporin (DS, 1.5pmole in total, 0.75pmole each side) pretreated rats following ankle joint inflammation. Paw withdrawal thresholds were significantly higher in the dermorphin-saporin group than in saline injected controls from 1 to 7d post CFA injection * p = 0.018,

dermorphin-saporin CFA v saline CFA, two-way ANOVA with repeated measures. There was no effect of pre-treatment on baseline paw withdrawal thresholds. **B).** Paw withdrawal thresholds of the contralateral hindpaw were not altered by CFA injection or by dermorphin-saporin pre-treatment, $p > 0.05$, three-way ANOVA with repeated measures. Data is presented as log2 (paw withdrawal threshold in g) and mean ± SEM, n = 8 in CFA groups, n = 6 /7 in sham groups.

The contralateral paw withdrawal thresholds were analysed in the same way using a three-way ANOVA with repeated measures but no main effects of time, CFA or dermorphin-saporin were found. The results of this analysis are given in table 5.7. This indicates neither CFA nor dermorphin-saporin treatment affected contralateral paw withdrawal thresholds (figure 5.6b).

Factor	df	F	Error	P
Time	14	1.273	350	0.222
Dermorphin-saporin	1	25	2677.524	0.897
CFA	1	0.467	25	0.349
Time x Dermorphin-saporin	14	0.647	350	0.825
Time x CFA	14	1.063	350	0.391
Time x Dermorphin-saporin x CFA	14	0.76	350	0.712

Table 5.7 Results of three-way ANOVA with repeated measures on contralateral paw withdrawal thresholds following 1.5pmole dermorphin-saporin.

At the end of the experiment, animals were culled by CO_2 asphyxiation and the dorsal quadrants of the lumbar spinal cord were dissected and frozen rapidly at -80^{o}C for later experiments (see chapter 6). The brains of these animals were also removed fresh and immersion fixed for 48h in 4% PFA. All brains were sectioned and stained using DAPI to identify the needle tracts. The approximate anterior-posterior, dorsal-ventral and lateral coordinates for the visible needle tracts were noted for all the animals from this experiment (table 5.8) and the approximate locations are illustrated for those in the CFA groups are shown (figure 5.7). The needle tracts of two animals from the saline-CFA group could not be identified, but for all other animals it was found that at least one of the bilateral injections was within

or close to the dorsal-ventral boundary of the RVM. Similarly the anterior-posterior coordinates were satisfactory for all animals (within the region of -10.5mm to -11.8mm from Bregma). Although those at -11.6mm and -11.8mm could be deemed caudal, the spread of the toxin is likely to be sufficient to ensure considerable depletion in the target area. For example in experiment 1, depletion of neurons was noted as far rostral as -10mm and as far caudal as -12.3mm from Bregma. The lateral coordinates were somewhat variable but bilateral injection would be expected to produce a sufficient distribution throughout the RVM.

Figure 5.7 Confirmation of bilateral microinjection sites of animals used in experiment 3. Only animals from the dermorpin-saporin + CFA group (dots labelled DS) and saline + CFA group (dots labelled saline) are shown. The numbers indicate the approximate anterior-posterior distance from Bregma in mm.

Group	Animal	AP	Right	Left	DV
Saline + CFA	1	11	0.8	0.8	9.2
	15	10.52	1	0.8	8.5
	19	11	0.4	0.4	8
	29	x	x	X	X
	39	x	x	X	X
	47	10.52	0.6	0.4	10
	49	10.52	0.3	0.9	10
	59	10.52	0.8	0.4	8.5
DS + CFA	3	11.8	0.6	0.8	9
	13	11	0.9	0.8	8.2
	21	10.8	0.6	0.5	8.8
	31	10.8	1	0.5	9.5
	35	10.8	0.5	0.6	9.5
	37	10.52	0.5	0.5	10
	45	11.6	1.2	0.4	9.5
	53	10.8	0.5	0.5	9.5
Saline + Sham	7	11	0.8	0.6	9
	9	10.8	0.8	0.6	8.7
	17	11.6	0.8	0.7	9.2
	25	10.52	0.8	0.6	9
	41	10.8	1	0	8
	51	10.52	0.4	0.4	10
DS + Sham	5	10.8	0.8	0.8	10
	11	11	0.8	0.4	9.5
	23	11.3	0.6	0.6	9.5
	27	10.8	0.4	0.4	9.5
	33	11	0.6	0.6	9.5
	55	10.3	0.5	0.8	10
	57	10.52	0.9	0.3	9

Table 5.8 Bilateral microinjection sites for all animals in experiment 3.

DS = dermorphin-saporin, AP = anterior-posterior (from Bregma), DV = dorsal-ventral (from top of brain surface), and right and left indicate lateral values are from the midline. Values are in mm.

5.4 Discussion

The selective neurotoxin dermorphin-saporin has been used in a number of studies to demonstrate a role for MOR+ neurons of the RVM in the maintenance phase of neuropathic pain behaviour (Bee and Dickenson,

2008; Burgess et al., 2002; Porreca et al., 2001; Zhang et al., 2009). As discussed in chapter 4, considerable evidence suggests a role for spinal 5-HT in the descending facilitation of cutaneous inflammatory pain (Géranton et al., 2008; LaGraize et al., 2010) and dorsal horn excitability in the MIA model of osteoarthritis (Rahman et al., 2009). Although it is known that some of the MOR+ neurons contain 5-HT (Marinelli et al., 2002; Wang and Wessendorf, 1999) to date the specific role of MOR+ neurons has not been studied in inflammatory joint pain. Using dermorphin-saporin lesion of the RVM we have demonstrated a role for these cells in the facilitation of inflammatory joint pain behaviour, suggesting that the 5-HT and MOR+ neurons of the RVM serve as partially overlapping but synergistic pathways in joint inflammation.

5.4.1 Dermorphin-saporin treatment: investigation of doses and side effects

The first experiment described in this chapter involved the use of 3pmole dermorphin-saporin injected into the RVM to ablate the MOR+ population of neurons within the region. This dose has been described previously in the literature, by a number of groups and in various pain models (Bee and Dickenson, 2008; Burgess et al., 2002; Vera-Portocarrero et al., 2006). These studies demonstrated that in neuropathic and pancreatitis-induced pain dermorphin-saporin pre-treatment attenuated the maintenance of behavioural hypersensitivity to mechanical stimuli but had no effect on the initial phase of the pain state. This chapter describes a similar experiment which found that this dose is also effective in attenuating inflammatory joint pain. Compared with behavioural studies of neuropathy and pancreatitis, the magnitude of the effect described here is smaller as we do not see a complete reversal of behavioural hypersensitivity (Bee and Dickenson, 2008; Burgess et al., 2002; Vera-Portocarrero et al., 2006). Also notable is that even at 6h post CFA injection attenuation of behavioural hypersensitivity is

observed. This suggests that this dose of dermorphin-saporin is effective in attenuating both the early (6h) and late (up to 7d) phases of inflammatory joint pain.

Importantly however it was found in the initial pilot study that bilateral injections of this dose resulted in adverse effects in 50% of animals, requiring them to be culled. These effects included motor impairments such as loss of balance, catalepsy and lack of coordination of limbs. Considerable weight loss was also observed in some animals. No previous reports of unwanted effects with this dose have been described (Porreca et al. 2001; Burgess et al. 2002; Vera-Portocarrero et al. 2006; Bee and Dickenson 2008; Zhang et al. 2009). However three observations suggest that these effects were indeed related to the extent of cell loss within the medulla. Firstly, saline injected control animals never developed any complications suggesting that it is not due to the microinjection technique or surgery. Second, these side effects consistently emerged at 1 to 2 weeks following microinjection. This is the point at which saporin is likely to cause cell death (Mantyh et al., 1997). Finally these adverse effects appear to be directly proportional to the number of MOR+ cells lost by dermorphin-saporin treatment as at the lower doses described in the second experiment, where the decrease in MOR+ cell number is reduced, no adverse effects were observed. It is also possible that higher doses of dermorphin-saporin could lead to dissociation of the complex, and death of non-specific death of MOR- cells.

The finding that a 'high' dose of dermorphin-saporin results in adverse effects highlights the difficulty in using lesion techniques in a small, complex brain region. The RVM is typically defined as consisting of the NRM and GiA regions. However within the anatomical boundary outlined by the GiA are a number of additional nuclei, including the nucleus raphe pallidus (RPa). The RPa is located along the midline, ventral to the NRM. Although the role of

the RPa in nociception has not been directly investigated it is known that MOR+ cells are located in this region (Phillips et al., 2012) and therefore likely to be affected by dermorphin-saporin treatment. The RPa as well as the more caudal raphe obscurus (ROb) are implicated in the modulation of feeding behaviour (Takase and Nogueira, 2008) therefore depletion of neurons in these regions may contribute to the weight loss observed in a number of animals. In addition these regions project to brainstem regions involved in motor control and directly to the ventral horn (Veasey et al., 1995) which may explain the motor impairments observed. Interestingly high doses of muscimol, a $GABA_A$ receptor agonist, was found to cause similar neurological impairments when injected to the RVM at co-ordinates comparable with those used here (Gilbert and Franklin, 2001). These authors suggest that at higher doses, the drug may reach more caudal regions of the RVM which play a role in motor control. The same may be true in our work. Higher doses of dermorphin-saporin may lead to a broader distribution and result in lesion of cells required for other important functions. In general it should be noted that the medullary raphe nuclei play a crucial role in cardiovascular, gastrointestinal and respiratory controls (Lovick 1997). Manipulation of the region in the study of nociceptive responses may therefore lead to alterations in these crucial homeostatic functions. Monitoring motor behaviours and weight gain following microinjection of toxins to the RVM is therefore important in these types of studies.

By carrying out a small dose-response experiment, it was found that injection of lower doses of dermorphin-saporin also leads to attenuation of hypersensitivity, however importantly these lower doses do not result in the unwanted toxicity of the higher dose. The attenuation of hypersensitivity is smaller than that observed for the 3pmole dose, resulting in only a 20% reduction in mechanical hypersensitivity. The dose-response effect suggests this is due to fewer MOR+ cells depleted by lower dermorphin-saporin doses. This was confirmed by MOR+ cell counts, which indicated that at the

two lower doses fewer MOR+ cells are lost. Interestingly there was no significant effect of the lowest dose (0.75pmole) on MOR+ cell numbers compared to saline controls, despite a significant effect on behaviour at this dose. One possible explanation for this discrepancy is that lower doses of dermorphin-saporin may take longer to cause death of MOR+ neurons. Despite the immunohistochemical detection of many MOR+ neurons in this treatment group, some of these neurons may be in the process of dying and not functioning optimally, leading to significant attenuation of hypersensitivity compared to the saline group. At the 6h, 1d, 2d and 7d time points post CFA injection there is a direct correlation between MOR+ cell number and mechanical paw withdrawal thresholds per individual animal. This suggests that the behavioural effects observed in our lesion studies are strongly dependent on the number of cells depleted.

This study is therefore the first to suggest that depletion of even a small number of MOR+ neurons can lead to a reduction in behavioural hypersensitivity. Conversely the complete reversal in neuropathic pain sensitivity described in previous studies (Burgess et al., 2002; Porreca et al., 2001; Zhang et al., 2009) would likely require a complete ablation of MOR+ neurons. As demonstrated in this chapter this is difficult to achieve without considerable adverse effects. Interestingly, adverse effects of dermorphin-saporin microinjection to the RVM had not been described by others previously and the source of this discrepancy is not clear. In most cases the same dose of toxin was used, in the same size and strain of rat, and at similar microinjection sites (Bee and Dickenson, 2008; Burgess et al., 2002; Porreca et al., 2001; Zhang et al., 2009). One possible explanation is batch to batch variation in dermorphin-saporin. Notably, one recent study has described the use of a dose of 1.8pmole dermorphin-saporin in the study of stress induced hyperalgesia (Reynolds et al., 2011). These authors mention that this dose is modified from the Porreca et al. study, however do not discuss if adverse effects were identified at higher does. Nonetheless along

with our findings, this highlights the importance of determining an optimal working concentration by individual laboratories.

Regardless of the cause of this discrepancy, in our studies a compromise between the extent of the lesion and efficacy in attenuation of behavioural hypersensitivity was required. Notably, survival of MOR- neurons within the RVM has not been convincingly demonstrated in these previous studies. Here we have demonstrated that the effects of dermorphin-saporin on behaviour are dose-dependent, and also that the selectivity of the lesion for MOR+ expressing neurons can be confirmed, at least at the lower doses than described previously in the literature.

5.4.2 Role of MOR+ cells in descending facilitation from 1d post CFA injection

Carrying out a complete, fully blinded and controlled experiment with this lower dose of dermorphin-saporin, it was found that attenuation of mechanical hypersensitivity only occurs from 1d onwards and that in the early stages of inflammation, at 2h and 6h post CFA, MOR+ cells are not required for behavioural hypersensitivity. As explained above, this may be due to insufficient ablation of MOR+ neurons, with the surviving cells having a facilitatory effect in this initial window. More likely however is that this behavioural experiment indicates important differences in the timing of descending modulation in neuropathic and inflammatory pain. Lesion of the RVM with dermorphin-saporin has no effect in the first 5 days of neuropathic pain behaviour (Burgess et al., 2002; Porreca et al., 2001; Zhang et al., 2009), and from that point onwards, a gradual reversal of sensitivity occurs. In contrast we find that attenuation of inflammatory joint pain occurs earlier but that the magnitude of attenuation is consistent throughout the period studied. This indicates that during joint inflammation descending facilitation via the MOR+ pathway becomes active from 24h onwards but does not increase or decrease in magnitude from that time.

This supports previous electrophysiological findings indicating that following inflammation, increased descending inhibition occurs in the acute phase (Cervero et al., 1991; Ren and Dubner, 1996; Schaible et al., 1991) but that this is not present in the maintenance phase (Danziger et al., 2001). In our experiment, in which descending facilitatory cells are depleted, this would explain why no apparent change occurs in the initial 24 hours of inflammation as at this point descending inhibitory controls may predominate. The effects of dermorphin-saporin lesion on descending facilitation are only unmasked later when descending inhibition is decreased.

Notably, dermorphin-saporin lesion has no effect on paw withdrawal thresholds before CFA treatment. This suggests that in the normal healthy animal, before induction of hypersensitivity by injection of CFA, there is no effect of dermorphin-saporin lesion on the response to mechanical stimulation. Although this may be due to a failure of our measure of paw withdrawal threshold to detect changes in nociceptive responses, it most likely indicates that in order for the descending facilitatory system to become active there must be an initial increase in nociceptive input. This supports previous findings regarding the electrophysiological responses of dorsal horn neurons to stimulation following dermorphin-saporin depletion of the MOR+ cell population, in which innocuous mechanical stimulation with von Frey hairs is not affected by the depletion (Bee and Dickenson, 2008)

5.4.3 Potential mechanisms underlying descending facilitation via MOR+ cells

MOR+ cells represent approximately half of all dorsal horn projecting RVM neurons (Gutstein et al., 1998; Kalyuzhny and Wessendorf, 1998; Mansour et al., 1994; Wang and Wessendorf, 1999), and approximately half of spinally projecting 5-HT expressing neurons are MOR+ (Kalyuzhny and

Wessendorf, 1998). Chapter 4 has described the role of descending 5-HT in facilitating behavioural hypersensitivity at 1d and 2d post inflammation. In this chapter the role of descending facilitation via MOR+ RVM neurons is addressed in a separate lesion experiment, however the results should be interpreted with the understanding that part of the effect of dermorphin-saporin lesion is via a reduction in 5-HT fibres projecting to the dorsal horn. However in contrast to the data from the 5,7-DHT experiment, an overall attenuation of hypersensitivity is observed following dermorphin-saporin treatment from 1 – 7 d post inflammation. This suggests that other mechanisms besides descending 5-HT are involved in MOR+ cell mediated descending facilitation.

Another important transmitter within the RVM during pain states is cholecystokinin (CCK). CCK is a peptide expressed within many of the same regions as endogenous opioids and has been shown to antagonise their analgesic effects (Faris et al., 1983). Within the RVM CCK administration has pro-nociceptive effects on visceral pain by colorectal distension (Friedrich and Gebhart, 2003) and contributes to morphine induced hyperalgesia (Xie et al., 2005). Administration of a CCK_2 antagonist to the RVM has been shown to reverse neuropathic hypersensitivity (Kovelowski et al., 2000) and CCK is known to increase ON cell firing (Heinricher and Neubert, 2004). Recently it has been shown that the MOR+ population overlaps considerably with the CCK_2 receptor (Zhang et al., 2009). Importantly it was shown that depletion of these neurons by administration of CCK_2-saporin leads to attenuation of neuropathic pain sensitivity (Zhang et al., 2009), comparable to that observed previously following dermorphin-saporin lesion (Burgess et al., 2002). This strongly suggests that the effects of dermorphin-saporin observed in the present study are also driven through the loss of these CCK_2 expressing cells. Recently it has been shown that CCK administration to the RVM results in an increase in PGE_2 release in the dorsal horn (Marshall et al., 2012). PGE_2 within the dorsal horn can cause central sensitisation (Baba et

al., 2001) and has been shown to contribute to inflammatory pain (Hay et al., 1997). Although the source of PGE_2 in response to CCK activation of RVM neurons is not clear, release within the spinal cord may play an important role in mediating descending facilitation by part of the ON cell population.

Another mechanism of action of descending facilitation by the MOR+ cell population which has been proposed is increased release of neurotransmitters from primary afferent terminals, and indeed it has been shown that following dermorphin-saporin lesion of the RVM, enhanced capsaicin evoked release of CGRP in neuropathic rats is attenuated (Gardell et al., 2003). This study suggests the interesting concept whereby pain facilitating neurons could influence primary afferent release. One possible mechanism that could explain this is the activation of 5-HT_3 receptors, some of which are expressed on peripheral nerve terminals in the dorsal horn (Maxwell et al., 2003). As explained in chapter 4, the 5-HT_3 receptor is a ligand gated ion channel, and so its activation could lead to an influx of calcium and increased transmitter release. Recently it has been demonstrated that LTP at primary afferent-dorsal horn synapses is driven in part by presynaptic mechanisms of neurotransmitter release (Luo et al., 2012). The ability of descending pathways to interact with primary afferent terminals may therefore contribute to presynaptic mechanisms of LTP within the dorsal horn.

It should also be noted that some GABA expressing projection neurons within the RVM are MOR+ and so may be lost by dermorphin-saporin lesion (Kalyuzhny and Wessendorf, 1998). Although these neurons would intuitively be expected to exert an inhibitory effect within the dorsal horn, the net effects of this inhibitory input will depend on the cell target within the dorsal horn. A facilitatory effect of these neurons via inhibition of inhibitory dorsal horn interneurons is a possibility, and loss of these neurons may contribute to the attenuation of hypersensitivity observed here. Further

immunohistochemical studies to quantify the extent of MOR+ double labelling with GABA and 5-HT, and their depletion following dermorphin-saporin treatment, could be used to clarify the relative contribution of these two neurotransmitters to MOR+ mediated descending facilitation.

5.4.4 Conclusion

This study is the first to investigate the role of RVM MOR+ neurons in inflammatory joint pain behaviour. In contrast to previous findings in neuropathic pain the effect of MOR+ cell depletion is small, but is involved earlier in the pain process. Relatively little is known about the underlying mechanism of MOR+ cell facilitation of spinal cord excitability. To address this question, we next carried out microarray analysis to investigate the contribution of this pathway to gene expression changes within the dorsal horn.

6. Descending regulation of dorsal horn gene expression

6.1 Introduction

Long term plasticity requires changes in gene expression and protein synthesis, for example during memory formation (Bailey et al., 1996; Costa-Mattioli et al., 2009) and central sensitisation (Kim et al., 1998). As shown in this thesis and by others previously, descending facilitation contributes to the development of increased spinal excitability and behavioural sensitivity. Therefore descending controls are also likely to drive molecular changes in the dorsal horn which are required for plasticity. Some studies have demonstrated that the expression of proteins in the dorsal horn such as the immediate-early genes c-Fos (Géranton et al., 2008) and zif-268 (Rygh et al., 2006) as well as the transcriptional regulator MeCP2 (Géranton et al., 2008) are subject to regulation by descending controls, but in general the underlying molecular mechanisms in the dorsal horn are not well understood.

Microarray analysis is a powerful technique used to study the expression levels of many genes within a sample simultaneously. The method was originally described by Schena et al., 1995 and involves binding of fluorescence-labelled cDNA, derived from a biological sample of interest, and applying it to a chip containing many probes representing individual genes. Hybridisation between cDNA strands of the sample and the probes on the chips allows for the extent of fluorescence at each probe to give a readout of levels of expression for that gene within the sample (Schena et al., 1995). Since its initial conception microarray technology has become progressively more sophisticated (including more and more genes on the chip) and is now a widely used technique in biology, including neuroscience

research. There are two main advantages to the use of microarrays to study gene expression. One is the high throughput nature of the microarray, allowing the screening of many thousands of genes at once within a sample. The other advantage is that it allows an unbiased approach to studying gene expression. Rather than selecting a gene of interest based on existing knowledge of the biological process, whole genome studies can reveal novel and unexpected roles for 'new' genes in a particular process (Mogil and McCarson, 2000).

Microarrays have been used in a number of studies to investigate changes in gene expression in the different components of the pain pathway, including the dorsal horn. This has been carried out following peripheral nerve injury (Griffin et al., 2007; Lacroix-Fralish et al., 2006; Yang et al., 2004), herpes zoster induced allodynia (Takasaki et al., 2012), and plantar inflammation (Rodriguez Parkitna et al., 2006). Recently, a number of innovative studies have used microarrays of distinct groups of animals with different behavioural responses to identify molecular mechanisms underlying these distinct pain phenotypes. For example, in young rats neuropathic injury does not lead to pain as it does in the adult (Howard et al., 2005). Microarray analysis has proved useful in identifying a role for the complement signalling cascade in microglia which is active in the adult, but not in the young animal. This has been proposed as an explanation for the difference in pain response to neuropathic injury in these age groups (Costigan et al., 2009a). Microarrays of the dorsal horn have also been used to identify changes in gene expression associated with re-injury after an earlier inflammatory insult with carrageenan (Yukhananov and Kissin, 2008), which suggests the existence of a molecular memory or trace of the initial pain state. Another interesting example is a recent investigation into electroacupuncture induced analgesia. This procedure is more successful in some animals than others, and microarray analysis has identified genes related to immune cell function, such as the pro-inflammatory cytokines Il-6, Il-1β and TNF-α, that

are expressed at a higher level in the low responders. This is believed to contribute to their insensitivity to the procedure (Wang et al., 2012). These studies demonstrate that comparing gene expression in groups with subtle differences in pain behaviours can provide important information on the molecular mechanisms underlying those differences.

Our group has previously used microarray analysis to characterise changes in dorsal horn gene expression associated with ankle joint inflammation (Géranton et al., 2007a). This study revealed waves of transcriptional regulation at different stages following inflammation, with the induction phase (2 – 24h post inflammation) broadly associated with an increase in gene expression and the maintenance phase (7d) associated predominantly with downregulation of genes. This study demonstrated that in a model of joint pain substantial changes in dorsal horn gene expression occur, which may correlate with the behavioural changes observed. In this thesis, chapter 4 and chapter 5 describe experiments which have demonstrated that descending facilitation contributes to behavioural hypersensitivity in this model. While the contribution of descending facilitation to central sensitisation and pain behaviour has been studied frequently (Bee and Dickenson, 2008; Burgess et al., 2002; Géranton et al., 2008; Wei et al., 2010) little is known about the molecular mechanisms underlying descending facilitation.

6.1.1 Hypothesis

In this chapter I have tested the hypothesis that gene expression changes in the dorsal horn following ankle joint inflammation are regulated by descending facilitation via MOR+ neurons.

6.2 Methods

6.2.1 Animals

The first part of this chapter describes work which used tissue from the behavioural experiment described in section 5.3.3. This cohort of animals received microinjection to the RVM of either 1.5pmole (48ng, 0.75pmole each side) dermorphin-saporin or saline. The animals were subsequently divided into two groups receiving either CFA injection to the ankle or undergoing a sham procedure. The ipsilateral dorsal horn of a subset of these animals (n = 5, dermorphin-saporin + CFA and saline + CFA) was used for microarray analysis and qPCR validation of target genes (experiment 1). The aim of the part of the study was to focus on the specific contribution of descending facilitation to the regulation of dorsal horn gene expression at the 7d time point. For this reason, microarray analysis was carried out on two groups of animals only. Both groups underwent CFA injection, and dermorphin-saporin or saline pre-treatment was the only variable. In this way our analysis revealed genes that are differentially regulated in the pain state by the MOR+ cell pathway.

The second part of this chapter describes immunohistochemistry and western blot experiments carried out on two other groups of animals. Animals underwent dermorphin-saporin or saline microinjection to the RVM followed by ankle injection of CFA (as before for the microarray experiment) and the ipsilateral dorsal horn of these animals (n= 6) were used for western blot analysis (experiment 2). A final group of animals were used which did not undergo RVM injection, and received either CFA injection or sham procedure (experiment 3). These were either perfused, or protein extracted from the ipsilateral dorsal horn for western blot analysis (n = 6 per group). In all cases tissue was collected at 7d post CFA injection. An outline of the treatment and tissue obtained from different sets of animals is listed in table 6.1.

	Experiment 1	Experiment 2	Experiment 3
RVM injection	DS or saline	DS or saline	None
CFA	CFA or sham	CFA or sham	CFA or sham
Used for	RNA: microarray and RT-qPCR	Protein: western blot	Protein: western blot or immunohistochemistry

Table 6.1 Outline of experimental groups used in chapter 6.

All tissue was obtained at 7d post CFA injection. DS = dermorphin-saporin.

6.2.2 Microarray analysis

6.2.2.1 RNA Extraction

Tissue was homogenised by hand in 700ul Qiazol (Qiagen) for 1 to 2min. The sample was removed and passed through a Qiashredder column and spun in the centrifuge at 14,000rpm for 2min. The sample was then left at room temperature for 5min before the RNA was extracted using the Qiagen RNeasy kit. 140µl chloroform was added to the sample and the tube was capped and shaken vigorously for 15s. The samples were then left at room temperature for 3min followed by centrifugation at 12,000 rpm at 4°C for 15min.

The upper aqueous phase was transferred to a new tube, with care taken to minimise cellular debris remaining in the sample. 53% EtOH was added to the removed aqueous phase. This was mixed well by pipetting up and down, and added to the RNeasy spin column, and centrifuged to remove the EtOH. A wash step using buffer RW1 (from the RNeasy kit) was carried out before adding DNAase I incubation mix (Qiagen) to the column for 15min. A series of further washes using buffer RW1 and RPE from the RNeasy kit were then performed, before a final drying step and elution of the RNA in 25ul of RNase free H_2O. 1µl of each RNA sample was applied to a Nanodrop spectrophotometer and the concentration of RNA per sample was determined in ng/µl. The contamination levels of organic solvents (indicated by a low 260/230 value) and protein contamination (indicated by a low

260/280 value) were also determined using the Nanodrop. RNA was then stored at -80°C until further use.

6.2.2.2 Microarray analysis

RNA derived from the ipsilateral dorsal horn from two groups of animals, one group with dermorphin-saporin lesion of the RVM and the other without, was used for microarray analysis of gene expression (experiment 1, see table 6.1). 5 replicates per group were used. RNA samples were normalised to a concentration of 50ng/µl in RNase free H_2O before submission to the UCL genomics service. Complementary DNA (cDNA) synthesis was carried out using the Ambion WT expression kit (see below section 6.2.5 for description of cDNA synthesis for RT-qPCR experiments). This was followed by labelling of the cDNA using the Affymetrix WT terminal labelling kit. Labelled cDNA was then hybridised to Affymetrix rat gene 1.0 ST arrays and the intensity of fluorescence of the arrays was measured using an Affymetrix gene chip scanner.

6.2.2.3 Data analysis

The raw data was obtained in the form of .CEL files, which contain the results of the intensity calculations per chip. Analysis of the raw data was carried out in the R, a language and environment for statistical computing and graphics (www.r-project.org), and the Bioconductor plugin for microarray analysis was used (www.bioconductor.org). The Bioconductor package was used for three different aspects of analysing the raw data: normalising, measuring differential expression of probe sets, and providing functional annotations for each probe from the gene ontology (GO) database.

The robust multi-array average (RMA) package was used to generate an expression matrix from the CEL files and to normalise the data. Limma testing was used to assess differential expression between the two

treatment groups. Limma testing produces a table of containing the probe ID, the log-fold difference between the two treatment groups, the average expression across samples, the t-statistic describing the differential expression, the p value and adjusted p value for the significance of any expression difference, and the log odds ratio. The adjusted p values were not significant for any of the probe sets, and for further analysis, the non-adjusted p value was used. Previous published work by our group has also used the non-adjusted p value (Géranton et al., 2007a).

6.2.2.4 Bioinformatics analysis

In order to identify biologically meaningful genes from this list, the online bioinformatics tool DAVID was used (http://david.abcc.ncifcrf.gov/). The DAVID functional annotation tool examines functional annotations of the genes in a list. It incorporates annotations from the gene ontology (GO) database and performs statistical analysis to identify annotations overrepresented in a gene list compared to the background list, in our case the rat genome. The advantage of using the DAVID analysis system rather than carrying out traditional gene annotation analysis is that it groups similar or redundant annotations together, minimising repetition and redundancy (Huang, Sherman, and Lempicki 2009). This is referred to as functional annotation clustering. Genes are grouped on the basis of similarities in functional annotations allowing the user to quickly identify common functions between genes.

Following the microarray experiment, the gene list was inserted into the DAVID analysis system using the official gene symbols as identifiers. The background list was designated as the Rattus norvegicus genome. The source of annotations chosen for analysis was the Gene Ontology (GO) database. This consists of annotations of gene function using defined GO terms in three areas: biological process (BP), cellular compartment (CC) and molecular function (MF) (Ashburner et al., 2000). The analysis produced two

sets of findings, a list of enriched annotations by traditional analysis, and functional annotation clustering which groups similar and redundant annotations together to simplify the identification of biologically interesting groups of genes.

The DAVID analysis system has two methods of studying functional annotations within a list of genes. The first lists all significantly enriched annotations found within the gene list. This is calculated from an EASE score, which is generated from a Fisher's exact test to determine if the overrepresentation of the annotation is random or not, with a p value of < 0.05 deemed to be a significant enrichment. As multiple annotations are tested in this way, a correction by Benjamini test is also carried out, and ideally these values should also be significant. This produces a list of significantly enriched annotations within the gene list.

The second analysis method sorts similar annotations into clusters. Within these groups, the individual EASE scores for the annotation are combined to produce an overall enrichment score. This is the geometric mean of the p-values for the individual annotations, followed by minus log transformation. This means that the higher the enrichment score the more significant the cluster is, and a value of approximately 1.3 corresponds to the non-transformed value of p = 0.05. However this does not rule out further investigation into clusters with an enrichment value < 1.3, as within the clusters there may be many significantly enriched annotations. Furthermore, the number of genes in a cluster may be of interest. If a large number of genes with similar functions are all differentially regulated in the experiment, it provides a strong clue towards an underlying mechanism and may warrant further investigation (Huang et al., 2009).

6.2.3 Quantitative real-time PCR (RT-qPCR)

6.2.3.1 cDNA synthesis for RT-qPCR

Complementary DNA (cDNA) was synthesised from the RNA samples. The reaction was carried by adding 0.5µg RNA sample to a mix of 0.2µl Oligo dT20 (Invitrogen), 0.8µl random nonamers (Sigma), 1µl PCR nucleotide mix (Promega) and bringing the reaction volume to 13µl by adding RNase free H20. This was then incubated at 65°C for 5min. The samples were then quickly chilled on ice for 5min. The tubes were briefly centrifuged to collect the mixture, and 4µl first strand buffer (Invitrogen), 1µl DTT (Invitrogen), 1µl RNaseIN ribonuclease inhibitor (Invitrogen) and 1µl of the key reaction component, reverse transcriptase (Superscript III, Invitrogen) were added. This was gently mixed by pipetting up and down and the samples were then incubated at 25°C for 5min, 50°C for 50min and 70°C for 15min. The cDNA samples were then placed quickly on ice before storage at -20°C until use in RT-qPCR assays.

6.2.3.2 Reverse transcriptase real time qPCR (RT-qPCR) assay

Oligonucleotide primers were designed to target selected genes based on the Affymetrix probe sequences (Sigma). A list of primer sequences is given in table 6.2. RT-qPCR assays were carried out on 96 well plates, with cDNA samples run in triplicate and controls for master mix contamination (no cDNA added) and cDNA contamination (negative control from the cDNA synthesis, without transcriptase added) included in each plate. A master mix solution was prepared for each plate so that each well contained 12.5µl SYBR green (Sigma), 9.5µl RNase free H_2O, and 1µl stock solution of the forward and reverse primers of the target gene. 1µl cDNA was added to the wells after they were filled with the master solution.

The Sigma 3-step amplification protocol was used with a Bio-Rad CFX96 PCR C100 thermal cycler (see table 6.3). Data was analysed using Bio-Rad CFX96

software. Ct values (threshold cycle, which is the number of cycles taken for the fluorescence labelling to increase above background) were obtained for each target gene. This value is inversely proportional to the log of the copy number of the cDNA in the sample. Actin was used as a housekeeping gene. Relative gene expression was calculated using the 2ΔCt method, where the data for each gene is expressed in the form 2 to the power of (Ct Actin – Ct target).

Gene name	Primer	Sequence
Cyclin B2	Ccnb2F	CTAAGAGCCATGTGACTGTC
	Ccnb2R	CAGAACTGTAGGTTTCGG
Chemokine (C-X-C motif) ligand 10	Cxcl10F	ATACTCACAGGAACCTAGACAT
	Cxcl10R	CCATCCAACACATCTTGTAATATG
Ribosomal protein L32	Rpl32F	GTTCATCAGGCACCAGTC
	Rpl32R	TGACATCGTGGACCAGAA
Chemokine (C-X-C motif) ligand 9	Cxcl9F	GATGAAGCCCTTTCATACTGC
	Cxcl9R	GTGGTTGTGAGTTTTGCTCCAATC
Chemokine (C-X-C motif) receptor 3	Cxcr3F	AGCCCTCACCTGCATAGTTG
	Cxcr3R	GCCACTAGCTGCAGTACACG
Nitric oxide synthase 2	Nos2F	GATATCTTCGGTGCGGTCTT
	Nos2R	GGCCAGATGCTGTAACTCTT

Table 6.2 Forward and reverse primer sequences used for RT-qPCR validation of selected genes.

Step	Temperature °C	Time
1. Denaturation	94	2min
2. Denaturation	94	15s
3. Annealing	60	30s
4. Extension	72	30s
5. Read Plate		
6. Return to step2, repeat x39		

Table 6.3 Sigma three step amplification protocol.

6.2.4 Western blot

Full details of all solutions used for western blot analysis are listed in appendix A2. As the primary aim was to determine if some of the genes validated by RT-qPCR were also regulated at the protein level, we limited western blot analysis to two groups of animals only for the dermorphin-saporin component of the experiment. As with the microarray analysis, both groups received CFA injection, and dermorphin-saporin or saline pre-treatment was the only variable (tissue from experiment 2). However, separate experiments were carried out on 'normal' CFA and sham tissue, to determine if protein levels are modulated by CFA treatment alone (tissue from experiment 3).

6.2.4.1 Protein extraction

Tissue was homogenised in 1ml RIPA buffer, 10µl protease inhibitor (Sigma) 10µl phosphatase inhibitor cocktail 1 (Sigma) and 10µl phosphatase inhibitor cocktail 2 (Sigma). 150µl of this mixture was used per dorsal horn quadrant. Tissue was placed in centrifuge tubes with ceramic beads and then placed in a FastPrep biopulverizer machine (MP Biomedicals Europe) for 20s at setting 5. Tubes were spun twice and left on ice for 1h, followed by 2 more spins and a final 1h on ice. Finally tubes were centrifuged at 12,000rpm for 15min at 4°C. The supernatant was removed, leaving the pellet left behind. Samples were stored at -20°C until use.

Protein quantity per sample was determined using a bicinchoninic acid (BCA) assay (Thermo Scientific). Bicinchoninic acid and 4 % copper sulphate solution were mixed in a 50:1 ratio, and 200µl of the mixture was added to protein standards, and unknown samples, on a 96-well plate. This was incubated at 37°C for 30min and a spectrophotometer was used to measure the colour emitted by the samples, allowing a standard curve to be generated and the unknown protein concentrations calculated.

6.2.4.2 Electrophoresis and protein transfer

Samples for western blot were prepared by adding sufficient protein sample to obtain a standard protein concentration of 35µg. The appropriate amount of loading buffer (Invitrogen) was added to obtain a final volume of 19.5µl per sample. Samples were boiled for 5min to denature the proteins, and cooled on ice prior to loading of the gel. Samples were loaded alongside a protein standard ladder (Bio-Rad) to pre-cast 12% agarose gels (Bio-Rad Criterion) in a tank with MOPS running buffer. Proteins were separated using SDS-polyacrylamide gel electrophoresis (SDS-PAGE), at 180V for 1hr using a power pack (Bio-Rad).

Meanwhile transfer buffer was prepared (see appendix A.2) and 2 sponges and 4 filter papers per gel were soaked for 15min. PVDF membrane (Bio-Rad) was activated in MeOH for 5min then soaked in transfer buffer prior to preparation of the sandwich within a plastic cassette. Sponges and filter paper (Bio-Rad) were also soaked in transfer buffer prior to use. This gel sandwich was prepared in the following order: sponge, 2 x filter paper, gel, PVDF membrane, 2x filter paper and sponge. The cassette was placed in a tank with transfer buffer and ran at 100V for 1h to complete the transfer, and the buffer was kept cool by addition of an ice pack.

6.2.4.3 Blocking, primary antibody and detection

Following completion of protein transfer, the membrane was blocked in blocking solution (4% skimmed milk solution in PBS-tween) for 1h. The primary antibody was diluted as required in blocking solution and the membrane incubated in a rolling tube overnight at 4°C. The primary antibodies and concentrations used are given in table 6.4.

After the overnight incubation, the membrane was then washed 3 times for 10min in PBS-tween on a rocker. The membrane was then incubated with a rabbit horseradish peroxidase-conjugated secondary antibody (Santa Cruz,

1:1000), diluted in blocking solution, for 1h at room temperature. This was followed by 3 more washes. The membrane was developed using the Bio-Rad Chemi-doc system, with a horseradish peroxidase (HRP) substrate developing kit (Thermo-Scientific). The HRP developing substrate was applied to the membrane for as long as required to see bands at the target molecular weight. Images of the developed blots were saved for later analysis.

All proteins of interest were normalised to the expression of calnexin, a housekeeping protein expressed in the endoplasmic reticulum membrane. Following the exposure of the first antibody, the membrane was incubated with the calnexin antibody (1:1000, rabbit, Biovision) overnight at 4°C. The next day the secondary HRP-conjugated antibody was applied, and developing of the blot was carried out as for the first primary antibody.

Antigen	Host	Company	Concentration	Molecular Weight
CXCL10	Rabbit	Peprotech	1:500	10kDA
CXCR3	Rabbit	Santa Cruz	1:50	38kDA
Calnexin	Rabbit	Biovision	1:1000	67kDA

Table 6.4 Primary antibodies used for western blot analysis.

6.2.4.4 Analysis

Western blots were analysed using Bio-rad Quantity One software. The volume analysis tool was used to quantify the intensity of band staining. Volume analysis involves creating a rectangle of equal size around each of the bands, and measures the volume within that rectangle. The volume is defined as the sum of pixel intensities x the area within the defined boundary. The global background volume is subtracted from these values, and is obtained by combining intensity data from three separate objects as representative of the background. For each band the background-adjusted intensity of the band at the appropriate molecular weight was normalised to

the background-adjusted intensity of calnexin, imaged on the same blot. The normalised data is then expressed as a proportion of the mean of the control group (either saline + CFA or sham, depending on the experiment).

6.2.5 Immunohistochemistry

Fluorescence immunohistochemistry with tyramide signal amplification was carried out as described in section 2.4. 40µm sections of the lumbar spinal cord (L4-L6) were taken across 6 wells, so that within each well all sections were at least 240µm apart.

Antibodies used were for CXCR3 and CXCL10, and double labelling was carried out with a number of cellular markers. These were NeuN (marker of neuronal nuclei), IBA1 (ionized calcium binding adaptor molecule 1, found in microglia), GFAP (glial fibrillary acidic protein, found in astrocytes) and CGRP (calcitonin gene related peptide, expressed in peptidergic primary afferents terminating in the dorsal horn), as appropriate. Primary antibodies and concentrations used for immunohistochemistry are given below in table 6.5.

Confocal microscopy (see section 2.4.6) was carried out to determine the extent of colabelling of CXCR3 and CXCL10 with these markers in the dorsal horn of animals with ankle injection of CFA. Controls were carried out to ensure that the secondary antibodies were specific to their primary antibody targets. This was carried out by removing either the first primary antibody or the second primary antibody from the procedure, to ensure no non-specific labelling by the secondary antibodies.

Antigen	Host	Company	Concentration	Method	Fluorophore
CXCL10	Rabbit	Peprotech	1:1000	TSA	FITC
CXCR3	Rabbit	Santa Cruz	1:200	TSA	FITC
NeuN	Mouse	Chemicon	1:1000	Direct	Alexa 594
CGRP	Rabbit	Sigma	1:4000	Direct	Alexa 594
IBA1	Rabbit	Wako	1:1000	Direct	Alexa 594
GFAP	Rabbit	Dako	1:4000	Direct	Alexa 594

Table 6.5 Primary antibodies, concentrations and detection methods for immunohistochemistry.

6.2.6 Statistical analysis of RT-qPCR and western blot experiments

For RT-qPCR and western blot experiments, data is presented as mean ± SEM per group. Independent samples t-tests were used to compare means between two groups and a p-value of < 0.05 was deemed significant.

6.3 Results

6.3.1 Microarray analysis

Following analysis of the microarray data in Bioconductor a list of all genes with corresponding fold changes and significance values was generated. Only those genes with a non-adjusted p value of < 0.05 were included as differentially regulated (2616 transcripts in total). Genes without an official gene symbol were also removed (leaving 1668 transcripts in total). The remaining transcripts were then ranked by fold change. A fold change cut-off was set at 1.2 and this resulted in a final list of 129 genes which was used for further analysis. Table 6.6 lists these genes, along with their ranking on the list based on fold change, gene name, official gene symbol, direction of change in dermorphin-saporin group (+ = upregulated in dermorphin-saporin, - = downregulated in dermorphin-saporin), fold change value, and

non-adjusted p value. The majority of the genes (76%) were downregulated in the dermorphin-saporin group. Within this list, two genes appear repeatedly (*Rpl21* and *Rpl7a*). This repetition can arise as each gene is represented on the array with multiple probes targeting different regions on the same gene. For ease of reference, genes are listed in alphabetical order (based on gene symbol).

List of genes differentially regulated in dermorphin-saporin group

Rank	Gene Name	Symbol		Fold	p value
27	ankyrin repeat, family A (RFXANK-like), 2	Ankra2	+	1.35	0.016
39	brain expressed gene 4	Bex4	+	1.30	0.021
26	biphenyl hydrolase-like (serine hydrolase)	Bphl	-	1.35	0.001
113	coiled-coil domain containing 79	Ccdc79	+	1.20	0.007
4	cyclin B2	Ccnb2	+	1.85	0.015
94	chemokine (C-C motif) receptor 1-like 1	Ccr1l1	-	1.21	0.000
115	cholinergic receptor, nicotinic, beta 3	Chrnb3	-	1.20	0.014
28	claudin 1	Cldn1	-	1.34	0.024
99	clarin 2	Clrn2	-	1.21	0.002
84	cytochrome c oxidase, subunit VIa, polypeptide 2	Cox6a2	-	1.22	0.005
34	chemokine (C-X-C motif) ligand 10	Cxcl10	-	1.32	0.000
42	chemokine (C-X-C motif) ligand 9	Cxcl9	-	1.30	0.042
127	chemokine (C-X-C motif) receptor 3	Cxcr3	-	1.20	0.005
109	cytochrome P450, family 2, subfamily b, polypeptide 12	Cyp2b12	-	1.20	0.010
81	defensin, alpha 5, Paneth cell-specific	Defa	-	1.22	0.001
75	defensin beta 40	Defb40	-	1.22	0.031
85	elongation factor RNA polymerase II-like 3	Ell3	-	1.22	0.003
47	ferritin, light polypeptide	Ftl	-	1.28	0.034
119	glyceraldehyde-3-phosphate dehydrogenase	Gapdh	-	1.20	0.013
82	glycoprotein (transmembrane) nmb	Gpnmb	-	1.22	0.021
67	GTP binding protein 4	Gtpbp4	+	1.23	0.027
51	histone cluster 1, H2bc	Hist1h2bc	-	1.26	0.004
54	histone cluster 1, H2bc	Hist1h2bc	-	1.26	0.006
102	histone cluster 3, H2a	Hist3h2a	+	1.21	0.008
40	high mobility group box 1	Hmgb1	-	1.30	0.006
123	heterogeneous nuclear ribonucleoprotein A3 ABREVIATED	Hnrnpa3	+	1.20	0.012
122	5-hydroxytryptamine (serotonin) receptor 1D	Htr1d	-	1.20	0.002
3	isopentenyl-diphosphate delta isomerase 2-like	Idi2l	-	1.98	0.043
59	indolethylamine N-methyltransferase	Inmt	-	1.25	0.005
106	intelectin 1 (galactofuranose binding)	Itln1	-	1.21	0.007
114	keratin 31	Krt31	-	1.20	0.037
104	keratin associated protein 4-7	Krtap4-7	-	1.21	0.045
19	NADH dehydrogenase (ubiquinone) 1 beta subcomplex 4	LOC100361934	-	1.38	0.006
117	epithelial cell transforming sequence 2 oncogene-like	LOC100361997	-	1.20	0.049
45	rCG59045-like	LOC100364529	-	1.29	0.002
78	hypothetical LOC290577	LOC290577	-	1.22	0.004
43	similar to hypothetical protein	LOC292449	-	1.29	0.006

9	similar to hypothetical protein 4930509O22	LOC300308	-	1.67	0.001
93	Ac2-224	LOC362921	-	1.21	0.000
24	hypothetical protein LOC499339	LOC499339	+	1.36	0.002
97	LRRGT00154	LOC499544	-	1.21	0.010
68	similar to hypothetical protein FLJ25692	LOC500392	+	1.23	0.004
52	hypothetical LOC502825	LOC502825	-	1.26	0.003
2	similar to Discs large homolog 5	LOC681283	-	2.06	0.005
76	hypothetical protein LOC683753	LOC683753	-	1.22	0.025
15	similar to Heterogeneous nuclear ribonucleoprotein A1	LOC689196	-	1.44	0.010
125	rCG20053-like /// mCG1042722-like	LOC691054	-	1.20	0.009
112	mast cell protease 8	Mcpt8	-	1.20	0.027
36	mannosyl (alpha-1,3-) ABREVIATED	Mgat4a	-	1.31	0.036
66	similar to melanoma antigen family A, 5	MGC114492	-	1.23	0.015
126	microRNA mir-152	Mir152	-	1.20	0.003
17	microRNA mir-344-1	Mir344-1	+	1.41	0.013
38	microRNA mir-374	Mir374	+	1.30	0.013
69	microRNA mir-377	Mir377	+	1.23	0.009
83	microRNA mir-384	Mir384	+	1.22	0.033
25	microRNA mir-421	Mir421	+	1.36	0.011
64	microRNA mir-544	Mir544	+	1.24	0.041
111	M-phase phosphoprotein 8	Mphosph8	-	1.20	0.001
58	mitochondrial ribosomal protein L18	Mrpl18	+	1.25	0.003
91	melanoma associated antigen (mutated) 1-like 1	Mum1l1	+	1.21	0.005
10	NADH dehydrogenase subunit 6	ND6	+	1.65	0.003
62	neurogenin 1	Neurog1	-	1.24	0.010
71	nuclear transcription factor, X-box binding-like 1	Nfxl1	+	1.23	0.015
72	nuclear transcription factor, X-box binding-like 1	Nfxl1	+	1.22	0.004
79	natural killer cell group 7 sequence	Nkg7	-	1.22	0.011
118	nitric oxide synthase 2, inducible	Nos2	-	1.20	0.000
31	NAD(P)H dehydrogenase, quinone 2	Nqo2	+	1.33	0.022
49	olfactory receptor 1598	Olr1598	-	1.27	0.030
95	olfactory receptor 1695	Olr1695	-	1.21	0.004
128	olfactory receptor 1733	Olr1733	+	1.20	0.028
63	olfactory receptor 1743	Olr1743	-	1.24	0.002
80	olfactory receptor 326	Olr326	-	1.22	0.009
65	olfactory receptor 446	Olr446	-	1.24	0.022
90	olfactory receptor 514	Olr514	-	1.21	0.008
13	olfactory receptor 707	Olr707	-	1.50	0.018
44	olfactory receptor 733	Olr733	-	1.29	0.044
5	olfactory receptor 780 /// olfactory receptor 779	Olr780	-	1.83	0.001
60	olfactory receptor 94	Olr94	-	1.25	0.010
124	polyadenylate-binding protein-interacting protein 2-like 1	Paip2l1	+	1.20	0.002

108	Prolactin family 3, subfamily d, member 1 ABREVIATED	Prl3d1	-	1.21	0.035
74	proline-rich protein 15 /// RGD1559532	Prp15	-	1.22	0.000
120	parathyroid hormone	Pth	-	1.20	0.000
88	RNA binding motif 31, Y-linked	Rbm31y	-	1.21	0.000
23	REST corepressor 2	Rcor2	+	1.36	0.042
107	renin	Ren	-	1.21	0.002
101	similar to Neuronal pentraxin II precursor (NP-II) (NP2)	RGD1311190	-	1.21	0.007
20	similar to NADH:ubiquinone oxidoreductase B15 subunit	RGD1560088	+	1.36	0.010
11	similar to RIKEN cDNA 1700001F22	RGD1561558	+	1.56	0.014
21	similar to putative protein kinase	RGD1561706	-	1.36	0.002
35	similar to putative protein kinase	RGD1561706	-	1.32	0.040
129	similar to Na+ dependent glucose transporter 1	RGD1561777	-	1.19	0.011
18	similar to TDPOZ3	RGD1563667	+	1.40	0.020
116	similar to chromosome 10 open reading frame 71	RGD1564899	-	1.20	0.004
53	similar to ATP synthase, ABREVIATED	RGD1565438	-	1.26	0.002
70	similar to Spindlin-like protein 2 (SPIN-2)	RGD1565862	-	1.23	0.007
6	similar to 60S ribosomal protein L12 /// ribosomal protein L12	Rpl12	+	1.81	0.016
37	ribosomal protein L19	Rpl19	+	1.30	0.023
12	ribosomal protein L21	Rpl21	-	1.51	0.050
22	ribosomal protein L21	Rpl21	+	1.36	0.022
32	ribosomal protein L21	Rpl21	+	1.33	0.025
46	ribosomal protein L21	Rpl21	+	1.28	0.039
8	ribosomal protein L32	Rpl32	-	1.68	0.015
55	ribosomal protein L35a	Rpl35a	+	1.26	0.025
14	ribosomal protein L7a	Rpl7a	-	1.45	0.011
33	ribosomal protein L7a	Rpl7a	-	1.32	0.014
77	ribosomal protein L7a	Rpl7a	-	1.22	0.020
121	ribosomal protein L7a	Rpl7a	-	1.20	0.016
29	ribosomal protein L9	Rpl9	-	1.34	0.018
30	ribosomal protein S2 /// ribosomal protein S2-like	Rps2	+	1.33	0.007
96	ribosomal protein S23 /// similar to ribosomal protein S23	Rps23	+	1.21	0.016
16	RT1 class Ib	RT1-N1	-	1.42	0.041
87	RT1 class Ib, locus O1	RT1-O1	+	1.22	0.040
110	Sin3-associated polypeptide 18	Sap18	+	1.20	0.013
86	SEC16 homolog B (S. cerevisiae)	Sec16b	-	1.22	0.002
73	sema domain	Sema4c	-	1.22	0.003
61	serine (or cysteine) proteinase inhibitor, clade B, member 1a	Serpinb1a	-	1.24	0.001
1	serine (or cysteine) peptidase inhibitor, clade B, member 1b	Serpinb1b	-	4.08	0.002
89	solute carrier family 7 ABREVIATED	Slc7a7	-	1.21	0.003
92	serine peptidase inhibitor, Kazal type 3	Spink3	-	1.21	0.045
56	storkhead box 1	Stox1	-	1.26	0.014

50	taste receptor, type 2, member 38	Tas2r38	-	1.27	0.004
105	tektin 5	Tekt5	-	1.21	0.001
98	transmembrane protein 27	Tmem27	-	1.21	0.016
57	transmembrane protease, serine 4	Tmprss4	-	1.25	0.002
48	tripartite motif-containing 42	Trim42	-	1.27	0.000
7	vomeronasal 1 receptor, D15	V1rd15	+	1.70	0.006
103	vestigial like 2 (Drosophila)	Vgll2	-	1.21	0.005
100	vomeronasal 2 receptor, 51	Vom2r51	-	1.21	0.010
41	xin actin-binding repeat containing 1	Xirp1	-	1.30	0.000

Table 6.6 Genes identified by microarray analysis.

129 genes with a p-value of < 0.05 and a fold change of > 1.2 were identified. The + or – symbols indicate upregulation or downregulation in the dermorphin-saporin group. Genes are listed alphabetically, based on gene symbol.

6.3.2 Bioinformatics analysis

To identify biological functions of genes in this list which may be of interest, DAVID bioinformatics software was used. This is a freely available online tool (http://david.abcc.ncifcrf.gov), and it was used to perform functional annotation of the genes in the list based on the gene ontology (GO) database. This analysis indicated there are 35 GO terms enriched within the list, however many of these annotations are similar. Functional annotation clustering was then carried out, to identify groups of annotations with similar functions and the genes they contain. This resulted in the identification of 20 clusters. These clusters are illustrated in figure 6.1, and the genes contained in each cluster are shown in table 6.7.

The enrichment score for each cluster was calculated as the log transformation of the geometric mean of the EASE scores for individual annotations within the cluster. Higher enrichment scores therefore correspond to greater significance. The enrichment scores for each cluster are also given in table 6.7 (values in bold). Interestingly, the most significantly enriched cluster corresponded to genes with ribosomal function. The annotations of this category refer to ribosomal structural

proteins, as well as genes involved in translation and those with a cytosolic location. This included several large ribosomal subunit components (e.g. *Rpl32* and *Rpl21*). Also within this group was *Ccnb2*, which encodes the cell-cycle mediator cyclin B2. This was one of the highest ranking fold changes identified with a 1.85 increase in the dermorphin-saporin group.

The next most significant cluster contains genes with annotations for defence response, which includes a number of genes involved in immune system function. Among these was *Nos2*, which encodes the enzyme nitric oxide synthase 2 (inducible nitric oxide synthase), which is implicated in inflammatory responses (MacMicking et al., 1997). The next cluster contains genes associated with chemotaxis, which are also involved in immune system function and inflammatory responses. This cluster included the chemokines *Cxcl9* and *Cxcl10*. All of these immune system and chemotaxis related genes were downregulated in the dermorphin-saporin group, suggesting that immune cell activation in the dorsal horn may be reduced in the dermorphin-saporin group.

Surprisingly, no clusters directly related to neuronal activity were identified. However within the GPCR signalling cluster the 5-HT receptor 5-HT1D (*Htr1d*) and the nicotinic receptor β subunit (*Chrnb3*) were identified. Both were downregulated 1.2 fold in the dermorphin-saporin group. This cluster also contained a large number of olfactory receptors, as well as the chemokine receptor *Cxcr3*, which binds the chemotaxis ligands *Cxcl9* and *Cxcl10*.

These functional annotation clusters helped identify interesting biological roles for some of the genes identified in the array, with a particular role for ribosomal function and immune cell activity.

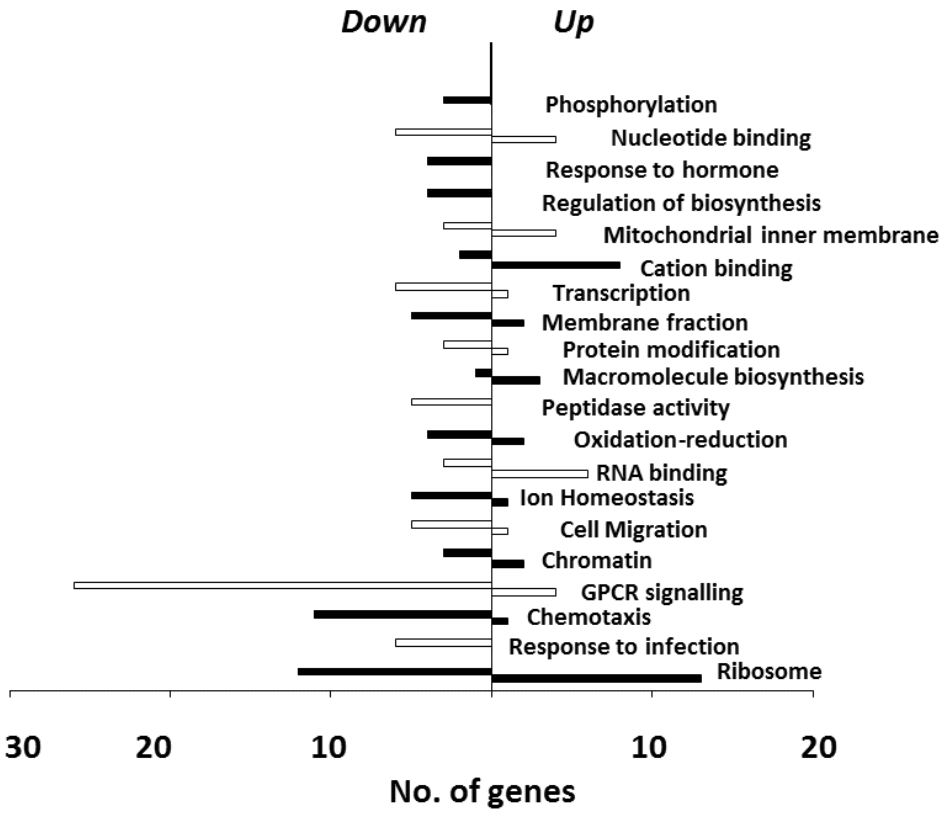

Figure 6.1 Functional annotation clustering analysis.

20 functional annotation clusters were identified using the DAVID online bioinformatics tool. The horizontal bars indicate the number of genes that are upregulated (to the right) or downregulated (to the left) in each cluster. Joined bars indicate the up- and downregulated genes for each cluster. For clarity, alternate black and white bars are used between clusters. For details of the genes contained in each cluster see table 6.7.

Functional annotation clusters generated by DAVID analysis

	Down	Up
1. Ribosome	Cldn1	Ankra2
2.88	Ftl	Ccnb2
	Gapdh	Gtpbp4
	Hist1h2bc	Hist3h2a
	Hmgb1	Rcor2
	Hnrnpa3	Rpl12
	Krt31	Rpl19
	LOC499339	Rpl35a
	Mphosph8	Rps2
	Mrpl18	Rps23
	Nos2	Tekt5
	Rpl21	
	Rpl32	
	Rpl7a	
	Rpl9	
2. Defence response	Cxcl10	
1.16	Defa	
	Defb40	
	Hist1h2bc	
	Mphosph8	
	Nos2	
3. Chemotaxis	Cxcl10	Gtpbp4
1.16	Cxcl9	
	Defa	
	Defb40	
	Hmgb1	
	Mcpt8	
	Mgat4a	
	Prl3d1	
	Pth	
	Ren	
	Spink3	
4. GPCR	Chrnb3	ND6
0.76	Cldn1	Nqo2
	Cxcl10	Olr1733
	Cxcl9	V1rd15
	Cxcr3	
	Gpnmb	
	Htr1d	
	Mgat4a	
	Nkg7	
	Nos2	
	Olr1598	
	Olr1695	
	Olr1743	
	Olr326	

	Olr446 Olr514 Olr707 Olr733 Olr780 Olr94 Pth RT1-N1 Slc7a7 Tas2r38 Tmem27 Vom2r51	
5. Chromatin **0.64**	Hist1h2bc Hmgb1 Mphosph8	Hist3h2a Rcor2
6. Cell migration **0.62**	Cxcl10 Cxcl9 Nos2	Gtpbp4 Hmgb1 Xirp1
7. Cell ion homeostasis **0.55**	Cldn1 Cxcr3 Ftl Pth Xirp1	Ccnb2
	Down	Up
8. RNA binding **0.5**	Ell3	Gtpbp4 Hmgb1 Hnrnpa3 LOC499339 Rpl12 Rpl35a Rpl9 Rps2
9. Oxidation-reduction **0.43**	Cyp2b12 Ftl Gapdh Nos2	ND6 Nqo2
10 Peptidase activity **0.37**	Mcpt8 Ren RGD1561777 Tmem27 Tmprss4	
11. Macromolecular biosythnthesis **0.29**	Chrnb3	Hist1h2bc Hist3h2a Rps2

12. Regulation of protein modification **0.24**	Hmgb1 Itln1 Spink3	Gtpbp4
13. Membrane fraction **0.17**	Chrnb3 Cyp2b12 Gapdh Hmgb1 Rpl9	Ankra2 Ccnb2
14. Transcription **0.17**	Ell3 Hmgb1 Itln1 Neurog1 Pth Vgll2	
15. Cation binding **0.16**	Cyp2b12 Ftl Gapdh Mgat4a Nos2 Rpl9 Spink3 Trim42	ND6 Nqo2
16. Mitochondrial inner membrane **0.13**	Bphl Cox6a2 RGD1565438 Rpl35a	Mrpl18 ND6 RGD1560088
17. Negative regulation of biosynthetic process **0.12**	Hmgb1	Gtpbp4 Rcor2 Spink3
18. Response to hormone stimulation **0.07**	Cxcl10 Cyp2b12 Hmgb1 Ren	

19. Adenyl nucleotide binding **0.07**	Gapdh Gtpbp4 LOC292449 LOC300308 LOC500392 Nos2 RGD1564899 Rpl9	Hnrnpa3 RGD1561706
20. Phosphorylation **0.02**	LOC300308 RGD1561706 RGD1565438	

Table 6.7 Functional annotation clustering using the DAVID bioinformatics tool. This analysis identified 20 clusters of genes with related annotations from the gene ontology (GO) database. Each cluster is listed with a sample annotation from that cluster (underlined). The genes in each cluster are divided into lists of upregulated (up) and downregulated (down) columns, and listed alphabetically by gene symbol. The full names of each gene can be found in table 6.6. The value highlighted in bold for each cluster is the enrichment score for that cluster. This is a measure of how significantly enriched the gene list is for that cluster of annotations, and is calculated as the geometric mean of the individual p value for each annotation in that cluster, and expressed on a log scale. Therefore the higher the enrichment value the greater the significance for that cluster.

6.3.3 Validation of selected genes by RT-qPCR

Following microarray analysis, it is necessary to validate gene expression changes by RT-qPCR. In choosing which genes to validate, a number of criteria are taken into account. A first consideration was the magnitude of fold changes observed for each gene, as genes with high fold changes may be of particular biological relevance. Another consideration is to identify genes on the list with known roles in nociceptive signalling within the dorsal horn, and those involved in other aspects of neuronal plasticity such as LTP. Genes related to molecular mechanisms such as the regulation of transcription and translation are also of interest, as these mechanisms are known to contribute to central sensitisation and behavioural hypersensitivity within the dorsal horn. Finally genes related to immune cell function may be of interest in pain studies, as immune cell related genes have been

previously identified in the dorsal horn in a number of pain models (Costigan et al., 2009a; Yukhananov and Kissin, 2008), and immune cells are known to contribute to central sensitisation and behavioural hypersensitivity in a number of different pain states (Calvo et al., 2012; Clark et al., 2012; Sagar et al., 2011). Based on these criteria a number of genes were selected for validation by RT-qPCR.

Ccnb2, encoding the protein Cyclin B2, was one of the highest fold gene changes on the list with a 1.85 fold increase in the dermorphin-saporin treated animals and ranking number 4 on the list. It was also among the minority of genes that were upregulated in the dermorphin-saporin group. This increase was confirmed by RT-qPCR, with a significant increase in expression found in the dermorphin-saporin + CFA treated group compared with saline + CFA controls ($p = 0.0041$, figure 6.2).

The next consideration was to investigate genes that were already known to contribute to central sensitisation within the dorsal horn. Relatively few genes fell into this category, however *Nos2*, encoding the enzyme nitric oxide synthase 2 (inducible nitric oxide synthase), is one example. *Nos2* has been shown to play a role in central sensitisation in both inflammatory and neuropathic pain states (Gühring et al., 2000; Infante et al., 2007; Kuboyama et al., 2011; Tang et al., 2007). *Nos2* was identified within the 'response to infection' cluster, which was the second most enriched cluster of genes and was found to be downregulated in the dermorphin-saporin group. RT-qPCR confirmed a significant decrease in *Nos2* expression in the dermorphin-saporin group ($p = 0.022$, figure 6.2).

The most statistically significant cluster (with the highest enrichment score) contained genes with ribosomal functions. Ribosomal proteins are of interest because translation is important in many forms of neuronal plasticity, including pain states (Costa-Mattioli et al., 2009; Géranton et al., 2009; Jiménez-Díaz et al., 2008). The ribosomal protein *Rpl32* had a fold

decrease of 1.68 on the microarray. The decrease in *Rpl32* was confirmed as significant by RT-qPCR ($p = 0.0399$, figure 6.2).

Another consideration was to investigate genes with roles in mediating immune system processes, as immune cells play an important role in central sensitisation in the dorsal horn (Clark et al., 2012; Costigan et al., 2009a; Raghavendra et al., 2004; Sagar et al., 2011). Interestingly, immune cell responses did feature prominently within the list of genes identified, as 'response to infection' and 'chemotaxis' were two of the most enriched clusters within the gene list. *Cxcl9* and *Cxcl10* were among the genes in the chemotaxis cluster. These are structurally similar chemokines from the same family, and are ligands for the G-protein coupled chemokine receptor *Cxcr3* (Müller et al., 2010) which was also identified on the microarray. *Cxcl9*, *Cxcl10* and *Cxcr3* were all downregulated in the dermorphin-saporin group in the microarray analysis, and RT-qPCR confirmed a significant decrease in all three genes (*Cxcl10* $p = 0.0132$, *Cxcl9* $p = 0.0329$, *Cxcr3* $p = 0.0379$, figure 6.2). This strongly suggested that this chemokine-receptor family is involved in mediating descending facilitation via the MOR+ cell pathway. As this chemokine family has not previously been described in the dorsal horn in pain states, it was decided to characterise the expression of CXCL10 and CXCR3 protein in the dorsal horn following CFA treatment, and dermorphin-saporin treatment.

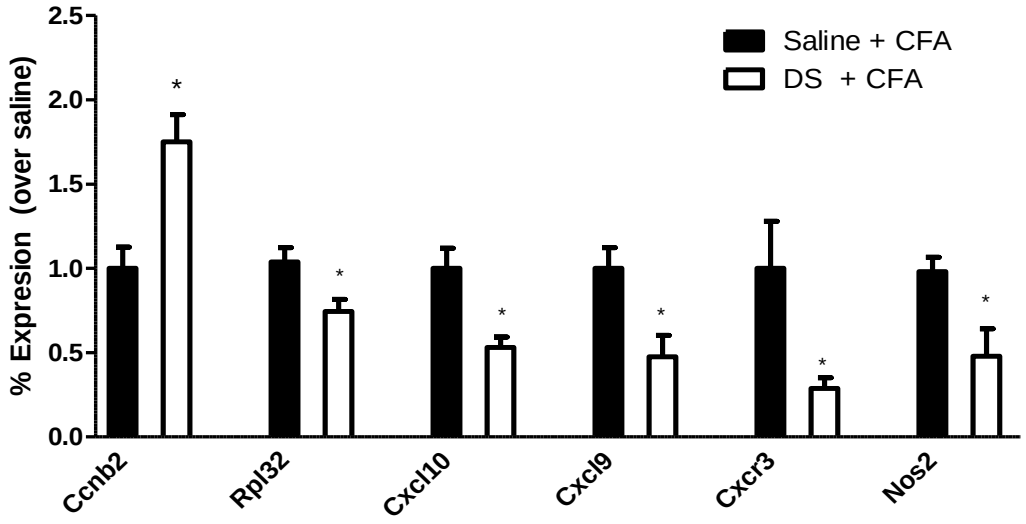

Figure 6.2 RT-qPCR validation of selected genes.

A number of genes were selected for validation by RT-qPCR. 2∆Ct values were obtained for each group, using actin as the housekeeping gene. Data is presented as % expression of the dermorphin-saporin (DS) + CFA group over the saline + CFA control group, mean ± SEM. n = 4 – 6 per group, * $p < 0.05$ independent samples t-test.

6.3.4 Characterising CXCL10 protein expression in the dorsal horn

Western blot analysis of CXCL10 was carried out on tissue from dermorphin-saporin + CFA and saline injected + CFA groups (experiment 2) and in 'normal' CFA and sham animals (without RVM injection, experiment 3). Bands were detected at the correct molecular weight (at approximately 10kDA), however comparison between groups indicated no significant differences when band intensity was normalised to the housekeeping protein calnexin, in either experiment 2 (dermorphin-saporin v saline, $p = 0.5753$, independent samples t-test), or experiment 3 (CFA v sham, $p = 0.96$) (figure 6.3). Nonetheless the ability of western blot analysis to detect considerable levels of CXCL10 protein in all samples, including sham controls, suggests that this protein may be expressed constitutively in the dorsal horn.

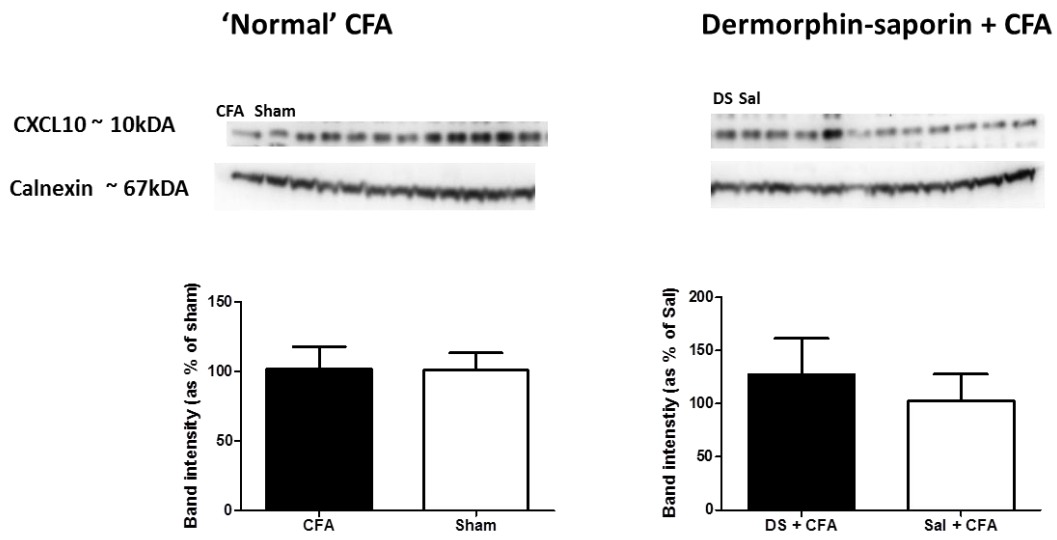

Figure 6.3 No effect of CFA or dermorphin-saporin on CXCL10 protein levels.

Two sets of tissue were used for western blot analysis. 'Normal' CFA corresponds to experiment 3, and dermorphin-saporin + CFA corresponds to experiment 2 (see table 6.1). Lanes are loaded alternately with CFA followed by Sham for the 'normal CFA' experiment and dermorphin-saporin (DS) followed by saline (sal) for the dermorphin-saporin + CFA experiment. No differences in CXCL10 expression were identified in either experiment. $p > 0.05$, independent samples t-test, $n = 6$ all groups, data is presented as mean ± SEM.

To identify the cellular localisation of CXCL10 protein within the dorsal horn, immunohistochemistry was carried out in animals at 7d following CFA injection or sham procedure. As with the western blot analysis, there did not appear to be any difference in CXCL10 expression between CFA and sham animals, with relatively high levels of staining in both groups. For this reason images from the sham treated group are not shown here. Confocal imaging was carried out with various cellular markers to identify the cellular localisation of CXCL10. Analysis of single plane images indicated there was no colabelling of CXCL10 in IBA1 positive cells (microglia) or GFAP positive cells (astrocytes). Strikingly, most CXCXL10 labelling appeared to be within a subset of neurons (NeuN), both in the dorsal and ventral horns. This suggested that within the dorsal horn CXCL10 is predominantly neuronal (figure 6.4).

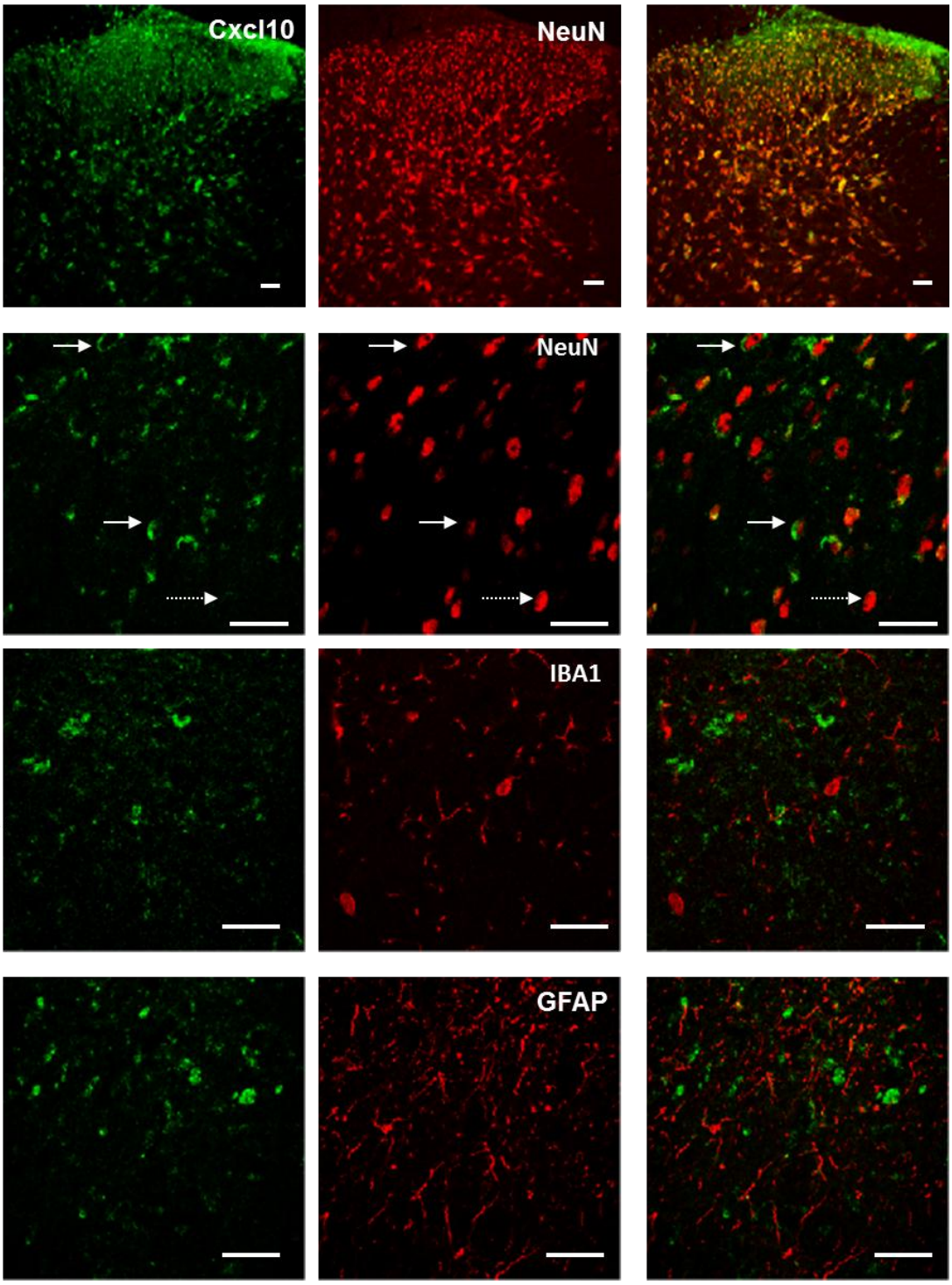

Figure 6.4 Neuronal localisation of CXCL10.

Images shown are single plane confocal images, from 7d CFA treated animals. Green indicates CXCL10 and red indicates the double labelled antigen, as indicated. The top panel is a low power image of CXCL10 and NeuN in the dorsal horn, and the panel below is a high power image from the same region. The full arrows indicate examples of double labelled CXCL10 and NeuN cells, while the dashed arrow is an example of a NeuN positive, CXCL10

negative cell. No double labelling was observed with IBA1 (a marker of microglia) or GFAP (a maker of astrocytes). Scale bars indicate 100µm for top panel and 25µm in all other images.

6.3.5 Characterising CXCR3 protein expression in the dorsal horn

Western blot analysis of CXCR3 was also carried out on tissue from dermorphin-saporin + CFA and saline injected + CFA groups (experiment 2) and in 'normal' CFA and sham animals (without RVM injection, experiment 3). Bands were detected at the correct molecular weight (at approximately 38kDA), however comparison between groups indicated no differences when band intensity was normalised to the housekeeping protein calnexin, either in experiment 2 (dermorphin-saporin v saline, p = 0.98) or experiment 3 (CFA v sham, p = 0.7188) (figure 6.5).

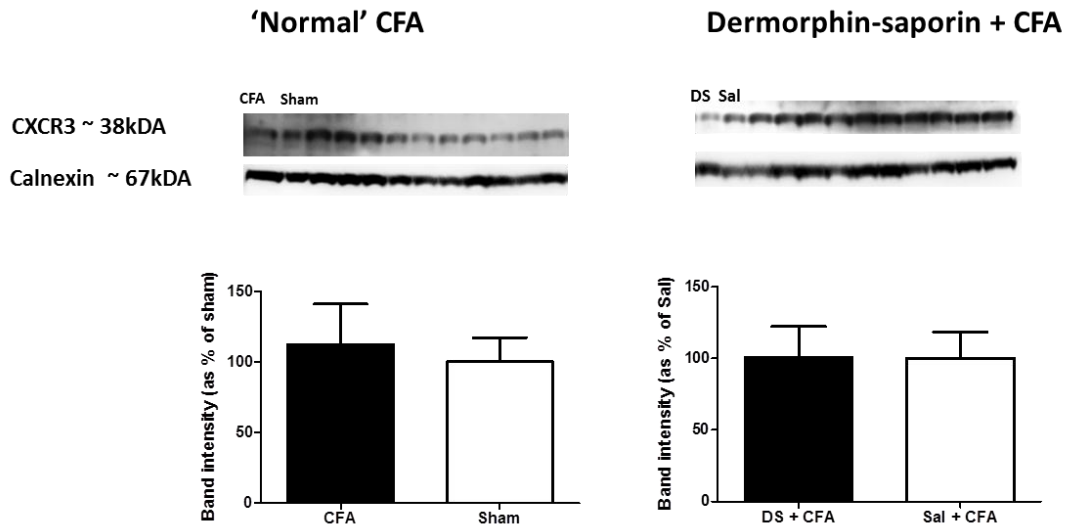

Figure 6.5 No effect of CFA or dermorphin-saporin on CXCR3 protein levels.

Two sets of tissue were used for western blot analysis. 'Normal' CFA corresponds to experiment 3, and dermorphin-saporin + CFA corresponds to experiment 2 (see table 6.1). Lanes are loaded alternately with CFA followed by Sham for the 'normal CFA' experiment and dermorphin-saporin (DS) followed by saline (sal) for the dermorphin-saporin + CFA experiment. No differences in CXCR3 expression were identified in either experiment. $p > 0.05$, independent samples t-test, n = 6 all groups, data is presented as mean ± SEM.

To characterise the cellular localisation of CXCR3 protein within the dorsal horn, immunohistochemistry was carried out in animals at 7d following CFA injection or sham procedure. As with the western blot analysis, there did not appear to be any difference in CXCR3 expression between CFA and sham groups. For this reason images from the sham treated group are not shown here. In contrast to CXCL10 labelling, CXCR3 had a discrete, punctate pattern of staining within the superficial laminae of the dorsal horn. The punctate pattern of staining suggested that CXCR3 could be expressed on afferent terminals. Double labelling with CGRP, a marker of peptidergic primary afferents, indicated that CXCR3 is expressed in CGRP+ terminals in some cases (figure 6.6). Analysis of single plane images indicated there was no colabelling of CXCR3 in IBA1 positive cells (microglia) or GFAP positive cells (astrocytes) (figure 6.6).

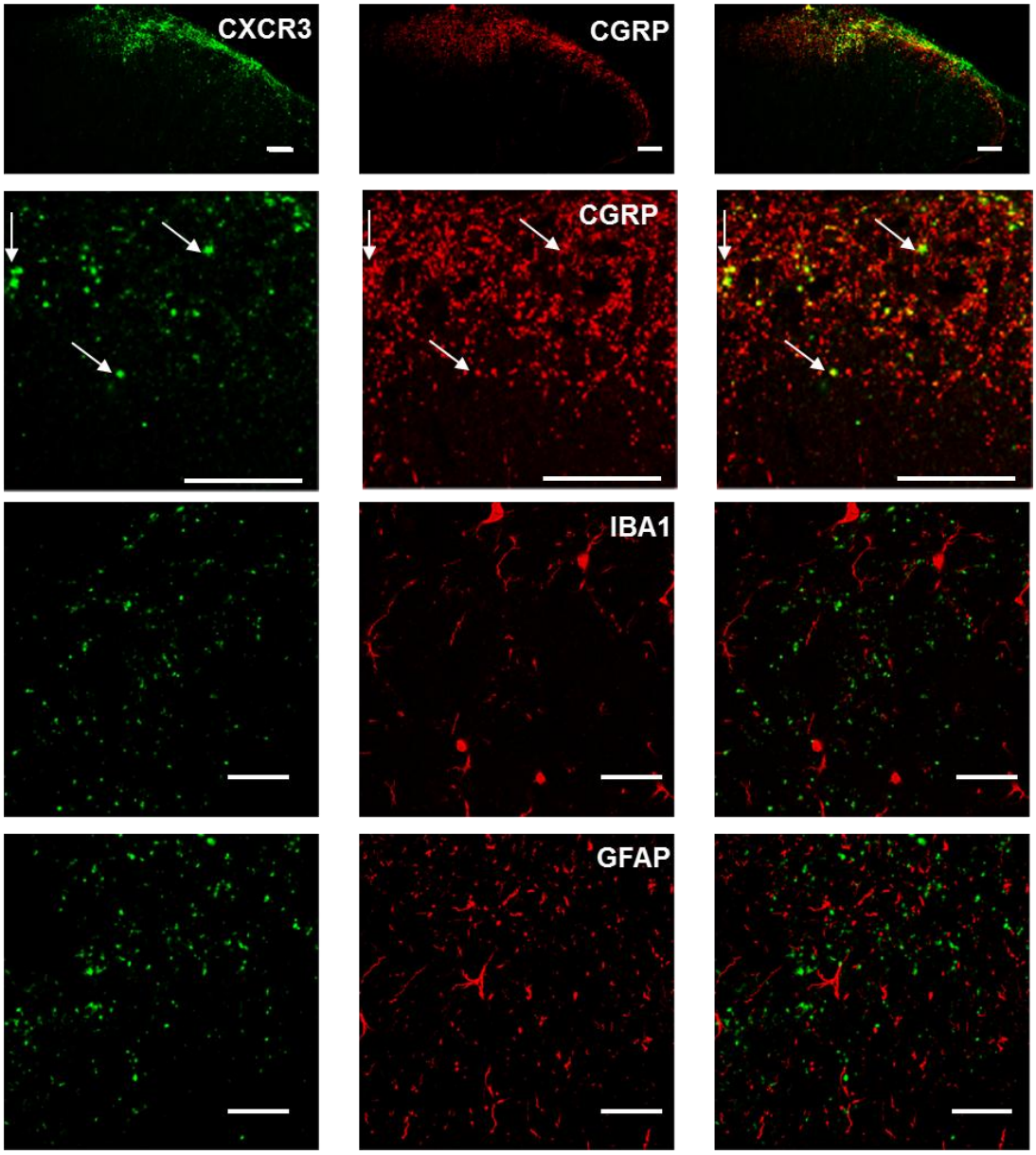

Figure 6.6 Double labelling of CXCR3 and CGRP terminals.

Images shown are single plane confocal images, from 7d CFA treated animals. Green indicates CXCR3 staining and red indicates the double labelled antigen. The top panel indicates a low power image of CXCR3 and CGRP labelling in the superficial dorsal horn, and directly below is a higher power image from the same area. Arrows indicate examples of CXCR3 double labelling with CGRP. No double labelling was observed with IBA1 (a marker of microglia) or GFAP (a maker of astrocytes). Scale bars indicate 100µm for top panel and 25µm in all other images.

6.4 Discussion

Previous work by others (Bee and Dickenson, 2008; Burgess et al., 2002; Porreca et al., 2001) has demonstrated that the MOR+ cells of the RVM contribute to behavioural sensitivity in neuropathic pain models. The previous chapter in this thesis has demonstrated that these cells also play a role in behavioural hypersensitivity following joint inflammation. Despite a number of studies on the role of these cells in facilitation of pain behaviour, relatively little is known regarding the spinal mechanisms underlying this facilitation. To investigate molecular mechanisms involved in descending facilitation by this pathway, we carried out microarray analysis of the dorsal horn following MOR+ cell depletion and CFA injection, compared with non-lesioned controls.

A number of cellular mechanisms could potentially contribute to descending facilitation of dorsal horn excitability. Changes in receptor availability, presynaptic release of neurotransmitters, post-synaptic changes in intracellular signalling pathways, transcriptional regulation and immune cell activation are all key features of central sensitisation (Latremoliere and Woolf, 2009) and could be subject to descending facilitation. However, surprisingly few genes with neuronal annotations were identified in our analysis, while many genes associated with immune cell function were identified. This fits with the prominent role of immune cells in the dorsal horn in mediating central sensitisation and behavioural hypersensitivity, and immune related genes are a feature of many other microarray studies of the dorsal horn (Costigan et al., 2009a; Griffin et al., 2007; Yukhananov and Kissin, 2008).

Of particular interest was the identification of a number of genes from the CXC chemokine-receptor family, which were found to be downregulated in the dermorphin-saporin group. Chemokines have emerged as important mediators of immune cell activation and central sensitisation in the dorsal

horn (Old and Malcangio, 2012). The identification here of the CXC chemokine family, previously uncharacterised in the dorsal horn, is a promising subject for future work on the descending facilitation of pain.

6.4.1 Dorsal horn genes regulated by descending facilitation

6.4.1.1 Microarray analysis

Microarray technology is widely used in many areas of biology as a high throughput method for identifying many differentially regulated genes in parallel. However one of the main limitations of this type of study is the generation of false positives and false negatives from the data set due to the high number of individual genes studied. To minimise the problem of false positives, fold change thresholds are often set at a high value, for example fold changes > 2. Used in conjunction with a p value of < 0.05, such strict criteria will reduce the likelihood of false positives. However the problem of false negatives remains, as many genes that are significantly regulated will not be identified as they fail to meet the conservative fold change requirement. In studies of the dorsal horn quadrant this can be a particular problem. Lamina I, II, and V are the key areas involved in receiving nociceptive input and projecting to the brain (Todd, 2002) and therefore inclusion of lamina III and IV as well as the surrounding white matter is likely to dilute the magnitude of gene expression changes within these laminae of interest. For this reason the use of lower fold changes as a cut-off may be more appropriate.

A recent study of the spinal cord in inflammatory pain has used a p value of < 0.01 as the sole criterion for identifying differentially regulated genes with no reference to fold changes (Yukhananov and Kissin, 2008). These authors were able to validate a number of targets by RT-qPCR suggesting that a fold change cut-off is not absolutely required in such studies. Our own group has also published data using a combination of statistical significance and fold change > 1.3 to identify gene changes in the dorsal horn associated with

ankle joint inflammation (Géranton et al., 2007a). In the Géranton et al. study comparison was made between naive and CFA treated animals, with an obvious difference in behaviour between these groups. Such a profound difference in the pain behaviour would suggest that a number of large increases in gene expression could occur within the dorsal horn. In the present study, microarray analysis was carried out on groups with and without RVM lesion by dermorphin-saporin, and both with CFA injection. As the lesioned group demonstrate a subtle attenuation of behavioural sensitivity it would be expected that the fold differences in gene expression changes would also be relatively low. For this reason it was decided that the fold change should be reduced to 1.2. This provided a balance between reducing false positives, by including a fold change in the interpretation of the results, while reducing the likelihood of false negatives by setting the fold change criterion at a relatively low level.

Using these criteria, 129 Affymetrix gene IDs were identified as differentially regulated in the dermorphin-saporin treated group. This suggests that descending facilitation by RVM MOR+ cells contributes to changes in gene expression within the dorsal horn following ankle joint inflammation. The majority of these were downregulated in the dermorphin-saporin group suggesting that in the normal pain state, these genes are positively regulated by descending facilitation. Functional annotation analysis was carried out on these genes which revealed that two of the major categories of genes regulated by the MOR+ cell descending pathway were those associated with ribosomal function and immune cell processes.

6.4.1.2 Ribosomal proteins regulated by descending facilitation

Differences in the expression of ribosomal related genes in this study suggests that descending facilitation from the RVM has a profound effect on the transcription of ribosomal RNA (rRNA) within the dorsal horn. Decreased ribosome biogenesis is a feature of some neurodegenerative responses

(Rieker et al., 2011) however it has also been found that rRNA transcription is subject to regulation by the mammalian target of rapamycin (mTOR) signalling pathway (Iadevaia et al., 2012). It is known that translational regulation is a key component of neuronal plasticity (Costa-Mattioli et al., 2009) and in particular the mTOR pathway is activated in the dorsal horn during persistent inflammation and contributes to behavioural hypersensitivity (Géranton et al., 2009; Norsted Gregory et al., 2010; Obara et al., 2011). It is possible that descending facilitation contributes to this activation which is reflected in changes in rRNA levels. Downregulation of the gene *Rpl32* was confirmed by RT-qPCR and other genes in this category may warrant further investigation.

Although RT-qPCR is widely used in the study of gene expression, and is an important step following microarray analysis for the validation of selected genes, there are some intrinsic limitations associated with this technique. One such limitation arises in the choice of a reference or housekeeping gene, required for the normalisation of expression data (Coulson et al., 2008). The ideal reference gene is one that is expressed at a stable level in the tissue of interest under all experimental conditions. However it has been reported that many common reference genes, such as glyceraldehyde-3-phosphate dehydrogenase (GAPDH) are themselves differentially regulated under certain experimental conditions (Winer et al., 1999). Indeed the microarray data obtained in the present experiment indicated that *Gapdh* is downregulated in the dorsal horn group. Actin was used as the sole reference gene in the RT-qPCR validation experiments described in this chapter. Actin has been used widely as the single reference gene for many published studies of the dorsal horn of the rat (Fu et al., 2007; Géranton et al., 2007; Ren et al., 2005; Tochiki et al., 2012). However it has been proposed that use of more than one reference gene within an experiment can produce more reliable data (Huggett et al., 2005). Therefore in further studies it may beneficial to include additional appropriate housekeeping

genes, such as hypoxanthine guanine phosphoribosyl transferase (HGPRT) in the analysis of the RT-qPCR data (Tochiki et al., 2012). This would reduce the possibility of generating misleading data due to fluctuations in expression levels of actin within the dorsal horn.

6.4.1.3 Immune system related genes regulated by descending facilitation

It is now widely accepted that immune cells such as microglia, astrocytes and infiltrating T cells play a crucial role in a number of chronic pain states following nerve injury (Costigan et al., 2009a), cutaneous inflammation (Raghavendra et al., 2004), and joint pain (Clark et al., 2012; Sagar et al., 2011). Activation of dorsal horn immune cells is generally thought to be driven by nociceptive input from the periphery, particularly during neuropathic injury (Calvo et al., 2012; Meller et al., 1994). Recently however it has been suggested that descending facilitation could contribute to immune cell activation within the dorsal horn. It has been shown that activation of the spinal 5-HT_3 receptor leads to the release of the chemokine CX3CL1 (fractalkine) from primary afferent terminals and subsequent microglial and astrocytic activation leading to enhanced pain responses (Gu et al., 2011). This suggests that descending 5-HT is involved in the activation of spinal immune cells in pain states, and may be one way in which descending controls result in increased pain responses.

In line with this hypothesis our study identified of a number of genes with functions within the immune system. Indeed the gene with the highest fold change was the serine peptidase inhibitor *Serpinb1b*, which was found to be downregulated 4-fold in the dermorphin-saporin treated group. A closely related gene *Serpinb1a* was also found to be significantly downregulated on the array. Serpin proteins are expressed in neutrophils and are required for the modulation of neutrophil serine protease activity and neutrophil survival (Benarafa et al., 2007). Neutrophil infiltration of the spinal cord (Mitchell et

al., 2008) and prefrontal cortex (Poh et al., 2012) has been shown to occur during peripheral inflammation and may contribute to increased pain processing in these regions. Downregulation of *Serpinb1a* and *Serpinb1b* in our study may therefore reflect a decrease in neutrophil activity within the spinal cord. This raises the interesting possibility that descending facilitation could contribute to immune cell infiltration and activation within the dorsal horn.

The gene *Nos2*, which encodes the enzyme inducible nitric oxide synthase (iNOS), was also found to be downregulated in the dermorphin-saporin treated group, and this decrease was confirmed by RT-qPCR. *Nos2* expression is induced in peripheral immune cells during inflammation, and has also been shown to be upregulated in microglia and astrocytes (Amitai, 2010). Nitric oxide (NO) itself has been implicated in central sensitisation in various pain states (Coderre and Yashpal, 1994; Gühring et al., 2000; Malmberg and Yaksh, 1993; Meller et al., 1994a; Moore et al., 1991; Wu et al., 2001). Although the focus has largely been on neuronal NOS as the enzyme responsible for spinal production of NO, a number of reports have implicated *Nos2* gene (and iNOS protein) in inflammatory and neuropathic pain (Gühring et al., 2000; Infante et al., 2007; Kuboyama et al., 2011; Tang et al., 2007). Bilateral induction of *Nos2* gene expression in the dorsal horn has been shown to occur following ankle injection of CFA (Infante et al., 2007), and our present data suggests that *Nos2* gene expression may be modulated, at least in part, by descending pathways. Interestingly upregulation of *Nos2* occurs in the spinal cord in a model of stress induced hyperalgesia, and CCK signalling within the RVM is required for this process (Rivat et al., 2010). Our finding supports this work and suggests that *Nos2* may be an important mediator of descending facilitation within the spinal cord.

6.4.2 Regulation of CXC chemokines by descending facilitation

Chemokines are small molecular weight proteins which traditionally have been shown to regulate leukocyte migration and activation and therefore act as a key component of the immune response (Fernandez and Lolis, 2002). There are four families of chemokine, based on the structural arrangements of cysteine residues in the N-terminus (see figure 6.7). Chemokines are involved in the migration of peripheral immune cells to the CNS during neuro-inflammatory disorders such as multiple sclerosis or viral infection (Ransohoff et al., 2007). In addition, chemokines and receptors have been found to be expressed on both neurons and glial cells within the normal, healthy CNS and may therefore play an intrinsic role in CNS function (Adler et al., 2005). Chemokines within the dorsal horn have been shown to play a role in a number of pain models. One well studied example is the chemokine CX3CL1 (fractalkine) which is released by neurons within the dorsal horn, and activates its receptor CX3CR1 on microglia, leading to enhanced release of pronociceptive mediators such as the cytokines IL-1β and IL-6, and nitric oxide (NO) (Old and Malcangio, 2012). CX3CL1 in the dorsal horn has been implicated in both neuropathic and inflammatory pain states (Clark et al., 2012). CCL2, a member of the CC family of chemokines, has also been implicated in neuropathic pain states (Zhang et al., 2007). In both cases, it appears that the chemokine is released by primary afferents and activates microglia or other cell types expressing the target receptor within the dorsal horn.

Figure 6.7 Classification of chemokine families.

Classification of chemokines into four families is based on the structural organisation of the N-terminus cysteine residues. To date, CCL2 and fractalkine are the most widely studied in the dorsal horn in pain states. Adapted from Old and Malcangio, 2011.

Given the established role of chemokines in a number of models of pain, one of the interesting findings of the functional annotation analysis was the enrichment of terms associated with chemotaxis. Within this cluster two members of the same family of chemokines were identified, *Cxcl9* and *Cxcl10*. These are members of the interferon gamma (IFN-γ) inducible subset of CXC chemokines (figure 6.7). A number of previous studies have suggested a role for the cytokine IFN-γ within the dorsal horn in chronic pain states. IFN-γ receptor knockout mice show reduced mechanical hypersensitivity in a neuropathic pain model (Robertson et al., 1997). Application of IFN-γ to the spinal cord increases nociceptive reflexes (Xu et al., 1994b) and the IFN-γ receptor has been shown to be expressed at synapses in the dorsal horn (Vikman et al., 1998). Recently it has been shown that IFN-γ application to the spinal cord leads to reduced GABAergic inhibition which may contribute to increased nociception (Vikman et al., 2007). As targets of IFN-γ signalling, *Cxcl9* and *Cxcl10* may therefore be involved in nociception in the dorsal horn. Notably the shared receptor for these chemokines, *Cxcr3*, was also identified in the microarray analysis. RT-qPCR analysis confirmed that *Cxcl9*, *Cxcl10* and *Cxcr3* are all downregulated in the dermorphin-saporin treated group, suggesting that this chemokine-receptor signalling pathway may contribute to descending facilitation of the pain state.

As mentioned above, a recent study has identified a role for descending 5-HT in the release of CX3CL1 (fractalkine) from primary afferents, leading to the activation of microglia and astrocytes within the dorsal horn, which leads to behavioural hypersensitivity (Gu et al., 2011) . This work indicated that descending facilitation by 5-HT is mediated, at least in part, by primary afferent release of pro-inflammatory chemokines. The findings presented in this chapter suggest that MOR+ cell mediated descending facilitation may act via a different subset of chemokines within the dorsal horn (figure 6.8). It

should be noted however that some of the data in the publication by Gu et al., 2011 has since been retracted, and therefore needs to be repeated.

Western blot analysis indicated that both CXCL10 and CXCR3 are expressed in the dorsal horn, however no significant increase was found in protein levels of either the receptor or the ligand at 7d following ankle injection of CFA. In addition, no change in protein levels was identified in the dermorphin-saporin and saline treated animals. This suggests that although gene expression is decreased in the dorsal horn in the dermorphin-saporin group, this is not reflected in overall protein levels. This may be due to a difference in time course of the changes in mRNA levels and changes in expression of the protein itself. Both CXCL10 and CXCR3 were expressed within the dorsal horn in the sham treated animals, suggesting that this chemokine-receptor pathway may play a role in normal transmission within the spinal cord. For this reason it was of interest to determine the cellular localisation of both the receptor and ligand within the cord using immunohistochemistry.

Surprisingly, no evidence was found for microglial or astrocytic expression of either CXCR3 or CXCL10. CXCL10 was found to be localised to a subset of neurons throughout the spinal cord, as identified by NeuN double labelling. Further work to determine the proportion of NeuN cells expressing CXCL10 will be carried out, as well as double labelling studies to identify specific neuronal subpopulations that express CXCL10. Studies have reported upregulation of *Cxcl10* within the DRG during inflammation and herpes zoster infection (Steain et al., 2011; Strong et al., 2012) and it is possible that *Cxcl10* is also upregulated in the DRG following ankle injection of CFA. However we found no evidence for CXCL10 expression on afferent terminals within the dorsal horn, suggesting that if *Cxcl10* is upregulated within DRG neurons in our model, the protein product is not transported to the primary afferent terminals. The immunohistochemistry data presented here suggests

that CXCL10 protein expression is restricted to a subpopulation of intrinsic dorsal horn neurons.

As with western blot analysis, there was no apparent upregulation of CXCL10 in the CFA treated animals, suggesting that the CXCL10 is constitutively expressed in these neurons. Although most studies of CXCL10 in the CNS have focused on its expression in immune cells and role in neuroinflammation (Müller et al., 2010), one study has demonstrated that CXCL10 is expressed constitutively in neurons in culture, and may be released tonically at low levels (Vinet et al., 2010). Furthermore exposure of hippocampal neurons in vitro to exogenous CXCL10 causes increased excitability (Cho et al., 2009). The identification of CXCL10 protein within dorsal horn neurons suggests that this ligand may be released by neurons within the dorsal horn and could contribute to synaptic activity in other neighbouring neurons. Although to date, chemokines within the CNS have been investigated predominantly as modulators of immune cells, in future it may be of interest to investigate their roles in neuronal transmission. Indeed chemokine-receptor interactions have previously been proposed as an additional neurotransmission system in the CNS, as a variety of chemokines and their corresponding G-protein coupled receptors have been identified in the CNS of healthy animals (Adler et al., 2005).

In support of a direct role for CXCL10 in neuronal modulation, no evidence of expression of the receptor CXCR3 was found in microglia and astrocytes of the dorsal horn using immunohistochemistry. In contrast to the CXCL10 ligand, the distribution of the receptor was restricted to the superficial laminae, and had a more punctate appearance. This suggested that CXCR3 could be located either presynaptically or postsynaptically. As explained, activation of the CXCR3 receptor by CXCL10 *in vitro* causes increased neuronal excitability, suggesting that CXCR3 activation within the dorsal horn may similarly contribute to neuronal excitability. Some double

labelling with CGRP was observed suggesting that CXCR3 expression occurs on a subset of peptidergic terminals in the dorsal horn. This suggests that CXCL10 (and other CXC ligands) could act directly on these terminals.

Not all CGRP+ terminals express the CXCR3 receptor, and work is currently underway within the group to quantify the proportion of double labelled CXCR3+ CGRP terminals, and within the cell bodies of the DRG. As many joint nociceptors express CGRP (Ivanavicius et al., 2004; Jimenez-Andrade et al., 2010; Nakajima et al., 2008) it would be expected that at least some of these double labelled afferent terminals originate in the joint. Future studies using anterograde tracing from the joint and skin could be used to determine the proportion of CGRP+/CXCR3+ terminals arising from the joint.

Interestingly descending facilitation via the MOR+ cell pathway has been implicated in the release of CGRP from primary afferent terminals (Gardell et al., 2003). Therefore one mechanism by which dermorphin-saporin exerts its effects on pain behaviour may be via regulation of the CXCR3 receptor within peptidergic primary afferent terminals (figure 6.8). Recently it has been demonstrated that LTP at primary afferent-dorsal horn synapses is driven in part by presynaptic mechanisms of neurotransmitter release (Luo et al., 2012). The ability of descending pathways to interact with primary afferent terminals may therefore contribute to presynaptic mechanisms of LTP within the dorsal horn.

Figure 6.8 Contribution of descending facilitation to immune cell and chemokine activation in the dorsal horn.

Activation of 5-HT_3 receptors on primary afferent terminals in the dorsal horn has been shown to cause release of the chemokine fractalkine (CX3CL1) from primary afferent terminals. This leads to activation of microglia, release of Il-18, activation of astrocytes, and release of IL-1β, which contributes to central sensitisation in cutaneous inflammation (Gu et al., 2011). The data provided in this thesis suggests that the MOR+ cell pathway may also result in the activation of a chemokine-receptor signalling mechanism. The CXCR3-receptor

localises to primary afferent terminals expressing CGRP, and CXCL10 ligand localises to neuronal cell bodies in the dorsal horn. These may be regulated by descending facilitation via the MOR+ cell pathway, and contribute to behavioural hypersensitivity. (NB. Some of the data in the publication by Gu et al., 2011 has since been retracted, and therefore needs to be repeated).

Chemokine receptors are G-protein coupled, signalling to Gi proteins and leading to activation of a variety of intracellular signalling pathways (Sallusto and Baggiolini, 2008). Therefore the expression of CXCR3 on primary afferent terminals suggests that activation could modulate the excitability of these fibres. *In vitro* studies have demonstrated that activation of the CXCR3 receptor by CXCL10 results in ERK phosphorylation and increased neuronal excitability in hippocampal cultures (Bajova et al., 2008; Xia et al., 2000). Notably, exposure of DRG neurons in culture to CXCL10 can induce calcium transients suggesting that DRGs express the CXCR3 receptor and respond to CXCL10 binding (Oh et al., 2001). Neuronal expression of the CXCR3 receptor and excitation of neurons by CXCL10 has not been demonstrated previously *in vivo*, however it is an interesting possibility that CXCL10 - CXCR3 signalling could contribute to neuronal excitability in the nociceptive system.

The expression of CXCR3 on primary afferent terminals is somewhat puzzling, given that our interest in this receptor arose from transcriptional changes in the dorsal horn, and these would largely reflects changes in transcription at the cell body. However it is known that local translation occurs in primary afferent terminals, presumably of mRNA transcripts that are present at those terminals (Géranton et al., 2009; Jiménez-Díaz et al., 2008). Therefore it is possible that mRNA transcripts localised to primary afferent terminals contribute to the changes identified by microarray and RT-qPCR analysis of the dorsal horn.

Upregulation of *Cxcl0* has been shown previously within the dorsal horn in a model of post-herpetic allodynia (Takasaki et al., 2012), and upregulation of *Cxcl10* has also been shown occur within the DRG during inflammation

(Strong et al., 2012) and following herpes zoster infection (Steain et al., 2011). Our work is the first to identify changes in both *Cxcl10* and *Cxcr3* genes simultaneously, and to attempt to characterise the cellular localisation of their protein products. Importantly changes in gene expression of *Cxcr3* and *Cxcl10* were only unmasked following depletion of the descending facilitatory system, suggesting an important role for the MOR+ pathway in the regulation of these molecules. Further work is needed to fully characterise this chemokine-receptor system in the dorsal horn but it is a promising target for further work on descending facilitation in pain.

6.4.3 Conclusion

Microarray analysis of the dorsal horn in animals with CFA injection and prior RVM injection of either dermorphin-saporin or saline led to the identification of genes regulated by descending facilitation. Many of these are immune related, and downregulated in the lesioned group. This fits with existing knowledge of the importance of immune cells to chronic pain states and the potential role of descending pathways in the activation of these processes.

7. General Discussion

Joint pain is a significant clinical problem, and to date most research has focused on the peripheral causes of joint injury as the source of pain, rather than addressing plasticity in the nociceptive system. Treatment approaches are also based largely on modification of peripheral pathology, such as joint replacement in osteoarthritis, or the use of immunosuppressant drugs in rheumatoid arthritis.

Clinically it has been demonstrated that patients with OA and RA have increased pain sensitivity at sites beyond the affected joints (Graven-Nielsen et al., 2012; Morris et al., 1997). This suggests that joint pain is caused in part by changes within the nociceptive system, in addition to the peripheral joint pathology. In some cases, pain may persist even after interventions to treat the peripheral cause of pain, such as joint replacement surgery (Wylde et al., 2011). Understanding the changes that occur in the nociceptive system during joint pain is important for the development of better pharmacological treatments (Kidd et al., 2007).

Studies have begun to address the role of dorsal horn sensitisation in animal models of joint pain (Schaible et al., 2009), and descending facilitation via the RVM is known to contribute to spinal excitability in other models, including neuropathic pain and cutaneous inflammation (Ossipov et al., 2010). To date however relatively few studies have addressed the role of the descending system in joint pain, and those that have investigated the role of descending inhibition, and only in the acute phase of injury (Cervero et al., 1991; Danziger et al., 1999; Schaible et al., 1991). The aim of this thesis was to investigate the role of descending facilitation in a model of joint inflammation. Using lesion techniques combined with behavioural studies and molecular analysis of the dorsal horn, I have demonstrated that descending facilitation contributes to mechanical hypersensitivity of the

hindpaw and transcriptional changes within the dorsal horn following joint inflammation.

7.1 Summary of findings

7.1.1 Changes in the RVM following joint inflammation

Ankle injection of CFA in the rat is a widely used model of inflammatory joint pain (Butler et al., 1992). Recent studies have demonstrated that the dorsal horn of the spinal cord is involved in the development of behavioural hypersensitivity in this model (Géranton et al., 2007a; Shan et al., 2007; Vikman et al., 2003; Yao et al., 2011). To date however the role of the RVM has not been investigated. Chapter 3 of this thesis investigated if activation of the RVM occurs following ankle joint inflammation, which would suggest recruitment of descending controls. Activation of ERK by phosphorylation is considered a hallmark of neuronal activity, and pERK immunohistochemistry has been used previously to demonstrate activation of the RVM following cutaneous inflammation (Imbe et al., 2005) and in a model of neuropathic pain (Géranton et al., 2010). As in these other pain models, ankle joint inflammation led to an increase in pERK positive neurons within the RVM. This effect was transient, as pERK was only significantly increased at 6h post CFA injection and not at later time points. Furthermore it was shown that this increase in pERK occurs largely within the 5-HT expressing population of RVM neurons, supporting a role these neurons in the modulation of pain in this model. Importantly, mechanical hypersensitivity of the hindpaw remains elevated for many days after this time point, suggesting that the activation of the ERK signalling pathway in the RVM contributes to the induction, but not the maintenance, of the pain state. ERK activation at this early time point may indicate the onset of descending modulation via the RVM.

Another approach used was to investigate if GABAergic signalling in the RVM is altered following joint inflammation. Many of the synapses formed onto

RVM neurons are GABAergic (Cho and Basbaum, 1991) suggesting an important role for GABA in modulating the output of the RVM. Recently it has been suggested that decreased GABAergic inhibition in the region contributes to increased excitability of the RVM-dorsal horn projection neurons in a model of cutaneous inflammation (Zhang et al., 2011). To investigate if this occurs in the ankle joint model, an antibody specific to C-terminus of VGAT, which is only accessible within actively recycling synapses, was injected into the RVM at 3d post CFA injection. This method labels active GABAergic synapses *in vivo* and quantification of this labelling indicated a decrease in GABAergic transmission occurs at 3d post CFA injection. This provides evidence supporting the view that decreased inhibition of RVM neurons occurs during the maintenance of inflammatory joint pain.

Taken together, these anatomical experiments have confirmed that the RVM is activated during joint inflammation, suggesting descending modulation from this region may contribute to behavioural hypersensitivity.

7.1.2 Descending facilitation plays a time dependent role in mechanical hypersensitivity of the hindpaw following joint inflammation

Behavioural hypersensitivity was measured following ankle injection of CFA using von Frey hairs applied to ipsilateral hindpaw. Increased mechanical hypersensitivity of the hindpaw is predominantly a reflection of secondary hyperalgesia and allodynia (see below section 7.2.1), which requires central sensitisation. To investigate the role of descending facilitation in this process two lesion experiments were carried out. Firstly lesion of the descending 5-HT input to the dorsal horn was performed by intrathecal administration of the toxin 5,7-dihydroxytryptamine (5,7-DHT). This selectively ablates all fibres containing 5-HT. This lesion was found to attenuate mechanical hypersensitivity, but only at 1d and 2d post CFA injection. This suggested

that descending 5-HT containing neurons play a time dependent role in the development of mechanical hypersensitivity.

As many previous studies had implicated the 5-HT_3 receptor in the facilitatory effects of 5-HT within the spinal cord (Dogrul et al., 2009; Donovan-Rodriguez et al., 2006; LaGraize et al., 2010; Suzuki et al., 2002), a further experiment investigated the role of this receptor. Intrathecal injection of ondansetron, a 5-HT_3 specific antagonist, was carried out at 1d following CFA injection. This led to a brief attenuation of established mechanical hypersensitivity. As the magnitude of attenuation was comparable to that observed following 5,7-DHT lesion, this suggested that 5-HT acting at the 5-HT_3 receptor is an important facilitatory pathway in joint pain.

Only a small proportion of electrophysiologically defined ON cells, believed to be facilitatory, contain 5-HT (Marinelli et al., 2002). This suggests other non-5-HT neurons are also likely to contribute to descending facilitation. Although ON cells do not have a single neurochemical identity, they can be identified by their direct responsiveness to morphine suggesting they express the mu opioid receptor (MOR) (Heinricher et al., 1994; Marinelli et al., 2002). This characteristic has been exploited previously to selectively ablate the MOR expressing (MOR+) neurons of the RVM using the selective neurotoxin dermorphin-saporin (Bee and Dickenson, 2008; Burgess et al., 2002; Porreca et al., 2001; Zhang et al., 2009). To investigate the role of these neurons in the inflammatory joint pain model, microinjection of dermorphin-saporin to the RVM was carried out prior to CFA injection. Unlike previous studies of neuropathic pain (Burgess et al., 2002; Zhang et al., 2009), MOR+ cell depletion did not lead to a full reversal of mechanical hypersensitivity. Instead a significant attenuation of hypersensitivity, of a similar magnitude to that observed in the 5,7-DHT experiment, was found. However in contrast to the 5,7-DHT depletion experiment, MOR+ cell

depletion had a more prolonged effect on behavioural hypersensitivity, with significant attenuation observed from 1-7d post CFA injection.

These behavioural experiments have demonstrated that both 5-HT and non-5-HT mechanisms of descending facilitation contribute to secondary hyperalgesia following joint inflammation. The time course of attenuation by these two pathways overlaps but is not identical, suggesting that these two pathways have different roles in inflammatory joint pain.

7.1.3 Changes in gene expression associated with descending facilitation

In comparison to our understanding of descending facilitation via the 5-HT pathway, relatively little is known about the dorsal horn mechanisms underlying ON/MOR+ cell mediated facilitation. Chronic pain states are associated with transcriptional changes within the dorsal horn (Géranton et al., 2007; Kim et al., 1998), and indeed a number of molecular changes have been shown to occur directly in response to the 5-HT pathway (Géranton et al., 2008; Rygh et al., 2006). To identify possible mechanisms by which MOR+ cells contribute to pain facilitation in the spinal cord, microarray analysis was carried out to identify changes in dorsal horn gene expression associated with this descending pathway.

This analysis led to the identification of a number of immune system related genes which may be of interest for further studies. This is in line with a number of other microarray studies which have found upregulation of immune related genes within the dorsal horn in persistent pain states (Costigan et al., 2009a; Yukhananov and Kissin, 2008). Of particular interest were the genes for the chemokine *Cxcl10* and its receptor *Cxcr3*, both of which were downregulated in the dermorphin-saporin group. A number of other chemokines have been implicated in pain signalling within the dorsal horn (Old and Malcangio, 2012). However neither CXCL10 nor the CXCR3 receptor proteins have been identified previously within the dorsal horn, although *Cxcl10* expression has been identified in the DRG in a number of

experimental conditions such as inflammation and herpes zoster infection (Steain et al., 2011; Strong et al., 2012; Takasaki et al., 2012). The downregulation of both genes in the dermorphin-saporin group suggest they may be targets of MOR+ mediated descending facilitation at the dorsal horn level.

Unexpectedly immunohistochemistry within the dorsal horn indicated that the protein products of these genes were not localised to microglia or astrocytes. The apparent neuronal localisation of CXCL10 and CXCR3 suggests that these may play a role in attracting immune cells to the dorsal horn during inflammatory pain, or as a novel neuronal signalling pathway contributing to central sensitisation.

7.2 Descending facilitation in joint inflammation

7.2.1 Measuring mechanical hypersensitivity of the hindpaw: a note on terminology

In humans, allodynia refers to an increased pain response to normally innocuous stimuli, and hyperalgesia refers to an increased response to painful stimuli. My behavioural experiments have investigated increased mechanical sensitivity of the hindpaw following joint inflammation in the rat. To avoid making assumptions as to whether this hypersensitivity is a reflection of allodynia or hyperalgesia, which is difficult to address in an animal model, I have used the term mechanical hypersensitivity to describe this data. However in this study it is important to distinguish between primary and secondary hyperalgesia. In models of cutaneous inflammation in humans, primary hyperalgesia refers to increased pain sensitivity that occurs at the site of injury while secondary hyperalgesia occurs at sites adjacent to but not at the site of injury (Hardy et al., 1950; Treede et al., 1992). A comparable distinction can also be made in conditions of joint pain, where pain in the affected joint is primary, and pain arising distal to the

injured joint is secondary, and presumably driven by central mechanisms (Graven-Nielsen et al., 2012). In the experiments described in this thesis, mechanical hypersensitivity of the hindpaw predominantly reflects secondary mechanisms, as increased paw sensitivity is secondary to the site of injury within the ankle joint.

To summarise, although I use the term mechanical hypersensitivity to describe the behavioural results in this thesis, this hypersensitivity is predominantly a reflection of secondary hyperalgesia (and/or allodynia), which is driven by central sensitisation (Treede et al., 1992).

7.2.2 Descending facilitation of mechanical hypersensitivity of the hindpaw

This study has provided new information regarding descending facilitation in chronic pain states. Although it seems that both descending 5-HT and the MOR+ cell pathway play a role in secondary hyperalgesia associated with joint inflammation, the magnitude of attenuation in both lesion studies is considerably smaller than that observed in neuropathic pain states. Depletion of MOR+ cells in the RVM results in a complete reversal of mechanical pain hypersensitivity at the later stages of neuropathic pain (Burgess et al., 2002; Zhang et al., 2009). Similarly 5-HT plays a small role in the behavioural experiments described in this thesis. This contrasts with previous findings in neuropathic pain, in which depletion of endogenous 5-HT completely reverses hypersensitivity (Rahman et al., 2006). This suggests there are important differences in neuropathic and joint pain processing at the supraspinal level, with neuropathic pain models more heavily dependent upon facilitation from the RVM.

The time of onset of descending facilitation is also different in the present study than that shown previously for neuropathic pain. The previous dermorphin-saporin studies of neuropathic pain indicated that descending facilitation is required for the maintenance but not the induction of

behavioural hypersensitivity (Bee and Dickenson, 2008; Burgess et al., 2002; Zhang et al., 2009). In contrast, descending facilitation of joint pain is evident from one day onwards. This suggests that in neuropathic pain, descending facilitation is required for the maintenance of pain, whereas in joint pain, descending facilitation contributes to both the induction and maintenance phases. Neuropathic and inflammatory pain models have different peripheral causes and onset of hypersensitivity. While peak behavioural hypersensitivity in the joint model is observed within hours, neuropathic pain may take longer to develop resulting in later activation of the descending facilitatory system. The differences in descending facilitation of joint pain and neuropathic pain may also indicate that central sensitisation, and subsequent secondary hyperalgesia, is more prominent in neuropathic than in joint pain.

Not only do the present findings differ from those in neuropathic models, they also highlight some differences between 5-HT modulation of joint and cutaneous inflammation. The contribution of descending 5-HT to cutaneous inflammatory pain has been investigated in a number of studies. For example our group previously found that 5,7-DHT depletion attenuates mechanical hypersensitivity following plantar inflammation from 1h to 1d post CFA injection (Géranton et al., 2008). This contrasts with the present findings in which 5-HT does not play a significant role until 1d post CFA injection to the ankle.

Interestingly a more recent study, which used siRNA within the RVM to silence the tryptophan hydroxylase (TPH) enzyme and so reduce 5-HT synthesis, showed slightly different results in the same cutaneous model (Wei et al., 2010). They found that there was no effect on mechanical hypersensitivity until 1d – 3d following plantar injection of CFA. The timing of the involvement of 5-HT in this study supports the present findings, suggesting that 5-HT plays a time dependent role in the facilitation of

inflammatory pain. Nonetheless the magnitude of changes observed in the Wei et al. study were larger than those identified here, again suggesting a greater contribution of descending facilitation to pain of cutaneous origin than that from arising the joint.

One of the major anatomical differences between joint and cutaneous nociceptors is the termination of joint afferents in lamina I, and absence of direct joint terminations in lamina II (Doyle and Hunt, 1999; Mense and Prabhakar, 1986; Neugebauer et al., 1994). Lamina II interneurons are believed to play an important role in the development of mechanical hypersensitivity in neuropathic pain and cutaneous inflammation (Malmberg et al., 1997; Martin et al., 2001). More recently genetic ablation of the IB4+, non-peptidergic C-fibre population, which terminate in lamina II has been shown to reduce mechanical hypersensitivity in cutaneous inflammation and neuropathic pain (Cavanaugh et al., 2009). This population of fibres do not innervate the joint (Ivanavicius et al., 2004; Jimenez-Andrade et al., 2010; Nakajima et al., 2008). Therefore pain arising from the joint may not result in direct activation of lamina II neurons in the dorsal horn. As descending projections from the RVM terminate in both lamina I and lamina II, direct actions on the peripheral nociceptive terminals may be more prominent in cutaneous inflammation than in joint inflammation (Millan, 2002).

These differences may also reflect a more prominent role of descending inhibition in joint pain than in cutaneous pain. The earliest investigations of descending controls in joint pain indicated that at least in the acute stage, inhibition of spinal nociception occurs (Cervero et al., 1991; Schaible et al., 1991). Although this inhibition may not persist beyond the acute phase of inflammation it raises the possibility that both facilitation and inhibition occur simultaneously, and which system predominates may depend on the nature of the nociceptive input (cutaneous or joint).

The findings presented in this thesis indicate that during inflammation of the joint, descending facilitation from the RVM contributes in a time dependent manner to mechanical hypersensitivity of the hindpaw, a reflection of secondary hyperalgesia. Previous work on descending controls in joint pain has largely focused on descending inhibition of spinal excitability during joint inflammation (Cervero et al., 1991; Schaible et al., 1991), although one study has demonstrated a role for descending 5-HT in the facilitation of spinal excitability in osteoarthritic pain (Rahman et al., 2009). No behavioural studies have been carried out to date in a joint model. The lesion experiments described here demonstrate that in addition to these inhibitory influences descending facilitation is important, in particular in mediating secondary mechanical hyperalgesia. This supports previous findings suggesting that descending modulation differentially affects primary and secondary hyperalgesia during cutaneous inflammation (Pertovaara, 2000; Vanegas, 2004; Zhuo and Gebhart, 1990).

Notably, no effect of descending 5-HT on weight bearing was observed in the present study suggesting that following ankle injection of CFA the same principles may apply. Primary hyperalgesia of the inflamed joint may be inhibited by descending controls, while descending facilitation could contribute to secondary mechanical hyperalgesia of the adjacent cutaneous tissue. Recent studies have addressed the role of descending 5-HT in pain behaviour following plantar inflammation, in which the primary and secondary components of hyperalgesia are difficult to distinguish (Géranton et al., 2008; LaGraize et al., 2010; Wei et al., 2010). The behavioural data presented in this thesis provides direct evidence that following peripheral inflammation, secondary hyperalgesia of adjacent non-inflamed tissue is facilitated by descending pathways from the RVM. Secondary hyperalgesia at sites distant from the inflamed joint has been reported in patients with RA (Edwards et al., 2009) and OA (Gwilym et al., 2009). Therefore cutaneous secondary mechanical hyperalgesia appears to be a clinically relevant

outcome measure in studies of joint pain. Secondary hyperalgesia requires central sensitisation (Treede et al., 1992), therefore studying secondary hyperalgesia in animal models is also useful as a measure of central sensitisation in the spinal cord.

The size of the weight bearing chamber available during these experiments was a limiting factor, and we were unable to carry out weight bearing analysis on the larger animals (400 – 500g) of the dermorphin-saporin experiments. Future work with a modified weight bearing chamber could provide useful information on the relative contribution of the descending 5-HT and MOR+ pathways to weight bearing on the inflamed joint. The question of primary hyperalgesia of the joint itself has not been explicitly addressed in this thesis, and it is possible that descending inhibition predominates over facilitation at the primary injury site. In future it would be of interest to fully characterise the role of descending facilitation in primary hyperalgesia of the inflamed joint using weight bearing apparatus, and indeed other measures such as hindlimb grip force (Chandran et al., 2009; Lee et al., 2011b).

7.2.2.1 Limitations of the lesion approach

Traditional electrolytic lesion techniques have been used in the RVM to investigate the net contribution of the neurons of this region in pain processing in a number of models (Terayama et al., 2002; Urban and Gebhart, 1999). However interpretation of results from such studies is complicated as the RVM is a heterogeneous population of cells, and non-selective ablation of the region will therefore include both the inhibitory and facilitatory circuitry. Selective lesion of components of the descending pathway such as those used in this thesis are an improvement on this technique, as it is possible to attribute the behavioural effects of the lesion to the loss of the cell type targeted. Nonetheless as with any experimental technique these methods are not without limitations.

Intrathecal administration of 5,7-DHT results in an almost complete loss of 5-HT containing neurons that project to the dorsal horn. The results of the ondansetron experiment in chapter 4 strongly suggest that the behavioural effects observed by 5,7-DHT depletion are driven largely by a loss of 5-HT itself. However it is important to bear in mind that by using lesion of whole fibres, other transmitters contained within those descending 5-HT fibres will also be lost. The loss of other transmitters may contribute to the behavioural effects observed. This is also true of the dermorphin-saporin experiment described in chapter 5. As shown in this chapter, loss of neurons in the RVM region can have unintended adverse effects on the animal which must be avoided.

7.2.3 Neurochemistry of descending facilitation

In this thesis the roles of two distinct but overlapping descending pathways via 5-HT cells and MOR expressing (MOR+) neurons were investigated in parallel experiments. This allows conclusions to be drawn about how these pathways interact in the intact animal. It is known that some MOR+ neurons contain 5-HT (Marinelli et al., 2002; Sikandar et al., 2012), but there are also many MOR negative (MOR-) 5-HT neurons, and 5-HT negative MOR+ cells. These three different categories of RVM neurons may have different contributions to the facilitation of joint pain behaviour.

Activation of ERK at 6h post CFA injection occurs largely within the 5-HT expressing population. This supports the behavioural findings in chapter 4 which indicate that depletion of the 5-HT population attenuates behavioural hypersensitivity at 1 and 2d post CFA injection, but not at later time points. These effects of 5-HT will incorporate those neurons that also express the MOR, therefore the effects of dermorphin-saporin lesion at 1d and 2d following CFA injection may be mediated partly by a 5-HT mechanism. Notably, little pERK labelling is observed in the more dorsal regions of the RVM, which is rich in MOR+ neurons. Therefore it is likely that many of the

MOR+, 5-HT negative neurons do not express pERK following ankle injection of CFA. As peak ERK activation occurs at the 6h time point, this suggests that these pERK negative neurons may play a role in the later phase of facilitation, from 3 to 7d post CFA injection.

By quantifying the number of active GABAergic synapses in the RVM it was found that inflammation induces a decrease in GABAergic inhibition in the RVM at 3d post CFA injection. This suggests that the effects of descending facilitation on pain maintenance are due in part to decreased inhibition in the RVM. Others have demonstrated previously that at 3d following cutaneous inflammation, GABAergic inhibition is decreased while MOR+ cell excitability increased, suggesting that MOR expressing cells are preferentially affected by this loss of inhibition (Zhang et al., 2011). Although here I have not addressed this directly it seems likely that decreased GABAergic inhibition of MOR+ cells at this later time point may contribute to facilitation by these neurons in the later phases of inflammation.

One hypothesis based on the anatomical data presented in chapter 3 and the behavioural experiments in chapter 4 and 5 is that in the acute phase of inflammatory joint pain, descending facilitation does not contribute to behavioural hypersensitivity, as no effects are observed by either 5,7-DHT or dermorphin-saporin lesion. 5-HT contributes to behavioural hypersensitivity at 1 and 2 d following inflammation, but not at later time points. Activation of ERK within the TPH population at 6h following CFA may contribute to setting up this behavioural effect. MOR+ cell depletion results in a more prolonged attenuation. At the 1d and 2d time points, at least some of this effect may be mediated by 5-HT mechanisms. At the later time points, from 3d to 7d, non 5-HT mechanisms must be involved. This would support a mechanism by which decreased GABAergic inhibition, as identified here at 3d following CFA injection, could result in increased excitability of MOR+

(non-5-HT) neurons, which contributes to the maintenance phase of behavioural hypersensitivity.

The main limitation of the findings presented here is our lack of knowledge of the transmitter content of these MOR+, non-5-HT neurons. At least some of these are GABAergic (Kalyuzhny and Wessendorf, 1998). Crucially the effect of the MOR+ projection neurons will depend on the cell type they synapse onto within the cord. In the case of the MOR+ 5-HT population we could assume that at least part of the effect is mediated via the 5-HT_3 receptor. For GABAergic MOR+ neurons, the facilitatory effects would be expected to be mediated via a disinhibitory mechanism, by synapsing onto inhibitory interneurons of the cord. A further complication is that not all MOR+ cells project to the cord. Some GABAergic MOR+ expressing neurons act locally within the RVM, presumably inhibiting OFF cells or other inhibitory projection neurons (Kaplan and Fields, 1991).

7.2.4 Immune related genes as targets of descending facilitation

While the contribution of descending facilitation to central sensitisation and pain behaviour has been studied frequently (Bee and Dickenson, 2008; Burgess et al., 2002; Géranton et al., 2008; Wei et al., 2010) little is known about the molecular mechanisms underlying descending facilitation. Our group has previously used microarray analysis to characterise changes in dorsal horn gene expression at various time points following ankle injection of CFA (Géranton et al., 2007). The aim of the present study was to focus on the specific contribution of descending facilitation in the regulation of gene expression at the 7d time point. For this reason, microarray analysis was carried out on two groups of animals only, both groups with CFA inflammation and dermorphin-saporin or saline pretreatment as the only variable. In this way our analysis revealed genes that are differentially regulated in the pain state in the presence or absence of the MOR+ cell pathway. One limitation of this approach is that we are unable to compare

gene expression between CFA and sham animals in the present work, however dorsal horn gene expression changes at various times post inflammation have been investigated by our group previously (Géranton et al., 2007).

Immune cells play an important role in mediating central sensitisation both in neuropathic (Beggs et al., 2012) and inflammatory (Clark et al., 2012; Sagar et al., 2011; Sun et al., 2012) pain states. Many molecular studies have identified immune related genes in the dorsal horn in various models of chronic pain (Costigan et al., 2009a; Yukhananov and Kissin, 2008). Therefore it was not surprising that in the microarray analysis carried out in this study many of the identified genes had immune system related annotations. Importantly this demonstrates that part of the mechanism by which descending controls mediate their effects in the spinal cord is via immune cell responses. This has been proposed by others for the descending 5-HT pathway (Gu et al., 2011). These authors suggest that 5-HT exerts its facilitatory effects via activation of the 5-HT_3 receptor on primary afferent terminals, which leads to the release of fractalkine (CX3CL1) from those terminals. CX3CL1 then signals to microglia and astrocytes, which contribute to behavioural hypersensitivity. This recent development provides an important framework in which our present molecular data can be interpreted. For example, descending signalling via the MOR+ pathway may contribute to the transcription of immune related genes such as Nos2, Serpinb1a and Serpinb1b. Exactly how this occurs is not yet established, as the neurochemical basis of descending facilitation by the MOR+ cell pathway within the dorsal horn is not clear. However the present data suggests that one mechanism by which descending facilitation has excitatory effects in the dorsal horn is via modulation of immune cells such as microglia and astrocytes.

The role of CXC chemokines is of particular interest as two chemokines of this family and their common receptor were simultaneously identified on the array. This strongly suggests that the downregulation of these genes is related to the decreased pain sensitivity observed in the dermorphin-saporin CFA group. CXCL10 and the receptor CXCR3 have previously been implicated in inflammatory disorders within the CNS, such as viral infection, multiple sclerosis and Alzheimer's disease (Müller et al., 2010). Although this would suggest a prominent role for this ligand-receptor pathway in neuronal-immune cell signalling in the dorsal horn, the immunohistochemistry data presented in chapter 6 suggests this is not in fact the case. Both the ligand and the receptor appear to be neuronally expressed, with no indication of being present within microglia or astrocytes. This poses an intriguing possibility in which chemokine-receptor signalling could be involved in the normal intrinsic function of the dorsal horn, as well as increased excitability in pain states. Some limited *in vitro* evidence is in place to suggest that CXCXL10-CXCR3 signalling is indeed involved in neuronal excitability. Firstly both the receptor and ligand have been localised to neurons (Vinet et al., 2010), at least in culture. Secondly CXCL10 application to neurons leads to alterations in calcium transients and cell excitability (Cho et al., 2009). In addition CXCL10 treatment causes increases in levels of phosphorylated cAMP response element binding protein (CREB) and phosphorylated ERK in cells, which are both hallmarks of neuronal activation (Bajova et al., 2008). It will be of interest to determine if this occurs *in vivo* within the dorsal horn, as it could represent a novel interneuronal signalling mechanism.

7.2.5 Clinical implications

Rheumatoid arthritis (RA) affects 1% of the population (Lee and Weinblatt, 2001) and is associated with resting pain in the joints, joint stiffness and inflammation. Although joint stiffness and functional disability are major symptoms which impair quality of life for patients, treatments which

suppress the peripheral inflammatory mechanisms are not always effective (Kidd et al., 2007). Therefore understanding changes in the nociceptive system and improving pain management remains an important goal.

Rodent models of inflammatory polyarthritis can result in complications which may impair nociceptive testing, such as skin lesions and weight loss (Neugebauer et al., 2007). To address this problem, models of inflammatory monoarthritis have also been developed, including injection of CFA to the ankle joint (Butler et al., 1992). Although not a model of human RA per se, this method produces a reliable, localised inflammation of the ankle joint and results in stable behavioural hypersensitivity lasting up to 2 weeks post inflammation. RA patients have increased pain sensitivity at sites away from the inflamed joints (Edwards et al., 2009) and this may reflect increased central sensitisation within the dorsal horn of these patients (Kidd et al., 2007; Morris et al., 1997, Lee et al., 2011). Ankle injection of CFA has been used to demonstrate that central sensitisation occurs within the dorsal horn following joint inflammation (Neugebauer and Schaible, 1990). Increased descending inhibition has been demonstrated in this model in the acute phase (Cervero et al., 1991; Schaible et al., 1991) suggesting that tonic inhibition from supraspinal regions is increased in the early stages of this model.

To date, little is known regarding the role of descending facilitation via the RVM in inflammatory joint pain. The findings presented in this thesis demonstrate for the first time that behavioural hypersensitivity in inflammatory joint pain is dependent in part on descending facilitation via the RVM. In addition to peripheral pathology and spinal cord sensitisation, brainstem contributions should also be taken into account in the treatment of joint inflammatory conditions such as RA. Our findings may also be of relevance to other joint pain conditions such as osteoarthritis. In summary, the contribution of descending facilitation to behavioural hypersensitivity,

which has been established in models of neuropathic pain (Bee and Dickenson, 2008; Burgess et al., 2002; Rahman et al., 2009), should also be taken into account in the study and treatment of joint pain.

7.3 Future directions

The behavioural studies described in this thesis add to the existing body of evidence indicating that descending facilitation contributes to central sensitisation and hyperalgesia in a number of persistent pain states. However a number of questions remain regarding the role of the RVM in nociceptive processing, in this and other pain models. The identification of immune related genes in the dorsal horn also raises a number of interesting questions and possibilities for further study.

One of the fundamental questions remaining regarding descending facilitation is the neurochemistry of the MOR+ neurons. It is thought that the ON cell, MOR+ population of neurons is a heterogeneous group of cells. Some of these contain 5-HT, which in part explains the facilitatory role of these cells, presumably acting via pro-nociceptive 5-HT_3 receptors in the dorsal horn (Bardin, 2011). Other MOR+ cells are known to be GABAergic (Kalyuzhny and Wessendorf, 1998), however if these are projection neurons it is not known which component of the dorsal horn circuitry they synapse onto. Future work could include further characterisation of this cell population. Anatomical studies to quantify the numbers of MOR+ projection and non-projection neurons as well as double labelling studies to determine the proportion of 5-HT and GABA containing neurons within the RVM would be useful in this regard. Another transmitter which may be involved in descending facilitation is cholecystokinin (CCK). This peptidergic neurotransmitter has pronociceptive effects within the spinal cord, and has been shown to contribute to the descending facilitation of secondary hyperalgesia in a model of cutaneous mustard oil application (Urban et al., 1996). CCK containing neurons are found in the RVM and many of these

project to the dorsal horn (Mantyh and Hunt, 1984). It is not known if these CCK expressing neurons are MOR+, and this would be an interesting possibility for investigation. Although this descending pathway has received little attention in comparison to the extensive investigation of 5-HT pathways it may be an important avenue for future research.

The role of GABAergic signalling within the RVM has not been well studied to date. The method of labelling active GABAergic synapses *in vivo* described in chapter 3 would be a useful method of studying GABAergc signalling in further experiments. A starting point would be to study further time points after CFA injection. The time point of 3d was chosen based on previous findings that GABAergic signalling in the region is decreased at 3d following plantar inflammation (Zhang et al., 2011), however this does not rule out changes at earlier or later time points. Injection of a GABAergic agonist to the RVM would also be a useful functional experiment to determine if the decrease observed here is required for increased descending facilitation.

My behavioural studies investigated the role of both the 5-HT and MOR+ mediated descending facilitatory pathways in mechanical hypersensitivity of the ipsilateral hindpaw in joint inflammation. This measure is a correlate of secondary hyperalgesia in the animal as it reflects hypersensitivity at a site adjacent to but removed from the inflamed region. It is known that secondary hyperalgesia is driven by central mechanisms and our work has demonstrated a role for descending facilitation in this process in the joint inflammation model. An investigation of weight bearing in the 5,7-DHT experiment, described in chapter 4, suggests that primary hyperalgesia of the inflamed joint itself is not attenuated by the depletion. This adds further evidence to the hypothesis that descending inhibition prevails in primary hyperalgesia, while descending facilitation contributes to secondary hyperalgesia (Urban et al., 1999; Vanegas and Schaible, 2004). An

investigation to determine how primary hyperalgesia is affected by the MOR+ cell or 5-HT descending pathways may be of interest in the future.

The role of 5-HT in descending facilitation is complex with both inhibitory and facilitatory roles reported, depending on the receptor subtype activated at the spinal cord level (Bardin, 2011). The intrathecal ondansetron experiment carried out in chapter 4 suggests that as in other chronic pain models, the 5-HT_3 receptor has a pro-nociceptive role in the joint inflammation model. A limitation of this pilot study is the use of only one dose of drug, based on previous published work in which a single intrathecal injection of 10µg ondansetron was sufficient to fully reverse thermal hypersensitivity associated with plantar inflammation (LaGraize et al., 2010). However it is possible that the optimal dose may differ for the ankle joint model, and for the measurement of mechanical hypersensitivity. Future work could include a range of doses to generate a dose response curve specific to the joint inflammatory model of mechanical hypersensitivity.

It is also important to note that we cannot rule out the involvement of other pro-nociceptive 5-HT receptors in mediating descending facilitation. Recent studies have shown that the 5-HT_{2A} receptor may be involved in neuropathic pain, and this may warrant investigation in the joint inflammation model (Aira et al., 2012). However, it is also likely that parallel systems of 5-HT mediated inhibition and facilitation exist in chronic pain states, as has been suggested in a neuropathic model (Dogrul et al., 2009). Therefore it may be of interest to investigate if 5-HT plays a role in inhibition in the joint inflammation model.

The microarray analysis carried out in this study has identified the CXC family of chemokines and receptor as a potential signalling pathway within the dorsal horn, regulated by descending facilitation. Our finding that CXCL10 is expressed within neurons of the dorsal horn, and CXCR3 is found in part on CGRP expressing primary afferent terminals, suggests a

mechanism by which primary afferent input could be modulated by this chemokine family. This is the first study to characterise protein expression of CXCL10 and CXCR3 in the dorsal horn however much work is required to determine if this receptor-ligand pair play a role in inflammatory joint pain, and projects are ongoing in our group to determine if this is the case. The first step is to determine if upregulation of protein occurs after the 7d time point. Future work could include inhibiting the receptor or the ligand within the dorsal horn by to determine if they play a role in nociception.

Notably, the expression of CXCL9 and CXCL10 is increased in the joints of patients with rheumatoid arthritis (Laragione et al., 2011; Yoshida et al., 2012) suggesting that these chemokines may contribute to the joint pathology associated with the disease. Furthermore a humanised anti-CXCL10 antibody has been shown to be safe and effective in treating the pain in rheumatoid arthritis (Yellin et al., 2012). In animal models CXCR3 receptor antagonists have also been shown to be effective in decreasing the pathogenesis of a model of rheumatoid arthritis (Jenh et al., 2012). Therefore safe and effective pharmacological tools exist to investigate the role of this chemokine pathway within the CNS in inflammatory pain states. If CXL10 to CXCR3 signalling is shown to be pronociceptive within the dorsal horn, this would provide further support for the use of such agents in the systemic treatment of joint pain states.

7.4 Conclusion

The data presented in this thesis demonstrates for the first that time that descending facilitation via the RVM contributes to behavioural hypersensitivity following joint inflammation. This suggests that in addition to targeting the underlying joint pathology, patients suffering from joint pain symptoms may benefit from treatments that reduce central sensitisation and descending facilitation.

8. References

Adler, M., Geller, E., Chen, X., Rogers, T., 2005. Viewing chemokines as a third major system of communication in the brain. The AAPS Journal 7, E865–E870.

Aguzzi, A., Barres, B.A., Bennett, M.L., 2013. Microglia: scapegoat, saboteur, or something else? Science 339, 156–161.

Aira, Z., Buesa, I., Gallego, M., Caño, G.G. del, Mendiable, N., Mingo, J., Rada, D., Bilbao, J., Zimmermann, M., Azkue, J.J., 2012. Time-Dependent Cross Talk between Spinal Serotonin 5-HT2A Receptor and mGluR1 Subserves Spinal Hyperexcitability and Neuropathic Pain after Nerve Injury. J. Neurosci. 32, 13568–13581.

Al-Khater, K.M., Todd, A.J., 2009. Collateral projections of neurons in laminae I, III, and IV of rat spinal cord to thalamus, periaqueductal gray matter, and lateral parabrachial area. J. Comp. Neurol. 515, 629–646.

Amitai, Y., 2010. Physiologic role for “inducible” nitric oxide synthase: A new form of astrocytic–neuronal interface. Glia 58, 1775–1781.

Andrews, N., Legg, E., Lisak, D., Issop, Y., Richardson, D., Harper, S., Huang, W., Burgess, G., Machin, I., Rice, A.S.C., 2011. Spontaneous burrowing behaviour in the rat is reduced by peripheral nerve injury or inflammation associated pain. Eur J Pain.

Apkarian, A.V., Bushnell, M.C., Treede, R.-D., Zubieta, J.-K., 2005. Human brain mechanisms of pain perception and regulation in health and disease. Eur J Pain 9, 463–484.

Ashburner, M., Ball, C.A., Blake, J.A., Botstein, D., Butler, H., Cherry, J.M., Davis, A.P., Dolinski, K., Dwight, S.S., Eppig, J.T., Harris, M.A., Hill, D.P., Issel-Tarver, L., Kasarskis, A., Lewis, S., Matese, J.C., Richardson, J.E., Ringwald, M., Rubin, G.M., Sherlock, G., 2000. Gene ontology: tool for the unification of biology. The Gene Ontology Consortium. Nat. Genet. 25, 25–29.

Averill, S., Inglis, J.J., King, V.R., Thompson, S.W.N., Cafferty, W.B.J., Shortland, P.J., Hunt, S.P., Kidd, B.L., Priestley, J.V., 2008. Reg-2 expression in dorsal root ganglion neurons after adjuvant-induced monoarthritis. Neuroscience 155, 1227–1236.

Baba, H., Kohno, T., Moore, K.A., Woolf, C.J., 2001. Direct activation of rat spinal dorsal horn neurons by prostaglandin E2. J. Neurosci. 21, 1750–1756.

Bailey, C.H., Bartsch, D., Kandel, E.R., 1996. Toward a molecular definition of long-term memory storage. Proc. Natl. Acad. Sci. U.S.A. 93, 13445–13452.

Bajova, H., Nelson, T.E., Gruol, D.L., 2008. Chronic CXCL10 alters the level of activated ERK1/2 and transcriptional factors CREB and NF-κB in

hippocampal neuronal cell culture. Journal of Neuroimmunology 195, 36–46.

Bär, K.-J., Natura, G., Telleria-Diaz, A., Teschner, P., Vogel, R., Vasquez, E., Schaible, H.-G., Ebersberger, A., 2004. Changes in the effect of spinal prostaglandin E2 during inflammation: prostaglandin E (EP1-EP4) receptors in spinal nociceptive processing of input from the normal or inflamed knee joint. J. Neurosci. 24, 642–651.

Barbaro, N.M., Heinricher, M.M., Fields, H.L., 1986. Putative pain modulating neurons in the rostral ventral medulla: reflex-related activity predicts effects of morphine. Brain Res. 366, 203–210.

Bardin, L., 2011. The complex role of serotonin and 5-HT receptors in chronic pain. Behav Pharmacol 22, 390–404.

Bardin, L., Jourdan, D., Alloui, A., Lavarenne, J., Eschalier, A., 1997. Differential influence of two serotonin 5-HT3 receptor antagonists on spinal serotonin-induced analgesia in rats. Brain Res. 765, 267–272.

Bardin, L., Tarayre, J.P., Koek, W., Colpaert, F.C., 2001. In the formalin model of tonic nociceptive pain, 8-OH-DPAT produces 5-HT1A receptor-mediated, behaviorally specific analgesia. Eur. J. Pharmacol. 421, 109–114.

Barres, B.A., 2008. The mystery and magic of glia: a perspective on their roles in health and disease. Neuron 60, 430–440.

Basbaum, A.I., Bautista, D.M., Scherrer, G., Julius, D., 2009. Cellular and molecular mechanisms of pain. Cell 139, 267–284.

Basbaum, A.I., Marley, N.J., O'Keefe, J., Clanton, C.H., 1977. Reversal of morphine and stimulus-produced analgesia by subtotal spinal cord lesions. Pain 3, 43–56.

Baumgarten, H.G., Lachenmayer, L., 2004. Serotonin neurotoxins--past and present. Neurotox Res 6, 589–614.

Bedson, J., Croft, P.R., 2008. The discordance between clinical and radiographic knee osteoarthritis: a systematic search and summary of the literature. BMC Musculoskelet Disord 9, 116.

Bee, L.A., Dickenson, A.H., 2008. Descending facilitation from the brainstem determines behavioural and neuronal hypersensitivity following nerve injury and efficacy of pregabalin. Pain 140, 209–223.

Beggs, S., Trang, T., Salter, M.W., 2012. P2X4R+ microglia drive neuropathic pain. Nat. Neurosci. 15, 1068–1073.

Ben Achour, S., Pascual, O., 2010. Glia: the many ways to modulate synaptic plasticity. Neurochem. Int. 57, 440–445.

Benarafa, C., Priebe, G.P., Remold-O'Donnell, E., 2007. The neutrophil serine protease inhibitor serpinb1 preserves lung defense functions in Pseudomonas aeruginosa infection. J. Exp. Med. 204, 1901–1909.

Bennell, K.L., Hunter, D.J., Hinman, R.S., 2012. Management of osteoarthritis of the knee. BMJ 345, e4934–e4934.

Berger, M., Gray, J.A., Roth, B.L., 2009. The Expanded Biology of Serotonin. Annual Review of Medicine 60, 355–366.

Bessou, P., Perl, E.R., 1969. Response of cutaneous sensory units with unmyelinated fibers to noxious stimuli. J Neurophysiol 32, 1025–1043.

Birrell, G.J., McQueen, D.S., Iggo, A., Grubb, B.D., 1990. The effects of 5-HT on articular sensory receptors in normal and arthritic rats. Br J Pharmacol 101, 715–721.

Boettger, M.K., Hensellek, S., Richter, F., Gajda, M., Stöckigt, R., Von Banchet, G.S., Bräuer, R., Schaible, H.-G., 2008. Antinociceptive effects of tumor necrosis factor alpha neutralization in a rat model of antigen-induced arthritis: evidence of a neuronal target. Arthritis Rheum. 58, 2368–2378.

Bourquin, A.-F., Süveges, M., Pertin, M., Gilliard, N., Sardy, S., Davison, A.C., Spahn, D.R., Decosterd, I., 2006. Assessment and analysis of mechanical allodynia-like behavior induced by spared nerve injury (SNI) in the mouse. PAIN 122, 14.e1–14.e14.

Bowker, R.M., Westlund, K.N., Sullivan, M.C., Coulter, J.D., 1982. Organization of descending serotonergic projections to the spinal cord. Prog. Brain Res. 57, 239–265.

Breivik, H., Collett, B., Ventafridda, V., Cohen, R., Gallacher, D., 2006. Survey of chronic pain in Europe: Prevalence, impact on daily life, and treatment. European Journal of Pain 10, 287–287.

Brenchat, A., Nadal, X., Romero, L., Ovalle, S., Muro, A., Sánchez-Arroyos, R., Portillo-Salido, E., Pujol, M., Montero, A., Codony, X., Burgueño, J., Zamanillo, D., Hamon, M., Maldonado, R., Vela, J.M., 2010. Pharmacological activation of 5-HT7 receptors reduces nerve injury-induced mechanical and thermal hypersensitivity. PAIN 149, 483–494.

Brenn, D., Richter, F., Schaible, H.-G., 2007. Sensitization of unmyelinated sensory fibers of the joint nerve to mechanical stimuli by interleukin-6 in the rat: an inflammatory mechanism of joint pain. Arthritis Rheum. 56, 351–359.

Burgess, P.R., Perl, E.R., 1967. Myelinated afferent fibres responding specifically to noxious stimulation of the skin. J Physiol 190, 541–562.

Burgess, S.E., Gardell, L.R., Ossipov, M.H., Malan, T.P., Vanderah, T.W., Lai, J., Porreca, F., 2002. Time-dependent descending facilitation from the rostral ventromedial medulla maintains, but does not initiate, neuropathic pain. J. Neurosci 22, 5129–5136.

Butler, S.H., Godefroy, F., Besson, J.M., Weil-Fugazza, J., 1992. A limited arthritic model for chronic pain studies in the rat. Pain 48, 73–81.

Calvo, M., Dawes, J.M., Bennett, D.L.H., 2012. The role of the immune system in the generation of neuropathic pain. Lancet Neurol 11, 629–642.

Carlson, J.D., Maire, J.J., Martenson, M.E., Heinricher, M.M., 2007. Sensitization of pain-modulating neurons in the rostral ventromedial medulla after peripheral nerve injury. J. Neurosci. 27, 13222–13231.

Caterina, M.J., Rosen, T.A., Tominaga, M., Brake, A.J., Julius, D., 1999. A capsaicin-receptor homologue with a high threshold for noxious heat. Nature 398, 436–441.

Cavanaugh, D.J., Lee, H., Lo, L., Shields, S.D., Zylka, M.J., Basbaum, A.I., Anderson, D.J., 2009. Distinct subsets of unmyelinated primary sensory fibers mediate behavioral responses to noxious thermal and mechanical stimuli. Proc Natl Acad Sci U S A 106, 9075–9080.

Cervero, F., Schaible, H.G., Schmidt, R.F., 1991. Tonic descending inhibition of spinal cord neurones driven by joint afferents in normal cats and in cats with an inflamed knee joint. Exp Brain Res 83, 675–678.

Chandran, P., Pai, M., Blomme, E.A., Hsieh, G.C., Decker, M.W., Honore, P., 2009. Pharmacological modulation of movement-evoked pain in a rat model of osteoarthritis. Eur. J. Pharmacol. 613, 39–45.

Chaplan, S.R., Bach, F.W., Pogrel, J.W., Chung, J.M., Yaksh, T.L., 1994. Quantitative assessment of tactile allodynia in the rat paw. J. Neurosci. Methods 53, 55–63.

Cheng, Z.F., Fields, H.L., Heinricher, M.M., 1986. Morphine microinjected into the periaqueductal gray has differential effects on 3 classes of medullary neurons. Brain Res. 375, 57–65.

Cho, H.J., Basbaum, A.I., 1991. GABAergic circuitry in the rostral ventral medulla of the rat and its relationship to descending antinociceptive controls. The Journal of Comparative Neurology 303, 316–328.

Cho, I.-H., Lee, M.J., Jang, M., Gwak, N.G., Lee, K.Y., Jung, H.-S., 2012. Minocycline markedly reduces acute visceral nociception via inhibiting neuronal ERK phosphorylation. Mol Pain 8, 13.

Cho, J., Nelson, T.E., Bajova, H., Gruol, D.L., 2009. Chronic CXCL10 alters neuronal properties in rat hippocampal culture. J. Neuroimmunol. 207, 92–100.

Clark, A.K., Grist, J., Al-Kashi, A., Perretti, M., Malcangio, M., 2012. Spinal cathepsin S and fractalkine contribute to chronic pain in the collagen-induced arthritis model. Arthritis Rheum. 64, 2038–2047.

Coderre, T.J., Yashpal, K., 1994. Intracellular messengers contributing to persistent nociception and hyperalgesia induced by L-glutamate and substance P in the rat formalin pain model. Eur. J. Neurosci. 6, 1328–1334.

Conte, D., Legg, E.D., McCourt, A.C., Silajdzic, E., Nagy, G.G., Maxwell, D.J., 2005. Transmitter content, origins and connections of axons in the spinal cord that possess the serotonin (5-hydroxytryptamine) 3 receptor. Neuroscience 134, 165–173.

Costa-Mattioli, M., Sossin, W.S., Klann, E., Sonenberg, N., 2009. Translational control of long-lasting synaptic plasticity and memory. Neuron 61, 10–26.

Costigan, M., Moss, A., Latremoliere, A., Johnston, C., Verma-Gandhu, M., Herbert, T.A., Barrett, L., Brenner, G.J., Vardeh, D., Woolf, C.J., Fitzgerald, M., 2009a. T-Cell Infiltration and Signaling in the Adult

Dorsal Spinal Cord Is a Major Contributor to Neuropathic Pain-Like Hypersensitivity. J. Neurosci. 29, 14415–14422.

Costigan, M., Scholz, J., Woolf, C.J., 2009b. Neuropathic Pain. Annu Rev Neurosci 32, 1–32.

Coull, J.A.M., Beggs, S., Boudreau, D., Boivin, D., Tsuda, M., Inoue, K., Gravel, C., Salter, M.W., De Koninck, Y., 2005. BDNF from microglia causes the shift in neuronal anion gradient underlying neuropathic pain. Nature 438, 1017–1021.

Coulson, D.T., Brockbank, S., Quinn, J.G., Murphy, S., Ravid, R., Irvine, G.B., Johnston, J.A., 2008. Identification of valid reference genes for the normalization of RT qPCR gene expression data in human brain tissue. BMC Molecular Biology 9, 46.

Cox, J.J., Reimann, F., Nicholas, A.K., Thornton, G., Roberts, E., Springell, K., Karbani, G., Jafri, H., Mannan, J., Raashid, Y., Al-Gazali, L., Hamamy, H., Valente, E.M., Gorman, S., Williams, R., McHale, D.P., Wood, J.N., Gribble, F.M., Woods, C.G., 2006. An SCN9A channelopathy causes congenital inability to experience pain. Nature 444, 894–898.

Crisp, T., Stafinsky, J.L., Spanos, L.J., Uram, M., Perni, V.C., Donepudi, H.B., 1991. Analgesic effects of serotonin and receptor-selective serotonin agonists in the rat spinal cord. Gen. Pharmacol. 22, 247–251.

Cruz, C.D., Neto, F.L., Castro-Lopes, J., McMahon, S.B., Cruz, F., 2005. Inhibition of ERK phosphorylation decreases nociceptive behaviour in monoarthritic rats. Pain 116, 411–419.

D'Mello, R., Dickenson, A.H., 2008. Spinal cord mechanisms of pain. Br J Anaesth 101, 8–16.

Danziger, N., Weil-Fugazza, J., Bars, D.L., Bouhassira, D., 1999. Alteration of Descending Modulation of Nociception during the Course of Monoarthritis in the Rat. J. Neurosci. 19, 2394–2400.

Danziger, N., Weil-Fugazza, J., Le Bars, D., Bouhassira, D., 2001. Stage-dependent changes in the modulation of spinal nociceptive neuronal activity during the course of inflammation. Eur. J. Neurosci 13, 230–240.

Deakin, J.F.W., Dostrovsky, J.O., 1978. Involvement of the periaqueductal grey matter and spinal 5-hydroxytryptaminergic pathways in morphine analgesia. Br J Pharmacol 63, 159–165.

Decosterd, I., Woolf, C.J., 2000. Spared nerve injury: an animal model of persistent peripheral neuropathic pain. Pain 87, 149–158.

Deval, E., Gasull, X., Noël, J., Salinas, M., Baron, A., Diochot, S., Lingueglia, E., 2010. Acid-Sensing Ion Channels (ASICs): Pharmacology and implication in pain. Pharmacology & Therapeutics 128, 549–558.

Dogrul, A., Ossipov, M.H., Porreca, F., 2009. Differential mediation of descending pain facilitation and inhibition by spinal 5HT-3 and 5HT-7 receptors. Brain Research 1280, 52–59.

Dogrul, A., Seyrek, M., 2006. Systemic morphine produce antinociception mediated by spinal 5-HT7, but not 5-HT1A and 5-HT2 receptors in the spinal cord. Br. J. Pharmacol. 149, 498–505.

Doly, S., Fischer, J., Brisorgueil, M.-J., Vergé, D., Conrath, M., 2005. Pre- and postsynaptic localization of the 5-HT7 receptor in rat dorsal spinal cord: immunocytochemical evidence. J. Comp. Neurol. 490, 256–269.

Donovan-Rodriguez, T., Urch, C.E., Dickenson, A.H., 2006. Evidence of a role for descending serotonergic facilitation in a rat model of cancer-induced bone pain. Neurosci. Lett. 393, 237–242.

Doyle, C.A., Hunt, S.P., 1999. Substance p receptor (neurokinin-1)-expressing neurons in lamina i of the spinal cord encode for the intensity of noxious stimulation: a c-fos study in rat. Neuroscience 89, 17–28.

Drower, E.J., Hammond, D.L., 1988. GABAergic modulation of nociceptive threshold: effects of THIP and bicuculline microinjected in the ventral medulla of the rat. Brain Res. 450, 316–324.

Duan, J., Sawynok, J., 1987. Enhancement of clonidine-induced analgesia by lesions induced with spinal and intracerebroventricular administration of 5,7-dihydroxytryptamine. Neuropharmacology 26, 323–329.

Dubuisson, D., Dennis, S.G., 1977. The formalin test: a quantitative study of the analgesic effects of morphine, meperidine, and brain stem stimulation in rats and cats. Pain 4, 161–174.

Edwards, R.R., Wasan, A.D., Bingham, C.O., 3rd, Bathon, J., Haythornthwaite, J.A., Smith, M.T., Page, G.G., 2009. Enhanced reactivity to pain in patients with rheumatoid arthritis. Arthritis Res. Ther. 11, R61.

Eijkelkamp, N., Linley, J.E., Baker, M.D., Minett, M.S., Cregg, R., Werdehausen, R., Rugiero, F., Wood, J.N., 2012. Neurological perspectives on voltage-gated sodium channels. Brain 135, 2585–2612.

Faris, P.L., Komisaruk, B.R., Watkins, L.R., Mayer, D.J., 1983. Evidence for the neuropeptide cholecystokinin as an antagonist of opiate analgesia. Science 219, 310–312.

Fernandez, E.J., Lolis, E., 2002. Structure, Function, and Inhibition of Chemokines. Annual Review of Pharmacology and Toxicology 42, 469–499.

Fernihough, J., Gentry, C., Malcangio, M., Fox, A., Rediske, J., Pellas, T., Kidd, B., Bevan, S., Winter, J., 2004. Pain related behaviour in two models of osteoarthritis in the rat knee. Pain 112, 83–93.

Fields, H., 2004. State-dependent opioid control of pain. Nature Reviews Neuroscience 5, 565–575.

Fields, H.L., Bry, J., Hentall, I., Zorman, G., 1983. The activity of neurons in the rostral medulla of the rat during withdrawal from noxious heat. J. Neurosci. 3, 2545–2552.

Fields, H.L., Heinricher, M.M., 1985. Anatomy and physiology of a nociceptive modulatory system. Philos. Trans. R. Soc. Lond., B, Biol. Sci. 308, 361–374.

Fields, H.L., Heinricher, M.M., 1989. Brainstem Modulation of Nociceptor-Driven Withdrawal Reflexes. Annals of the New York Academy of Sciences 563, 34–44.

Fields, H.L., Heinricher, M.M., Mason, P., 1991. Neurotransmitters in Nociceptive Modulatory Circuits. Annual Review of Neuroscience 14, 219–245.

Fields, H.L., Malick, A., Burstein, R., 1995. Dorsal horn projection targets of ON and OFF cells in the rostral ventromedial medulla. J. Neurophysiol. 74, 1742–1759.

Frankfurt, M., Azmitia, E., 1984. Regeneration of serotonergic fibers in the rat hypothalamus following unilateral 5,7-dihydroxytryptamine injection. Brain Res. 298, 273–282.

Friedrich, A.E., Gebhart, G.F., 2003. Modulation of visceral hyperalgesia by morphine and cholecystokinin from the rat rostroventral medial medulla. Pain 104, 93–101.

Fu, X., Wang, Y.-Q., Wang, J., Yu, J., Wu, G.-C., 2007. Changes in expression of nociceptin/orphanin FQ and its receptor in spinal dorsal horn during electroacupuncture treatment for peripheral inflammatory pain in rats. Peptides 28, 1220–1228.

Gao, Y.-J., Ji, R.-R., 2010. Targeting astrocyte signaling for chronic pain. Neurotherapeutics 7, 482–493.

Gao, Y.-J., Xu, Z.-Z., Liu, Y.-C., Wen, Y.-R., Decosterd, I., Ji, R.-R., 2010. The c-Jun N-terminal kinase 1 (JNK1) in spinal astrocytes is required for the maintenance of bilateral mechanical allodynia under a persistent inflammatory pain condition. Pain 148, 309–319.

Gardell, L.R., Vanderah, T.W., Gardell, S.E., Wang, R., Ossipov, M.H., Lai, J., Porreca, F., 2003. Enhanced evoked excitatory transmitter release in experimental neuropathy requires descending facilitation. J. Neurosci 23, 8370–8379.

Gauriau, C., Bernard, J.-F., 2002. Pain pathways and parabrachial circuits in the rat. Exp. Physiol. 87, 251–258.

Gauriau, C., Bernard, J.-F., 2004. Posterior triangular thalamic neurons convey nociceptive messages to the secondary somatosensory and insular cortices in the rat. J. Neurosci. 24, 752–761.

George Paxinos, 1998. The rat brain in stereotaxic coordinates / George Paxinos, Charles Watson.

Géranton, S.M., Fratto, V., Tochiki, K.K., Hunt, S.P., 2008. Descending serotonergic controls regulate inflammation-induced mechanical sensitivity and methyl-CpG-binding protein 2 phosphorylation in the rat superficial dorsal horn. Mol Pain 4, 35.

Géranton, S.M., Jiménez-Díaz, L., Torsney, C., Tochiki, K.K., Stuart, S.A., Leith, J.L., Lumb, B.M., Hunt, S.P., 2009. A rapamycin-sensitive signaling

pathway is essential for the full expression of persistent pain states. J. Neurosci 29, 15017–15027.

Géranton, S.M., Morenilla-Palao, C., Hunt, S.P., 2007. A role for transcriptional repressor methyl-CpG-binding protein 2 and plasticity-related gene serum- and glucocorticoid-inducible kinase 1 in the induction of inflammatory pain states. J. Neurosci. 27, 6163–6173.

Géranton, S.M., Tochiki, K.K., Chiu, W.W., Stuart, S.A., Hunt, S.P., 2010. Injury induced activation of extracellular signal-regulated kinase (ERK) in the rat rostral ventromedial medulla (RVM) is age dependant and requires the lamina I projection pathway. Mol Pain 6, 54.

Gilbert, A.-K., Franklin, K.B.., 2001. GABAergic modulation of descending inhibitory systems from the rostral ventromedial medulla (RVM). Dose-response analysis of nociception and neurological deficits. Pain 90, 25–36.

Gold, M.S., Gebhart, G.F., 2010. Nociceptor sensitization in pain pathogenesis. Nat. Med. 16, 1248–1257.

Goldberg, Y.P., MacFarlane, J., MacDonald, M.L., Thompson, J., Dube, M.-P., Mattice, M., Fraser, R., Young, C., Hossain, S., Pape, T., Payne, B., Radomski, C., Donaldson, G., Ives, E., Cox, J., Younghusband, H.B., Green, R., Duff, A., Boltshauser, E., Grinspan, G.A., Dimon, J.H., Sibley, B.G., Andria, G., Toscano, E., Kerdraon, J., Bowsher, D., Pimstone, S.N., Samuels, M.E., Sherrington, R., Hayden, M.R., 2007. Loss-of-function mutations in the Nav1.7 gene underlie congenital indifference to pain in multiple human populations. Clin. Genet. 71, 311–319.

Gonçalves, L., Almeida, A., Pertovaara, A., 2007. Pronociceptive changes in response properties of rostroventromedial medullary neurons in a rat model of peripheral neuropathy. European Journal of Neuroscience 26, 2188–2195.

González-Maeso, J., Ang, R.L., Yuen, T., Chan, P., Weisstaub, N.V., López-Giménez, J.F., Zhou, M., Okawa, Y., Callado, L.F., Milligan, G., Gingrich, J.A., Filizola, M., Meana, J.J., Sealfon, S.C., 2008. Identification of a serotonin/glutamate receptor complex implicated in psychosis. Nature 452, 93–97.

Graven-Nielsen, T., Wodehouse, T., Langford, R.M., Arendt-Nielsen, L., Kidd, B.L., 2012. Normalization of widespread hyperesthesia and facilitated spatial summation of deep-tissue pain in knee osteoarthritis patients after knee replacement. Arthritis & Rheumatism 64, 2907–2916.

Griffin, R.S., Costigan, M., Brenner, G.J., Ma, C.H.E., Scholz, J., Moss, A., Allchorne, A.J., Stahl, G.L., Woolf, C.J., 2007. Complement induction in spinal cord microglia results in anaphylatoxin C5a-mediated pain hypersensitivity. J. Neurosci. 27, 8699–8708.

Grubb, B.D., Stiller, R.U., Schaible, H.G., 1993. Dynamic changes in the receptive field properties of spinal cord neurons with ankle input in

rats with chronic unilateral inflammation in the ankle region. Exp Brain Res 92, 441–452.

Gu, M., Miyoshi, K., Dubner, R., Guo, W., Zou, S., Ren, K., Noguchi, K., Wei, F., 2011. Spinal 5-HT3 Receptor Activation Induces Behavioral Hypersensitivity via a Neuronal-Glial-Neuronal Signaling Cascade. The Journal of Neuroscience 31, 12823 –12836.

Gu, M., Wessendorf, M., 2007. Endomorphin-2-immunoreactive fibers selectively appose serotonergic neuronal somata in the rostral ventral medial medulla. The Journal of Comparative Neurology 502, 701–713.

Guan, Y., Guo, W., Robbins, M.T., Dubner, R., Ren, K., 2004. Changes in AMPA receptor phosphorylation in the rostral ventromedial medulla after inflammatory hyperalgesia in rats. Neurosci. Lett. 366, 201–205.

Guan, Y., Guo, W., Zou, S.-P., Dubner, R., Ren, K., 2003. Inflammation-induced upregulation of AMPA receptor subunit expression in brain stem pain modulatory circuitry. Pain 104, 401–413.

Gühring, H., Görig, M., Ates, M., Coste, O., Zeilhofer, H.U., Pahl, A., Rehse, K., Brune, K., 2000. Suppressed injury-induced rise in spinal prostaglandin E2 production and reduced early thermal hyperalgesia in iNOS-deficient mice. J. Neurosci. 20, 6714–6720.

Guilbaud, G., Iggo, A., Tegnér, R., 1985. Sensory receptors in ankle joint capsules of normal and arthritic rats. Exp Brain Res 58, 29–40.

Guo, W., Robbins, M.T., Wei, F., Zou, S., Dubner, R., Ren, K., 2006. Supraspinal Brain-Derived Neurotrophic Factor Signaling: A Novel Mechanism for Descending Pain Facilitation. The Journal of Neuroscience 26, 126 –137.

Guo, W., Wang, H., Zou, S., Dubner, R., Ren, K., 2012. Chemokine signaling involving chemokine (C-C motif) ligand 2 plays a role in descending pain facilitation. Neurosci Bull 28, 193–207.

Gutstein, H.B., Mansour, A., Watson, S.J., Akil, H., Fields, H.L., 1998. Mu and kappa opioid receptors in periaqueductal gray and rostral ventromedial medulla. Neuroreport 9, 1777–1781.

Gwilym, S.E., Keltner, J.R., Warnaby, C.E., Carr, A.J., Chizh, B., Chessell, I., Tracey, I., 2009. Psychophysical and functional imaging evidence supporting the presence of central sensitization in a cohort of osteoarthritis patients. Arthritis Rheum. 61, 1226–1234.

Hama, A.T., Fritschy, J.M., Hammond, D.L., 1997. Differential distribution of (GABA)A receptor subunits on bulbospinal serotonergic and nonserotonergic neurons of the ventromedial medulla of the rat. J. Comp. Neurol. 384, 337–348.

Hannon, J., Hoyer, D., 2008. Molecular biology of 5-HT receptors. Behav. Brain Res. 195, 198–213.

HARDY, J.D., WOLFF, H.G., GOODELL, H., 1950. Experimental evidence on the nature of cutaneous hyperalgesia. J. Clin. Invest. 29, 115–140.

Hargreaves, K., Dubner, R., Brown, F., Flores, C., Joris, J., 1988. A new and sensitive method for measuring thermal nociception in cutaneous hyperalgesia. Pain 32, 77–88.

Hay, C.., Trevethick, M.., Wheeldon, A., Bowers, J.., De Belleroche, J.., 1997. The potential role of spinal cord cyclooxygenase-2 in the development of Freund's complete adjuvant-induced changes in hyperalgesia and allodynia. Neuroscience 78, 843–850.

Heinricher, M.M., Kaplan, H.J., 1991. GABA-mediated inhibition in rostral ventromedial medulla: role in nociceptive modulation in the lightly anesthetized rat. Pain 47, 105–113.

Heinricher, M.M., Morgan, M.M., Fields, H.L., 1992. Direct and indirect actions of morphine on medullary neurons that modulate nociception. Neuroscience 48, 533–543.

Heinricher, M.M., Morgan, M.M., Tortorici, V., Fields, H.L., 1994. Disinhibition of off-cells and antinociception produced by an opioid action within the rostral ventromedial medulla. Neuroscience 63, 279–288.

Heinricher, M.M., Neubert, M.J., 2004. Neural basis for the hyperalgesic action of cholecystokinin in the rostral ventromedial medulla. J. Neurophysiol. 92, 1982–1989.

Heinricher, M.M., Tavares, I., Leith, J.L., Lumb, B.M., 2009. Descending control of nociception: Specificity, recruitment and plasticity. Brain Research Reviews 60, 214–225.

Herz, A., Albus, K., Metys, J., Schubert, P., Teschemacher, H., 1970. On the central sites for the antinociceptive action of morphine and fentanyl. Neuropharmacology 9, 539–551.

Hossaini, M., Goos, J.A.C., Kohli, S.K., Holstege, J.C., 2012. Distribution of Glycine/GABA Neurons in the Ventromedial Medulla with Descending Spinal Projections and Evidence for an Ascending Glycine/GABA Projection. PLoS ONE 7, e35293.

Howard, R.F., Walker, S.M., Mota, P.M., Fitzgerald, M., 2005. The ontogeny of neuropathic pain: postnatal onset of mechanical allodynia in rat spared nerve injury (SNI) and chronic constriction injury (CCI) models. Pain 115, 382–389.

Huang, D.W., Sherman, B.T., Lempicki, R.A., 2009. Systematic and integrative analysis of large gene lists using DAVID bioinformatics resources. Nat Protoc 4, 44–57.

Huang, J., Spier, A.D., Pickel, V.M., 2004. 5-HT3A receptor subunits in the rat medial nucleus of the solitary tract: subcellular distribution and relation to the serotonin transporter. Brain Res. 1028, 156–169.

Huggett, J., Dheda, K., Bustin, S., Zumla, A., 2005. Real-time RT-PCR normalisation; strategies and considerations. Genes Immun. 6, 279–284.

Hughes, E.G., Elmariah, S.B., Balice-Gordon, R.J., 2010. Astrocyte secreted proteins selectively increase hippocampal GABAergic axon length, branching, and synaptogenesis. Mol. Cell. Neurosci. 43, 136–145.

Hunt, S.P., Mantyh, P.W., 2001. The molecular dynamics of pain control. Nat. Rev. Neurosci. 2, 83–91.

Hunt, S.P., Rossi, J., 1985. Peptide- and non-peptide-containing unmyelinated primary afferents: the parallel processing of nociceptive information. Philos. Trans. R. Soc. Lond., B, Biol. Sci. 308, 283–289.

Iadevaia, V., Huo, Y., Zhang, Z., Foster, L.J., Proud, C.G., 2012. Roles of the mammalian target of rapamycin, mTOR, in controlling ribosome biogenesis and protein synthesis. Biochem. Soc. Trans. 40, 168–172.

Ilkjaer, S., Petersen, K.L., Brennum, J., Wernberg, M., Dahl, J.B., 1996. Effect of systemic N-methyl-D-aspartate receptor antagonist (ketamine) on primary and secondary hyperalgesia in humans. Br J Anaesth 76, 829–834.

Imbe, H., Kimura, A., Okamoto, K., Donishi, T., Aikawa, F., Senba, E., Tamai, Y., 2008. Activation of ERK in the rostral ventromedial medulla is involved in hyperalgesia during peripheral inflammation. Brain Res. 1187, 103–110.

Imbe, H., Murakami, S., Okamoto, K., Iwai-Liao, Y., Senba, E., 2004. The effects of acute and chronic restraint stress on activation of ERK in the rostral ventromedial medulla and locus coeruleus. Pain 112, 361–371.

Imbe, H., Okamoto, K., Okamura, T., Kumabe, S., Nakatsuka, M., Aikawa, F., Iwai-Liao, Y., Senba, E., 2005. Effects of peripheral inflammation on activation of ERK in the rostral ventromedial medulla. Brain Res. 1063, 151–158.

Impey, S., Obrietan, K., Storm, D.R., 1999a. Making New Connections: Role of ERK/MAP Kinase Signaling in Neuronal Plasticity. Neuron 23, 11–14.

Impey, S., Obrietan, K., Storm, D.R., 1999b. Making New Connections: Role of ERK/MAP Kinase Signaling in Neuronal Plasticity. Neuron 23, 11–14.

Infante, C., Díaz, M., Hernández, A., Constandil, L., Pelissier, T., 2007. Expression of nitric oxide synthase isoforms in the dorsal horn of monoarthritic rats: effects of competitive and uncompetitive N-methyl-D-aspartate antagonists. Arthritis Res. Ther. 9, R53.

Inglis, J.J., McNamee, K.E., Chia, S.-L., Essex, D., Feldmann, M., Williams, R.O., Hunt, S.P., Vincent, T., 2008. Regulation of pain sensitivity in experimental osteoarthritis by the endogenous peripheral opioid system. Arthritis & Rheumatism 58, 3110–3119.

Inglis, J.J., Notley, C.A., Essex, D., Wilson, A.W., Feldmann, M., Anand, P., Williams, R., 2007. Collagen-induced arthritis as a model of

hyperalgesia: functional and cellular analysis of the analgesic actions of tumor necrosis factor blockade. Arthritis Rheum. 56, 4015–4023.

Ivanavicius, S.P., Blake, D.R., Chessell, I.P., Mapp, P.I., 2004. Isolectin B4 binding neurons are not present in the rat knee joint. Neuroscience 128, 555–560.

Jenh, C.-H., Cox, M.A., Cui, L., Reich, E.-P., Sullivan, L., Chen, S.-C., Kinsley, D., Qian, S., Kim, S.H., Rosenblum, S., Kozlowski, J., Fine, J.S., Zavodny, P.J., Lundell, D., 2012. A selective and potent CXCR3 antagonist SCH 546738 attenuates the development of autoimmune diseases and delays graft rejection. BMC immunology 13, 2.

Ji, R.R., Baba, H., Brenner, G.J., Woolf, C.J., 1999. Nociceptive-specific activation of ERK in spinal neurons contributes to pain hypersensitivity. Nat. Neurosci. 2, 1114–1119.

Ji, R.-R., Befort, K., Brenner, G.J., Woolf, C.J., 2002. ERK MAP kinase activation in superficial spinal cord neurons induces prodynorphin and NK-1 upregulation and contributes to persistent inflammatory pain hypersensitivity. J. Neurosci. 22, 478–485.

Ji, R.-R., Gereau IV, R.W., Malcangio, M., Strichartz, G.R., 2009. MAP kinase and pain. Brain Research Reviews 60, 135–148.

Jimenez-Andrade, J.M., Mantyh, W.G., Bloom, A.P., Xu, H., Ferng, A.S., Dussor, G., Vanderah, T.W., Mantyh, P.W., 2010. A phenotypically restricted set of primary afferent nerve fibers innervate the bone versus skin: Therapeutic opportunity for treating skeletal pain. Bone 46, 306–313.

Jiménez-Díaz, L., Géranton, S.M., Passmore, G.M., Leith, J.L., Fisher, A.S., Berliocchi, L., Sivasubramaniam, A.K., Sheasby, A., Lumb, B.M., Hunt, S.P., 2008. Local translation in primary afferent fibers regulates nociception. PLoS ONE 3, e1961.

Jones, B.E., Holmes, C.J., Rodriguez-Veiga, E., Mainville, L., 1991. GABA-synthesizing neurons in the medulla: their relationship to serotonin-containing and spinally projecting neurons in the rat. J. Comp. Neurol. 313, 349–367.

Julius, D., Basbaum, A.I., 2001. Molecular mechanisms of nociception. Nature 413, 203–210.

Kalyuzhny, A.E., Wessendorf, M.W., 1998. Relationship of mu- and delta-opioid receptors to GABAergic neurons in the central nervous system, including antinociceptive brainstem circuits. J. Comp. Neurol. 392, 528–547.

Kaplan, H., Fields, H.L., 1991. Hyperalgesia during acute opioid abstinence: evidence for a nociceptive facilitating function of the rostral ventromedial medulla. The Journal of Neuroscience 11, 1433–1439.

Kauppila, T., Kontinen, V.K., Pertovaara, A., 1998. Influence of spinalization on spinal withdrawal reflex responses varies depending on the submodality of the test stimulus and the experimental pathophysiological condition in the rat. Brain Res. 797, 234–242.

Kawasaki, Y., Kohno, T., Zhuang, Z.-Y., Brenner, G.J., Wang, H., Van Der Meer, C., Befort, K., Woolf, C.J., Ji, R.-R., 2004. Ionotropic and metabotropic receptors, protein kinase A, protein kinase C, and Src contribute to C-fiber-induced ERK activation and cAMP response element-binding protein phosphorylation in dorsal horn neurons, leading to central sensitization. J. Neurosci 24, 8310–8321.

Kawasaki, Y., Zhang, L., Cheng, J.-K., Ji, R.-R., 2008. Cytokine Mechanisms of Central Sensitization: Distinct and Overlapping Role of Interleukin-1β, Interleukin-6, and Tumor Necrosis Factor-α in Regulating Synaptic and Neuronal Activity in the Superficial Spinal Cord. J. Neurosci. 28, 5189–5194.

Kidd, B., Langford, R., Wodehouse, T., 2007. Arthritis and pain. Current approaches in the treatment of arthritic pain. Arthritis Research & Therapy 9, 214.

Kim, S.E., Coste, B., Chadha, A., Cook, B., Patapoutian, A., 2012. The role of Drosophila Piezo in mechanical nociception. Nature 483, 209–212.

Kim, S.J., Thomas, K.S., Calejesan, A.A., Zhuo, M., 1998. Macromolecular synthesis contributes to nociceptive response to subcutaneous formalin injection in mice. Neuropharmacology 37, 1091–1093.

Kincaid, W., Neubert, M.J., Xu, M., Kim, C.J., Heinricher, M.M., 2006. Role for medullary pain facilitating neurons in secondary thermal hyperalgesia. J. Neurophysiol. 95, 33–41.

King, T., Vera-Portocarrero, L., Gutierrez, T., Vanderah, T.W., Dussor, G., Lai, J., Fields, H.L., Porreca, F., 2009. Unmasking the tonic-aversive state in neuropathic pain. Nat. Neurosci. 12, 1364–1366.

Kovelowski, C.J., Ossipov, M.H., Sun, H., Lai, J., Malan, T.P., Porreca, F., 2000. Supraspinal cholecystokinin may drive tonic descending facilitation mechanisms to maintain neuropathic pain in the rat. Pain 87, 265–273.

Kuboyama, K., Tsuda, M., Tsutsui, M., Toyohara, Y., Tozaki-Saitoh, H., Shimokawa, H., Yanagihara, N., Inoue, K., 2011. Reduced spinal microglial activation and neuropathic pain after nerve injury in mice lacking all three nitric oxide synthases. Molecular Pain 7, 50.

Kuner, R., 2010. Central mechanisms of pathological pain. Nat. Med. 16, 1258–1266.

Kwiat, G.C., Basbaum, A.I., 1992. The origin of brainstem noradrenergic and serotonergic projections to the spinal cord dorsal horn in the rat. Somatosens Mot Res 9, 157–173.

Lacroix-Fralish, M.L., Tawfik, V.L., Tanga, F.Y., Spratt, K.F., DeLeo, J.A., 2006. Differential spinal cord gene expression in rodent models of radicular and neuropathic pain. Anesthesiology 104, 1283–1292.

LaGraize, S.C., Guo, W., Yang, K., Wei, F., Ren, K., Dubner, R., 2010. Spinal cord mechanisms mediating behavioral hyperalgesia induced by neurokinin-1 tachykinin receptor activation in the rostral ventromedial medulla. Neuroscience 171, 1341–1356.

Laragione, T., Brenner, M., Sherry, B., Gulko, P.S., 2011. CXCL10 and its receptor CXCR3 regulate synovial fibroblast invasion in rheumatoid arthritis. Arthritis Rheum. 63, 3274–3283.

Latremoliere, A., Woolf, C.J., 2009. Central Sensitization: A Generator of Pain Hypersensitivity by Central Neural Plasticity. The Journal of Pain 10, 895–926.

Lee, D.M., Weinblatt, M.E., 2001. Rheumatoid arthritis. Lancet 358, 903–911.

Lee, Y., Nassikas, N., Clauw, D., 2011a. The role of the central nervous system in the generation and maintenance of chronic pain in rheumatoid arthritis, osteoarthritis and fibromyalgia. Arthritis Research & Therapy 13, 211.

Lee, Y., Pai, M., Brederson, J.-D., Wilcox, D., Hsieh, G., Jarvis, M.F., Bitner, R.S., 2011b. Monosodium iodoacetate-induced joint pain is associated with increased phosphorylation of mitogen activated protein kinases in the rat spinal cord. Mol Pain 7, 39.

Lewis, T., 1938. Study of Somatic Pain. Br Med J 1, 321–325.

Light, A.R., Casale, E.J., Menétrey, D.M., 1986. The effects of focal stimulation in nucleus raphe magnus and periaqueductal gray on intracellularly recorded neurons in spinal laminae I and II. J. Neurophysiol. 56, 555–571.

Linley, J.E., Rose, K., Ooi, L., Gamper, N., 2010. Understanding inflammatory pain: ion channels contributing to acute and chronic nociception. Pflugers Arch. 459, 657–669.

Löken, L.S., Wessberg, J., Morrison, I., McGlone, F., Olausson, H., 2009. Coding of pleasant touch by unmyelinated afferents in humans. Nature Neuroscience 12, 547–548.

Luo, C., Gangadharan, V., Bali, K.K., Xie, R.-G., Agarwal, N., Kurejova, M., Tappe-Theodor, A., Tegeder, I., Feil, S., Lewin, G., Polgar, E., Todd, A.J., Schlossmann, J., Hofmann, F., Liu, D.-L., Hu, S.-J., Feil, R., Kuner, T., Kuner, R., 2012. Presynaptically Localized Cyclic GMP-Dependent Protein Kinase 1 Is a Key Determinant of Spinal Synaptic Potentiation and Pain Hypersensitivity. PLoS Biol 10, e1001283.

MacMicking, J., Xie, Q., Nathan, C., 1997. Nitric Oxide and Macrophage Function. Annual Review of Immunology 15, 323–350.

Malmberg, A.B., Chen, C., Tonegawa, S., Basbaum, A.I., 1997. Preserved Acute Pain and Reduced Neuropathic Pain in Mice Lacking PKCγ. Science 278, 279–283.

Malmberg, A.B., Yaksh, T.L., 1993. Spinal nitric oxide synthesis inhibition blocks NMDA-induced thermal hyperalgesia and produces antinociception in the formalin test in rats. Pain 54, 291–300.

Mansikka, H., Pertovaara, A., 1997. Supraspinal influence on hindlimb withdrawal thresholds and mustard oil-induced secondary allodynia in rats. Brain Res. Bull. 42, 359–365.

Mansour, A., Fox, C.A., Burke, S., Meng, F., Thompson, R.C., Akil, H., Watson, S.J., 1994. Mu, delta, and kappa opioid receptor mRNA expression in the rat CNS: an in situ hybridization study. J. Comp. Neurol. 350, 412–438.

Mantyh, P.W., Hunt, S.P., 1984. Evidence for cholecystokinin-like immunoreactive neurons in the rat medulla oblongata which project to the spinal cord. Brain Res. 291, 49–54.

Mantyh, P.W., Rogers, S.D., Honore, P., Allen, B.J., Ghilardi, J.R., Li, J., Daughters, R.S., Lappi, D.A., Wiley, R.G., Simone, D.A., 1997. Inhibition of hyperalgesia by ablation of lamina I spinal neurons expressing the substance P receptor. Science 278, 275–279.

Marinelli, S., Vaughan, C.W., Schnell, S.A., Wessendorf, M.W., Christie, M.J., 2002. Rostral Ventromedial Medulla Neurons That Project to the Spinal Cord Express Multiple Opioid Receptor Phenotypes. The Journal of Neuroscience 22, 10847–10855.

Marshall, T.M., Herman, D.S., Largent-Milnes, T.M., Badghisi, H., Zuber, K., Holt, S.C., Lai, J., Porreca, F., Vanderah, T.W., 2012. Activation of descending pain-facilitatory pathways from the rostral ventromedial medulla by cholecystokinin elicits release of prostaglandin-E2 in the spinal cord. PAIN 153, 86–94.

Martens, H., Weston, M.C., Boulland, J.-L., Grønborg, M., Grosche, J., Kacza, J., Hoffmann, A., Matteoli, M., Takamori, S., Harkany, T., Chaudhry, F.A., Rosenmund, C., Erck, C., Jahn, R., Härtig, W., 2008. Unique luminal localization of VGAT-C terminus allows for selective labeling of active cortical GABAergic synapses. J. Neurosci. 28, 13125–13131.

Martin, W.J., Malmberg, A.B., Basbaum, A.I., 2001. PKCgamma contributes to a subset of the NMDA-dependent spinal circuits that underlie injury-induced persistent pain. J. Neurosci. 21, 5321–5327.

Maxwell, D.J., Kerr, R., Rashid, S., Anderson, E., 2003. Characterisation of axon terminals in the rat dorsal horn that are immunoreactive for serotonin 5-HT3A receptor subunits. Exp Brain Res 149, 114–124.

Mayer, M.L., Westbrook, G.L., Guthrie, P.B., 1984. Voltage-dependent block by Mg2+ of NMDA responses in spinal cord neurones. Nature 309, 261–263.

McCleane, G.J., Suzuki, R., Dickenson, A.H., 2003. Does a single intravenous injection of the 5HT3 receptor antagonist ondansetron have an analgesic effect in neuropathic pain? A double-blinded, placebo-controlled cross-over study. Anesth. Analg. 97, 1474–1478.

Meller, S.T., Cummings, C.P., Traub, R.J., Gebhart, G.F., 1994a. The role of nitric oxide in the development and maintenance of the hyperalgesia produced by intraplantar injection of carrageenan in the rat. Neuroscience 60, 367–374.

Meller, S.T., Dykstra, C., Grzybycki, D., Murphy, S., Gebhart, G.F., 1994b. The possible role of glia in nociceptive processing and hyperalgesia in the spinal cord of the rat. Neuropharmacology 33, 1471–1478.

Melzack, R., Wall, P.D., Ty, T.C., 1982. Acute pain in an emergency clinic: latency of onset and descriptor patterns related to different injuries. Pain 14, 33–43.

Mense, S., Prabhakar, N.R., 1986. Spinal termination of nociceptive afferent fibres from deep tissues in the cat. Neurosci. Lett. 66, 169–174.

Miki, K., Zhou, Q.-Q., Guo, W., Guan, Y., Terayama, R., Dubner, R., Ren, K., 2002. Changes in Gene Expression and Neuronal Phenotype in Brain Stem Pain Modulatory Circuitry After Inflammation. Journal of Neurophysiology 87, 750 –760.

Millan, M.J., 2002. Descending control of pain. Prog. Neurobiol. 66, 355–474.

Mills, C., Leblond, D., Joshi, S., Zhu, C., Hsieh, G., Jacobson, P., Meyer, M., Decker, M., 2012. Estimating efficacy and drug ED50's using von Frey thresholds: impact of weber's law and log transformation. J Pain 13, 519–523.

Mitchell, K., Yang, H.-Y.T., Tessier, P.A., Muhly, W.T., Swaim, W.D., Szalayova, I., Keller, J.M., Mezey, E., Iadarola, M.J., 2008. Localization of S100A8 and S100A9 expressing neutrophils to spinal cord during peripheral tissue inflammation. Pain 134, 216–231.

Mogil, J.S., 2009. Animal models of pain: progress and challenges. Nat. Rev. Neurosci. 10, 283–294.

Mogil, J.S., McCarson, K.E., 2000. Identifying pain genes: Bottom-up and top-down approaches. The Journal of Pain 1, 66–80.

Moore, P.K., Oluyomi, A.O., Babbedge, R.C., Wallace, P., Hart, S.L., 1991. L-NG-nitro arginine methyl ester exhibits antinociceptive activity in the mouse. Br. J. Pharmacol. 102, 198–202.

Morris, V.H., Cruwys, S.C., Kidd, B.L., 1997. Characterisation of capsaicin-induced mechanical hyperalgesia as a marker for altered nociceptive processing in patients with rheumatoid arthritis. Pain 71, 179–186.

Müller, M., Carter, S., Hofer, M.J., Campbell, I.L., 2010. Review: The chemokine receptor CXCR3 and its ligands CXCL9, CXCL10 and CXCL11 in neuroimmunity – a tale of conflict and conundrum. Neuropathology and Applied Neurobiology 36, 368–387.

Naeini, R.S., Cahill, C.M., Ribeiro-da-Silva, A., Ménard, H.A., Henry, J.L., 2005. Remodelling of spinal nociceptive mechanisms in an animal model of monoarthritis. European Journal of Neuroscience 22, 2005–2015.

Nagy, J.I., Hunt, S.P., 1982. Fluoride-resistant acid phosphatase-containing neurones in dorsal root ganglia are separate from those containing substance P or somatostatin. Neuroscience 7, 89–97.

Nakajima, T., Ohtori, S., Inoue, G., Koshi, T., Yamamoto, S., Nakamura, J., Takahashi, K., Harada, Y., 2008. The characteristics of dorsal-root ganglia and sensory innervation of the hip in rats. J Bone Joint Surg Br 90-B, 254–257.

Nassar, M.A., Stirling, L.C., Forlani, G., Baker, M.D., Matthews, E.A., Dickenson, A.H., Wood, J.N., 2004. Nociceptor-specific gene deletion

reveals a major role for Nav1.7 (PN1) in acute and inflammatory pain. Proc. Natl. Acad. Sci. U.S.A. 101, 12706–12711.

Neugebauer, V., Han, J.S., Adwanikar, H., Fu, Y., Ji, G., 2007. Techniques for assessing knee joint pain in arthritis. Mol Pain 3, 8.

Neugebauer, V., Lücke, T., Schaible, H.G., 1993. Differential effects of N-methyl-D-aspartate (NMDA) and non-NMDA receptor antagonists on the responses of rat spinal neurons with joint input. Neurosci. Lett. 155, 29–32.

Neugebauer, V., Schaible, H.G., 1990. Evidence for a central component in the sensitization of spinal neurons with joint input during development of acute arthritis in cat's knee. J Neurophysiol 64, 299–311.

Neugebauer, V., Schaible, H.G., Weiretter, F., Freudenberger, U., 1994. The involvement of substance P and neurokinin-1 receptors in the responses of rat dorsal horn neurons to noxious but not to innocuous mechanical stimuli applied to the knee joint. Brain Res. 666, 207–215.

Neugebauer, V., Vanegas, H., Nebe, J., Rümenapp, P., Schaible, H.G., 1996. Effects of N- and L-type calcium channel antagonists on the responses of nociceptive spinal cord neurons to mechanical stimulation of the normal and the inflamed knee joint. J. Neurophysiol. 76, 3740–3749.

Nichols, M.L., Allen, B.J., Rogers, S.D., Ghilardi, J.R., Honore, P., Luger, N.M., Finke, M.P., Li, J., Lappi, D.A., Simone, D.A., Mantyh, P.W., 1999. Transmission of chronic nociception by spinal neurons expressing the substance P receptor. Science 286, 1558–1561.

Nielsen, K., Brask, D., Knudsen, G.M., Aznar, S., 2006. Immunodetection of the serotonin transporter protein is a more valid marker for serotonergic fibers than serotonin. Synapse 59, 270–276.

Nishimune, H., Vasseur, S., Wiese, S., Birling, M.C., Holtmann, B., Sendtner, M., Iovanna, J.L., Henderson, C.E., 2000. Reg-2 is a motoneuron neurotrophic factor and a signalling intermediate in the CNTF survival pathway. Nat. Cell Biol. 2, 906–914.

Nitanda, A., Yasunami, N., Tokumo, K., Fujii, H., Hirai, T., Nishio, H., 2005. Contribution of the peripheral 5-HT 2A receptor to mechanical hyperalgesia in a rat model of neuropathic pain. Neurochem. Int. 47, 394–400.

Norsted Gregory, E., Codeluppi, S., Gregory, J.A., Steinauer, J., Svensson, C.I., 2010. Mammalian target of rapamycin in spinal cord neurons mediates hypersensitivity induced by peripheral inflammation. Neuroscience 169, 1392–1402.

Oatway, M.A., Chen, Y., Weaver, L.C., 2004. The 5-HT3 receptor facilitates at-level mechanical allodynia following spinal cord injury. Pain 110, 259–268.

Obara, I., Tochiki, K.K., Géranton, S.M., Carr, F.B., Lumb, B.M., Liu, Q., Hunt, S.P., 2011. Systemic inhibition of the mammalian target of rapamycin (mTOR) pathway reduces neuropathic pain in mice. Pain 152, 2582–2595.

Obata, H., Saito, S., Sakurazawa, S., Sasaki, M., Usui, T., Goto, F., 2004. Antiallodynic effects of intrathecally administered 5-HT(2C) receptor agonists in rats with nerve injury. Pain 108, 163–169.

Obata, H., Saito, S., Sasaki, M., Ishizaki, K., Goto, F., 2001. Antiallodynic effect of intrathecally administered 5-HT(2) agonists in rats with nerve ligation. Pain 90, 173–179.

Obreja, O., Biasio, W., Andratsch, M., Lips, K.S., Rathee, P.K., Ludwig, A., Rose-John, S., Kress, M., 2005. Fast modulation of heat-activated ionic current by proinflammatory interleukin 6 in rat sensory neurons. Brain 128, 1634–1641.

Oh, S.B., Tran, P.B., Gillard, S.E., Hurley, R.W., Hammond, D.L., Miller, R.J., 2001. Chemokines and glycoprotein120 produce pain hypersensitivity by directly exciting primary nociceptive neurons. J. Neurosci. 21, 5027–5035.

Okamoto, K., Imbe, H., Tashiro, A., Kumabe, S., Senba, E., 2004. Blockade of peripheral 5HT3 receptor attenuates the formalin-induced nocifensive behavior in persistent temporomandibular joint inflammation of rat. Neurosci. Lett. 367, 259–263.

Old, E.A., Malcangio, M., 2012. Chemokine mediated neuron-glia communication and aberrant signalling in neuropathic pain states. Curr Opin Pharmacol 12, 67–73.

Ossipov, M.H., Dussor, G.O., Porreca, F., 2010. Central modulation of pain. J. Clin. Invest. 120, 3779–3787.

Oyama, T., Ueda, M., Kuraishi, Y., Akaike, A., Satoh, M., 1996. Dual effect of serotonin on formalin-induced nociception in the rat spinal cord. Neurosci. Res. 25, 129–135.

Oz, M., Zhang, L., Morales, M., 2002. Endogenous cannabinoid, anandamide, acts as a noncompetitive inhibitor on 5-HT3 receptor-mediated responses in Xenopus oocytes. Synapse 46, 150–156.

Palygin, O., Lalo, U., Verkhratsky, A., Pankratov, Y., 2010. Ionotropic NMDA and P2X1/5 receptors mediate synaptically induced Ca2+ signalling in cortical astrocytes. Cell Calcium 48, 225–231.

Pan, Z.Z., Tershner, S.A., Fields, H.L., 1997. Cellular mechanism for anti-analgesic action of agonists of the kappa-opioid receptor. Nature 389, 382–385.

Pertovaara, A., 2000. Plasticity in descending pain modulatory systems. Prog. Brain Res. 129, 231–242.

Pertovaara, A., Wei, H., Hämäläinen, M.M., 1996. Lidocaine in the rostroventromedial medulla and the periaqueductal gray attenuates allodynia in neuropathic rats. Neurosci. Lett. 218, 127–130.

Pezet, S., Malcangio, M., Lever, I.J., Perkinton, M.S., Thompson, S.W.N., Williams, R.J., McMahon, S.B., 2002. Noxious stimulation induces Trk receptor and downstream ERK phosphorylation in spinal dorsal horn. Mol. Cell. Neurosci. 21, 684–695.

Phillips, R.S., Cleary, D.R., Nalwalk, J.W., Arttamangkul, S., Hough, L.B., Heinricher, M.M., 2012. Pain-facilitating medullary neurons contribute to opioid-induced respiratory depression. J. Neurophysiol.

Plenderleith, M.B., Snow, P.J., 1993. The plant lectin Bandeiraea simplicifolia I-B4 identifies a subpopulation of small diameter primary sensory neurones which innervate the skin in the rat. Neurosci. Lett. 159, 17–20.

Poh, K.-W., Yeo, J.-F., Stohler, C.S., Ong, W.-Y., 2012. Comprehensive Gene Expression Profiling in the Prefrontal Cortex Links Immune Activation and Neutrophil Infiltration to Antinociception. J. Neurosci. 32, 35–45.

Porreca, F., Burgess, S.E., Gardell, L.R., Vanderah, T.W., Malan, T.P., Ossipov, M.H., Lappi, D.A., Lai, J., 2001. Inhibition of neuropathic pain by selective ablation of brainstem medullary cells expressing the mu-opioid receptor. J. Neurosci 21, 5281–5288.

Potrebic, S.B., Fields, H.L., Mason, P., 1994. Serotonin immunoreactivity is contained in one physiological cell class in the rat rostral ventromedial medulla. J. Neurosci. 14, 1655–1665.

Raghavendra, V., Tanga, F., DeLeo, J.A., 2003. Inhibition of microglial activation attenuates the development but not existing hypersensitivity in a rat model of neuropathy. J. Pharmacol. Exp. Ther. 306, 624–630.

Raghavendra, V., Tanga, F.Y., DeLeo, J.A., 2004. Complete Freunds adjuvant-induced peripheral inflammation evokes glial activation and proinflammatory cytokine expression in the CNS. Eur. J. Neurosci 20, 467–473.

Rahman, W., Bauer, C.S., Bannister, K., Vonsy, J.-L., Dolphin, A.C., Dickenson, A.H., 2009. Descending serotonergic facilitation and the antinociceptive effects of pregabalin in a rat model of osteoarthritic pain. Mol Pain 5, 45.

Rahman, W., Suzuki, R., Webber, M., Hunt, S.P., Dickenson, A.H., 2006. Depletion of endogenous spinal 5-HT attenuates the behavioural hypersensitivity to mechanical and cooling stimuli induced by spinal nerve ligation. Pain 123, 264–274.

RANDALL, L.O., SELITTO, J.J., 1957. A method for measurement of analgesic activity on inflamed tissue. Arch Int Pharmacodyn Ther 111, 409–419.

Ransohoff, R.M., Liu, L., Cardona, A.E., 2007. Chemokines and chemokine receptors: multipurpose players in neuroinflammation. Int. Rev. Neurobiol. 82, 187–204.

Raouf, R., Quick, K., Wood, J.N., 2010. Pain as a channelopathy. J. Clin. Invest. 120, 3745–3752.

Reichling, D.B., Basbaum, A.I., 1990. Contribution of brainstem GABAergic circuitry to descending antinociceptive controls: I. GABA-immunoreactive projection neurons in the periaqueductal gray and nucleus raphe magnus. J. Comp. Neurol. 302, 370–377.

Reid, K.J., Harker, J., Bala, M.M., Truyers, C., Kellen, E., Bekkering, G.E., Kleijnen, J., 2011. Epidemiology of chronic non-cancer pain in Europe: narrative review of prevalence, pain treatments and pain impact. Curr Med Res Opin 27, 449–462.

Ren, K., Dubner, R., 1996. Enhanced descending modulation of nociception in rats with persistent hindpaw inflammation. Journal of Neurophysiology 76, 3025 –3037.

Ren, K., Dubner, R., 2010. Interactions between the immune and nervous systems in pain. Nat. Med. 16, 1267–1276.

Ren, K., Novikova, S.I., He, F., Dubner, R., Lidow, M.S., 2005. Neonatal local noxious insult affects gene expression in the spinal dorsal horn of adult rats. Mol Pain 1, 27.

Ren, W., Neugebauer, V., 2010. Pain-related increase of excitatory transmission and decrease of inhibitory transmission in the central nucleus of the amygdala are mediated by mGluR1. Molecular Pain 6, 93.

REXED, B., 1952. The cytoarchitectonic organization of the spinal cord in the cat. J. Comp. Neurol. 96, 414–495.

Reynolds, D.V., 1969. Surgery in the rat during electrical analgesia induced by focal brain stimulation. Science 164, 444–445.

Reynolds, J., Bilsky, E.J., Meng, I.D., 2011. Selective ablation of mu-opioid receptor expressing neurons in the rostral ventromedial medulla attenuates stress-induced mechanical hypersensitivity. Life Sciences 89, 313–319.

Rieker, C., Engblom, D., Kreiner, G., Domanskyi, A., Schober, A., Stotz, S., Neumann, M., Yuan, X., Grummt, I., Schütz, G., Parlato, R., 2011. Nucleolar disruption in dopaminergic neurons leads to oxidative damage and parkinsonism through repression of mammalian target of rapamycin signaling. J. Neurosci. 31, 453–460.

Rivat, C., Becker, C., Blugeot, A., Zeau, B., Mauborgne, A., Pohl, M., Benoliel, J.-J., 2010. Chronic stress induces transient spinal neuroinflammation, triggering sensory hypersensitivity and long-lasting anxiety-induced hyperalgesia. PAIN 150, 358–368.

Roberts, J., Ossipov, M.H., Porreca, F., 2009. Glial activation in the rostroventromedial medulla promotes descending facilitation to mediate inflammatory hypersensitivity. Eur. J. Neurosci. 30, 229–241.

Robertson, B., Xu, X.J., Hao, J.X., Wiesenfeld-Hallin, Z., Mhlanga, J., Grant, G., Kristensson, K., 1997. Interferon-gamma receptors in nociceptive pathways: role in neuropathic pain-related behaviour. Neuroreport 8, 1311–1316.

Rodriguez Parkitna, J., Korostynski, M., Kaminska-Chowaniec, D., Obara, I., Mika, J., Przewlocka, B., Przewlocki, R., 2006. Comparison of gene expression profiles in neuropathic and inflammatory pain. J. Physiol. Pharmacol. 57, 401–414.

Ruda, M.A., 1988. Spinal dorsal horn circuitry involved in the brain stem control of nociception. Prog. Brain Res. 77, 129–140.

Ruda, M.A., Bennett, G.J., Dubner, R., 1986. Neurochemistry and neural circuitry in the dorsal horn. Prog. Brain Res. 66, 219–268.

Rygh, L.J., Suzuki, R., Rahman, W., Wong, Y., Vonsy, J.L., Sandhu, H., Webber, M., Hunt, S., Dickenson, A.H., 2006. Local and descending circuits regulate long-term potentiation and zif268 expression in spinal neurons. Eur. J. Neurosci. 24, 761–772.

Sagar, D.R., Burston, J.J., Hathway, G.J., Woodhams, S.G., Pearson, R.G., Bennett, A.J., Kendall, D.A., Scammell, B.E., Chapman, V., 2011. The contribution of spinal glial cells to chronic pain behaviour in the monosodium iodoacetate model of osteoarthritic pain. Mol Pain 7, 88.

Sagar, D.R., Staniaszek, L.E., Okine, B.N., Woodhams, S., Norris, L.M., Pearson, R.G., Garle, M.J., Alexander, S.P.H., Bennett, A.J., Barrett, D.A., Kendall, D.A., Scammell, B.E., Chapman, V., 2010. Tonic modulation of spinal hyperexcitability by the endocannabinoid receptor system in a rat model of osteoarthritis pain. Arthritis & Rheumatism 62, 3666–3676.

Sallusto, F., Baggiolini, M., 2008. Chemokines and leukocyte traffic. Nature Immunology 9, 949–952.

Salter, M.W., Henry, J.L., 1991. Responses of functionally identified neurones in the dorsal horn of the cat spinal cord to substance P, neurokinin A and physalaemin. Neuroscience 43, 601–610.

Samad, T.A., Moore, K.A., Sapirstein, A., Billet, S., Allchorne, A., Poole, S., Bonventre, J.V., Woolf, C.J., 2001. Interleukin-1beta-mediated induction of Cox-2 in the CNS contributes to inflammatory pain hypersensitivity. Nature 410, 471–475.

Sanoja, R., Tortorici, V., Fernandez, C., Price, T.J., Cervero, F., 2010. Role of RVM neurons in capsaicin-evoked visceral nociception and referred hyperalgesia. Eur J Pain 14, 120.e1–9.

Schaible, H.-G., Ebersberger, A., Natura, G., 2011. Update on peripheral mechanisms of pain: beyond prostaglandins and cytokines. Arthritis Research & Therapy 13, 210.

Schaible, H.-G., Grubb, B.D., 1993. Afferent and spinal mechanisms of joint pain. Pain 55, 5–54.

Schaible, H.G., Neugebauer, V., Cervero, F., Schmidt, R.F., 1991. Changes in tonic descending inhibition of spinal neurons with articular input during the development of acute arthritis in the cat. Journal of Neurophysiology 66, 1021 –1032.

Schaible, H.-G., Richter, F., Ebersberger, A., Boettger, M.K., Vanegas, H., Natura, G., Vazquez, E., Segond von Banchet, G., 2009. Joint pain. Exp Brain Res 196, 153–162.

Schaible, H.G., Schmidt, R.F., 1988. Time course of mechanosensitivity changes in articular afferents during a developing experimental arthritis. J. Neurophysiol. 60, 2180–2195.

Schaible, H.G., Schmidt, R.F., Willis, W.D., 1987. Enhancement of the responses of ascending tract cells in the cat spinal cord by acute inflammation of the knee joint. Exp Brain Res 66, 489–499.

Schena, M., Shalon, D., Davis, R.W., Brown, P.O., 1995. Quantitative monitoring of gene expression patterns with a complementary DNA microarray. Science 270, 467–470.

Scholz, J., Woolf, C.J., 2002. Can we conquer pain? Nature Neuroscience 5, 1062–1067.

Seal, R.P., Wang, X., Guan, Y., Raja, S.N., Woodbury, C.J., Basbaum, A.I., Edwards, R.H., 2009. Injury-induced mechanical hypersensitivity requires C-low threshold mechanoreceptors. Nature 462, 651–655.

Shan, S., Hong, C., Mei, H., Ting-Ting, L., Hai-Li, P., Zhi-Qi, Z., Yu-Qiu, Z., 2007. New evidence for the involvement of spinal fractalkine receptor in pain facilitation and spinal glial activation in rat model of monoarthritis. Pain 129, 64–75.

Sherrington, C.S., 1903. Qualitative difference of spinal reflex corresponding with qualitative difference of cutaneous stimulus. J. Physiol. (Lond.) 30, 39–46.

Sherrington, C.S., 1906. Observations on the scratch-reflex in the spinal dog. J. Physiol. (Lond.) 34, 1–50.

Siegfried, B., Frischknecht, H.R., Nunes de Souza, R.L., 1990. An ethological model for the study of activation and interaction of pain, memory and defensive systems in the attacked mouse. Role of endogenous opioids. Neurosci Biobehav Rev 14, 481–490.

Sikandar, S., Bannister, K., Dickenson, A.H., 2012. Brainstem facilitations and descending serotonergic controls contribute to visceral nociception but not pregabalin analgesia in rats. Neurosci. Lett. 519, 31–36.

Skagerberg, G., Björklund, A., 1985. Topographic principles in the spinal projections of serotonergic and non-serotonergic brainstem neurons in the rat. Neuroscience 15, 445–480.

Sluka, K.A., 2002. Stimulation of deep somatic tissue with capsaicin produces long-lasting mechanical allodynia and heat hypoalgesia that depends on early activation of the cAMP pathway. J. Neurosci. 22, 5687–5693.

Sluka, K.A., Westlund, K.N., 1992. An experimental arthritis in rats: dorsal horn aspartate and glutamate increases. Neurosci. Lett. 145, 141–144.

Sommer, C., Kress, M., 2004. Recent findings on how proinflammatory cytokines cause pain: peripheral mechanisms in inflammatory and neuropathic hyperalgesia. Neurosci. Lett. 361, 184–187.

Spike, R.C., Puskár, Z., Andrew, D., Todd, A.J., 2003. A quantitative and morphological study of projection neurons in lamina I of the rat lumbar spinal cord. Eur. J. Neurosci. 18, 2433–2448.

Steain, M., Gowrishankar, K., Rodriguez, M., Slobedman, B., Abendroth, A., 2011. Upregulation of CXCL10 in human dorsal root ganglia during experimental and natural varicella-zoster virus infection. J. Virol. 85, 626–631.

Strong, J.A., Xie, W., Coyle, D.E., Zhang, J.-M., 2012. Microarray analysis of rat sensory ganglia after local inflammation implicates novel cytokines in pain. PLoS ONE 7, e40779.

Sufka, K.J., 1994. Conditioned place preference paradigm: a novel approach for analgesic drug assessment against chronic pain. Pain 58, 355–366.

Sun, L., Wu, Z., Hayashi, Y., Peters, C., Tsuda, M., Inoue, K., Nakanishi, H., 2012. Microglial cathepsin B contributes to the initiation of peripheral inflammation-induced chronic pain. J. Neurosci. 32, 11330–11342.

Suzuki, R., Morcuende, S., Webber, M., Hunt, S.P., Dickenson, A.H., 2002. Superficial NK1-expressing neurons control spinal excitability through activation of descending pathways. Nature Neuroscience 5, 1319–1326.

Svensson, C.I., Tran, T.K., Fitzsimmons, B., Yaksh, T.L., Hua, X.-Y., 2006. Descending serotonergic facilitation of spinal ERK activation and pain behavior. FEBS Lett. 580, 6629–6634.

Sweatt, J.D., 2004. Mitogen-activated protein kinases in synaptic plasticity and memory. Curr. Opin. Neurobiol. 14, 311–317.

Takasaki, I., Taniguchi, K., Komatsu, F., Sasaki, A., Andoh, T., Nojima, H., Shiraki, K., Hsu, D.K., Liu, F.-T., Kato, I., Hiraga, K., Kuraishi, Y., 2012. Contribution of spinal galectin-3 to acute herpetic allodynia in mice. Pain 153, 585–592.

Takase, L.F., Nogueira, M.I., 2008. Patterns of fos activation in rat raphe nuclei during feeding behavior. Brain Res. 1200, 10–18.

Tang, Q., Svensson, C.I., Fitzsimmons, B., Webb, M., Yaksh, T.L., Hua, X.-Y., 2007. Inhibition of spinal constitutive NOS-2 by 1400W attenuates tissue injury and inflammation-induced hyperalgesia and spinal p38 activation. Eur. J. Neurosci. 25, 2964–2972.

Terayama, R., Dubner, R., Ren, K., 2002. The roles of NMDA receptor activation and nucleus reticularis gigantocellularis in the time-dependent changes in descending inhibition after inflammation. Pain 97, 171–181.

Terayama, R., Guan, Y., Dubner, R., Ren, K., 2000. Activity-induced plasticity in brain stem pain modulatory circuitry after inflammation. Neuroreport 11, 1915–1919.

Terman, G.W., Shavit, Y., Lewis, J.W., Cannon, J.T., Liebeskind, J.C., 1984. Intrinsic mechanisms of pain inhibition: activation by stress. Science 226, 1270–1277.

Thakur, M., Rahman, W., Hobbs, C., Dickenson, A.H., Bennett, D.L.H., 2012. Characterisation of a peripheral neuropathic component of the rat monoiodoacetate model of osteoarthritis. PLoS ONE 7, e33730.

Tillu, D.V., Gebhart, G.F., Sluka, K.A., 2008. Descending facilitatory pathways from the RVM initiate and maintain bilateral hyperalgesia after muscle insult. PAIN 136, 331–339.

Tochiki, K.K., Cunningham, J., Hunt, S.P., Geranton, S.M., 2012. The expression of spinal methyl-CpG-binding protein 2, DNA methyltransferases and histone deacetylases is modulated in persistent pain states. Molecular Pain 8, 14.

Todd, A.J., 2002. Anatomy of primary afferents and projection neurones in the rat spinal dorsal horn with particular emphasis on substance P and the neurokinin 1 receptor. Exp. Physiol. 87, 245–249.

Todd, A.J., 2010. Neuronal circuitry for pain processing in the dorsal horn. Nat. Rev. Neurosci. 11, 823–836.

Tracey, I., Mantyh, P.W., 2007. The Cerebral Signature for Pain Perception and Its Modulation. Neuron 55, 377–391.

Treede, R.-D., Meyer, R.A., Raja, S.N., Campbell, J.N., 1992. Peripheral and central mechanisms of cutaneous hyperalgesia. Progress in Neurobiology 38, 397–421.

Uematsu, T., Sakai, A., Ito, H., Suzuki, H., 2011. Intra-articular administration of tachykinin NK1 receptor antagonists reduces hyperalgesia and cartilage destruction in the inflammatory joint in rats with adjuvant-induced arthritis. European Journal of Pharmacology 668, 163–168.

Urban, M.O., Gebhart, G.F., 1999. Supraspinal contributions to hyperalgesia. Proc Natl Acad Sci U S A 96, 7687–7692.

Urban, M.O., Jiang, M.C., Gebhart, G.F., 1996. Participation of central descending nociceptive facilitatory systems in secondary hyperalgesia produced by mustard oil. Brain Res. 737, 83–91.

Urban, M.O., Zahn, P.K., Gebhart, G.F., 1999. Descending facilitatory influences from the rostral medial medulla mediate secondary, but not primary hyperalgesia in the rat. Neuroscience 90, 349–352.

Van der Werf, Y.D., Witter, M.P., Groenewegen, H.J., 2002. The intralaminar and midline nuclei of the thalamus. Anatomical and functional evidence for participation in processes of arousal and awareness. Brain Res. Brain Res. Rev. 39, 107–140.

Vanegas, H., 2004. To the descending pain-control system in rats, inflammation-induced primary and secondary hyperalgesia are two different things. Neurosci. Lett. 361, 225–228.

Vanegas, H., Schaible, H.-G., 2004. Descending control of persistent pain: inhibitory or facilitatory? Brain Res. Brain Res. Rev 46, 295–309.

Vay, L., Gu, C., McNaughton, P.A., 2012. The thermo-TRP ion channel family: properties and therapeutic implications. British Journal of Pharmacology 165, 787–801.

Veasey, S.C., Fornal, C.A., Metzler, C.W., Jacobs, B.L., 1995. Response of serotonergic caudal raphe neurons in relation to specific motor activities in freely moving cats. J. Neurosci. 15, 5346–5359.

Vera-Portocarrero, L.P., Xie, J.Y., Yie, J.X., Kowal, J., Ossipov, M.H., King, T., Porreca, F., 2006. Descending facilitation from the rostral ventromedial medulla maintains visceral pain in rats with experimental pancreatitis. Gastroenterology 130, 2155–2164.

Verpoorten, N., Claeys, K.G., Deprez, L., Jacobs, A., Van Gerwen, V., Lagae, L., Arts, W.F., De Meirleir, L., Keymolen, K., Ceuterick-de Groote, C., De Jonghe, P., Timmerman, V., Nelis, E., 2006. Novel frameshift and splice site mutations in the neurotrophic tyrosine kinase receptor type 1 gene (NTRK1) associated with hereditary sensory neuropathy type IV. Neuromuscul. Disord. 16, 19–25.

Vikman, K., Robertson, B., Grant, G., Liljeborg, A., Kristensson, K., 1998. Interferon-gamma receptors are expressed at synapses in the rat superficial dorsal horn and lateral spinal nucleus. J. Neurocytol. 27, 749–759.

Vikman, K.S., Duggan, A.W., Siddall, P.J., 2003. Increased ability to induce long-term potentiation of spinal dorsal horn neurones in monoarthritic rats. Brain Research 990, 51–57.

Vikman, K.S., Duggan, A.W., Siddall, P.J., 2007. Interferon-gamma induced disruption of GABAergic inhibition in the spinal dorsal horn in vivo. Pain 133, 18–28.

Vinet, J., De Jong, E.K., Boddeke, H.W.G.M., Stanulovic, V., Brouwer, N., Granic, I., Eisel, U.L.M., Liem, R.S.B., Biber, K., 2010. Expression of CXCL10 in cultured cortical neurons. Journal of Neurochemistry 112, 703–714.

Von Banchet, G.S., Kiehl, M., Schaible, H.-G., 2005. Acute and long-term effects of IL-6 on cultured dorsal root ganglion neurones from adult rat. J. Neurochem. 94, 238–248.

Wallace, V.C.J., Segerdahl, A.R., Blackbeard, J., Pheby, T., Rice, A.S.C., 2008. Anxiety-like behaviour is attenuated by gabapentin, morphine and diazepam in a rodent model of HIV anti-retroviral-associated neuropathic pain. Neurosci. Lett. 448, 153–156.

Wang, H., Wessendorf, M.W., 1999. Mu- and delta-opioid receptor mRNAs are expressed in spinally projecting serotonergic and nonserotonergic neurons of the rostral ventromedial medulla. J. Comp. Neurol. 404, 183–196.

Wang, K., Zhang, R., Xiang, X., He, F., Lin, L., Ping, X., Yu, L., Han, J., Zhao, G., Zhang, Q., Cui, C., 2012. Differences in neural-immune gene expression response in rat spinal dorsal horn correlates with variations in electroacupuncture analgesia. PLoS ONE 7, e42331.

Wang, W., Wu, S.-X., Wang, Y.-Y., Liu, X.-Y., Li, Y.-Q., 2003. 5-hydroxytryptamine1A receptor is involved in the bee venom induced inflammatory pain. Pain 106, 135–142.

Wang, Y.-Y., Wei, Y.-Y., Huang, J., Wang, W., Tamamaki, N., Li, Y.-Q., Wu, S.-X., 2009. Expression patterns of 5-HT receptor subtypes 1A and 2A on GABAergic neurons within the spinal dorsal horn of GAD67-GFP knock-in mice. Journal of Chemical Neuroanatomy 38, 75–81.

Wei, F., Dubner, R., Zou, S., Ren, K., Bai, G., Wei, D., Guo, W., 2010. Molecular depletion of descending serotonin unmasks its novel facilitatory role in the development of persistent pain. J. Neurosci. 30, 8624–8636.

Wei, F., Guo, W., Zou, S., Ren, K., Dubner, R., 2008. Supraspinal Glial–Neuronal Interactions Contribute to Descending Pain Facilitation. J. Neurosci. 28, 10482–10495.

Widmann, C., Gibson, S., Jarpe, M.B., Johnson, G.L., 1999. Mitogen-Activated Protein Kinase: Conservation of a Three-Kinase Module From Yeast to Human. Physiol Rev 79, 143–180.

Wiklund, L., Björklund, A., 1980. Mechanisms of regrowth in the bulbospinal serotonin system following 5,6-dihydroxytryptamine induced axotomy. II. Fluorescence histochemical observations. Brain Res. 191, 109–127.

Wiley, R.G., 1992. Neural lesioning with ribosome-inactivating proteins: suicide transport and immunolesioning. Trends Neurosci. 15, 285–290.

Wiley, R.G., Oeltmann, T.N., Lappi, D.A., 1991. Immunolesioning: selective destruction of neurons using immunotoxin to rat NGF receptor. Brain Res. 562, 149–153.

Winer, J., Jung, C.K., Shackel, I., Williams, P.M., 1999. Development and validation of real-time quantitative reverse transcriptase-polymerase chain reaction for monitoring gene expression in cardiac myocytes in vitro. Anal. Biochem. 270, 41–49.

Wolfe, F., Michaud, K., 2007. Assessment of pain in rheumatoid arthritis: minimal clinically significant difference, predictors, and the effect of anti-tumor necrosis factor therapy. J. Rheumatol. 34, 1674–1683.

Woolf, C.J., 1983. Evidence for a central component of post-injury pain hypersensitivity. Nature 306, 686–688.

Woolf, C.J., 2010. What is this thing called pain? J. Clin. Invest. 120, 3742–3744.

Woolf, C.J., Costigan, M., 1999. Transcriptional and posttranslational plasticity and the generation of inflammatory pain. Proc. Natl. Acad. Sci. U.S.A. 96, 7723–7730.

Woolf, C.J., Ma, Q., 2007. Nociceptors—Noxious Stimulus Detectors. Neuron 55, 353–364.

Woolf, C.J., Salter, M.W., 2000. Neuronal plasticity: increasing the gain in pain. Science 288, 1765–1769.

Woolf, C.J., Thompson, S.W., 1991. The induction and maintenance of central sensitization is dependent on N-methyl-D-aspartic acid

receptor activation; implications for the treatment of post-injury pain hypersensitivity states. Pain 44, 293–299.

Woolf, C.J., Wall, P.D., 1986. Relative effectiveness of C primary afferent fibers of different origins in evoking a prolonged facilitation of the flexor reflex in the rat. J. Neurosci. 6, 1433–1442.

Wu, J., Fang, L., Lin, Q., Willis, W.D., 2001. Nitric oxide synthase in spinal cord central sensitization following intradermal injection of capsaicin. Pain 94, 47–58.

Wylde, V., Hewlett, S., Learmonth, I.D., Dieppe, P., 2011. Persistent pain after joint replacement: prevalence, sensory qualities, and postoperative determinants. Pain 152, 566–572.

Xia, M.Q., Bacskai, B.J., Knowles, R.B., Qin, S.X., Hyman, B.T., 2000. Expression of the chemokine receptor CXCR3 on neurons and the elevated expression of its ligand IP-10 in reactive astrocytes: in vitro ERK1/2 activation and role in Alzheimer's disease. J. Neuroimmunol. 108, 227–235.

Xie, J.Y., Herman, D.S., Stiller, C.-O., Gardell, L.R., Ossipov, M.H., Lai, J., Porreca, F., Vanderah, T.W., 2005. Cholecystokinin in the Rostral Ventromedial Medulla Mediates Opioid-Induced Hyperalgesia and Antinociceptive Tolerance. J. Neurosci. 25, 409–416.

Xu, W., Qiu, X.C., Han, J.S., 1994. Serotonin receptor subtypes in spinal antinociception in the rat. J. Pharmacol. Exp. Ther. 269, 1182–1189.

Yaksh, T.L., Wilson, P.R., 1979. Spinal serotonin terminal system mediates antinociception. J Pharmacol Exp Ther 208, 446–453.

Yaksh, T.L., Yeung, J.C., Rudy, T.A., 1976. Systematic examination in the rat of brain sites sensitive to the direct application of morphine: observation of differential effects within the periaqueductal gray. Brain Res. 114, 83–103.

Yanarates, O., Dogrul, A., Yildirim, V., Sahin, A., Sizlan, A., Seyrek, M., Akgül, O., Kozak, O., Kurt, E., Aypar, U., 2010. Spinal 5-HT7 receptors play an important role in the antinociceptive and antihyperalgesic effects of tramadol and its metabolite, O-Desmethyltramadol, via activation of descending serotonergic pathways. Anesthesiology 112, 696–710.

Yang, K.-H., Galadari, S., Isaev, D., Petroianu, G., Shippenberg, T.S., Oz, M., 2010. The nonpsychoactive cannabinoid cannabidiol inhibits 5-hydroxytryptamine3A receptor-mediated currents in Xenopus laevis oocytes. J. Pharmacol. Exp. Ther. 333, 547–554.

Yang, L., Zhang, F.-X., Huang, F., Lu, Y.-J., Li, G.-D., Bao, L., Xiao, H.-S., Zhang, X., 2004. Peripheral nerve injury induces trans-synaptic modification of channels, receptors and signal pathways in rat dorsal spinal cord. Eur. J. Neurosci. 19, 871–883.

Yao, Y.-X., Jiang, Z., Zhao, Z.-Q., 2011. Knockdown of synaptic scaffolding protein Homer 1b/c attenuates secondary hyperalgesia induced by complete Freund's adjuvant in rats. Anesth. Analg. 113, 1501–1508.

Yellin, M., Paliienko, I., Balanescu, A., Ter-Vartanian, S., Tseluyko, V., Xu, L.-A., Tao, X., Cardarelli, P.M., Leblanc, H., Nichol, G., Ancuta, C., Chirieac, R., Luo, A., 2012. A phase II, randomized, double-blind, placebo-controlled study evaluating the efficacy and safety of MDX-1100, a fully human anti-CXCL10 monoclonal antibody, in combination with methotrexate in patients with rheumatoid arthritis. Arthritis Rheum. 64, 1730–1739.

Yoshida, S., Arakawa, F., Higuchi, F., Ishibashi, Y., Goto, M., Sugita, Y., Nomura, Y., Niino, D., Shimizu, K., Aoki, R., Hashikawa, K., Kimura, Y., Yasuda, K., Tashiro, K., Kuhara, S., Nagata, K., Ohshima, K., 2012. Gene expression analysis of rheumatoid arthritis synovial lining regions by cDNA microarray combined with laser microdissection: up-regulation of inflammation-associated STAT1, IRF1, CXCL9, CXCL10, and CCL5. Scand. J. Rheumatol. 41, 170–179.

Yukhananov, R., Kissin, I., 2008. Persistent changes in spinal cord gene expression after recovery from inflammatory hyperalgesia: a preliminary study on pain memory. BMC Neurosci 9, 32.

Zapata, A., Pontis, S., Schepers, R.J., Wang, R., Oh, E., Stein, A., Bäckman, C.M., Worley, P., Enguita, M., Abad, M.A., Trullas, R., Shippenberg, T.S., 2012. Alleviation of Neuropathic Pain Hypersensitivity by Inhibiting Neuronal Pentraxin 1 in the Rostral Ventromedial Medulla. J. Neurosci. 32, 12431–12436.

Zeitz, K.P., Guy, N., Malmberg, A.B., Dirajlal, S., Martin, W.J., Sun, L., Bonhaus, D.W., Stucky, C.L., Julius, D., Basbaum, A.I., 2002. The 5-HT3 subtype of serotonin receptor contributes to nociceptive processing via a novel subset of myelinated and unmyelinated nociceptors. J. Neurosci. 22, 1010–1019.

Zhang, E.T., Craig, A.D., 1997. Morphology and distribution of spinothalamic lamina I neurons in the monkey. J. Neurosci. 17, 3274–3284.

Zhang, J., Shi, X.Q., Echeverry, S., Mogil, J.S., Koninck, Y.D., Rivest, S., 2007. Expression of CCR2 in Both Resident and Bone Marrow-Derived Microglia Plays a Critical Role in Neuropathic Pain. J. Neurosci. 27, 12396–12406.

Zhang, L., Lu, Y., Chen, Y., Westlund, K.N., 2002. Group I metabotropic glutamate receptor antagonists block secondary thermal hyperalgesia in rats with knee joint inflammation. J. Pharmacol. Exp. Ther. 300, 149–156.

Zhang, L., Sykes, K.T., Buhler, A.V., Hammond, D.L., 2006. Electrophysiological heterogeneity of spinally projecting serotonergic and nonserotonergic neurons in the rostral ventromedial medulla. J. Neurophysiol. 95, 1853–1863.

Zhang, W., Gardell, S., Zhang, D., Xie, J.Y., Agnes, R.S., Badghisi, H., Hruby, V.J., Rance, N., Ossipov, M.H., Vanderah, T.W., Porreca, F., Lai, J., 2009. Neuropathic pain is maintained by brainstem neurons co-expressing opioid and cholecystokinin receptors. Brain 132, 778–787.

Zhang, X., Huang, J., McNaughton, P.A., 2005. NGF rapidly increases membrane expression of TRPV1 heat-gated ion channels. EMBO J. 24, 4211–4223.

Zhang, Y., Yang, Z., Gao, X., Wu, G., 2001. The role of 5-hydroxytryptamine1A and 5-hydroxytryptamine1B receptors in modulating spinal nociceptive transmission in normal and carrageenan-injected rats. Pain 92, 201–211.

Zhang, Z., Cai, Y.-Q., Zou, F., Bie, B., Pan, Z.Z., 2011. Epigenetic suppression of GAD65 expression mediates persistent pain. Nature Medicine 17, 1448-55.

Zhuo, M., Gebhart, G.F., 1990. Characterization of descending inhibition and facilitation from the nuclei reticularis gigantocellularis and gigantocellularis pars alpha in the rat. Pain 42, 337–350.

Zhuo, M., Gebhart, G.F., 1991. Spinal serotonin receptors mediate descending facilitation of a nociceptive reflex from the nuclei reticularis gigantocellularis and gigantocellularis pars alpha in the rat. Brain Res. 550, 35–48.

Zhuo, M., Gebhart, G.F., 1992a. Characterization of descending facilitation and inhibition of spinal nociceptive transmission from the nuclei reticularis gigantocellularis and gigantocellularis pars alpha in the rat. J. Neurophysiol. 67, 1599–1614.

Zhuo, M., Gebhart, G.F., 1992b. Inhibition of a cutaneous nociceptive reflex by a noxious visceral stimulus is mediated by spinal cholinergic and descending serotonergic systems in the rat. Brain Res. 585, 7–18.

Zhuo, M., Gebhart, G.F., 1997. Biphasic modulation of spinal nociceptive transmission from the medullary raphe nuclei in the rat. J. Neurophysiol. 78, 746–758.

Zimmermann, K., Leffler, A., Babes, A., Cendan, C.M., Carr, R.W., Kobayashi, J., Nau, C., Wood, J.N., Reeh, P.W., 2007. Sensory neuron sodium channel Nav1.8 is essential for pain at low temperatures. Nature 447, 855–858.

Zylka, M.J., Rice, F.L., Anderson, D.J., 2005. Topographically distinct epidermal nociceptive circuits revealed by axonal tracers targeted to Mrgprd. Neuron 45, 17–25.

Appendix

A1. Solutions for immunohistochemistry

Phosphate buffer (0.1M, pH7.4)

190mM NaH_2PO_4

810mM $Na_2H\ PO_4$

Paraformaldehyde

4% paraformaldehyde

0.1M phosphate buffer

Heparinised saline

5IU/ml heparin

0.9% NaCl

Sucrose

30% or 5% sucrose

0.02% NaN_2 (Sigma)

Blocking solution - fluorescence detection:

0.1M PB

3% normal serum (species dependent on host of secondary antibody)

0.3% TritionX-100

Blocking solution - chromogenic detection:

0.1M PB

3% normal serum (species dependent on host of secondary an

2% H_2O_2 to quench endogenous peroxidase activity

0.3% TritonX-199

TTBS (Tris-Triton buffered saline)

0.05M Tris base

0.3% TritonX-100

0.9% NaCl

Preparation of gelatinised slides

2.5g gelatine in 500ml dH_2O, heat to < 50°C

Add 0.5g chrome alum (chromic potassium sulphate, Sigma)

Filter

Dip twin-frost slides in solution for 30s

Dry overnight

A2. Solutions for western blot analysis

RIPA

100mM NaCl

100mM NaF

20mM 4-(2-hydroxyethyl)-1-piperazineethanesulfonic acid (HEPES) ph7.4

5mM ethylenediametetraacetic acid (EDTA)

1mM Na_2VO_4

1% v/v NP-40

MOPS ph7.3

0.05M 3-(N-morpholino) propane sulphonic acid (MOPS)

0.5M Tris base

3.5mM SDS

1mM EDTA

Transfer buffer

48mM Tris base

39mM glycine

0.037% SDS

10% v/v methanol

Tris-buffered saline

0.05M Tris base

0.9% NaCl

PBS Tween

0.1 M phosphate-buffered saline (Sigma-Aldrich)

0.1 % v/v Tween 20

Appendix A3. Log2 transformation of von Frey hairs

g	log2 (g)
0.07	-3.84
0.16	-2.64
0.4	-1.32
0.6	-0.74
1	0.00
1.4	0.49
2	1.00
4	2.00
6	2.58
8	3.00
10	3.32
15	3.91
26	4.70
60	5.91